

AEROSOL DEPOSITION AND
AIRWAY - TO - PERFUSATE
TRANSFER IN THE
ISOLATED, PERFUSED RAT LUNG

Nesta Sian Rowlands Roberts

Submitted for the degree of Ph.D. to
The University of Aston in Birmingham.

March 1984.

ACKNOWLEDGEMENTS

I express my gratitude to Dr P. R. Byron and Dr. A. R. Rees for their guidance, advice and tolerance during the supervision of the research work presented in this thesis. I also thank The Pharmaceutical Society of Great Britain for their financial support, Dr I. Gonda, Mr. A. Hickey and Dr Y. S. Bakhle (Royal College of Surgeons, London) for their advice and Mr W. Field for the splendid photographic work displayed in this thesis. I am indebted to many of the technical staff in the Department of Pharmacy and to Mr P. Behan and the staff in the Animal House. Finally I must thank my long-suffering husband for his tireless efforts in word-processing this thesis.

Siân Roberts, March 1984.

DEDICATION

To Mum, Dad and Peter

The University of Aston in Birmingham

Aerosol deposition and airway-to-perfusate transfer in the isolated, perfused rat lung

Nesta Siân Rowlands Roberts

Ph.D. Thesis Summary, 1984

Although the lungs offer a potentially useful alternative route of drug administration, little is known about systemic absorption, after drug delivery to the respiratory tract as inhalation aerosols. A technique was developed and evaluated for the administration of inhalation aerosols to the isolated, perfused rat lung. Well characterised aerosols of disodium fluorescein were administered to the preparation under controlled respiratory regimes. Subsequent airway-to-perfusate transfer of this highly soluble material, mimicking systemic absorption in whole animals, was monitored by perfusate sampling. Fractional deposition and the time dependence of fractional transfer of this solute were investigated as functions of aerosol particle size distribution, lung tidal volume and ventilation rate, all of which could be held constant during an experiment.

Fractional deposition was greater at lower ventilation rates. This suggested that the primary mechanism of aerosol deposition in this model, for the aerosols studied, was sedimentation rather than impaction. Total fractional transfer and transfer rate increased with increasing tidal volume or decreasing particle size. This implied that rate and total fractional transfer were dependent upon regional deposition, greater penetration of the lower airways occurring with smaller particle sizes or larger tidal volumes. Also, transfer rate, and total fractional transfer, increased with increasing ventilation rate and decreasing lung residence time, a phenomenon which may have been due to different regional deposition of the aerosol when administered at different frequencies, induced by the dependence of hygroscopic growth kinetics upon particle size. Transfer kinetics were apparent first-order, but the transfer rate constants were largely independent of aerosol particle size distribution, lung respiratory regime and perfusate flow rate. This implied that rate constants were independent of regional deposition and that pulmonary epithelial permeability, the rate-determining process in this system, was similar in all perfused lung areas.

Keywords: Isolated lung, Aerosol, Pulmonary deposition, Systemic absorption, Absorption kinetics

CONTENTS

	Page
<u>Chapter 1. Introduction</u>	1
<u>Chapter 2. The isolated, perfused lung system</u>	10
2.1 Introduction	10
2.2 Materials and Methods	10
2.2.1 Animals	14
2.2.2 Anaesthesia	14
2.2.3 Viability Assessment	15
2.2.4 Isolation using continuous perfusion and continuous positive pressure ventilation	15
2.2.5 Isolation in the absence of ventilation and continuous perfusion	17
2.2.6 Isolation using a short period of positive pressure ventilation and continuous perfusion	19
2.2.7 An apparatus designed for the isolated, perfused rat lung preparation receiving positive pressure ventilation	22
2.2.8 An apparatus for the isolated, perfused rat lung preparation receiving negative pressure ventilation	24
2.3 Results and discussion	27
2.3.1 Isolation using continuous perfusion and continuous positive pressure ventilation	27
2.3.2 Isolation in the absence of ventilation and continuous perfusion	30
2.3.3 Isolation using a short period of positive pressure ventilation and continuous perfusion	33
2.3.4 Pulmonary oedema	34
2.3.5 An apparatus designed for the isolated, perfused rat lung preparation receiving positive pressure ventilation	35
2.3.6 An apparatus for the isolated, perfused rat lung preparation receiving negative pressure ventilation	38
<u>Chapter 3. Disodium fluorescein - marker compound for absorption studies in the rat lung</u>	52
3.1 Introduction	52

3.2 Materials and Methods	55
3.2.1 Fluorescein analysis	55
3.2.1.1 Analysis of disodium fluorescein powder	55
3.2.1.2 Determination of III in K4	55
3.2.1.3 General method of assay for III in rat lung perfusate	57
3.2.2 Airway-to-perfusate transfer following intratracheal instillation of disodium fluorescein solution	58
3.2.3 Control experiments to determine loss of fluorescein to the system	59
3.2.3.1 Loss of fluorescein to sand	59
3.2.3.2 Loss of fluorescein to apparatus	59
3.2.3.3 Loss of fluorescein due to binding and metabolism by the lung	60
a. Binding	60
b. Conjugation	60
c. Metabolism	61
3.2.4 Fluorescein transfer	62
3.3 Results and discussion	64
3.3.1 Analysis of disodium fluorescein powder	64
3.3.2 Determination of III in K4	65
3.3.3 Airway-to-perfusate transfer following intratracheal instillation of disodium fluorescein solution	66
3.3.4 Control experiments to determine loss of fluorescein to the system	68
3.3.4.1 Loss to sand	68
3.3.4.2 Loss of fluorescein to the apparatus	68
3.3.4.3 Loss of fluorescein due to binding or metabolism by the lung	69
a. Binding	69
b. Conjugation	70
c. Metabolism	70
3.3.5 Data correction for instillation experiments	71
3.3.6 Fluorescein transfer	72
<u>Chapter 4. Aerosol generation and administration <u>apparatus</u></u>	97
4.1 Introduction	97
4.2 Background	97
a. Generation	98
b. aerosol administration	103
4.3 Materials and Methods	106
4.3.1 3400FB airflow	106
4.3.2 3400FB mass aerosol output	106
4.3.2.1 Apparatus	107
4.3.2.2 Experimental details	108
4.3.3 Aerosol concentration in delivery tube	109

4.3.4 Aerosol particle size distributions	110
4.3.4.1 Apparatus	111
4.3.4.2 Experimental details	111
4.3.5 Sample analysis	112
4.3.5.1 Determination of mass aerosol output	112
4.3.5.2 Aerosol particle size distribution	112
4.4 Results	114
4.4.1 3400FB mass aerosol output	114
4.4.1.1 Output stability	114
4.4.1.2 Effect of powder feed rate	114
4.4.1.3 Effect of total airflow to fluidised bed	115
4.4.1.4 Effect of powder particle size	115
4.4.1.5 Reproducibility of particle size distribution	116
4.4.2 Aerosol concentration in delivery tube	117
4.4.3 Aerosol particle size distribution	117
4.5 Discussion	119
<u>Chapter 5. Aerosol administration to the isolated, perfused rat lung</u>	152
5.1 Introduction	152
5.2 Materials and Methods	154
5.3 Results	158
5.3.1 Reproducibility	158
5.3.2 Fractional deposition	159
5.3.2.1 Effect of respiratory frequency	159
5.3.2.2 Effect of tidal volume	160
5.3.2.3 Effect of aerosol particle size	160
5.3.3 Fractional transfer	161
5.3.3.1 Effect of perfusate flow rate	161
5.3.3.2 Effect of respiratory frequency	161
5.3.3.3 Effect of tidal volume	161
5.3.4 Solution versus aerosol transfer rates	162
5.4 Discussion	164
5.4.1 Reproducibility	164
5.4.2 Effects of respiratory frequency, tidal volume and aerosol particle size upon fractional deposition	165
5.4.3 Effects of perfusate flow, respiratory frequency, tidal volume and aerosol particle size on fractional transfer	168
5.4.4 Apparent first-order kinetics	171
5.4.5 Solution versus aerosol transfer rates	175
<u>Chapter 6. General discussion</u>	227
<u>Plates 1 to 15</u>	232
<u>Appendix A</u>	247
<u>References</u>	271

LIST OF TABLES

TABLE	Page	
2.1	Dry-to-wet weight lung ratios and their lack of correlation with oedema	41
3.1	Water content of disodium fluorescein powder	75
3.2	Sodium fluorescein elemental analysis	76
3.3	Percent fluorescein by weight, as determined by fluorimetric analysis and titration	76
3.4	Amounts of III (μg) transferred from airway - to - perfusate with time for the instillation experiments I and II	77
3.5	Fraction of deposited amount of III transferred from airway - to - perfusate with time for instillation experiments I and II	78
3.6	Amounts of III found after analysis of the various samples collected in instillation experiments I and II	79
3.7	Fractional losses of fluorescein to apparatus: (a) unsiliconised and (b) siliconised, 1 and 60min after bolus injection	80
3.8	Amounts of fluorescein (μg) recovered and unrecoverable from isolated rat lungs, following the intratracheal instillation of a range of doses	81
3.9a	Comparison of the amounts of III found after analysis of perfusate samples, collected in instillation experiments I and II treated (a) with, and (b) without, β -glucuronidase	82
3.9b	Comparison of the amounts of III found after analysis of lung homogenate supernatants from instillation experiments I and II treated (a) with, and (b) without, β -glucuronidase	83
3.10	Summary of results from control experiments	83
3.11	Perfusate - to - lung fluorescein transfer:- lack of evidence for reversibility	84
5.1	Effect of respiratory frequency (RF) on fractional deposition	178
5.2	Effect of tidal volume on fractional deposition	179
5.3	Effect of aerosol particle size distribution on fractional deposition	180
5.4	Amounts of III and fractions to be transferred with time, for the instillation experiments I and II	181
5.5	The lack of correlation between values for f_{∞} as an index of depth of RT penetration, and the transfer rate constant, k , for aerosol and instilled solution administration experiments	182

5.6 Values for the transfer rate constant, k , following the deposition of a range of transferable amounts (A) of III, as aerosol, in the isolated, perfused rat lung preparation 183

LIST OF FIGURES

FIGURE	Page
2.1 Rat neck, ventral-side uppermost, displaying sterno-hyoid muscle	42
2.2 Exposed and cannulated rat trachea	44
2.3 Apparatus for the isolated, perfused rat lung preparation receiving positive pressure ventilation	46
2.4 The artificial thorax apparatus for the isolated, perfused rat lung preparation receiving negative pressure ventilation	48
2.5 Apparatus for the isolated, perfused rat lung preparation receiving negative pressure ventilation	50
3.1 Molecular formulae of fluorescein (I), disodium fluorescein (II) and the fluorescein dianion (III)	85
3.2 Calibration curves (relative intensity versus fluorescein dianion, III, concentration) for solutions containing fluorescein in pH12SGB or pH12 K4 supernatant and fluorescein solution alkalinised to pH12 and diluted in pH12K4 supernatant	87
3.3 Schematic diagram of fraction transferred versus time, representing insignificant and significant fluorescein metabolism during the course of an experiment	89
3.4 Amount of fluorescein transferred from the airways to the perfusate versus time in instillation experiments I and II	91
3.5 Fraction transferred versus time for instillation experiments I and II	93
3.6 Insignificant III metabolism in the isolated, perfused rat lung, as shown by the random distribution of normalised data for fractional transfer about 1 (times greater than 70min) in aerosol administration experiments	95
4.1 Comparison of mass III aerosol output versus running time for the constant liquid feed atomiser and 3400 fluidised-bed generator	124
4.2 Schematic diagram of aerosol generation apparatus featuring the constant liquid feed atomiser	126
4.3 Schematic diagram (cross sectional view) of 3400FB (fluidised-bed aerosol generator)	128

4.4	Design of glass administration tube (C) used in the aerosol administration studies described in Chapter 5	130
4.5	Air flow rate ($l\ min^{-1}$) from the outlet of the 3400FB aerosol generator versus bed flow setting (%) obtained at a variety of bead purge settings	132
4.6	Schematic diagram of the aerosol generating apparatus featuring the fluidised-bed aerosol generator. The overlay details the apparatus for determining mass III aerosol output	134
4.7	Schematic diagram of the aerosol generating apparatus featuring the fluidised-bed aerosol generator. The overlay details the apparatus used for determining aerosol particle size distributions utilising a cascade impactor	136
4.8-13	Mass III aerosol output versus running time for the 3400 fluidised-bed aerosol generator under various operating conditions	138
4.14	Concentration of III in aerosols generated from powder sub-batch A in main aerosol stream and delivery tube	145
4.15	Concentration of III in aerosols generated from powder sub-batch D in main aerosol stream and delivery tube	147
4.16	Aerosol particle size distribution determined using a cascade impactor <u>before</u> aerosol administration to the iprl	149
4.17	Aerosol particle size distribution determined using a cascade impactor <u>after</u> aerosol administration to the iprl	151
5.1	Schematic diagram of apparatus used to administer aerosols of II to the isolated, perfused rat lung preparation	184
5.2-12	Fraction transferred versus time profiles resulting from the administration of aerosols of II to a number of isolated, perfused rat lung preparations	186
5.2	Test of reproducibility	186
5.3	Test of reproducibility	188
5.4	Effect of perfusate flow rate (PF) on transfer	190
5.5	Effect of perfusate flow rate (PF) on fractional transfer	192
5.6	Effect of respiratory frequency (RF) on fractional transfer	194
5.7	Effect of respiratory frequency (RF) on fractional transfer	196
5.8	Effect of respiratory frequency (RF) on fractional transfer	198
5.9	Effect of tidal volume (TV) on fractional transfer	200
5.10	Effect of aerosol particle size distribution on fractional transfer	202
5.11	Effect of aerosol particle size distribution on fractional transfer	204

5.12	Effect of aerosol particle size distribution on fractional transfer	206
5.13	Fraction transferred versus time profiles resulting from aerosol administration and solution instillation	208
5.14	Log-linear plots of fraction to be transferred versus time (data from Fig 5.13)	210
5.15	Schematic representation of the pulmonary circulation	212
5.16-25	Log-linear plots of fraction to be transferred versus time, for values obtained after aerosol administration was complete	214
5.26	Amounts of III transferred versus time following deposition, from aerosols, of a range of transferable amounts	225

LIST OF PLATES

PLATE		Page
1.	Oedematous lungs	232
2.	A non-viable, mottled lung	233
3.	A non viable lung after perfusion. Grey and patchy, indicating loss of viability	234
4.	Tracheotomised rat receiving positive pressure ventilation	235
5.	Tracheotomised rat receiving positive pressure ventilation - thorax is open, displaying the heart and lungs	236
6.	Cannulation of the pulmonary artery and clearance of blood from the ventilating lungs with K4	237
7.	Isolated, perfused rat lungs, ventral view, with the pulmonary artery cannula tied in place, without ventilation	238
8.	Isolated, perfused rat lungs, without ventilation. The pulmonary artery and left ventricle are cannulated	239
9.	Viable, unventilated, isolated, perfused rat lung with bar through the oesophagus for horizontal suspension in the artificial thorax	240
10.	Isolated, perfused lungs, suspended horizontally in artificial thorax (AT) and maintained under slight negative pressure by withdrawal of air from the AT by syringe	241
11.	Aerosol generation apparatus featuring the constant liquid feed atomiser	242
12.	Close-up view of constant liquid feed atomiser and associated equipment	243
13.	Aerosol characterisation: determination of aerosol mass output	244
14.	Aerosol characterisation: determination of particle size distribution using a cascade impactor	245
15.	Apparatus used for aerosol generation and administration to the isolated, perfused rat lung preparation	246

CHAPTER ONE

INTRODUCTION

The gaseous exchange role played by the lungs during respiration is the primary, but not the only, important function which they perform in the body. Over the past ten to fifteen years, increasing attention has been devoted to the metabolic (1 - 16, 37, 38) and binding (1, 5, 16, 17) capacity of the lungs for both endogenous and exogenous substances. Of particular therapeutic interest is the removal of certain drug entities from the systemic circulation and their accumulation within the lungs. At therapeutic dose levels, drugs like imipramine and chlorpromazine exhibit tissue/plasma concentration ratios of above 50 (18), so that any minor redistribution from high capacity storage sites like the lungs, could lead to a dramatic increase in plasma levels with subsequent pharmacological and toxicological activity (5).

In recent years, research workers have begun to investigate systemic absorption of drugs from the airways of the lung. Research motives vary considerably. Some workers are concerned with systemic toxicity resulting from inhalation of insecticides, herbicides, industrial chemicals and other airborne substances (6, 14, 16, 19). While the

pharmaceutical industry attempts to formulate inhalation aerosols, usually containing compounds (bronchodilators, anti-inflammatory steroids and certain antibiotics) which have a local effect within the respiratory tract (RT) (20 - 22), other workers investigate the undesirable systemic effects which result from the absorption of these drugs and their vehicles (20, 23). Some studies have been performed, with selected solutes, in order to characterise the permeability of RT epithelia, in both healthy and diseased lungs. A measure of permeability could be used in the early diagnosis of some diseased lung conditions (24 - 26). Another field of enquiry has been the use of the RT for the administration of systemically active compounds. The large surface area of the lung, approximately 30m² in man (27), provides an absorptive area (which can be reached in seconds) comparable with that of the gastro-intestinal tract (GIT). Thus the RT could offer an alternative delivery route for drugs which, at present, require injection, because of either poor absorption or chemical or biological inactivation within the GIT.

The administration of compounds to the RT is by no means a new idea. The route, although little understood, has been used for centuries (28). The work described in this thesis was designed to improve our understanding of certain aspects of drug administration and absorption via the RT, by using a non - pharmacologically active marker compound. Because the major areas of research interest described above, really differ only in the type of compound being administered to the RT, some of the work in this thesis is

of relevance to each major area. Nevertheless, much of the work to be described, is presented according to the author's own, pharmaceutical interest in understanding the effects of aerosol characteristics and respiratory variables upon drug absorption from the RT.

Many workers have studied systemic absorption, following intratracheal solution instillation of a wide variety of compounds in various species (rat, 23, 28 - 35; dog, 36; rabbit, 37, 38). Rates of absorption vary considerably, depending upon the physico-chemical properties of the compounds and on whether absorption is perfusion or diffusion rate-limited or occurs via a carrier-mediated process. Studies to date suggest that the pulmonary or RT epithelium has the characteristics of the classic "lipid-pore model" of biological membranes (24, 40). The most significant factor affecting the movement of "lipophilic" solutes, such as gases and alcohols, is thought to be their partition coefficient. They penetrate the RT barriers so rapidly, that equilibration between fluid injected into the alveoli, and blood in the capillaries, is nearly complete during the capillary transit time (~ 0.75 sec, 39). Clearance of such solutes from the lung is limited primarily by perfusion rather than diffusion (24). In contrast, "lipophobic" solutes, such as electrolytes and sugars are thought to be absorbed via extracellular pathways through aqueous membrane pores. Their absorption rates are not related to partition coefficient but are inversely related to molecular size (24, 40). Absorption of such solutes appears to be limited by diffusion rather than

perfusion. Furthermore, some anionic compounds, phenol red, disodium cromoglycate, and amino acid cycloleucine, appear to be absorbed in part by saturable, carrier-type transport processes (31, 35, 40).

Data presented in the literature concerning solute absorption following intratracheal solution instillation provides an important basis for the future exploitation of this route for systemically active drugs. The choice of dosage form for administration to the conscious human or animal RT however, is restricted to either vapours or aerosol systems due to the need for patient compliance and ease of administration. Although aerosol systems are most flexible for drug administration to the RT, many difficulties remain to be overcome if reliable, systemically active aerosols are to be developed.

Major problems are concerned with the prediction of regional and total aerosol deposition in the RT and the resultant drug absorption into the pulmonary circulation. Aerosol deposition in the human RT has been widely reported under a variety of respiratory regimes (41, 42, 49) alongside deposition in synthetic and theoretical human RT models (43, 44). The applicability of these data and models to therapeutic aerosols however, is limited, because of the use of water-insoluble, rather than soluble, aerosol systems. Hygroscopic growth of water-soluble, therapeutic aerosols is known to occur in regions of high relative humidity, as found in the RT (45, 48, 66, 91). This phenomenon is thought to greatly affect aerosol deposition patterns (46, 47, 50, 91, 92) and, perhaps, resultant drug

absorption (40). Synthetic models of the RT have been used to estimate the rate and extent of growth of soluble aerosols (48, 91, 92) although extrapolation of these findings is at present, virtually impossible. Despite the difficulties associated with quantitative prediction, factors known to affect regional and total aerosol deposition within the RT include inspiratory flow rate (25, 42, 49, 94), tidal volume (25, 41, 42, 49, 94), breath holding time (25, 27, 50, 94), aerosol particle size distribution (42, 47, 49, 51), particulate growth (46, 47, 92) and mucociliary clearance (25, 93, 102; which occurs in all of the lower respiratory tract except the terminal structures and depends upon both site of deposition and particle solubility). Studies to date however, do not include the investigation of the deposition and absorption of well characterised soluble aerosols given systematic alteration of aerosol particle size and respiratory variables.

The literature provides a great deal of information on drug absorption via the lung following solution instillation. Little similar data is available however, after aerosol administration. Brown and Shanker (40) looked at ^{drug} absorption following the administration of a number of rather poorly characterised aerosols, administered in unknown quantities, to the rat lung in situ. They concluded that transfer rate constants were first order (ranging 0.0201 to 1.03min⁻¹) for the compounds studied, except where carrier-mediated transport was implicated. They also found that absorption from aerosols occurred approximately twice

as fast as that for the same compound administered as a solution instillation to the RT. They hypothesised that this was due to differences in regional deposition and a greater permeability of the alveolar, as opposed to tracheobronchial, epithelial membranes. These hypotheses should be tested. The rates of drug absorption are important for aerosols containing compounds intended for either local or systemic effect. A slow rate of absorption is preferable for local activity, in order to reduce the frequency of dosage, while the converse may be true for a systemically active compound. Alteration of chemical entity may be employed to change absorption rate (28), for example the administration of the sodium salt of an organic acid, as opposed to the acid itself. Absorption studies however, must also include investigations into the drug binding and metabolising capacity of the lung (1 - 5, 17).

It is clear that a great amount of basic research remains to be performed if serious attempts are to be made to quantify drug delivery via the RT, whether for local or systemic activity. The ultimate therapeutic goal for administration via this route would be to deposit known quantities of drug-containing aerosol in the RT, reproducibly, under a constant respiratory regime, such that absorption^{of drug}, in a systemically active form, occurred at predictable rates. The goal of the work presented in this thesis was to develop a means of investigating some of the factors which influence aerosol deposition and subsequent airway-to-vasculature solute transfer. In order to achieve this objective, it was necessary to choose, and suitably

adapt, an animal lung model in which deposition and absorption could be quantified. Well characterised aerosols, in various size ranges, were then to be administered to this model, and the effects of particle size distribution (psd), lung tidal volume and respiratory frequency investigated.

Several methods have been used to estimate the rate and extent of drug absorption from the lung. These evaluate either drug disappearance from the lung (19, 22, 23, 28 - 35, 40), or drug appearance in the circulation (36 - 38). Disadvantages of the disappearance methodology are found when significant metabolism occurs or, in the case of radio-labelled compounds, where the label becomes detached from the drug. Furthermore, the entire RT has to be analysed, requiring a large number of animals, with associated variability, per experiment. In this thesis, an isolated, perfused lung preparation was chosen. This system permitted quantitative determination of the administered compound in the perfusate (vasculature) as a function of time, after administration to the airways. Whole body complications (induced by variations in a compound's pharmacokinetics) are removed, by removing the body, so that absorption can be assessed directly. Also, because various respiratory regimes and perfusate flows could be imposed upon an isolated lung preparation, the effects of these variables, could be studied with relative ease, compared to the difficulties encountered with whole animals. Rats were chosen as a lung source, because they were cheap, easy to handle and readily available. A suitable apparatus, to maintain isolated lungs, in viable condition, under

controlled, but variable respiratory regimes required design. This design was undertaken, after reviewing a number of different systems utilised by other workers (6 - 8, 10, 11, 13, 15, 21, 52 - 54).

A water soluble compound had to be selected, which was thought representative of a therapeutic entity but which was non-toxic, easily detectable and without pharmacologic activity in the rat lung. Disodium fluorescein, the marker compound selected for these investigations, satisfied all of these criteria.

Solid, rather than liquid aerosol systems, were preferred because they were capable of carrying a greater quantity of the solute, making subsequent detection in the perfusate solutions more precise. Given the many aerosol generators available, one was selected with the capacity to produce aerosols with various psd's, for prolonged periods, at effectively constant concentrations. A system to convey the aerosol, from the generator to the lungs was designed and constructed. It was necessary, in this design, to cope with the need to dispose of large quantities of aerosol waste, without contamination of laboratory air.

In order to study the effects of aerosol psd upon deposition and absorption in these investigations, it was not felt sufficient to characterise the aerosol (concentration and psd) after its generation, owing to inevitable particulate segregation in the apparatus conveying aerosol to lungs. Attempts were made in these studies to use techniques which determined aerosol characteristics for the inhaled systems. This contrasts with

recently published work by Brown and Shanker (40), who used an aerosol administration system with the rat lungs at right angles to the main aerosol stream, while determining aerosol psd in the main stream alone. It is likely that particulate segregation occurred in their system at this anisokinetic junction.

Difficulties are acknowledged in the literature concerning inhalation aerosol administration, regarding the accurate determination of aerosol mass deposition in the RT (37, 38, 40, 55). Thus, in this thesis, mass-balance was first established for disodium fluorescein, instilled intratracheally in known amounts in aqueous solution. In aerosol administration experiments, when the problem of dose estimation arose, it was then possible to determine the amount deposited retrospectively, after analysis.

The major objectives of this thesis have been outlined above. The remaining chapters describe the rational development (design and evaluation) of the model used to study fluorescein aerosol deposition and subsequent solute transfer to the vasculature, under various experimental conditions. The effects of aerosol particle size and respiratory regime are documented and explained in Chapter 5. The relationships between this work, in the isolated, perfused rat lung preparation, and aerosol deposition and solute absorption from the human RT can only be speculative at present. It is to be hoped however, that the material presented in this thesis, will contribute to the literature in a research area where, although groundwork is minimal, interest is growing rapidly.

CHAPTER TWO

THE ISOLATED, PERFUSED LUNG SYSTEM

2.1 INTRODUCTION

The work described in this chapter concerns the design and development of an in vitro model aimed at providing quantitative information on the availability of a marker compound, delivered as a solid aerosol to the lungs.

The model, or system, consisted of an isolated, perfused rat lung preparation, and an apparatus suitable for maintaining its viability. The procedures involved in isolation and perfusion of the rat lung are frequently documented (5, 8, 10 - 17, 19, 21, 28, 52 - 54, 58) however, the use of such a preparation in aerosol studies is novel. As a result, developing a system suitable for the aerosol studies described in this thesis, required the amalgamation of many techniques employed by other workers, and the development of new ideas related to procedure and apparatus design.

The system will be described in two sections, i) the development of surgical techniques consistent with the

maintainence of lung viability and ii) the design of an apparatus to maintain viability, permit aerosol administration and enable monitoring of airway-to-perfusate transfer of dissolved material.

Although surgical procedures to isolate and perfuse the rat lung are frequently documented, as yet unpublished is a comprehensive technique which can readily be learned and which overcomes the many, often unreported, problems associated with such procedures. A detailed description of the surgical techniques involved in successful lung isolation and perfusion is therefore presented together with the development of these procedures. It is hoped that this description may help future workers in this area to acquire the necessary surgical expertise.

The path to a successful technique for rat lung isolation and perfusion will be described in three subsections:

2.2.4 Isolation using continuous perfusion and continuous positive pressure ventilation.

2.2.5 Isolation in the absence of ventilation and continuous perfusion.

2.2.6 Isolation using a short period of positive pressure ventilation and continuous perfusion.

The second part of the chapter concerns the design of an apparatus to house the isolated perfused lung. The apparatus evolved by combination of guidance from the literature (6 - 8, 10, 11, 13, 15, 21, 52 - 54, 58) and the necessity to enable aerosol administration. Fractional deposition, that is the amount of aerosol deposited in the

lungs expressed as a fraction of the total administered, and fractional transfer, the amount of dissolved aerosol transferred to the perfusate expressed as a fraction of the amount deposited, were to be studied as functions of aerosol particle size, lung tidal volume, ventilation rate and perfusion rate. Ultimately, the apparatus had to cater for:

1. Maintenance of lung viability for >3 hr.
2. Lung ventilation under controlled regimes with the facility to change ventilatory regime (tidal volume, ventilatory frequency) quickly and easily.
3. Aerosol administration in the ventilatory airstream.
4. Constant rate rather than constant pressure perfusion (and the facility to vary this rate).
5. Perfusate recirculation.
6. A large volume perfusate reservoir for mixing and sampling.

Lung viability was maintained by creating conditions recommended in the literature. The lungs were suspended in a humid atmosphere (6, 7, 37, 38) at 37°C (5 - 17, 21, 37, 38, 52 - 54) and perfused with Krebs Ringer bicarbonate solution (56) with 4%w/v bovine serum albumin, held at pH 7.35 to 7.4 (11, 16, 53), 37°C, with a partial pressure of oxygen (pO_2) greater than 400mm Hg (11). Because the withdrawable blood volume of a rat (approximately 10ml) was too small to enable the study of drug transfer, whole blood was not used in these investigations.

In some metabolic studies, single pass perfusion has been used (13, 15, 16). In the studies described in this thesis however, the perfusate was recirculated to enable

accurate assay of the small quantities of drug transferred from the airways. Constant rate, rather than constant pressure, perfusion of the isolated lung was employed. With constant pressure, the perfusion rate decreases as the resistance of the blood vessels in the lungs increases (10). This was considered non-ideal for studying the effects of certain controlled variables on airway-to-perfusate transfer of administered material.

The apparatus was designed with a large reservoir in which the perfusate could be mixed homogeneously. Sequential sampling then enabled solute transfer to be monitored. The first apparatus to be designed and tested (Fig 2.3) was constructed with the aim of satisfying criteria 1 to 6 above. Details of this apparatus are given in Section 2.2.7, and its limitations and necessary modifications in Section 2.3.5. The modified apparatus is described in Section 2.2.8 (Fig 2.5), and the results of testing this with the isolated perfused rat lungs, described in Section 2.3.6.

2.2 MATERIALS AND METHODS

The information provided in sub-sections 2.2.1, 2.2.2 and 2.2.3 applies to all animal experiments described in this thesis.

2.2.1 Animals

Adult male Wistar rats (Bantin and Kingman, Hull, U.K.) weighing 350 to 400g were housed in natural lighting at 21°C. Animals breathed filtered air, were fed on a specific diet (Heygates modified breeding diet, Northampton, U.K.) and drank tap water ad libitum. Large, rather heavy rats were used for these experiments to facilitate surgical procedures.

2.2.2 Anaesthesia

Rats were anaesthetised by intraperitoneal injection (I.P.) of sodium pentobarbitone (Sagatal, May and Baker Ltd, Dagenham, U.K.) (60mg kg^{-1}), and laid, ventral side uppermost, in a spread eagle position on a dissecting board. Because manoeuvrability of the rat was essential during lung isolation, the rats were not pinned in position.

2.2.3 Viability Assessment

Loss of lung viability due to oedema was easy to identify. Oedema, when it occurred, was rapid and could be recognised by the presence of fluid in the trachea, lungs swelling to three or four times their normal size and becoming spongy and mottled in appearance (Plates 1 and 2). Loss of viability in the absence of oedema, although not as dramatic, was also apparent. After removal of blood the lungs are white in colour (Plate 9). With a loss of viability, the lungs first become grey and patchy (Plate 3), they then turn pink, starting at the mid-line, the colour working radially across each lung. Loss of viability could also be assessed retrospectively. When this occurred during or after transfer of the marker compound from the lungs to the perfusate, perfusate concentration increased suddenly. This was probably because perfusate entered the bronchii and trachea and washed through untransferred material deposited higher in the respiratory tract.

2.2.4 Isolation using continuous perfusion and continuous positive pressure ventilation

A 3cm incision was made in the skin at the neck of the anaesthetised rat. The connective tissue under the skin was drawn aside by blunt dissection, to minimise blood loss, exposing the sterno-hyoid muscle surrounding the trachea (Fig 2.1). Care was taken not to damage the carotid arteries. The sterno-hyoid muscle was cut along its

mid-ventral axis to expose the trachea and, after detaching the trachea from this muscle (blunt dissection with round bladed scissors), two sutures (Dewhurst Strong Thread, Manchester, U.K.) were tied loosely around the trachea. The trachea was cut through half its diameter, between the 4th and 5th cartilage rings, caudally to the thyroid gland, and a nylon cannula (800/200/150/100, Portex Ltd., Hythe, U.K.) inserted (Fig 2.2). The cannula was tied in place and the lungs ventilated (Small animal ventilator, No. 5056, Scientific Research Instruments, Edenbridge, U.K.) at 60 cycles min^{-1} (14, 53, 54) with an approximate tidal volume of 2ml (53, 54).

A horizontal incision was made at the base, and vertical incisions each side of the sternum, which was then drawn back to expose the heart and associated vasculature. The thymus was carefully removed and a 0.5cm incision made in the right ventricle. A pulmonary artery nylon cannula (800/200/175/100, Portex Ltd., Hythe, U.K.) was inserted into the pulmonary artery via the right ventricle and held in place by a small artery clip (1 inch, stainless steel, Mercian Surgical Instruments, Birmingham, U.K.). The left ventricle was quickly cut away to permit escape of blood and perfusate, and the lungs cleared of blood by continuous perfusion with Krebs Ringer bicarbonate solution with 4%w/v bovine serum albumin (Fraction V, Sigma Chemical Co., St Louis, U.S.A.) (K4). The perfusate was supplied through a removable extension tube (m) between the pump and the rat (Fig 2.3).

The heart and lungs were removed carefully from the

thorax, whilst still being perfused and ventilated, by cutting through the remainder of the trachea and removing connective tissue with round bladed scissors. This was achieved by holding the trachea away from the rat body, while directing the scissors toward the body, to avoid piercing or touching the lungs. The heart and lungs were washed in K4 and suspended vertically by the trachea in the upper chamber (Fig 2.3). Perfusion at 15 ml min^{-1} , and ventilation were continued.

The total operation time, defined as the time from the first incision, to the lungs being suspended in the upper chamber, was 15min. After surgical expertise had been gained, the procedures were assessed using 10 isolated preparations. The duration of lung viability (maintained in the apparatus shown in Fig 2.3) and the suitability of the isolated lungs for aerosol administration purposes, were evaluated.

2.2.5 Isolation in the absence of ventilation and continuous perfusion

The isolated, perfused rat lungs, prepared using the procedures described in section 2.2.4 were unsuitable for aerosol administration studies. Reasons for this are given in section 2.3.1, along with suggestions for their modification (section 2.3.1,1,2,3,4) with the goal of improving the quality of the preparation in terms of duration of viability and suitability for use in aerosol studies. The modified procedure is described below.

The abdomen of the anaesthetised rat was cut horizontally, just below the diaphragm. The diaphragm was pierced and 500 international units (i.u.) heparin in 0.1ml normal saline injected into the right ventricle of the heart. The chest was opened (see section 2.2.4) and the pulmonary artery cannulated by clipping a hard tipped (800/200/200/100 nylon tubing, Portex Ltd., Hythe, U.K.), soft walled cannula (bore 0.2cm, wall 0.1cm, Esco(Rubber) Ltd., Twickenham, U.K.) in place (see section 2.3.1.2) instead of the nylon type used in section 2.2.4. The right and left ventricles of the heart were cut away and 20ml Krebs Ringer bicarbonate solution (KRB), at room temperature, injected through the pulmonary artery cannula to clear the lungs of blood. A suture (Dewhurst strong thread, Manchester, U.K.) to retain the cannula was placed around both the pulmonary artery and the aorta (due to the difficulty in placing the suture around the artery alone without damaging its wall). The pulmonary artery cannula was then tied in place, and the clip removed.

Tracheotomy was performed, the lungs removed from the thorax, as described in section 2.2.4, washed in K4 and suspended in the upper chamber (Fig 2.3). The lungs were inflated with 1.5ml air from a syringe and the trachea tied off (13, 15) to prevent their collapse. Continuous perfusion was initiated at 15ml min^{-1} . The approximate time that the lungs were without perfusion was 3.5min. The total operation time was reduced to 5min because of the ease of isolation in terms of avoiding lung contact (accidental piercing) in the absence of ventilation. Time was also saved by eliminating

the need for an extension tube from the perfusate pump to the rat (for continuous perfusion) in favour of a KRB-filled syringe for limited perfusion.

The techniques described above were tested experimentally on 15 rats. The procedures were assessed and stepwise modifications made in a further 20 experiments. The results of the first 15, together with the surgical modifications explored subsequently, are discussed in section 2.3.2.

2.2.6 Isolation using a short period of positive pressure ventilation and continuous perfusion

The surgical modifications suggested in section 2.3.2 were implemented. These were the re-introduction of continuous perfusion, tracheal cannulation with a stainless steel cannula, positive pressure ventilation for a limited period during surgery alone and cannulation of the left side of the heart to permit negative pressure ventilation of the horizontally suspended lungs in a sealed chamber. The procedures including these modifications are described in detail below.

Male Wistar rats were anaesthetised and a tracheotomy performed (section 2.2.4). A stainless steel cannula was tied in place in the trachea (Plate 4). The lungs were ventilated using positive pressure at 15 cycles min^{-1} , with tidal volume 1.5ml. The abdomen of the rat was cut horizontally, the diaphragm pierced and the associated vasculature exposed (Plate 5). A hard-tipped, soft-walled

cannula was clipped into the pulmonary artery and the tip of the heart removed (Plate 6). The lungs were continuously perfused as in section 2.2.4 and, when cleared of blood, ventilation was stopped. Total positive pressure ventilation time was approximately 1.5min. The heart and lungs were quickly and carefully removed from the thorax, as described in section 2.2.4. Special care was taken not to tug at the lungs when removing them, to avoid damage. Any contact with the lungs (surgical instruments or fingers) was strictly avoided. The pulmonary artery was tied in place and the clip removed (Plate 7).

The left ventricle was cannulated by gently pushing a hard-tipped, soft-walled cannula (similar to that used in arterial cannulation) into the left atrium, via the left ventricle, and withdrawing the cannula slightly so that the tip remained in the ventricle. This action widened the connection between the two chambers on the left side of the heart, by damaging the heart valves. This was essential in maintaining adequate perfusate flow. The presence of a cannula in the left ventricle, whilst the valves between the atrium and ventricle were intact, impaired flow. This resulted in back-pressure in the pulmonary veins and subsequent lung oedema. The ventricular cannula was held in place by carefully tightening a thick suture (No.2,U.S.P., Armour Laboratories, London, U.K.) around both the right and left ventricles (Plate 8). This suture tended to cut through the ventricle walls causing perfusate to leak from the left ventricle.

The isolated lungs were washed with K4 and a bar

gently pushed through the oesophagus (Plate 9). The lungs were then hung horizontally by the bar in the artificial thorax, AT (Plate 10), and were kept under a slight negative pressure to prevent collapse.

Two stainless steel cannulae, driven through two rubber bungs sealing orifices in the wall of the AT (I and II, Fig 2.4), allowed perfusate flow through the lungs once suspended in the upper chamber. The first cannula (I, Fig 2.4), was connected on the inside of the chamber to the pulmonary artery cannula and, on the outside, to the silicone rubber tubing supplying perfusate. The perfusate returned to the reservoir (c, Fig 2.5) via a second stainless steel cannula (II, Fig 2.4). This was connected on the inside of the chamber to a left ventricular cannula and, on the outside, to silicone rubber tubing. The perfusate dripped from the lungs, via the cannulae and tubing, into the reservoir.

Total operation time was 7 to 10 minutes. The increase in time over method 2.2.5 was largely due to cannulation of the left ventricle. Perfusion was continued at 15ml min^{-1} and ventilation could be initiated by altering the pressure within the AT (see section 2.2.8). A sigh (7), or one large inspiration (tidal volume approximately 3ml), was induced at the beginning of ventilation, to produce even ventilation of both lungs (the stroke volume of the volume-cycle ventilator (i, Fig 2.5) was increased by 1ml for one whole ventilation cycle). The effects of ventilation over prolonged periods, and other modifications introduced into the surgical procedures described in this sub-section, are discussed in

section 2.3.3.

2.2.7 An apparatus designed for the isolated, perfused rat lung preparation receiving positive pressure ventilation

The first apparatus to hold the preparation was designed with the goal of fulfilling criteria 1 to 6 in section 2.1. The apparatus is shown schematically in Fig 2.3. Temperature was maintained at 37°C throughout, by water jacketing (b,c,g, Fig 2.3), connected to a thermocirculator (Churchill Laboratory Thermocirculator, Churchill Instrument Co. Ltd., Perivale, U.K.). The upper chamber (b) was fitted with a ground-glass stopper, and housed the lungs, suspended vertically. The stopper had three openings; the ventilatory line to the trachea passed through 1 (Fig 2.3), the pulmonary cannula through 2, while 3 was sealed.

Perfusate drained from the upper chamber to the perfusate reservoir, c, where pH was monitored by a combined glass/reference electrode (GK2401C, PHM62, Radiometer, Copenhagen, Denmark). Perfusate pH was maintained within the physiological range 7.35 to 7.4 by addition of <0.25%v/v 0.1M NaOH or HCl.

Total perfusate volume ranged 130 to 150ml. A magnetic stirrer (e, Fig 2.3, Monotherm, Rodwell Scientific Instruments Ltd., London, U.K.) ensured homogeneous mixing of the perfusate by the 4 x 0.5cm magnetic flea, e'. Carbogen was passed over the perfusate in the reservoir (Fig 2.3; c) to maintain pO_2 in excess of 400mm Hg (early attempts to bubble carbogen through the perfusate caused

excessive foaming). The pO_2 of the perfusate was continuously monitored (Flow through oxygen electrode, Rank Bros., Cambridge, U.K. connected to a calibrated XY recorder; 2600A4 with time drive, Bryans Southern Instruments Ltd., Mitcham, U.K.). Perfusate was circulated continuously (H.R. Flowinducer, Watson-Marlow Ltd., Falmouth, U.K.).

A pressure-cycle small animal ventilator (No. 5056, Scientific Research Instruments, Edenbridge, U.K.) was adjusted to deliver approximately 2ml cycle^{-1} carbogen to the lungs at $60\text{ cycles min}^{-1}$. Carbogen flow to the ventilator and perfusate was controlled by an inline flow meter, j, and regulator, k (FCV/ 0.25inch S/L, Platons, Basingstoke, U.K.).

Test experiments were performed to assess the performance of the apparatus (Fig 2.3) in terms of criteria 1 to 6 (section 2.1). The experiments included attempts to maintain the isolated lungs, prepared either by method 2.2.4 (10 attempts) or 2.2.5 (15 attempts), in the apparatus for prolonged periods. Positive pressure ventilation was attempted in three of these fifteen preparations. The time taken to achieve homogeneous mixing throughout the perfusate system was determined by injecting a known amount of fluorescein in 0.1ml solution, into the perfusate in the reservoir. The perfusate was mixed by the magnetic flea and circulated throughout the apparatus at 15 ml min^{-1} . Samples were withdrawn from the reservoir at 30 sec intervals and assayed for fluorescein content (Chapter 3). Results of these test experiments are discussed in section 2.3.5.

2.2.8 An apparatus for the isolated, perfused rat lung preparation receiving negative pressure ventilation

Problems associated with the first apparatus (Fig 2.3) are discussed in section 2.3.1, 1 to 6, together with necessary modifications. These included the addition of a heating coil and a filter (No.13400, 2.5cm Sartorius membrane filter, Hamburg, W. Germany) in the circulatory system, omission of the oxygen electrode during lung perfusion, re-design of the upper chamber to make it airtight and the addition of a narrow-bore side arm to the perfusate reservoir.

The modified apparatus is shown schematically in Fig 2.5 (Plate 10). The upper chamber, or artificial thorax (AT) is detailed in Fig 2.4. Necessary connections (I,II,III,IV) from the inside to the outside of the AT were made via stainless steel cannulae pushed through rubber bungs. Connections I and II permitted perfusate flow to and from the lungs, respectively, III was attached to a 3-way tap, q, connecting the pressure transducer, m, and syringe, n, to the AT, while IV connected the volume-cycle ventilator.

The AT had two, small glass, cup-shaped supports on each side of the inner wall. These were to support a rod, located in the rat oesophagus (section 2.2.6), to suspend the lungs horizontally. The lungs were maintained under a small residual negative pressure by removing 4ml air from the 210ml AT with syringe, n, via q. Lungs were ventilated with a volume-cycle animal ventilator (i, Fig 2.5; Modified

Palmer ventilator, London, U.K.; The original bellows and non-return valve on this ventilator were replaced by a mounted 5ml hypodermic syringe in order to displace a known volume of air in each ventilatory cycle). To initiate ventilation, the ventilator removed a known volume of air, from the AT, causing the lungs to inhale via the tracheal cannula, o. Air replacement, during the second half of the ventilator cycle, caused exhalation. During aerosol administration, o was connected to the administration apparatus (C, Fig 5.1, Chapter 5) and the ventilatory regime monitored continuously as pressure within the AT versus time by the transducer, m, attached to a calibrated pen recorder (Devices M2, Welwyn Garden City, U.K.), via q.

The volume and elasticity of the isolated lungs is subject to inter-animal variation. Calculation of tidal volumes therefore, is not straightforward. The stroke volume (SV) of the ventilator could not be assumed to equal tidal volume. Indeed, if this were the case, then at constant temperature, the pressure at y (Fig 2.4) within the AT should remain constant.

Tidal volumes were calculated by assuming the validity of Boyle's Law at fixed temperature as

$$P_1V_1 = P_2V_2 \quad (\text{Eq 1})$$

within the AT (Fig 2.4). During ventilation the pressures P_1 and P_2 were measured respectively at the start and finish of an inspiration. The volume of the AT was known to be 210ml, and thus defining

$$V_1 = (\text{volume of AT}) - (\text{lung volume})_1 \quad (\text{Eq 2})$$

and

$$V_2 = (\text{volume of AT} + \text{SV}) - (\text{lung volume})_2 \quad (\text{Eq 3}),$$

subtracting Eq 3 from Eq 2, substituting for $TV = (\text{lung volume})_2 - (\text{lung volume})_1$, and rearranging gives

$$TV = V_1 - V_2 + SV \quad (\text{Eq 4}).$$

Given that SV was known and constant in any single experiment, a solution for $(V_1 - V_2)$ would enable calculation of TV from Eq.4. Values from a pressure trace for P_1 and P_2 however, are insufficient to enable explicit solution of Eq.1 for $(V_1 - V_2)$. Values for $(\text{lung volume})_1$ however, range 3 to 5 ml, and thus V_1 ranges 205 to 207ml (Eq.2; volume of AT = 210ml). Assuming, in turn, that $V_1 = 205$ or 207ml, calculating V_2 from (P_1V_1/P_2) , where P_1 and P_2 were determined experimentally in a number of cases with $SV = 3\text{ml}$, showed that calculation of TV from Eq.4, produced values with a coefficient of variation $< 3\%$. Thus tidal volumes throughout this thesis were calculated using Eq.4, after first assuming that $V_1 = 206\text{ml}$ to enable estimation of V_2 from Eq.1 and the experimental values P_1 and P_2 .

Preliminary experiments with the new apparatus (Fig 2.5) were undertaken. The duration of viability and tolerance of the lungs, under the conditions created in the

apparatus were examined. Tests involved negative-pressure ventilation of the lungs with dry air instead of carbogen, in order to assess the need for oxygen in maintaining lung viability. This was explored to facilitate subsequent aerosol administration experiments where aerosols were to be dispersed in dry air (Chapter 5).

2.3 RESULTS AND DISCUSSION

This chapter describes the development of an isolated, perfused rat lung system and an apparatus consistent with the maintenance of its viability, enabling both dry aerosol administration and assessment of airway-to-perfusate transfer of dissolved material. Surgical procedures were described in detail in order to present a comprehensive method by which the lungs could be isolated in good, viable condition.

2.3.1 Isolation using continuous perfusion and continuous positive pressure ventilation

The surgical procedures described in section 2.2.4 were performed on 20 anaesthetised rats. Of these, 10 lung preparations were damaged during isolation, 6 became oedematous within 20 minutes and 4 within 35 minutes of pulmonary artery cannulation. Damage incurred during isolation due to careless procedure was eliminated with practice. The two major reasons causing oedema are discussed below, together with surgical modifications to eliminate the problems (points 1 and 2). Points 3 and 4 detail minor modifications aimed at prolonging the viability of the preparation.

1. Continuous positive pressure ventilation during both surgical isolation and perfusion in the upper chamber, probably helped induce lung oedema. When removed from the chest the lungs no longer benefit from thoracic compliance which helps protect against over inflation. This point was especially important because of the use of a pressure-, rather than volume-, cycle device. Due therefore, to the inter-rat variability in lung elasticity, over inflation resulted in some cases of lung damage, which was manifested as oedema. The variability in tidal volumes using a pressure-cycle ventilator would, furthermore, have proved unacceptable in future aerosol administration experiments. Although positive pressure ventilation has been used successfully in whole animal experiments, its prolonged use to ventilate isolated lung preparations has been reported to cause oedema (7, 57), although some controversy still surrounds this point (10, 53, 54). In recent years, most workers have either tended to avoid ventilation altogether (13, 15), or to use negative pressure ventilation (2, 6, 7, 37, 38) by housing the lungs in an airtight chamber and inducing inhalation or exhalation through the externalised trachea by changing the pressure within the container. Prior to the ultimate design of an "artificial thorax" to house the lungs, further experiments were performed using the apparatus shown in Fig 2.3, to assess the duration of viability using controlled positive pressure ventilation for a short period during surgical isolation, but removing such ventilation while perfusing in the upper chamber.

2. The use of unsuitable cannulae for pulmonary artery

cannulation was thought to be another source of oedema (57). It was suggested (57) that to prevent early oedema, any cannula must not contort, or strain, the artery in such a way as to cause turbulent perfusate flow. The hard-walled cannula documented in section 2.2.4 was therefore replaced by a soft-walled, hard-tipped cannula, constructed by inserting 0.75cm hard-walled tubing (800/200/200/100 Nylon tubing, Portex Ltd., Hythe, U.K.) into the end of 12cm soft-walled tubing (0.2cm bore, 0.1cm wall thickness, Esco(Rubber) Ltd., Twickenham, U.K.). The hard tip of the cannula could be inserted into the artery and clipped, or tied, in place, without the cannula walls collapsing and occluding flow. Moreover, the flexible, soft-walled, portion, hung vertically from the artery, when the lungs were suspended, without contorting the vessel in relation to the isolated preparation. The cannula was tied, rather than clipped, in place to a) prevent perfusate leakage and b) reduce the weight (and strain) of the cannula when the lungs were suspended.

3. In order to isolate the lungs without ventilation, it was necessary to open the chest, cannulate the pulmonary artery, and perfuse the lungs before tracheotomy was performed. If tracheotomy was performed first, the animal was without ventilation or perfusion for a substantial period during the operation; this gave rise to the formation of emboli in the lung vasculature, making them impossible to clear of blood by subsequent perfusion.

4. It had been suggested (57), that continuous perfusion during surgery may have been unnecessary and that

clearance of blood from the lungs may be achievable by limited perfusion with only 20ml Kreb's Ringer bicarbonate solution (KRB), immediately after cannulation of the pulmonary artery. This simpler method of lung clearance was adopted to reduce total operation time in some experiments.

2.3.2 Isolation in the absence of ventilation and continuous perfusion

Modifications described under points 1 to 4 above, were employed in procedures described in section 2.2.5. Of the 15 experiments performed, ventilation was attempted in only 3. Of the 12 unventilated preparations, 3 became oedematous almost immediately, while 9 remained viable for 60 to 120 minutes. In 3 experiments where positive pressure ventilation was employed, almost immediate oedema resulted. A number of hypotheses were advanced to explain the variability of lung viability. These suggested surgical modifications to improve the quality of the preparation, although some changes were made to enable aerosol administration.

1. In all cases in these experiments, the lungs were incompletely cleared of blood. This was undesirable and variable. Emboli in lung vasculature may impair perfusate flow to certain parts of the lung, not only reducing duration of lung viability, but also making viability variable and dependent upon the number and distribution of the emboli. Several methods were explored with the aim of achieving reproducible and complete lung clearance^{of blood} KRB at

37°C was employed for the limited lung perfusion and showed no improvement in clearance versus KRB at 20°C. Similarly, no improvement was noted when K4 at 37°C was substituted for KRB. Carefully controlled positive pressure ventilation was re-introduced during surgery alone. This, together with limited perfusion with warm K4, brought about marked improvements in lung clearance but with variable results. Continuous perfusion with K4 at 37°C was therefore re-employed in conjunction with limited positive pressure ventilation during surgery. This technique was successful and reproducibly blanched the lungs. It was adopted for all subsequent experiments.

2. Three attempts to ventilate isolated lungs in the upper chamber (Fig. 2.3) using positive pressure failed. In each case the lungs became almost immediately oedematous. An airtight lung chamber, similar to that designed by Niemeier and Bingham (7) was designed. The use of such a chamber to house the preparation however, meant that some changes had to be made to the surgical procedures. Because perfusate could no longer simply drip, from the heart in the upper chamber, to the reservoir, once the upper chamber was sealed, the left ventricle of the heart had to be cannulated to allow perfusate flow from the lungs to the reservoir. This was achieved by connecting the ventricular cannula to a stainless steel cannula, piercing one of the rubber bungs sealing the upper chamber. These modifications are described in detail in section 2.2.6.

To improve the likelihood of success in future aerosol administration studies, two further changes were made to the

surgical procedures:

3. The nylon tracheal cannulae used in sections 2.2.4 and 2.2.5 was replaced by a stainless steel cannula preferred, because this could maintain its shape when an upper seal (V; Fig 2.4) was tightened around it and it could be used in all subsequent experiments. Variability in tracheal cannulae could affect aerosol deposition in the respiratory tract.

4. The lungs were suspended horizontally rather than vertically. In isolated lung-preparation studies by other workers, the lungs were often suspended vertically by the trachea. Such treatment causes the trachea to stretch under the weight of the preparation, a phenomenon which is subject to some variability. Although this is probably unimportant in metabolic and accumulation studies (1 - 17) or in studies of absorption from the lungs following solution instillation (19, 21, 23, 28 - 35), it is clearly unacceptable if aerosols are to be administered. The lungs were therefore suspended horizontally by a rod passing through the oesophagus, supported at either end by two, glass U-shaped cups on the internal wall of the upper chamber.

Problems associated with surgical procedures described in section 2.2.5 have been discussed above in points 1 to 4. The suggested modifications were introduced into the procedures described in section 2.2.6.

2.3.3 Isolation using a short period of positive pressure ventilation and continuous perfusion

Using these modifications, viability of the isolated, perfused rat lungs could be reproducibly maintained between 3 and 3.5 hours. This period was subsequently found adequate to permit the study of the transfer of the marker (fluorescein) from airways to perfusate, following intratracheal administration of dry aerosols (Chapter 5).

Lung ventilation, by application of negative pressures to the artificial thorax (Fig 2.4) was attempted for periods of up to 40 min, with, apparently, no detrimental effects (see "assessment of viability", section 2.2.3). The stainless steel tracheal cannula proved suitable for aerosol administration since it maintained constant shape when the seal was tightened around it (V; Fig 2.4). Fluorescein deposited in this cannula during administration could be quantified easily by washing and the cannula re-used.

Lung suspension horizontally in this AT required temporary disconnection of perfusate flow in order that flow could be re-directed through the stainless steel cannula passing through seal I (Fig 2.4). Perfusate flow was then re-connected to the pulmonary artery cannula. The period without flow was approximately 30 seconds and, providing no air was introduced into the circulation on re-connection, no adverse effects were observed.

Surgical procedures described in section 2.2.6 were employed successfully in the isolation and perfusion of rat lungs. Ventilation was possible with retention of viability.

These procedures were therefore adopted and used in subsequent aerosol administration studies.

2.3.4 Pulmonary oedema

Pulmonary oedema has been widely reported in literature concerning isolated lung preparations. Attempts have been made to quantify (12, 53, 54) and qualify the phenomenon. These methods were found to be either unreliable or unsuitable in the studies reported here. For example, Bassett and Fisher (53), suggested dry to wet weight ratios lower than 0.16 were indicative of oedema. Table 2.1 however, shows that measurement of this ratio in these investigations proved pointless. Consider for example, experiment 1 (Table 2.1) where the preparation was clearly oedematous but the ratio was 0.19. Conversely, in experiment 2, the ratio was 0.11, while the preparation appeared non-oedematous. Both observations contradict the findings of Bassett and Fisher.

Attempts to qualify and quantify oedema by estimation of potassium efflux (59) or histological examination of perfused and non-perfused tissue by electron microscopy (17, 59) however, were unsuitable in these studies, due to the need to assay the preparation at the end of an experiment for total retained aerosol. These techniques, from the literature, provide dubious information and would preclude the required analysis.

Because pulmonary oedema is such a problem in the isolated, perfused rat lung preparation, a brief summary of

points, which help guard against this phenomenon, is included here, for the benefit of the prospective worker in this area.

1. Keep operation time to a minimum and maintain lung temperature and moisture throughout isolation by bathing with warm saline.
2. Avoid all contact with the lungs.
3. Never pull or stretch the lungs and take special care when removing connective tissue during isolation.
4. Keep breaks in perfusion below 1min in duration and ensure that no air bubbles are introduced when disconnecting and re-connecting cannulae and tubing.
5. Perfuse with aerated Kreb's Ringer bicarbonate solution with 4%w/v bovine serum albumin at 37°C.
6. Use soft-walled, hard-tipped cannulae for cannulation of right and left sides of the heart.
7. Ensure the absence of air bubbles prior to perfusion.
8. Maintain the isolated lungs in a humid environment.
9. Maintain a small residual volume of air (approximately 1ml) within the lungs, to prevent their collapse.
10. Never over-inflate the lungs. One sigh, or large inspiration (approximately 3ml), is useful however, to promote even ventilation.

2.3.5 An apparatus designed for the isolated, perfused rat lung preparation receiving positive pressure ventilation

The first apparatus (Fig 2.3) was designed in an attempt to satisfy criteria 1 to 6 (section 2.1). It was

assessed using 15 isolated, perfused rat lung preparations, prepared according to section 2.2.5. Of these 15, three became oedematous almost immediately, 9 remained viable for between 60 and 120min and the remainder (3) became oedematous subsequent to initiating positive pressure ventilation in the upper chamber.

The apparatus fulfilled criteria 4,5 and 6 (section 2.1). Constant rate perfusion could be maintained and varied between 5 and 20 ml min⁻¹, without detrimental effect to the preparation. It has been reported (60), that perfusate flow rate may affect the rate of solute transfer from airway-to-perfusate. A rate of 15ml min⁻¹ was therefore selected with the aim of combining a reasonable transfer rate with maintenance of lung viability. In all experiments, pump rate had to be increased periodically, to compensate for decrease in flow, due to increasing resistance in the pulmonary circulation. If the pump was not adjusted, then flow decreased by approximately 3ml min⁻¹, to 12ml min⁻¹, between 90 and 180min perfusion. In the period 0 to 90min perfusion however, flow was effectively constant.

The peristaltic pump re-circulated perfusate through the system and the perfusate reservoir was an ideal design for sampling. Magnetic stirring ensured homogeneous mixing within 30sec of the administration of a bolus injection of fluorescein to the reservoir.

This apparatus (Fig 2.3) failed to satisfy criteria 1,2 and 3 (section 2.1) due to a variety of factors. These are discussed below:

1. Perfusate temperature fell by 10°C between the pump (h)

and the upper chamber (b).

2. The membrane of the oxygen electrode was rapidly poisoned by circulating perfusate (and possibly endogenous lung residues) causing false, low levels of oxygen to be recorded.

3. Total perfusate volume decreased during each experiment due to evaporation.

4. Positive pressure lung ventilation using a pressure-cycle ventilator resulted in both pulmonary oedema and unreliable ventilatory regimes (section 2.3.1.1)

These problems were overcome by employing the revised apparatus design shown in Fig 2.5. Alphabetical characters in the following discussion all refer to this figure:

i) A heating coil (a) was included between the perfusate pump and the upper chamber, to ensure that perfusate entering the lung was at 37°C.

ii) A filter (f) was placed, in line, between the reservoir (c) and the oxygen electrode (g), to prevent electrode "poisoning" by insoluble circulating residues. The filter and electrode were left in place, only until the pO_2 of the perfusate had risen above 400mm Hg. These two pieces of equipment were then removed from the system and pO_2 maintained by constant perfusate aeration, monitored by flowmeter (j). This manoeuvre was essential for the further reason that the electrode and filter often introduced, oedema-inducing, air bubbles. Their removal therefore, was effected prior to lung perfusion, after stabilisation of oxygen tension.

iii) To avoid decreasing perfusate volume due to

evaporation, the bottom reservoir was re-designed to include a narrow-bore side-arm (p). The height of the perfusate in this side-arm was maintained constant by periodic additions of double-distilled water (DDW) (61).

iv) The upper chamber was replaced by an airtight, "artificial thorax" (AT) (Fig 2.4). A volume-, rather than pressure-, cycle ventilator permitted negative pressure changes in the AT (section 2.2.6). Ventilatory regimes could be easily altered in terms of respiratory frequency and tidal volume. Thus, positive-pressure ventilation induced oedema was avoided and, the more normal manoeuvre of aerosol inspiration, rather than administration by forced inflation, made possible.

2.3.6 An apparatus for the isolated, perfused rat lung preparation receiving negative pressure ventilation

The modifications detailed above were included in the apparatus re-design which is described in section 2.2.8 and shown in Fig 2.5 and Plate 10. It supported lung viability for 3 to 3.5 hours, after preparation according to section 2.2.6. This duration of viability was considered sufficient for aerosol investigations (see section 2.3.3). Lungs were subjected to negative pressure ventilation with dry air for periods of up to 40min without suffering damage (62). The addition of the heating coil (a, Fig 2.5) successfully held the perfusate temperature at 37°C for flow rates of 5 to 20ml min⁻¹. Perfusate volume could be maintained in the reservoir, throughout the whole experimental period, at

200+1ml, by the periodic addition of small volumes of DDW to hold levels in the side-arm (p, Fig 2.5) constant. This modified apparatus (Fig 2.5) fulfilled all criteria described in section 2.1 (1 to 6) and was used to house, ventilate and support the viability of all lung preparations employed in the aerosol administration studies described in subsequent chapters of this thesis.

TABLE 2.1

Dry-to-wet weight lung ratios and their lack of correlation with oedema (see text, section 2.3.4)

```
*****
Experiment      Dry/wet weight ratio      Condition
*****
```

1	0.19	oedematous
2	0.11	non-oedematous
3	0.17	non-oedematous
4	0.09	oedematous

```
*****
```

FIGURE 2.1

Rat neck, ventral-side uppermost, displaying sterno-hyoid muscle (-----incision), which overlies the right and left carotid arteries.

- a sterno-hyoid muscle
- b sub-clavical vein
- c trachea
- d external jugular vein

FIGURE 2.1

Head

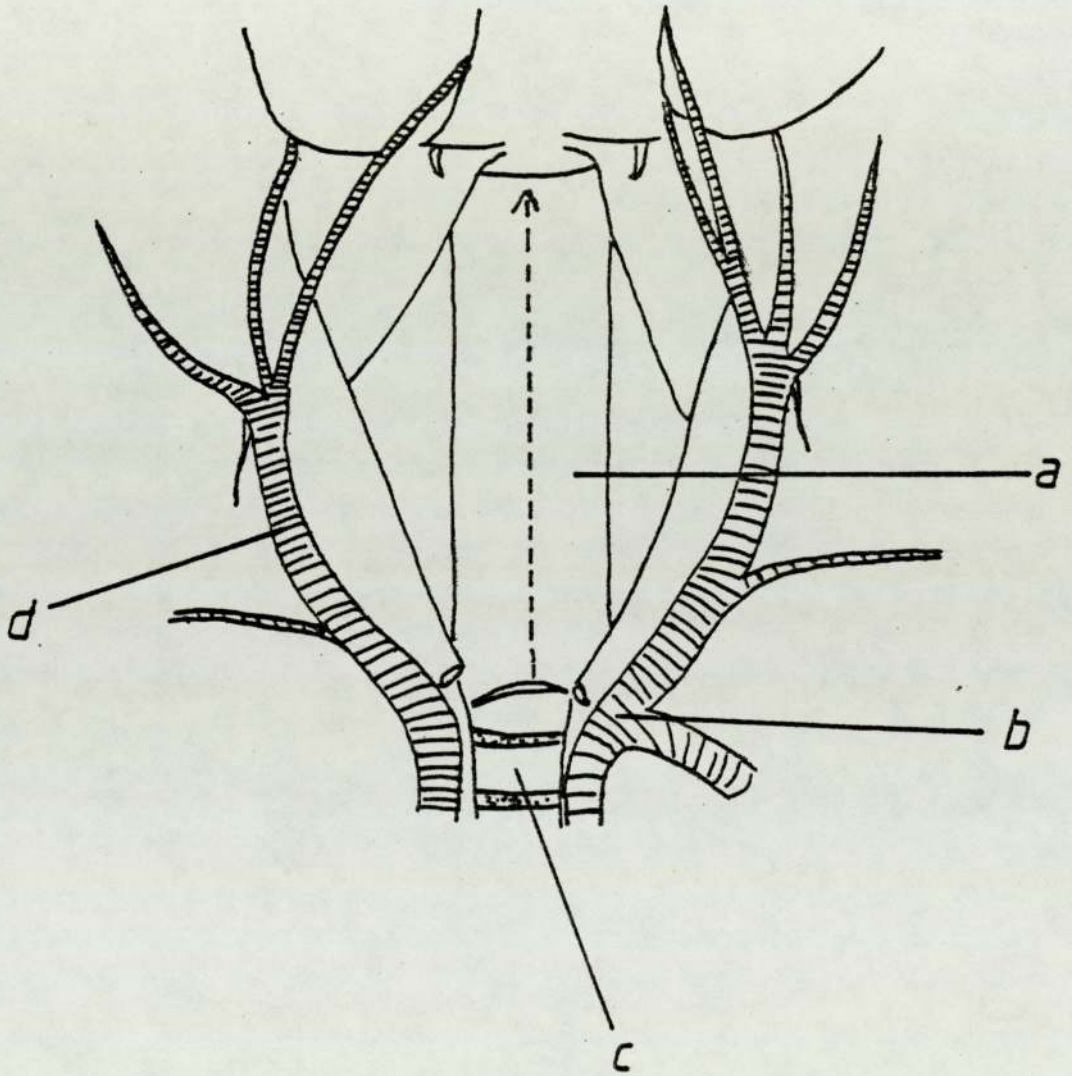


FIGURE 2.2

Exposed and cannulated rat trachea.

- a thyroid gland
- b right common carotid artery
- c tracheal cannula
- d incision in trachea
- e suture securing tracheal cannula
- f aorta
- g left common carotid artery
- h tracheal cartilage ring

FIGURE 2.2

Head

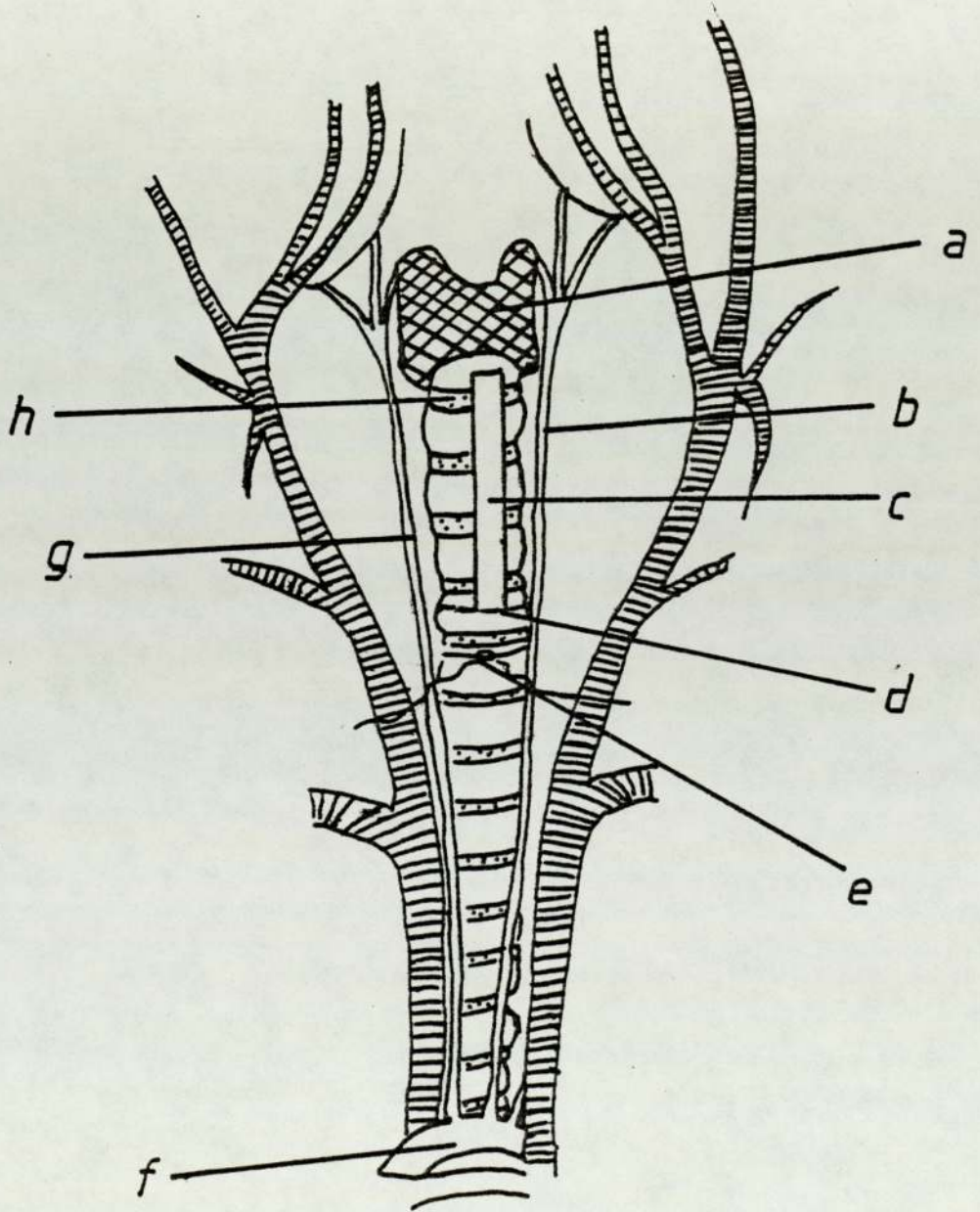
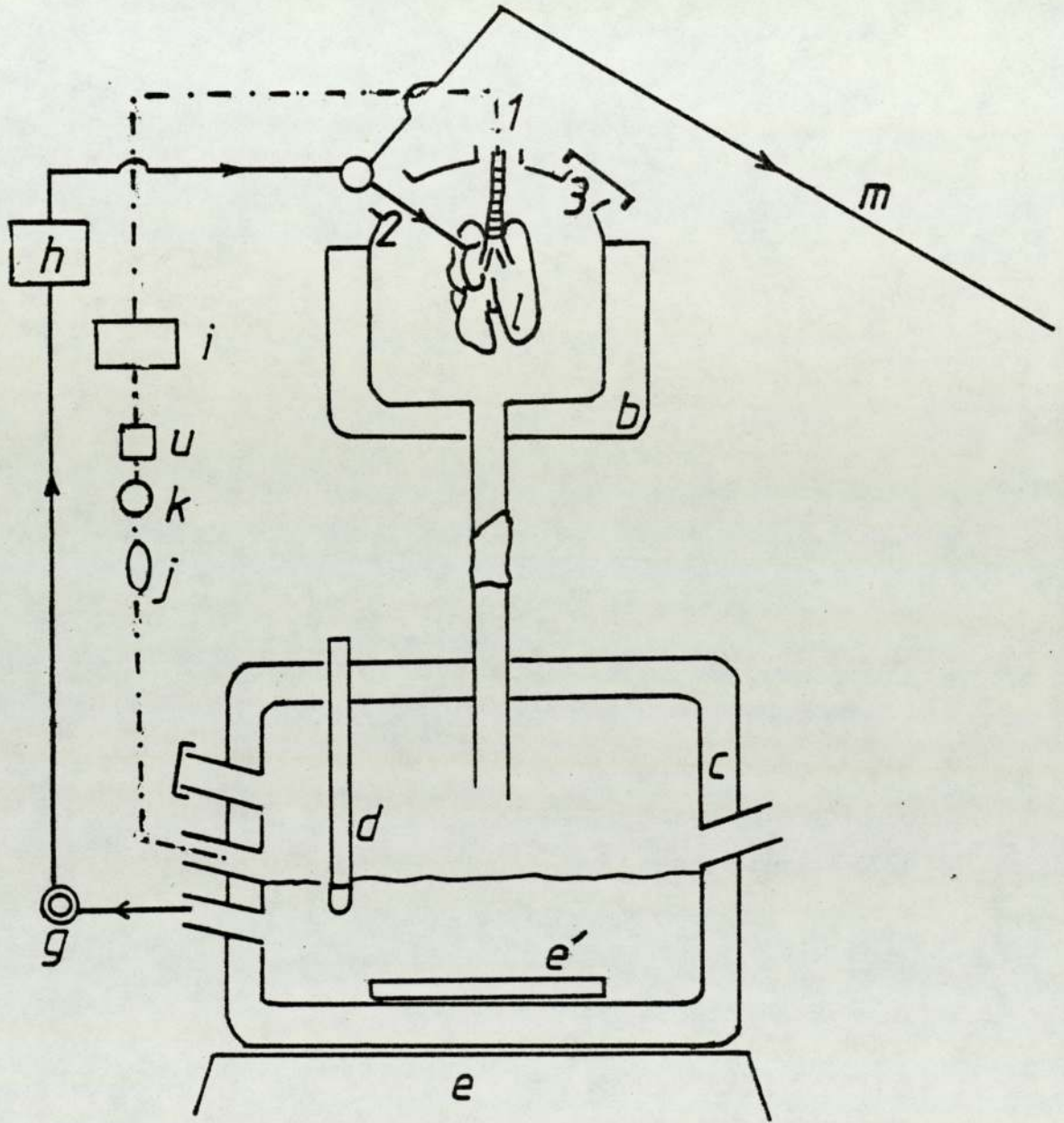


FIGURE 2.3

Apparatus for the isolated, perfused rat lung preparation receiving positive pressure ventilation.

- b upper chamber to house lungs
- c perfusate reservoir
- d pH meter electrode
- e magnetic stirrer
- e' magnetic flea
- g oxygen electrode
- h perfusate pump
- i positive-pressure ventilator (SRI, No 5056)
- j flow meter
- k flow regulator
- l lungs
- m removable extension tube
- u carbogen supply
- 1,2+3 see text p.22

FIGURE 2.3



→ *perfusate flow*

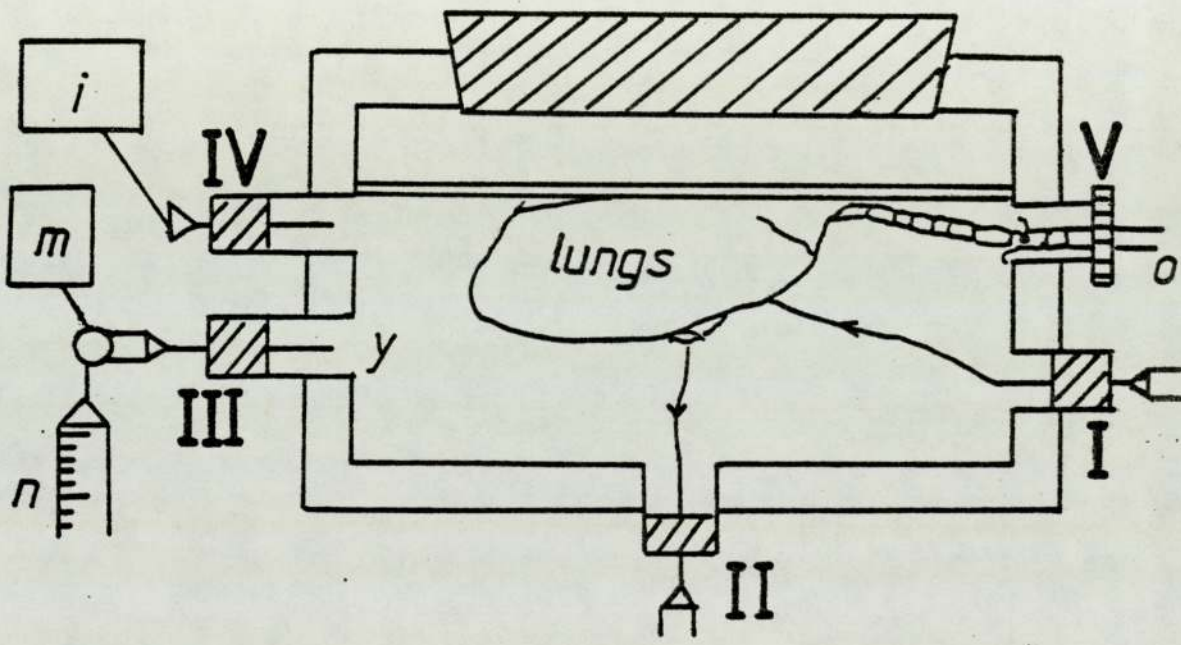
----- *carbogen flow*

FIGURE 2.4

The artificial thorax apparatus for the isolated, perfused rat lung preparation receiving negative pressure ventilation

- I,II,III,IV stainless steel cannulae
- I: perfusate supply to isolated lungs via pulmonary artery
- II: perfusate return to reservoir
- III: attached to 3-way tap, q, connecting pressure transducer, m, and syringe, n, to artificial thorax
- IV: ventilator connection to artificial thorax
- V: airtight seal around tracheal cannula, o.
- i volume cycle ventilator
- m pressure transducer
- q 3-way tap
- n syringe
- o tracheal cannula

FIGURE 2.4



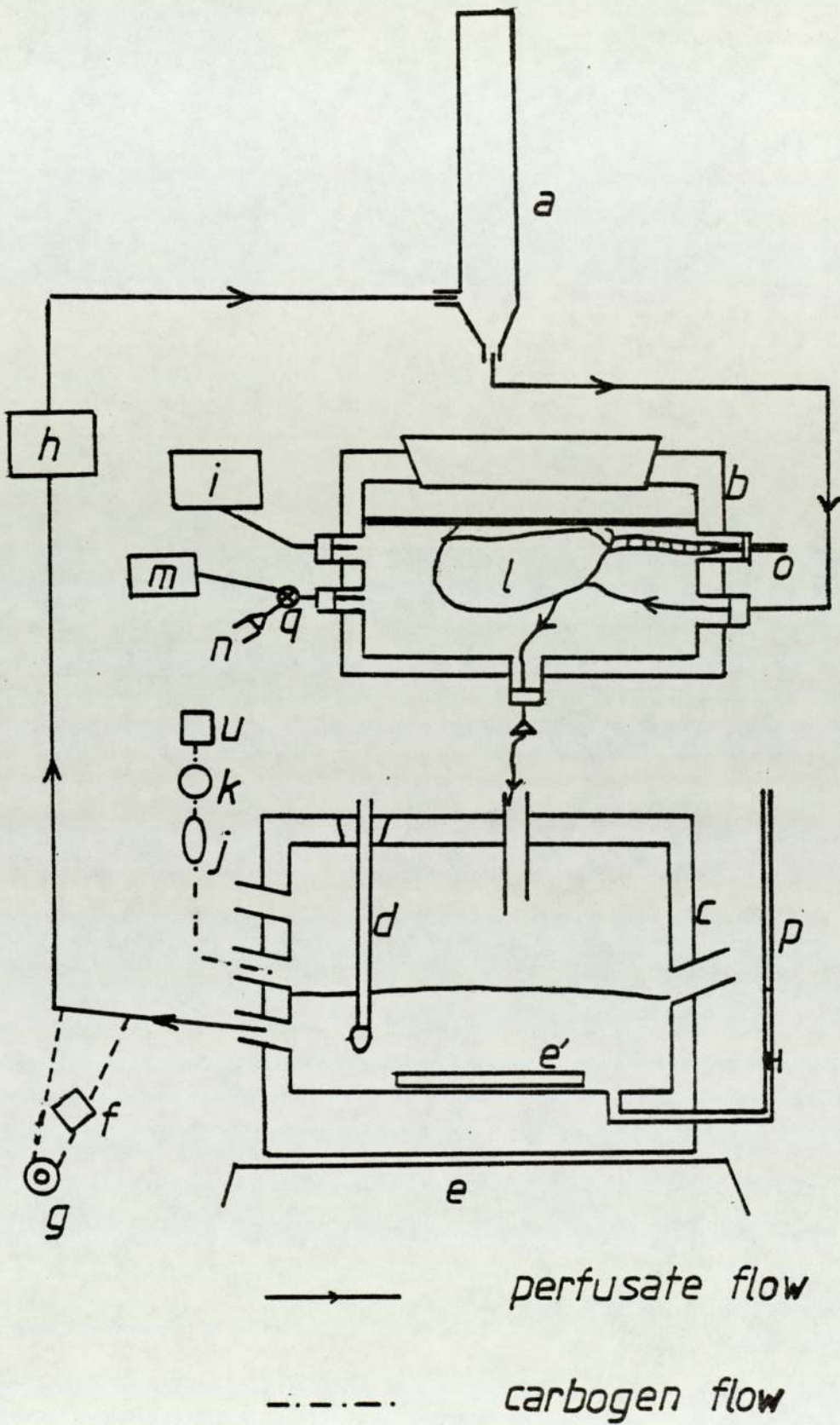
 *perfusate flow*

FIGURE 2.5

Apparatus for the isolated, perfused rat lung preparation receiving negative pressure ventilation.

- a heating coil
- b artificial thorax
- c perfusate reservoir
- d pH meter electrode
- e magnetic stirrer
- e' magnetic flea
- f filter
- g oxygen electrode
- h perfusate pump
- i volume-cycle ventilator
- j flow meter
- k flow regulator
- l isolated lungs
- m pressure transducer
- n syringe
- o tracheal cannula
- p narrow-bore reservoir side-arm
- q 3-way tap
- u carbogen supply

FIGURE 2.5



CHAPTER THREE

DISODIUM FLUORESCEIN - MARKER COMPOUND FOR ABSORPTION STUDIES IN THE RAT LUNG

3.1 INTRODUCTION

This chapter describes preliminary investigations involving:

1. Analysis of disodium fluorescein powder and development of an assay for its dianion in perfusate solutions.
2. Airway - to - perfusate transfer studies following intratracheal instillation of disodium fluorescein solutions to the isolated, perfused rat lung preparation.
3. Experiments to determine the source and magnitude of fluorescein losses in the system.
4. Development of a kinetic scheme to describe fluorescein transfer to the vasculature.

Fluorescein (I, Fig 3.1) is a weak dibasic acid, poorly soluble in water, and is thus, generally employed, as its disodium salt. Disodium fluorescein (II, Fig 3.1) is freely soluble in water. It possesses a characteristically intense fluorescence in neutral or basic solutions and can

be detected at concentrations as low as 1pg ml^{-1} (63). The salt shows no sign of degradation, in terms of loss of fluorescence, if stored under appropriate conditions. The powder, which is hygroscopic, should be stored in dessicators over silica gel and protected from light; solutions may be stored at room temperature (20°C), but kept in the dark.

Because the disodium salt is difficult to obtain in a pure state, this chapter reports the purity of the material used in these investigations. In order to study the transfer of the dianion (III, Fig 3.1) in the rat lung preparation (Chapter 2), a fluorimetric assay was developed for III in K4. Previous workers (66) had established that maximum fluorescence of III in pH 12 Sorensen's glycine buffer (64) occurred at excitation and emission wavelengths of 486 and 516nm respectively, using an Aminco-Bowman Type 4-8202 fluorimeter (American Instrument Co. Inc.). Using the same instrument, these wavelengths were found suitable for the assay of III in K4.

Investigations involving the intratracheal instillation of aqueous solutions of II to the isolated rat lung were performed to:

- i. ensure that the preparation developed in Chapter 2 was suitable for airway-to-perfusate transfer studies of compounds administered to the respiratory tract.
- ii. determine whether fluorescein was readily transferred.
- iii. determine the recoverable fraction of a known administered dose.

During ^{later} aerosol ⁿⁱ administration, unlike the instillation of a

known dose, known volumes of a given aerosol concentration would be inhaled. An unknown quantity of the aerosol however, would be exhaled. It was essential therefore, in these preliminary studies, in order to be able to state the retained dose of an aerosol, to establish mass-balance and account for 100% of the intratracheal dose of the administered compound. In this way, the mass of fluorescein recovered would equal the amount deposited after aerosol administration.

Initial experiments involved intratracheal instillation of known quantities of disodium fluorescein in solution, in order to determine the rate and extent of airway-to-perfusate transfer. Subsequent control experiments are described to document fluorescein losses to glassware and tubing. Because accumulation and metabolism of compounds by the lung has been documented (1 - 5, 17, 37, 38), and fluorescein conjugation by the lung reported (36, 65), some experiments are described to determine the extent and significance of loss due to binding or metabolism. The outcome of these experiments enabled a simple kinetic scheme to be developed to describe fluorescein transfer from airways-to-perfusate.

3.2 MATERIALS AND METHODS

3.2.1 Fluorescein analysis

Sections 3.2.1.1 and 3.2.1.2 detail the analysis of disodium fluorescein powder and the development of an assay for III in K4. Section 3.2.1.3 describes a general method of analysis for III in rat lung perfusate.

3.2.1.1 Analysis of disodium fluorescein powder

I am grateful for the assistance of I.C.I. Pharmaceuticals Analytical Division (Macclesfield, U.K.) for their elemental analysis of the disodium fluorescein powder (Koch-Light Laboratories, Colnbrook, U.K.) used in these studies. I must also thank Dr. A. R. Rees (Dept. Pharmacy, University of Aston in Birmingham, U.K.) for determination of III in different batches of II (Fig 3.1) by titration and fluorimetry. Results of these analyses are presented in section 3.3.1.

3.2.1.2 Determination of III in K4

A rectilinear relationship between fluorescent intensity and concentration of III in pH 12 Sorensen's

glycine buffer (pH 12 SGB), over the range 2 to 63 ng ml⁻¹, had previously been observed (66). To determine whether a similar relationship existed for III in K4, over the range 1 to 100 ng ml⁻¹, calibration curves were constructed for a series of III concentrations in both pH 12 SGB and K4, as described below.

Alkalinisation of pH 7.4 K4 to pH 12 was effected by addition of a small volume (<3%v/v) of 2M NaOH. The solution was centrifuged at 38000g (MSE high speed refrigerated centrifuge, Scientific Equipment Ltd., Crawley, U.K.) for 30mins, the supernate withdrawn and the white precipitate, formed by addition of the alkali, discarded. Fluorescein solutions were then prepared containing 1 to 100ng ml⁻¹ III in (a) pH 12 SGB and (b) pH 12 K4 supernatant (pH 12 K4). Calibration curves of relative fluorescent intensity (RI) versus anion concentration,

$$RI = T_s/T_r \quad (\text{Eq 3.1})$$

were constructed for systems (a) and (b) where T is fluorescent intensity and subscripts s and r refer to sample and reference or standard solution, respectively. Reference solutions in this instance contained 10ng ml⁻¹ III in pH 12 SGB or pH 12 K4, as appropriate. The fluorimeter (Aminco-Bowman Type 4802-2) was adjusted to read zero using the appropriate blank solution, without fluorescein. The assay employed excitation and emission wavelengths of 486 and 516nm, respectively, and was performed in 1cm path length, matched silica cuvettes (Hellma, Westcliffe-on-sea,

U.K.).

The loss of III to the precipitate, after alkalisation and centrifugation of K4, was determined in an additional experiment. A small volume of fluorescein solution (100ng ml^{-1} in K4) was alkalised to pH 12 with 2M NaOH. The precipitate was removed by spinning at $38000g$ for 30min and supernatant dilutions performed in pH 12 K4 to yield solutions containing ideally, 1 to 100ng ml^{-1} , III. The 10ng ml^{-1} standard, was prepared as for (b) above, by dilution of a non-alkalised III solution in pH 12 K4. The loss of fluorescein to the precipitate was assessed by comparison of the resultant calibration curve and those from systems (a) and (b) above, with the theoretical, ideal calibration curve (continuous line, Fig 3.2).

3.2.1.3 General method of assay for III in rat lung perfusate

Perfusate (K4 which has passed through the rat lung preparation) samples were collected after either intratracheal instillation of an aqueous solution of II or inhalation of II by the lungs. Samples (1.5ml) were alkalised by the addition of $30\mu\text{l}$ 2M NaOH. The samples were shaken and centrifuged at $9980g$ (Eppendorf Type 5412 centrifuge, Hamburg, Germany) for 5min. Supernatants were diluted with pH 12 Krebs Ringer supernatant (pH 12 KRB; prepared similarly to pH 12 K4 but without bovine serum albumin) and assayed for III against standard and blank solutions containing appropriate concentrations of bovine

serum albumin. Sample dilution was performed to achieve III concentrations ranging 1.0 to 60.0ng ml⁻¹. Concentration of III was calculated according to Eq 3.2 (section 3.3.2), based on the calibration curve Fig 3.2, after determination of T_e and T_r as documented previously (section 3.2.1.2)

3.2.2 Airway-to-perfusate transfer following intratracheal instillation of disodium fluorescein solution

Using surgical procedures described in Chapter 2 (section 2.2.5) and the apparatus in Fig 2.3, the isolated rat lungs (iprl) were suspended by the trachea in the upper chamber. Perfusion at 15ml min⁻¹ was initiated, and the lungs allowed to equilibrate for 10min. A 5ml blank perfusate sample was withdrawn, and replaced by 5ml fresh K4. One hundred microlitres of II solution (approximately 60ug, accurately known) was instilled into the trachea. A connector attached to the pressure-cycle ventilator was pushed into the tracheal cannula and the lungs made to expand 5 times with an approximate tidal volume = 2ml. This manoeuvre forced the administered fluorescein to the lower airways. No fluorescein was found subsequently, in the washings from the ventilator connector although allowance had to be made for material, not delivered to the lungs, which remained in the tracheal cannula.

The perfusate was sequentially sampled over the 60min time course of the experiment, each sample being replaced by an equal volume of K4. Samples were stored overnight at 3°C. At the end of perfusion the rat lungs were removed from the

upper chamber (Fig 2.3) and ground in a pestle and mortar with 8g of washed sand (B.D.H. Laboratory Chemical Division, Poole, U.K.). Forty ml 2M NaOH were added, the homogenate shaken and stored overnight, at 3°C. The whole apparatus, plus the tracheal cannula, were washed with DDW and the washings stored prior to assay. This experiment was performed in duplicate.

Assays for III were performed as follows: Perfusate samples were treated as described in section 3.2.1.3 and, together with cannulae and apparatus washings, diluted with pH 12 KRB and assayed fluorimetrically. Lung homogenates were shaken and 2 x 2ml samples centrifuged at 9980g for 30min. Supernatants were diluted 1 in 3 in pH 12 KRB and assayed for III against appropriate standard and blank solutions (containing the same concentration of bovine serum albumin as the diluted perfusate samples).

3.2.3 Control experiments to determine loss of fluorescein to the system

3.2.3.1 Loss of fluorescein to sand Fluorescein, in known amounts, 10 to 60ug in 0.1ml aqueous solution, was instilled into 8g sand (as used during lung homogenisation). Sand and fluorescein solution were thoroughly mixed with 40ml 2M NaOH and allowed to stand overnight at 3°C.

3.2.3.2 Loss of fluorescein to apparatus Fluorescein, in known amounts, 15 and 1000ug in 0.1ml, was delivered by bolus injection to different 200ml quantities of K4 in the

perfusate reservoir (c, Fig 2.3). In each case, the perfusate was mixed and circulated through the apparatus (identical to that described in section 3.2.2 but without lungs). Perfusate samples were taken as described in section 3.2.2, assayed and any loss of fluorescein to the apparatus recorded.

This experiment was repeated after first siliconising all apparatus, as described by other workers (6, 7) with 2% dimethyl dichlorosilane in 1,1,1 trichloroethane (B.D.H. Laboratory Chemicals Division, Poole, U.K.) to determine the effects of siliconisation.

3.2.3.3 Loss of fluorescein due to binding and metabolism by the lung

(a)Binding To examine the possibility of irreversible binding of fluorescein to the preparation, a number of lungs were cleared of blood and isolated (Chapter 2, section 2.2.5). Known amounts of fluorescein, 3 to 60ug in 0.1ml, were instilled into the trachea and forced to the lower airways (section 3.2.2). The preparation was not perfused after delivery of II solution. Each experiment was duplicated. Assay for III was performed according to the method described in section 3.2.2, after storage at 3°C overnight, in order to determine recoverable material.

(b)Conjugation The presence of fluorescein monoglucuronide in lung and perfusate samples taken from experiments described in section 3.2.2 was investigated. Samples were

treated with the enzyme β -glucuronidase (Sigma Chemical Co., St Louis, U.S.A.) using the method described by Chen et al (67). The enzyme cleaves glucuronidated fluorescein, regenerating the parent compound, which was determined fluorimetrically after sample treatment.

(c) Metabolism The absence of significant fluorescein metabolism, in the studies described in this thesis, was documented after analysis of data collected in the aerosol administration experiments described in Chapter 5. The method of data analysis and some necessary background material will be presented here.

Transfer of fluorescein from airways-to-perfusate is usually reported in Chapter 5 as fractional, f_t , rather than absolute (mass) transfer. In all aerosol administration experiments, using respiratory frequencies = 28 and 14 cycles min^{-1} , fractional transfer plateaued approximately 70min after administration commenced (see Figs 5.2 to 5.12) at values ranging 0.358 to 0.745, dependent upon aerosol particle size and respiratory regime. Other workers, using isolated, perfused rat lung preparations maintained similarly to those described in section 2.2.6, document the maintenance of enzyme activity in their preparations for periods >150min (5 - 7, 90). It follows therefore, that if significant fluorescein metabolism were occurring, values for f_t (proportional to perfusate concentration) should fall with increasing time, after 70min had elapsed. Cases of significant and insignificant metabolism are shown schematically in Fig 3.3.

To test for fluorescein metabolism, the variation in the data for f_t (time, $t > 70\text{min}$) from 10 different aerosol experiments (Tables A1 - A6, A12, A14, A16, A18) was determined after first normalising each value of f_t for $t > 70\text{min}$ by dividing by the average value of f_t ($t > 70\text{min}$) from that particular experiment $((f_{t1} + f_{t2} + \dots + f_{tn})/n)$. Clearly, if there was no data variation around a given plateau, then each "normalised" value for f_t would be unity (1). Because each determination of f_t however, was associated with some error, normalised values ranged above and below 1. The randomness of these deviations about unity (normalised f_t) was considered as a function of time ($t > 70\text{mins}$) for the ten experiments.

3.2.4 Fluorescein transfer

In experiments where fluorescein was administered to the perfusate, there were no reductions in perfusate concentration, other than those which could be accounted for as "losses to the apparatus" (section 3.3.4.2). In order to investigate the reversibility of fluorescein transfer in this system therefore, an experiment was designed to maximise possible transfer from the perfusate to the lung by reducing the volume of the donor-solution and increasing the potential binding areas of the lung, while minimising losses to the apparatus by reducing available surface area). Three solutions of K4 (pH = 7.35 to 7.4 were prepared with fluorescein concentrations $\sim 30, 60$ and 4000ng ml^{-1} . Six rat lungs were isolated using the method described

in section 2.2.5. Each lung was lead weighted, to prevent it floating, and placed in 1 of 6, siliconised glass flasks. The fluorescein solutions in K4 were added (flasks 1 and 2, $\sim 30\text{ng ml}^{-1}$; 3 and 4, $\sim 60\text{ng ml}^{-1}$; 5 and 6, $\sim 4000\text{ng ml}^{-1}$) to produce a total volume of 50ml in each flask. Three control flasks, containing fluorescein solution of each concentration, lead weight, but no lungs, were established for comparative purposes. The nine flasks were sealed and shaken in a water bath, in the dark, for 24hr at 37°C. Samples withdrawn at 12 and 24hr were assayed for III fluorimetrically.

3.3 RESULTS AND DISCUSSION

3.3.1 Analysis of disodium fluorescein powder

This section contains pertinent results, from the analysis of II used in these investigations, which were provided by ICI Pharmaceutical Division, Macclesfield, U.K. and Dr A. R. Rees, University of Aston.

Water content of the hygroscopic (68), powdered II ranged 11.9 to 21.6%w/w (Table 3.1), and varied, not only between different batches of disodium fluorescein, but also between different bottles from the same batch. Sodium content, determined experimentally in the batches analysed, was greater than theory predicted. Conversely, theoretical carbon content, was greater than that determined experimentally (Table 3.2), implying some inorganic contamination. After correction for water content, the percent purity of each batch of disodium fluorescein used in these investigations was determined. Titration of the phenolic hydroxyl^{group} (Fig 3.1) for one batch, and subsequent fluorimetry versus a reference solution from the^{same} batch gave values for purity >96% (Table 3.3, ranging through 100%). Concentrations and quantities of fluorescein quoted throughout this thesis therefore, are corrected for water content only and, unless stated otherwise, are expressed as the anhydrous dianion,

III (Fig 3.1).

3.3.2 Determination of III in K4

Figure 3.2 shows calibration curves for fluorescein in pH 12 SGB (\diamond) and pH 12 K4 (X). Calibration curves were identical when the method described in section 3.2.1.2 was employed using identical standard solution concentrations, showing that the supernatant of K4, after adjustment to pH 12 and spinning, did not interfere with the assay for III developed previously. The solid line represents the theoretical (ideal) calibration curve for the fluorescein standard used (10ng ml^{-1} , III). All calibration curves were rectilinear over the studied range. Subsequently therefore, concentrations of III in pH 12 K4 were calculated from

Unknown concentration = RI x Standard concentration (Eq 3.2)

The assay was accurate to $\pm 5\%$ for concentrations $>1\text{ng ml}^{-1}$ in pH 12 SGB and pH 12 K4.

Figure 3.2 also presents the calibration data for fluorescein added to K4 prior to alkalisation and centrifugation. The fact that this data is indistinguishable from the last, where fluorescein was added after centrifugation, shows insignificant fluorescein loss to the precipitate. Thus, there were no problems introduced to the general assay method due to the presence of bovine serum albumin (provided the standard solution possessed a similar concentration) or precipitation on sample alkalisation.

The method of analysis had a number of advantages. It was accurate and reliable and did not require extraction or purification of biological samples. The sensitivity of the assay was comparable with those employing other methods of fluorescein determination (69) incorporating extraction procedures - involving inevitable loss of fluorescein from the samples.

3.3.3 Airway-to-perfusate transfer following intratracheal instillation of disodium fluorescein solution

The duplicate experiments described in section 3.2.2 provided results representative of several similar experiments which showed that fluorescein was readily transferred from the airways to the perfusate following intratracheal instillation of aqueous II solutions. The transfer profiles, amount III transferred and fraction transferred versus time, for the two experiments described, are shown in Fig 3.4 and 3.5 respectively. The original data is presented in Table 3.4 and the data for fractional transference in Table 3.5. The actual amount of III deposited in the lungs in each experiment was considerably less than the ~60ug delivered by syringe (section 3.2.2), due to retention of up to 33% within the tracheal cannula. Doses deposited were 40.57 and 46.87ug in experiments I and II respectively (see section 3.3.5). When similar amounts of fluorescein were deposited by solution instillation into the tracheae of two consecutive iprl's, maintained in similar systems, subsequent rates of III transfer to the perfusate

were different (Fig 3.4, 3.5). The time after instillation, at which fluorescein was detectable in the perfusate varied, as did the asymptotes to which the curves in Fig 3.5 approached (total fractional transfer). It was interesting to observe however, that the speed at which the transfer process neared completion (rate at which the transferable amount approached a given fraction of a chosen starting value) was similar, once started.

The experimental variability documented in Figs 3.4 and 3.5, between two duplicate experiments, was not thought to be due to differences in retained doses and interanimal variability only. If fluorescein were deposited in, or proximal to, the perfused regions of the lung, it was hypothesised to be "available for transfer". Fluorescein in the trachea, which is unperfused in the isolated system however, was thought likely to remain "unavailable for transfer". It follows, if this hypothesis is true, that greater values for f_t , observed in experiment II, were probably due to a larger proportion of the deposited fluorescein reaching the lower, perfused airways after the small period of ventilation. In aerosol administration experiments however, interexperimental variability in transfer profiles should be smaller than that illustrated after solution instillation, because regional deposition, during a given ventilatory regime, should be much more reproducible (55).

In order to construct the transfer profiles shown in Fig 3.5 in this chapter, it was not necessary to be able to recover and account for all material instilled into the



system as a method of estimating the amount deposited in the lungs. This amount, (amount deposited), was determined from (amount instilled) - (amount retained in tracheal cannula). Table 3.6 shows the amounts of III found by assay of the various samples collected from the two experiments described in section 3.2.2. The sum of these amounts, determined at the end of each experiment, was less than the amount instilled. Control experiments, designed to account for missing fluorescein, are described in section 3.2.3.

3.3.4 Control experiments to determine loss of fluorescein in the system

3.3.4.1 Loss to sand The 40ml aliquots of 2M NaOH, containing 10 to 60ug fluorescein in 8g sand, were shaken, sampled and assayed for III, after centrifugation and supernatant withdrawal. Over the complete range of instilled quantities all fluorescein was recoverable. This showed that the fluorescein loss, which was apparent in experiments I and II of section 3.2.2, was not due to binding to the sand used for homogenisation of the lungs.

3.3.4.2 Loss of fluorescein to the apparatus When known amounts of fluorescein (15 and 1000ug) were circulated through the apparatus containing 200ml K4 (section 3.2.3.2), the fractional loss of fluorescein, due probably to adsorption (6, 7, 70), was approximately 0.1. When the same experiment was repeated using siliconised apparatus however, fractional loss decreased to 0.05 (Table 3.7). These losses,

when expressed as fractions, appeared to be independent of the amount instilled. Section 3.3.5 contains a reappraisal of the amounts of fluorescein recovered from the various sources sampled during experiments I and II (section 3.2.2). To take fractional loss from the perfusate to the apparatus into account, recoverable mass in the perfusate was multiplied by 1.05 (section 3.3.5).

3.3.4.3 Loss of fluorescein due to binding or metabolism by the lung

(a) Binding Following intratracheal instillation of 15 to 60ug quantities of fluorescein (section 3.2.3.3.a), an apparently constant amount (~ 3ug) was unrecoverable from the supernatant of the lung homogenate (Table 3.8). When only 3ug was instilled however, only approximately 0.6ug was lost. Fluorescein may have been irreversibly bound to homogenised lung constituents and lost during centrifugation prior to assay. This explanation is consistent with the loss of a fixed quantity when all sites are occupied (high concentrations), and smaller amounts prior to saturation. Alternatively, the compound may have been metabolised, or degraded by lung constituents during the extraction procedure (see (b) and (c) below). (Control experiments performed in the absence of the lungs, showed that solutions held under the same dark conditions at this pH, were stable and retained their starting fluorescence.)

Irrespective of the explanation, it was clear that when treating data where >12ug fluorescein was recovered

from the lung homogenate plus the perfusate, 3 μ g should be added to the total recovered, ^{for recovery > 12 μ g} to compensate for irreversible loss to the lungs.

(b) Conjugation Amounts of fluorescein recovered from perfusate and rat lung homogenate samples with and without β -glucuronidase treatment are shown in Table 3.9a and b. Treatment with the enzyme clearly made no difference to the results, showing the absence of any significant fluorescein loss over the 1hr period due to metabolism to the monoglucuronide (a phenomenon known to occur in intact rats (67, 99)).

(c) Metabolism The deviations of the normalised data for fractional transference, f_t , ($t > 70$ min), from unity, in the aerosol administration experiments is shown as a function of time in Fig 3.6. The coefficient of variance in this data was <2.5% and, more importantly, it is clear from Fig 3.6, that deviations in the normalised values for f_t , from the theoretical value of 1, show no time dependence in their random distribution about one. Thus, there were no detectable losses of fluorescein in this system, due to metabolism by the isolated lung.

A summary of the results from these control experiments is presented in Table 3.10. They were used to re-calculate amounts of fluorescein recovered in the instillation experiments I and II (section 3.2.2) and, subsequently, similar methods were used to calculate recovered quantities, after solution or aerosol administration, to isolated rat lungs.

3.3.5 Data correction for instillation experiments

Table 3.6 documents the amounts of fluorescein determined by analysis in the samples taken during experiments I and II (section 3.2.2), their sums being 56.92 and 55.48ug, respectively. In order to account for the total quantities instilled on each occasion (experiment I = 60.97ug, experiment II = 61.62ug), the amounts recovered in the perfusates must be multiplied by 1.05 (section 3.3.4.2), while 3ug should be added to the amount recovered from the homogenised lung (section 3.3.4.3.a). These corrections account for losses due to binding to apparatus and the lung homogenate, respectively and, when made in these experiments, provide values for accountable quantities = 61.11ug (experiment I) and 60.26ug (experiment II). Accountable fractions in these two experiments were therefore, 1.00 and 0.98, demonstrating the achievement of mass balance.

The results of these experiments were most important when aerosols of disodium fluorescein were to be administered to the isolated, perfused rat lung preparation. Under these circumstances, the amount of fluorescein retained by the lung during administration cannot easily be determined from (mass inhaled - mass exhaled), due to the difficulty in separating inhaled and exhaled aerosol. This problem was overcome for fluorescein in these investigations by determining retained material retrospectively, after analysis of the perfusate and lung homogenates and

correction of the results according to the methods detailed above.

The amounts of fluorescein deposited in the lung after aerosol administration (Chapter 5) were calculated, after analysis, by summation of (amount in perfusate \times 1.05) and (amount recovered from lung homogenate + 3 μ g). After solution instillation (experiments I and II, section 3.2.2) however, deposition may be determined by analysis and correction (above), or by subtracting the amounts in the tracheal cannulae from the amount administered. Fractional transference can then be determined, as the ratio of the amount in the perfusate at any time, to the amount deposited. Table 3.5 presents data for f_t versus time for experiments I and II (section 3.2.2).

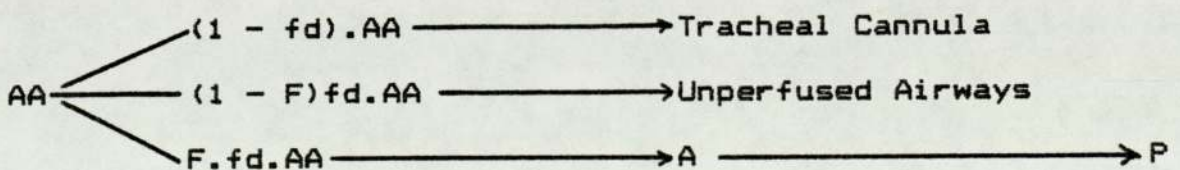
3.3.6 Fluorescein Transfer

Table 3.11 presents the concentrations of fluorescein in the nine flasks (prepared as described in section 3.2.4) at 12 and 24hr. Concentrations in control and test flasks were similar showing that, even when experiments were designed to maximise fluorescein loss from the perfusate to the lung, any transfer was insignificant. These observations, taken along with the rapid airway-to-perfusate transfer (Fig 3.4), but incomplete collection in the perfusate during instillation experiments (even though transfer was continuing at the end of the experiments, it is clear that not all of the deposited dose would be transferred; see also Chapter 5, section 5.3), permit the

construction of a simple kinetic scheme or model for fluorescein transfer in this system. The model must consist of at least two compartments (perfused-airways, A, and perfusate, P), with apparent, irreversible transfer of fluorescein from one to the other. The incomplete transfer of instilled fluorescein, requires the existence of a third, unperfused region of the airways, from which fluorescein transfer is unlikely. At time zero, the initial amount available for irreversible transfer to the perfusate, A_0 , depends upon

1. The amount of fluorescein instilled, or administered, into the tracheal cannula, AA.
2. That fraction, f_d , of the instilled amount, AA, which is deposited in the isolated tissue (and not the cannula, which retains $(1 - f_d)AA$, section 3.3.3).
3. The transferable fraction, F , of $f_d.AA$, that is the fraction deposited in, or proximal to, perfused regions (an amount, $(1-F)f_d.AA$, is untransferable and deposited in unperfused regions). Thus, the amount available for transfer at time zero, $A_0 = F.f_d.AA$.

The model can therefore be represented:



SCHEME 1

$$F = f_{\infty}$$

The observation of insignificant transference from perfusate to lung (Table 3.11), under the conditions described in section 3.2.4, suggests that fluorescein was not irreversibly bound in the intact lung. Transfer of the lipophobic fluorescein (existing almost entirely as the dianion at physiologic pH) was likely to occur via extracellular pathways (23, 24). Thus, fluorescein would not be expected to enter cells unless they were damaged (an effect ~~utilised~~ utilised in ^hophthalmic procedures to identify damaged tissues by fluorescein staining (68)). Fluorescein losses to lung fragments during analysis (section 3.3.4.3.a) therefore, were almost certainly due to binding to the intracellular constituents released during homogenisation.

In summary, this chapter described the analysis of II powder and the development of an assay for III in perfusate solutions. Experiments involving instillations of solutions of II into the trachea of a number of iprl's indicated that airway-to-perfusate transfer was rapid. Mass balance was established following instillation of known amounts of III, permitting the determination of deposited amounts of III in subsequent aerosol administration experiments (Chapter 5). A kinetic scheme was designed to describe the apparently irreversible III transfer from airway - to - perfusate.

TABLE 3.1

Water content of disodium fluorescein powder

```
*****  
Batch No          Bottle No          Water Content (%w/w)  
*****  
  
69305             1                 21.6  
                  2                 18.9  
                  3                 18.5  
81178             4                 12.4  
                  5                 12.0  
                  6                 11.9  
  
*****
```

TABLE 3.2

Disodium fluorescein elemental analysis. Results are percentages of carbon and sodium found alongside their theoretical values given the variable water contents (see Table 3.1).

```
*****
Batch No           Element           % Theoretical       % Found
*****
69305              carbon            51.7                50.7
                   sodium            9.9                 10.7
81178              carbon            56.0                54.2
                   sodium            10.7                12.4
*****
```

TABLE 3.3

Percent fluorescein by weight, as determined by fluorimetric analysis and titration (Batch 69305)

```
*****
Batch No           Fluorescein Content (%w/w)
*****
69305              97.0
81178              101.7
*****
```

TABLE 3.4

Amounts of III (ug) transferred from airway - to - perfusate with time for the instillation experiments I and II.

```
*****
Time (min)          -----Amount transferred (ug)-----
                    Experiment I           Experiment II
*****
```

5	1.7	5.87
10	6.6	12.77
15	9.63	19.33
20	16.37	25.65
30	18.71	30.09
45	20.48	32.31
53	23.88	--
60	--	35.59


```
*****
Amount III instilled  60.97ug           61.62ug
Amount III deposited  40.57ug           46.87ug
*****
```

TABLE 3.5

Fraction of deposited amount of III transferred from airway
- to - perfusate with time for instillation experiments I
and II

```
*****
Time (min)          -----Fraction Transferred (ft)-----
                    Experiment I           Experiment II
*****
```

5	0.04	0.10
10	0.11	0.27
15	0.24	0.41
20	0.40	0.56
30	0.46	0.64
45	0.50	0.69
53	0.59	--
60	--	0.76

```
*****

Amount III deposited    40.57ug           46.87ug

*****
```

TABLE 3.6

Amounts of III found after analysis of the various samples collected in instillation experiments I and II

```
*****
Sample          -----Amount III Recovered (ug)-----
                  Experiment I           Experiment II
*****
```

Perfusate	23.88	35.59
Lung homogenate	12.34	7.17
Tracheal cannula	20.70	12.72

Total recovered	56.92ug	55.48ug
Amount III instilled	60.97ug	61.62ug

TABLE 3.7

Fractional losses of fluorescein to apparatus: (a) unsiliconised and (b) siliconised, 1 and 60min after bolus injection

```
*****
Initial amount      -----Fractional loss-----
of fluorescein     -Unsiconised-      --Siliconised--
                   1min      60min      1min      60min
*****
```

15ug	0.11	0.09	0.04	0.05
1000ug	0.07	0.11	0.06	0.05

```
*****
```

TABLE 3.8

Amounts of fluorescein (ug) recovered and unrecoverable from isolated rat lungs, following the intratracheal instillation of a range of doses

Instilled dose Lung Amount recovered Amount lost

2.96	1	2.34	0.62
	2	2.41	0.55
16.03	3	13.05	2.98
	4	13.26	3.07
32.17	5	29.25	2.82
	6	28.72	3.45
63.28	7	59.82	3.46
	8	60.54	2.74

TABLE 3.9a

Comparison of the amounts of III (ug) found after analysis of perfusate samples, collected in instillation experiments I and II treated (a) with, and (b) without, β -glucuronidase.

```

*****
Time (min)          --Experiment I-      -Experiment II-
                   -(a)-      -(b)-      -(a)-      -(b)-
*****
5                   1.67      1.70      4.36      5.87
10                  5.83      6.60      12.67     12.77
15                 10.52     9.63      19.25     19.33
20                 16.39     16.37     24.89     25.65
30                 19.93     18.71     29.38     30.09
45                 21.22     20.48     32.91     32.31
53                 24.12     23.88     --        --
60                 --        --        35.53     35.59
*****

```

TABLE 3.9b

Comparison of the amounts of III (ug) found after analysis of lung homogenate supernatants from instillation experiments I and II treated (a) with, and (b) without, β -glucuronidase.

```
*****
Instilled dose                Amount in homogenate (ug)
                               -(a)-          -(b)-
*****
I:  60.97ug                   12.30          12.34
II: 61.62ug                   7.45           7.17
*****
```

TABLE 3.10

Summary of results from control experiments.

```
*****
Experiment                    Loss of fluorescein
*****
1. Sand                        No loss
2. Siliconised apparatus      5% loss
3. Intracellular binding      3ugx
4. Conjugation                None
5. Metabolism                 None
*****
X for recovery > 12ug
```

TABLE 3.11

Perfusate - to - lung fluorescein transfer:- lack of evidence for reversibility (control flasks did not contain an iprl).

```
*****
Flask                Fluorescein concentration (ng per ml)
                    12hr          24hr          Nominal
*****
```

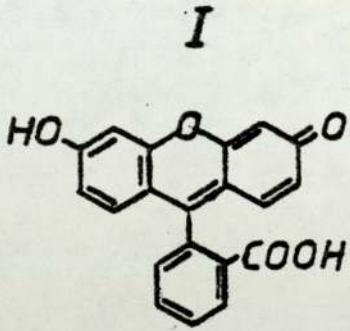
Control A	25.7	24.3	30
1	25.7	24.3	30
2	25.7	23.4	30
Control B	53.6	52.8	60
3	53.6	52.8	60
4	56.3	52.8	60
Control C	3793	3799	4000
5	3869	3817	4000
6	3865	3817	4000

```
*****
```

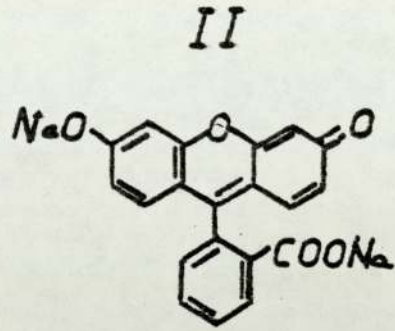
FIGURE 3.1

Molecular formulae of fluorescein (I), disodium fluorescein (II) and the fluorescein dianion (III).

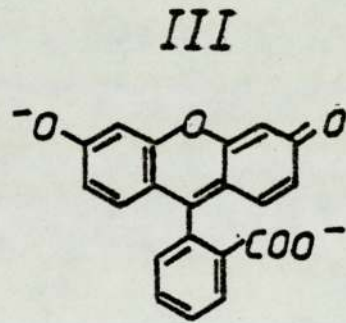
FIGURE 3.1



Fluorescein



Disodium Fluorescein



Fluorescein²⁻

FIGURE 3.2

Calibration curves (relative intensity versus fluorescein dianion, III, concentration) for solutions containing fluorescein in pH12SGB (\diamond) or pH12 K4 supernatant (X) and fluorescein solution alkalinised to pH12 and diluted in pH12K4 supernatant (O). The solid line represents the ideal calibration curve for the fluorescein standard used (10ng per ml III).

FIGURE 3.2

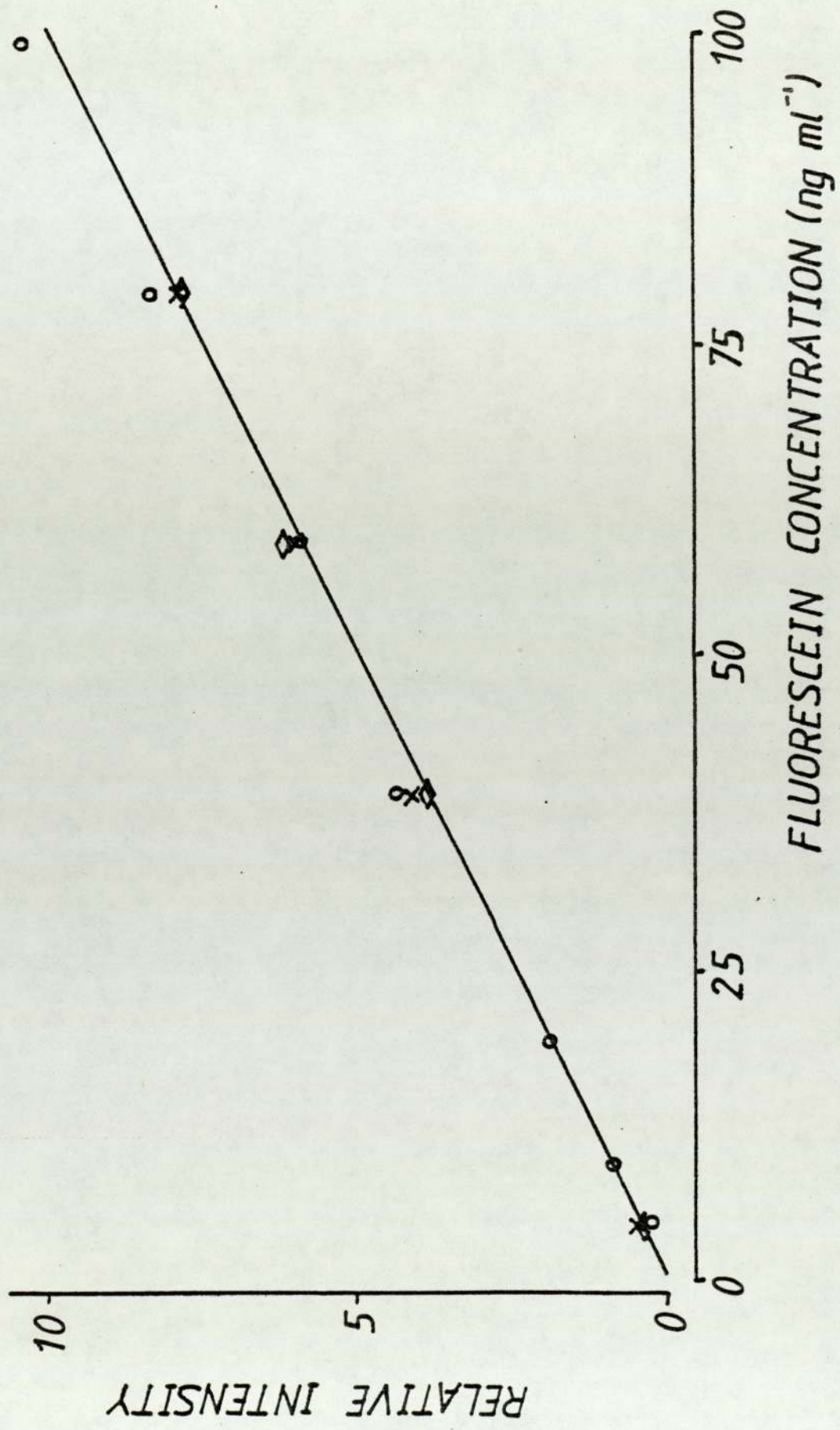


FIGURE 3.3

Schematic diagram of fraction transferred versus time, representing insignificant (solid line) and significant (dashed line) fluorescein metabolism during the course of an experiment.

FIGURE 3.3

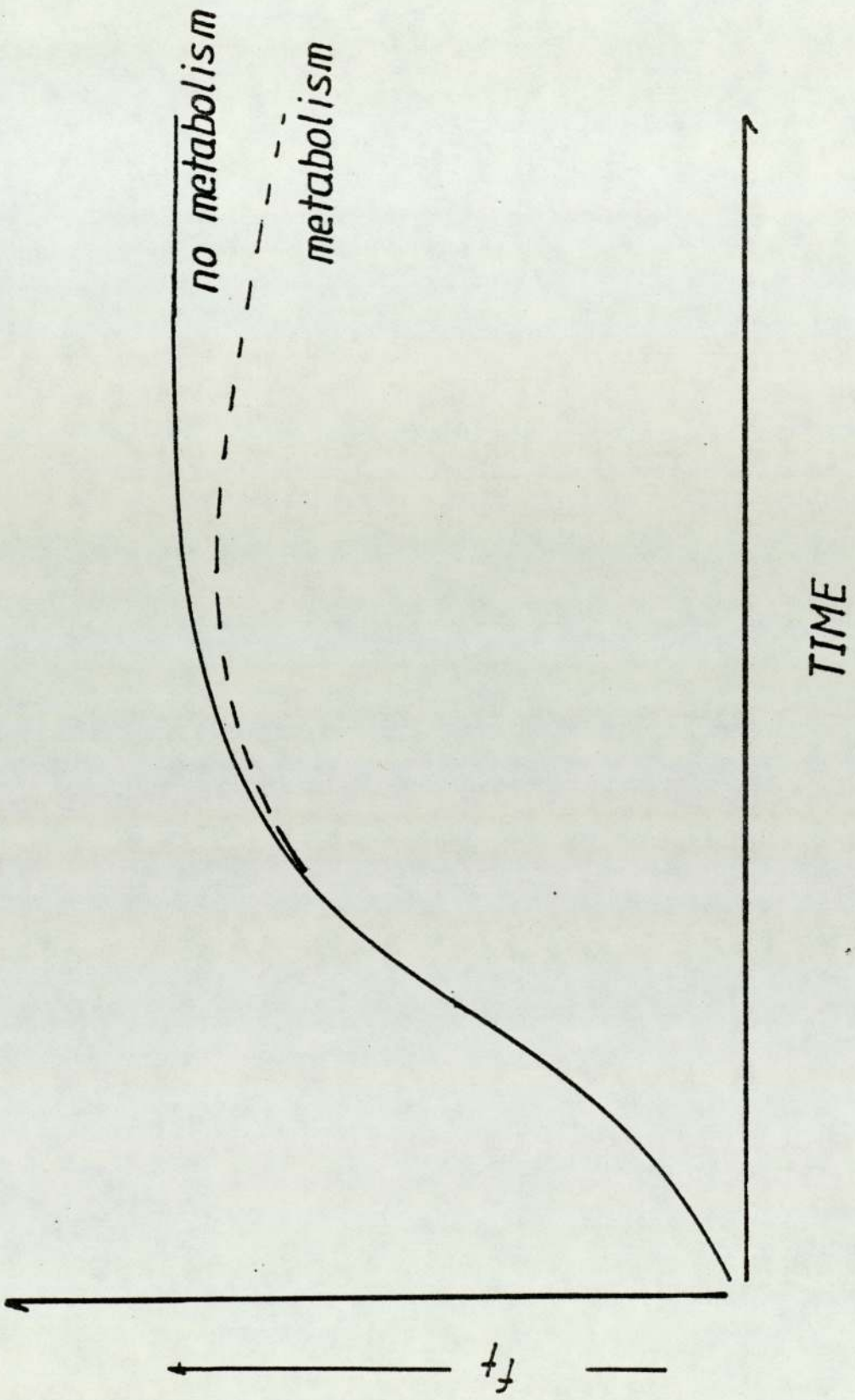


FIGURE 3.4

Amount of fluorescein transferred from the airways to the perfusate versus time in instillation experiments I and II.

FIGURE 3.4

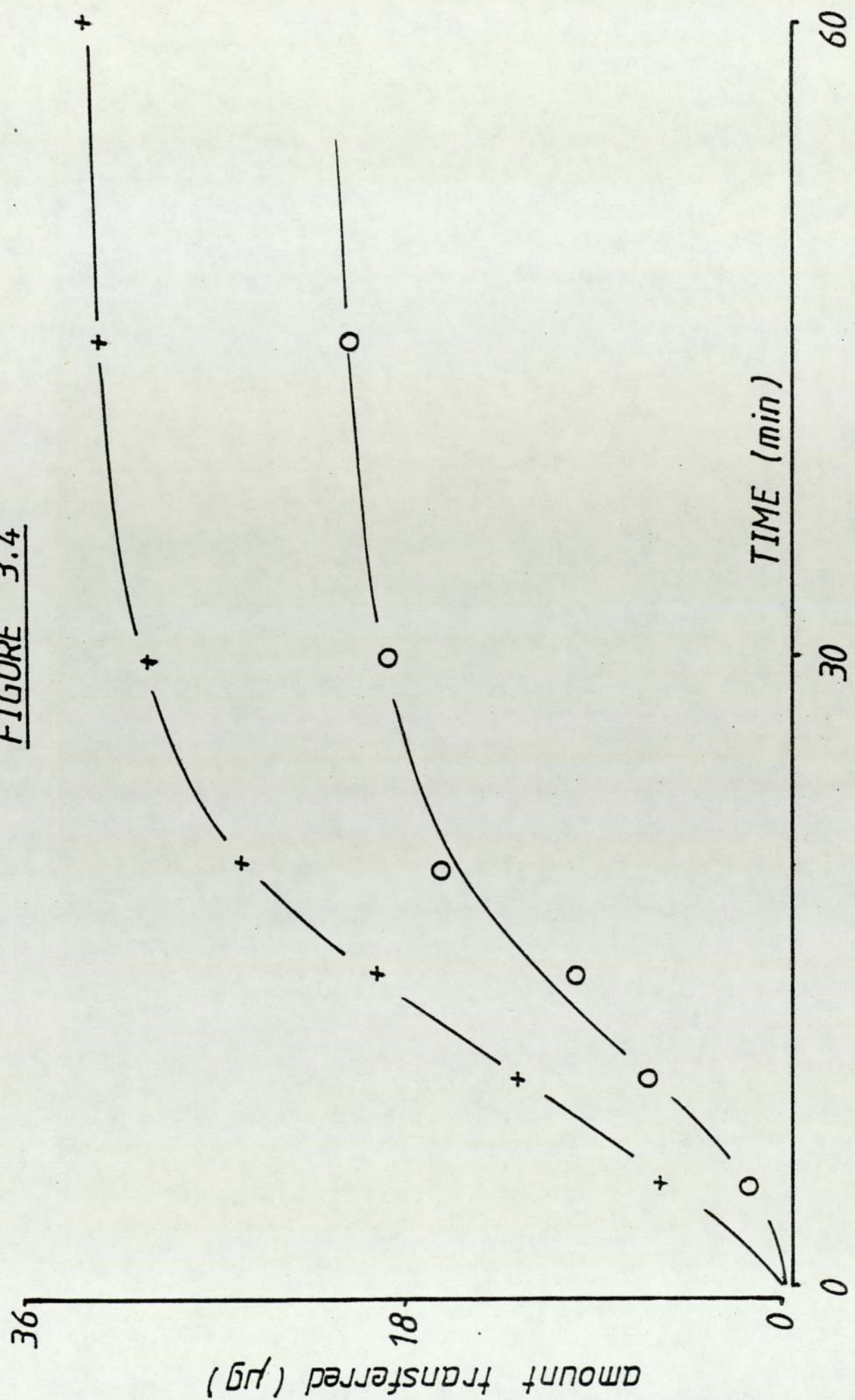


FIGURE 3.5

Fraction transferred versus time for instillation experiments I and II.

FIGURE 3,5

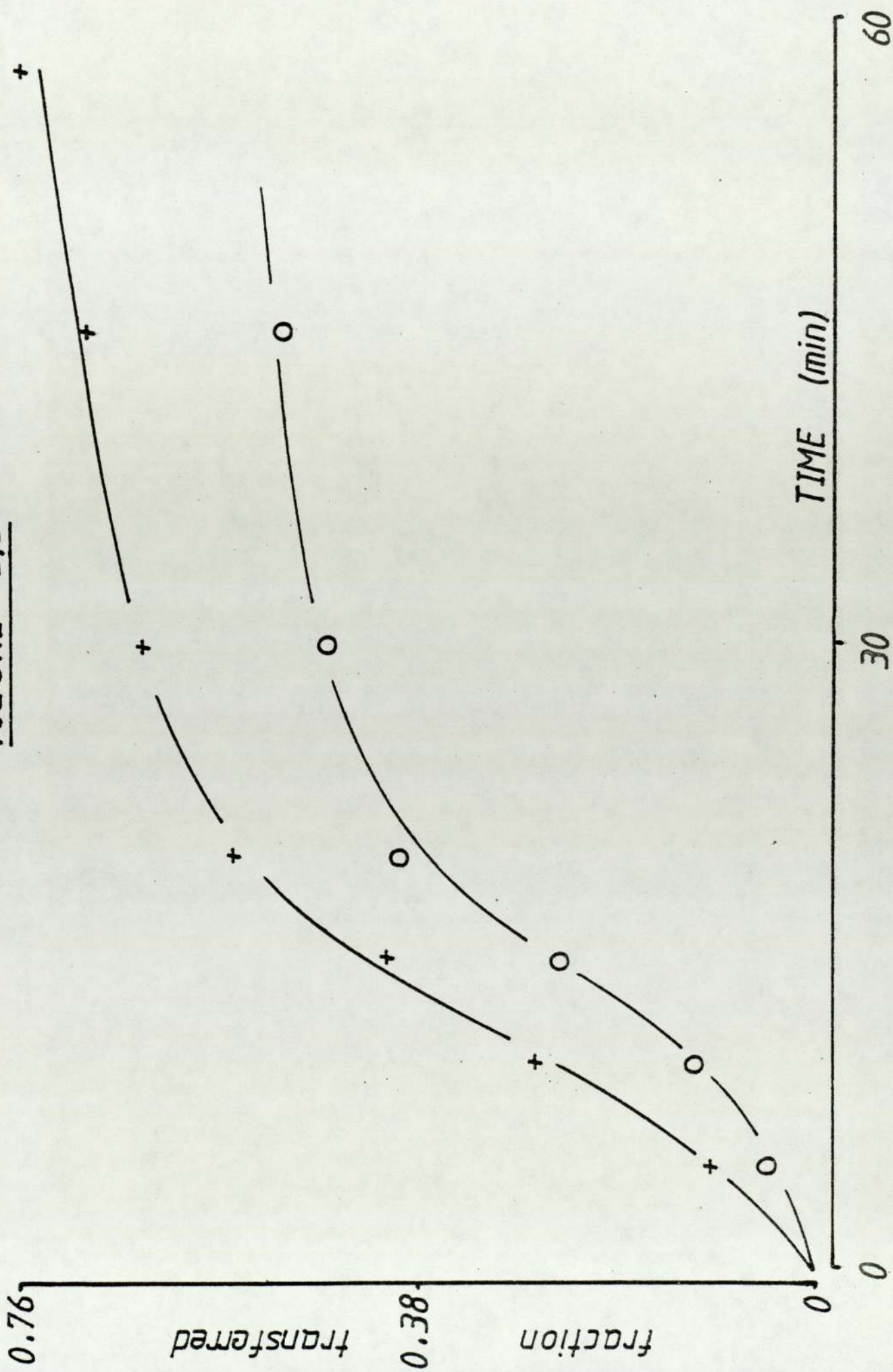
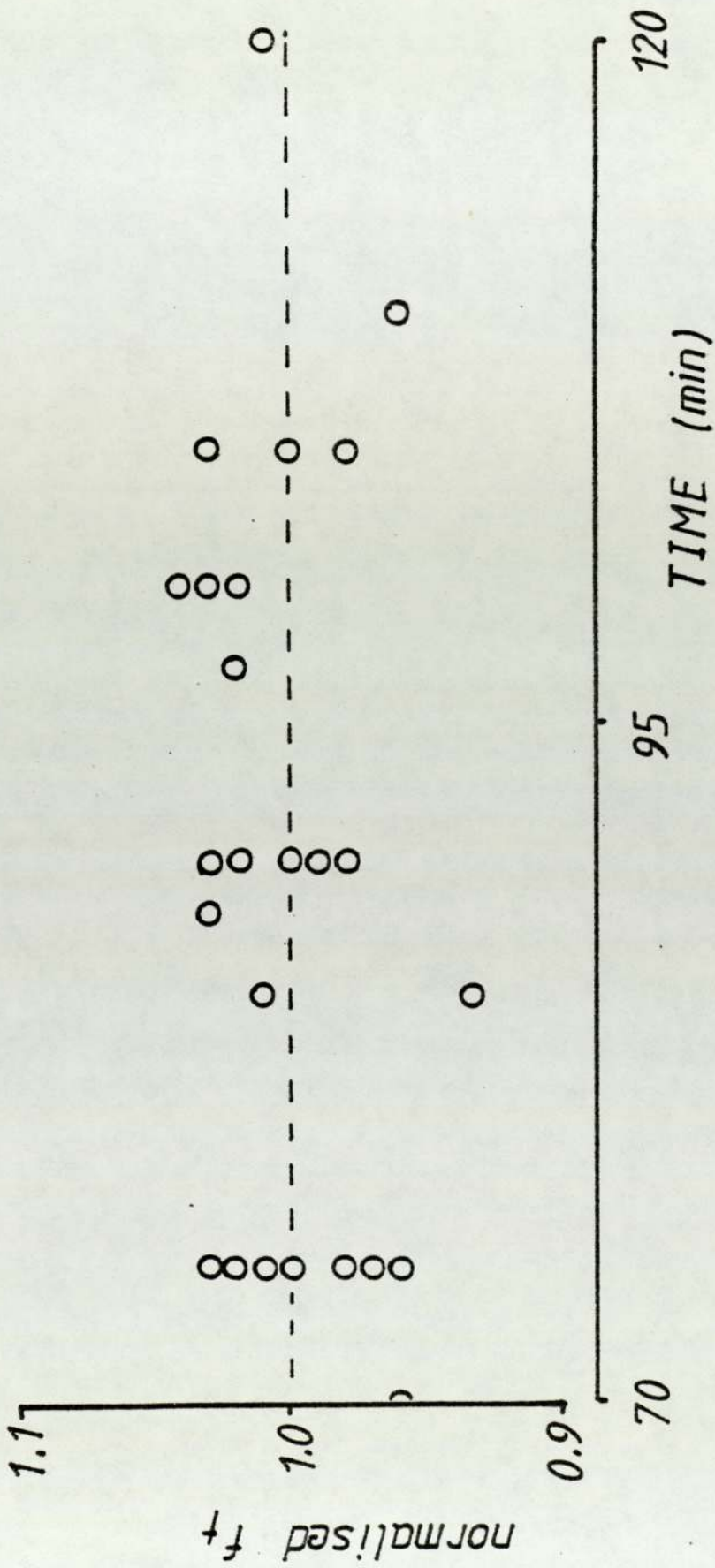


FIGURE 3.6

Insignificant III metabolism in the isolated, perfused rat lung, as shown by the random distribution of normalised data for fractional transfer about 1 (times greater than 70min) in aerosol administration experiments.

FIGURE 3.6



CHAPTER FOUR

AEROSOL GENERATION AND ADMINISTRATION APPARATUS

4.1 INTRODUCTION

This chapter describes factors influencing the selection of a generator with the capacity to produce aerosols suitable for administration studies in the iprl preparation. Generator characteristics are investigated and discussed. Also described are design, and experimental characteristics, of an administration tube which conveyed aerosol from generator to lungs. Techniques for aerosol sampling and waste disposal were developed, which permitted the dependence of aerosol characteristics upon generator variables to be investigated, prior to their administration to the iprl.

4.2 BACKGROUND

One purpose of these investigations was to document effects of aerosol particle size and respiratory variables upon airway-to-perfusate transfer of fluorescein. Once a model system had been devised therefore (Chapters 2 and 3),

means of (a) generating, (b) characterising and administering and (c) disposing of waste aerosols were needed.

(a) Generation Generators may be categorised according to their ability to produce either polydisperse or monodisperse aerosols. In practice, monodisperse systems consist of particles or droplets of approximately the same size. One of the few quantitative definitions of "monodispersity" in the literature (71) limits geometric standard deviations, σ_g to <1.22 (assuming a log-normal size distribution). Administration of monodisperse fluorescein aerosols to the iprl could have proved ideal for documenting effects of particle size on absorption. Quoted output concentrations of monodisperse generators however, were too small to enable adequate mass delivery to the iprl and subsequent accurate assay of III (Chapter 3, section 3.3.2). Similar reasoning caused the rejection of a number of generator candidates. The required aerosol output concentration from a generator, for administration to the iprl, was estimated to be $>100\text{ng ml}^{-1}$ (0.1g m^{-3}). This was based upon

1. A lung ventilation rate = 7 cycles min^{-1} (the slowest rate in these studies),
2. A rat lung tidal (inhaled) volume = 2ml ,
3. A total ventilatory period = 20min ,
4. A fractional deposition, $fd = 0.5$,
5. A transferable fraction, $F = 0.5$ and ^{finally 6.} a knowledge of the limits of accuracy of the assay for III in perfusate (Chapter 3, section 3.3.2).

The total inhaled volume under these conditions would be

280ml and, if the aerosol concentration = 100ng ml^{-1} , total eventual transference should equal 7 μg . In 200ml perfusate, this was considered to be adequate, representing a concentration of approximately 35ng ml^{-1} , after transference was complete.

Methods of aerosol generation include:

1. Controlled condensation from vapours
2. Atomisation of particulate suspensions
3. High frequency "chopping" of a jet of liquid into droplets
4. Centrifugal liquid atomisation
5. Air-blast liquid atomisation
6. Ultrasonic nebulisation
7. Dry powder dispersion.

Methods 1 to 4 are capable of producing "monodisperse", while 5 to 7 usually yield "polydisperse", aerosols. Most methods failed to satisfy the minimum concentration criterion and, because of the substantial difference in fluorescein carrying capacity between solid and solution aerosols, a generator for solid disodium fluorescein particles (in the respirable size range) was required. Method 6 was therefore unsuitable. Method 1 requires that the material is thermo-stable and therefore was also unsuitable for these studies (72, 73). Similarly, atomised suspensions are known to contain empty shells of, for these studies, undesirable surfactants (73).

The output characteristics of an aerosol generator, designed by Berglund and Liu (74), utilising ultrasonic vibration of a liquid jet were investigated. Theoretically,

after drying, an output concentration = $3.8 \times 10^{-9} \text{g m}^{-3}$ of monodisperse $2 \mu\text{m}$ particles of II was possible. It was hoped to collect these and re-aerosolise using a fluidised-bed generator (see below). In practice however, the actual aerosol yield proved prohibitively low and, as such, was rejected due to impractically long required generation periods. The spinning disc (or spinning top) generator (Method 4, above), is quoted as possessing higher output concentrations than the Berglund-Liu (75), while retaining the possibility of monodisperse, respirable, solid particulate aerosols, after drying in dilution air (76 - 79). This generator is noted for, and was rejected because of, its operation difficulties (78, 79).

Some air-blast solution atomisers were unsuitable, due to their time-dependent output (increasing solute concentration with solvent evaporation; 73, 80). Constant output was required, at least for the desired administration period (~20min). If droplets are dried after generation however, one constant liquid feed atomiser (81) overcomes this problem. Its output is reported stable, in terms of particle size and concentration, for prolonged periods. Preliminary investigations using this generator substantiated these reports (see Fig 4.1). The output concentration however, was only 0.09g m^{-3} (after determination using apparatus shown in Fig 4.2, Plates 11 and 12), a value at the lower limit for required concentration. The aerosol size range from this generator is restricted to sub-micron particles (81). Attempts were made to administer aerosols produced by this device to the iprl

with little success. Neither transference nor deposition, was found to be sufficiently high, to produce reliable results (probably because of a low value for f_d for sub-micron aerosols in this system).

The generator selected finally, for use with the iprl, was a fluidised-bed dust generator, designed by Marple et al (82), marketed by Thermo Systems Inc. (Model 3400, St Paul, Minnesota, U.S.A.). Its output concentration was high (up to 1.2g m^{-3}) and fairly stable. Theoretically, the device was capable of aerosol sizes in the range submicron to $20\mu\text{m}$ (manufacturer's specifications). Warm up time for this generator was however $\sim 2\text{hr}$, this being essential for stable output. More recently, a stable, high output, dry aerosol generator has been developed capable of concentrations $\sim 4\text{g m}^{-3}$ with a warm-up time of only 30min. The device was limited however, to particle sizes $< 1.8\mu\text{m}$ (83).

The experiments described in detail in this and Chapter 5, utilised the Model 3400 TSI fluidised-bed aerosol generator (3400 FB), as the most suitable, in conjunction with the iprl. A diagrammatic illustration of the generator is included as Fig 4.3. Its principles of operation are as follows:

Powder to be aerosolised is placed in the reservoir chamber (Fig 4.3), from where it is conveyed, by a variable-speed bead chain, into the fluidised bed. This bed consists of numerous brass beads of diameter $\sim 100\mu\text{m}$ (or at least 10 times larger than the powder to be aerosolised), supported by a porous plate, above an air plenum. Dried, filtered air enters from the plenum, to fluidise the bed.

The continuous action of the beads, deagglomerates the powder and dispersed particles are carried, in the air stream, to the outlet (The settling velocity of the brass beads is designed so as to be higher than the linear velocity of air in the fluidising chamber, which in turn should be higher than the gravitational settling velocity of the "dust" particles).

Brass bead contamination of the powder reservoir is prevented by a so called "bead-purge" airflow. This cleans the chain prior to its re-entry into the powder chamber. Both fluidised-bed and bead-purge airflows are adjustable. The optional use of a 1/2 inch cyclone separator, positioned at the aerosol outlet, allows only "respirable dust" to exit, given a total air flow = 9 l min^{-1} . This cyclone was not used in any of the investigations described in this thesis.

The particle size distribution of aerosols generated by this fluidised-bed generator depends largely upon the characteristics of the powder in the reservoir. Output concentration however, is a function of chain feed rate and volume gas flow through the bed. Prior to aerosol administration to the iprl, operating characteristics and performance of the generator were evaluated. Total air throughput was measured at variable bed flow and bead purge settings (inbuilt rotameters in the generator interact and require precalibration). The mass concentration and particle size distributions of polydisperse II aerosols were studied as functions of time to determine, (a) whether concentration and particle size distribution were suitable for

administration to the iprl and (b) the time taken to reach "steady-state" (constant concentration) aerosol output after starting up the generator.

(b) Aerosol administration Three administration tubes were designed to convey aerosol from the generator to the iprl. The suitability of these tubes was investigated. Only the final system is described in detail. The inadequacies of earlier designs are listed below. The final design, which was used successfully, in all aerosol administration experiments, was based upon several important criteria. Earlier designs failed to comply with one or more of the following requirements:

1. The dead space (between the aerosol streamline and the lung) should be minimised. The internal diameter of the aerosol delivery tube (Fig 4.4, S) however (2mm in this case), should be large enough to avoid clogging due to particulate impaction.
2. Entrance of aerosol to the trachea, should be in line with particle trajectories within the aerosol stream.
3. Essential bends in the administration tube should curve gently, to minimise loss due to impaction and resultant particulate segregation in the system.
4. Attention was paid to the linear velocity of aerosol particles in the tubing system. A compromise was necessary, when tubing diameters were assigned, between the need for low velocity particles (laminar flow and minimal impaction loss) with retention in the air stream (sufficient flow to minimise sedimentation prior to administration). Clearly, at a given volume flow rate, a decrease in linear velocity

- could be achieved by increasing the diameter of the tubing.
5. The administration tube (Fig 4.4) should be of constant diameter to avoid particulate acceleration or deceleration with changing bores.
 6. The length of the administration tube should be restricted to avoid unnecessary aerosol losses due to sedimentation.

Figure 4.4 illustrates the final administration tube design, which complied with these criteria. Figures 4.6 and 4.7 show the aerosol sampling and waste systems designed to complement the generator, administration tube and iprl system (Chapter 2). Generated, but not administered, aerosol (the vast majority) must be wasted without either building up back-pressures in the administration apparatus and generator or contaminating the environment. Sampling, to determine aerosol concentration and particle size distribution, must also be possible without perturbing either the administration system or laboratory air. This apparatus was designed to achieve these goals.

The rate at which aerosol is drawn through the small bore delivery tube (connecting the iprl to the administration tube; Fig 4.4, s) by the lungs must be variable due to the nature of respiration. Aerosol characterisation by isokinetic sampling (84) at the exit of this, rather than the main administration tube, is therefore impossible. Because aerosols were to be characterised in this main administration tube, immediately prior, and just after their administration to the iprl (Chapter 5), experiments are described in this chapter which show that in

this apparatus, aerosols administered to the lungs differed insignificantly from those travelling down the main administration tube. This was probably not the case for the administration experiments of other workers using less adequately designed systems (40). The Brown and Shanker administration apparatus almost certainly causes particulate segregation at the junction of the delivery tube and the aerosol mainstream (where their systems are also characterised). These criticisms have been described in more detail previously (Chapter 1).

4.3 MATERIALS AND METHODS

4.3.1 3400FB airflow

I am grateful to Dr A.R.Rees for her determinations of generator output airflow at variable bed flow and bead purge settings. Bead purge settings on the generator (Model 3400 fluidised-bed aerosol generator, Thermo Systems Inc., St Paul, Minnesota, U.S.A.) were held at 0, 25, 75 and 100%, while total output was determined as a function of bed flow settings, using a precalibrated rotameter. Results are detailed for the instrument used in these investigations in Fig 4.5.

4.3.2 3400FB mass aerosol output

A number of experiments were performed to evaluate the output of 3400FB as a function of time. Aerosols of II were produced from powders of different particle sizes. These powders were all produced from one large batch of II which had been contract-jet-milled (Cavadell Ltd., U.K.) into four sub-batches (A,B,C and D) of nominally different sizes. Mean sizes were originally thought to be ~1,3,5 and 7 μ m respectively. Aerosol output was determined in terms of concentration and particle size distribution, for each of

these sub-batches, under a variety of generating conditions.

4.3.2.1 Apparatus

A schematic diagram of the apparatus used in assessment of generator performance is shown in Fig 4.6 (Plate 13). Output from the generator, A, flowed through a 180° arched tube (internal diameter 9mm) into a column, B, containing a radioactive ^{85}Kr source (Model 3054, Thermo Systems Inc., St Paul, Minnesota, U.S.A.) designed to neutralise the charge on the aerosol particles (85). The column was inverted in order to reduce particulate losses (86). From the neutraliser, the aerosol flowed through the glass administration tube, C, and to waste via the glass cup, D. The latter two parts, C and D, had a ground glass, airtight interface at x (Fig 4.6). Removable tubing clips are represented by S1,C2,C3,D1 and R1, and vacuum sources by V1 and V2. The following section, which details the methodology used to sample aerosol flows, should also indicate how laboratory contamination was avoided using this apparatus design.

Mass concentrations in the main aerosol stream were measured at various times after generation commenced, by collecting total aerosol output for a known time on to a filter (5.5cm GF/B glass microfibre filter, Whatman, Maidstone, U.K.), held in a double-coned filter holder, F (overlay, Fig 4.6). During generation, aerosol output was wasted, at atmospheric pressure, at M1 and M2 (water and fibre aerosol traps). When sampling however, the filter

holder, F, was connected on one side to a glass cup, D', identical to D and, on the other, to a vacuum, V2, of flow rate greater than the airflow output from the generator. To avoid evacuating C, B and A during sampling, C2 was opened to allow additional laboratory air to be drawn through the filter and vacuum, alongside total generator output. The means of exchanging the cups D and D', without contaminating the laboratory, are detailed below.

4.3.2.2 Experimental details

Clean, dry, compressed air, was supplied to the 3400FB. Bead-purge and bed flow rates were both adjusted to 50% (values consistent with a total air throughput = 10 l min⁻¹; see Fig 4.5). Approximately 13g of sub-batch A, of II, previously oven dried for 2 days at 70°C, was placed in the powder reservoir. The bead chain speed was adjusted to a value between 25 and 100% (100% represents maximum powder delivery to the bed), and the chain activated (time, t = 0).

During routine aerosol generation, clips S1 and C2 were closed and vacuum V1 switched off (Fig 4.6). Aerosol therefore travelled via the open routes C3 and D1, at atmospheric pressure. Particulate material was removed from the airstream by the high capacity water and fibre traps (M1 and M2), which offered minimal resistance to airflow. Air from the generator escaped to waste via these traps, in this case down a laboratory sink via R1, containing flowing water. To sample the aerosol, C2 and V1 were opened, simultaneous to the closure of R1. This diverted all aerosol

flow to waste via C3. The glass cup D' was then clamped to C, in place of D. To draw total aerosol plus additional room air (via open C2) onto the filter F, V2^{was opened} and C3 and closed simultaneously. Samples were withdrawn for 1 minute periods, at regular intervals for some 14 hours after t=0 and the amount of III on the filters was determined (section 4.3.5.1) and added to the amount in DDW washings from the holder and tubing plus D', for each aerosol sample collected. At the end of each sampling period, procedures were reversed; C3^{was opened} and V2 closed simultaneously, D and D' exchanged and V1 and C2 closed.

Mass concentrations in the main aerosol stream were determined in this way, for each sub-batch of aerosolised II, using different 3400FB operating conditions (bed flow and chain feed rate variations).

4.3.3 Aerosol concentration in delivery tube

Two experiments were undertaken to ascertain whether aerosol concentrations determined in the main stream (at D, Fig 4.6) were representative of those in the delivery tube, S, during inhalation by the iprl. If concentrations differed, then this would almost certainly be due to particulate segregation at the junction of C and S. It can be reasoned furthermore, that large particles are most likely to be lost at such a junction due to turbulence-induced impaction. Because these large particles account for the bulk of the aerosol's concentration, insignificant loss of II at S would indicate that the

apparatus design was adequate for characterised aerosol delivery; ie. that both concentration and particle size distributions determined in the main stream were descriptive of aerosols administered to the trachea.

Quantities of the sub-batches A and D (the smallest and the largest nominally sized powders) were aerosolised by the 3400FB in two separate experiments. After output had risen to steady-state, aerosol was drawn from the main stream, C, through the delivery tube, S, by a vacuum, onto a filter (2.5cm GF/C glass microfibre paper, Whatman, Maidstone, U.K.) held in a holder (Millipore (UK) Ltd., London, U.K.) at 112, 56 and 28ml min⁻¹. These rates of withdrawal were chosen to be representative of the rates used by the ipr1, breathing with tidal volume = 2ml at 28, 14 and 7 cycles min⁻¹, the respiratory frequencies employed during aerosol administration (Chapter 5). Sampling times of 1, 2 and 4 min were employed using precalibrated vacuum flow rates, such that the total volume of aerosol withdrawn via S remained constant at 112ml. Aerosol concentrations determined in this way were compared to those determined at D (Fig 4.6) according to the method described in section 4.3.2.2.

4.3.4 Aerosol particle size distributions

Particle size distributions were determined using a precalibrated Battelle cascade impactor (Model DCI6, Delron Research Company, Powell, Ohio, U.S.A.)

4.3.4.1 Apparatus

The apparatus is shown schematically in Fig 4.7 (Plate 14). To draw an aerosol sample through the impactor, it was first necessary to divert aerosol flow, as described in section 4.3.2.2. Vacuum V1 was activated and tubing clip C2 was opened simultaneously, while R1 was closed (Fig 4.7). The glass cup, D, was replaced by a long, curved glass tube, E (Fig 4.7), with the same internal diameter as C. It was physically impossible to shorten or straighten tube E due to apparatus constraints, thus, the gentle bends in this sample tube, were intended to minimise aerosol losses en route to the impactor.

4.3.4.2 Experimental details

Aerosol was drawn through the impactor by closing C3 and opening V4 (Fig 4.7) simultaneously. A constant volume flow rate = 12.45 l min^{-1} was maintained through the cascade impactor, for the sampling period by application of a vacuum (Speedivac, Edwards High Vacuum, Crawley, U.K.) $<17\text{mm Hg}$ below a critical orifice situated in its base. Particles were collected at successive stages onto silicone fluid coated glass slides, according to the method of Groom and Gonda (87). The final stage of this impactor consisted of a glass fibre filter (76mm, Type AE, Gelman Instrument Co., Michigan, U.S.A.), designed to remove all non-impacted particles from the air stream.

One minute samples were taken, after which, V4 was

closed and C3 opened (Fig 4.7) simultaneously and the glass tube, E, replaced by the cup, D. Normal flow was restored in the system by closing C2 and V1 at the same time as opening R1. The procedure was executed at $t = 2\text{hr}$ and 10hr after generation commenced, to determine the stability of the aerosol's particle size distribution over prolonged periods.

4.3.5 Sample analyses

4.3.5.1 Determination of mass aerosol output

Subsequent to sampling (sections 4.3.2.2 and 4.3.3), filters were placed in separate beakers with 20ml 0.1M NaOH and left overnight at room temperature in the dark. Subsequently, each filter was rinsed repeatedly with DDW and the washings, plus NaOH solution made up to known volume with DDW. Resultant solutions were diluted in pH12 SGB and assayed according to section 3.2.1.2 in duplicate relative to a standard of known III concentration. The amount of III collected during a sampling period was calculated from the product of concentration (Eq 3.2) and volume of the sample solution, corrected for dilution.

4.3.5.2 Aerosol Particle size distribution

Fluorescein deposited on glass slides at successive stages of the cascade impactor was extracted using benzene (AR Grade, Fisons, Loughborough, U.K.) and pH 12 SGB as described by Groom and Gonda (87). The glassfibre filter was

extracted with buffer alone. Extracted fluorescein was diluted with pH 12 SGB and assayed fluorimetrically. The amount of fluorescein collected at each stage (concentration (Eq 3.2) x volume of solution) was expressed as percentage of total collected in the impactor during the sampling period.

4.4 RESULTS

The 3400FB aerosol output characteristics were assessed in terms of aerosol concentration at D and S (Fig 4.6) and particle size distribution at D (Fig 4.7), after the aerosols had passed through the administration apparatus. Each of the disodium fluorescein sub-batches A, B, C and D were used for aerosol production under various generator operating conditions.

4.4.1 3400FB mass aerosol output

4.4.1.1 Output stability

Figures 4.8 to 4.13 all show that the generation time required to reach steady-state output was between two and three hours. After this generator "warm up" period, output concentration was effectively constant. The time to reach steady-state operating conditions seemed to be independent of the particle size of the powder or the generator operating variables.

4.4.1.2 Effect of powder feed rate

The powder feed rate, from the reservoir to the

fluidised bed, had a dramatic effect upon steady-state aerosol output for a chosen powder. Figure 4.8 shows a six-fold increase in aerosol output for sub-batch A, resulting from a four-fold increase in chain speed (25 to 100%).

4.4.1.3 Effect of total airflow to fluidised bed

Using powder sub-batch D in the reservoir and a constant (50%) powder feed rate, a change in total airflow from 10 to 15 l min⁻¹ to the bed appeared to have no effect on steady-state output of III when expressed in mg min⁻¹. The aerosol concentration however, was reduced by a factor of 10/15 at the higher flow rate. The aerosol mass median aerodynamic diameter (MMD₅₀) appeared to be slightly smaller at the higher airflow (Fig 4.9).

4.4.1.4 Effect of powder particle size

The nominal particle sizes (1, 3, 5 and 7µm) quoted for the sub-batches A to D were broad approximations only. Because aerosol characteristics were ultimately important however, no attempts were made to size the sub-batches precisely. The particle size of powder in the reservoir appeared to have a variable effect on aerosol output concentration and particle size distribution. For example, Fig 4.10 shows output versus time for the two sub-batches B and C. When used for aerosol generation under similar production conditions (total air throughput = 10 l min⁻¹,

chain feed rate = 50%), both output and particle size distribution were similar. In contrast, sub-batches B and D (under identical generation conditions), had different distributions (MMD₅₀ and geometric standard deviation, σ_g) but similar output (mass and concentration) (Fig 4.11).

4.4.1.5 Reproducibility of particle size distribution

When the same powder sub-batch was subjected to aerosolisation in the 3400FB, under identical operating conditions, on different occasions, aerosol characteristics were rarely the same. Concentration or output varied little, but there was often a marked change in aerosol particle size distribution. The legend of Fig 4.12, for example, shows the MMD₅₀ of the aerosol generated from sub-batch B = 3.38 μ m on one occasion and 3.9 μ m on another. Similarly, MMD₅₀ varied by up to 1 μ m (2.6 to 3.59 μ m; Fig legend 4.13) for sub-batch A on different occasions. It should perhaps be emphasised here, that not all of these differences were necessarily properties of the generator. Experiments were designed to display the operating characteristics of the whole aerosol administration apparatus and thus, some of these observations may well be due to slight differences in the geometry of the interconnecting pipework, charge neutraliser and administration apparatus, which required dismantling and cleaning (as indeed did the 3400FB) between experiments.

4.4.2 Aerosol concentration in delivery tube

The aerosol concentration withdrawn from the main stream via S (Fig 4.6), according to the method detailed in section 4.3.3, was calculated by dividing the amount found from analysis by the volume of aerosol sampled (a constant 112ml). Figures 4.14 and 4.15 show that for both the small (sub-batch A) and large (sub-batch D) aerosolised powders, aerosol concentrations in the main stream and the delivery tube were similar, indicating a lack of significant particulate segregation in these cases.

4.4.3 Aerosol particle size distribution

Particle size distributions were determined according to section 4.3.4.2, using a cascade impactor. The cumulative % total aerosol mass collected up to and including each stage (n) can be plotted versus the D50 (aerodynamic diameter collected with a 50% efficiency) of the stage above (n-1), as log probability plots (see, for example, Figs 4.16 and 4.17). In all cases, for aerosols described throughout this thesis, such plots were apparently rectilinear, indicating that aerosols were log-normally distributed. To show the constancy of 3400FB particle size distribution during steady-state, Figs 4.16 and 4.17 present such data for one aerosol generation sampled at t = 2hr and 10hr, respectively. If the mass median aerodynamic diameter, MMD_{50} , is to be obtained from such plots, then this is defined as the particle size above and below which 50% of

the mass resides (MMD_{50} 2.32 and 2.6 μ m in Figs 4.16 and 4.17 respectively). The geometric standard deviation, the term commonly used to indicate the spread of log-normal distributions is given by

$$\sigma_g = (D_{50} \text{ at } 84\% \text{ undersize}) / (MMD_{50}) \quad (\text{Eq 4.1})$$

where D_{50} is aerodynamic diameter. Deciding the exact location of a straight line on such a plot may lead to large errors in estimates for MMD_{50} and σ_g . Furthermore, the accuracy of such a method relies upon the validity of theoretical impactor calibration curves which are known to be incorrect for the device used in these studies (66). Mass data from this precalibrated impactor was therefore subjected to weighted non-linear least squares regression analysis, according to the method of Raabe (83), using an interactive computer program devised by Gonda (89). Calculated values for MMD_{50} and σ_g (from the data in Figs 4.16 and 4.17) using this method were 2.67 μ m ($\sigma_g = 1.5$) at $t = 2$ and 2.57 μ m ($\sigma_g = 1.5$) at $t = 10$ hr, respectively. Thus, the particle size distribution of an aerosol produced by the 3400FB during steady-state, remained effectively constant over this period. Subsequent values quoted in this thesis, for aerosol MMD_{50} and σ_g , are the average of the values determined for two cascade impaction samples taken during each steady-state aerosol generation (before and after administration to the ipr1).

4.5 DISCUSSION

The 3400FB aerosol generator reached steady-state output in 2 to 3 hr, a time which appeared independent of the various operating conditions employed. This finding concurs with those of Marple et al (82) who observed a time ~ 3 hr for their prototype to achieve stable operation.

Aerosol mass output of II by the 3400FB was dictated primarily by the rate of powder feed to the fluidised bed (Fig 4.8) but the particle size of powder in the reservoir also had an effect. The lower bead chain speed (25%) employed for aerosol generation from the smallest powder sub-batch A (Figs 4.8 and 4.13) was used in response to the large outputs observed in pilot studies at 100% chain speed. Mass output, when expressed as amount per unit time, appeared to be independent of air throughput (Fig 4.9). Aerosol concentrations however, were obviously changed by this manoeuvre.

According to the manufacturer, the volume feed rate to the fluidised bed is adjustable between 3 and $30\text{mm}^3\text{ min}^{-1}$; a value which has been shown to be independent of the material employed (82). For a chain speed of 100% (see Fig 4.8), maximum delivery should therefore correspond to $30\text{mm}^3\text{ min}^{-1}$. Assuming the bulk density of II to be 1.46g cm^{-3} (86; water

content was unspecified), 30mm^3 should weigh 43.8mg , corresponding to approximately 36mg III after taking account of the water content of the powder used in this experiment. The values shown for mass output in Fig 4.8, ranged from 10.9 to 11.9mg min^{-1} , some 30% of that theoretically conveyed to the bed. Some particles undoubtedly fail to escape from the exit port of the generator while others are possibly too large to be aerosolised. A substantial quantity of II remained in the fluidised bed chamber at the end of each experiment. Possibly this "bed charge" must be accumulated before steady-state is reached. Much of the difference between the theoretical and experimental yield of this generator was due to loss in the interconnecting pipework, most occurring in the arched outlet tube from the 3400FB (Fig 4.6).

In all experiments mass output varied. Variations were greater for aerosols of larger particle size (compare Fig 4.8, $\text{MMD}_{50} = 2.6\mu\text{m}$ with Fig 4.9, $\text{MMD}_{50} = 4.31$ and $4.00\mu\text{m}$). Although cyclic variations in aerosol concentration, with a frequency corresponding to the rate of entry of a new bead chain section into the fluidised bed, have been reported (82), these fluctuations were only of the order of $\pm 5\%$ of the average concentration, which should remain constant. The output fluctuations during steady-state (Figs 4.9 to 4.13) may have resulted from re-entrainment of material, previously deposited in the pipework, due to movement or vibration in the apparatus. The larger variations in output, which occur with the larger aerosols, are consistent with this explanation. Re-entrainment of larger particles

of greater mass into the air stream, would cause more marked changes in output. These observations indicated the need, during administration experiments, to fix all apparatus and pipework as rigidly as possible to ensure stable aerosol concentrations.

Mass aerosol output of the 3400FB at the sampling point (D, Fig 4.6) appeared to increase as particles became smaller, necessitating decreased rates of supply to the fluidised bed for the smaller powders. With the larger sized aerosols, increased deposition occurred in pipework and the administration tube, (C, Fig 4.6). Thus larger particles, at volume flow rates = 10 l min^{-1} , almost certainly sediment from the main stream in areas prior to the sampling point (for this reason, the sampling point, D, occurs in the same vertical plane as the opening of the delivery tube S; Fig 4.6). Sedimentation therefore, probably played an important role in setting an upper limit for aerosol particle size in this administration system. An attempt to decrease its importance was made in order to increase particle size at D (Fig 4.6). Increasing volume flow rate through the apparatus however, failed to significantly affect mass output from sub-batch D (Fig 4.9), perhaps because of a coincident increase in the importance of impaction (The small decrease in MMD_{50} at the higher airflow would be consistent with this explanation, although this may have been due to lack of reproducibility between different aerosol generations; section 4.4.1.5).

Particle size distributions of aerosols produced, from the same sub-batch, during different generations were

administration to the isolated, perfused rat lung preparation. Effectively constant aerosol output was demonstrated within 2 to 3hr of commencing generation. An administration apparatus was described which enabled aerosols to be drawn from the main supply which were similar in particle size distribution and concentration to those flowing in the main stream. Methods of aerosol characterisation were designed to prevent contamination of the environment or perturbations (pressure changes) in the administration system. The size range of aerosols that could be tested in the iprl, by withdrawal from the apparatus as described, appeared to have an upper limit (approximately 4 to 5 μ m) dictated by particulate losses in the system.

FIGURE 4.1

Comparison of mass III aerosol output versus running time for the constant liquid feed atomiser (X) and 3400 fluidised-bed generator (O).

FIGURE 4.1

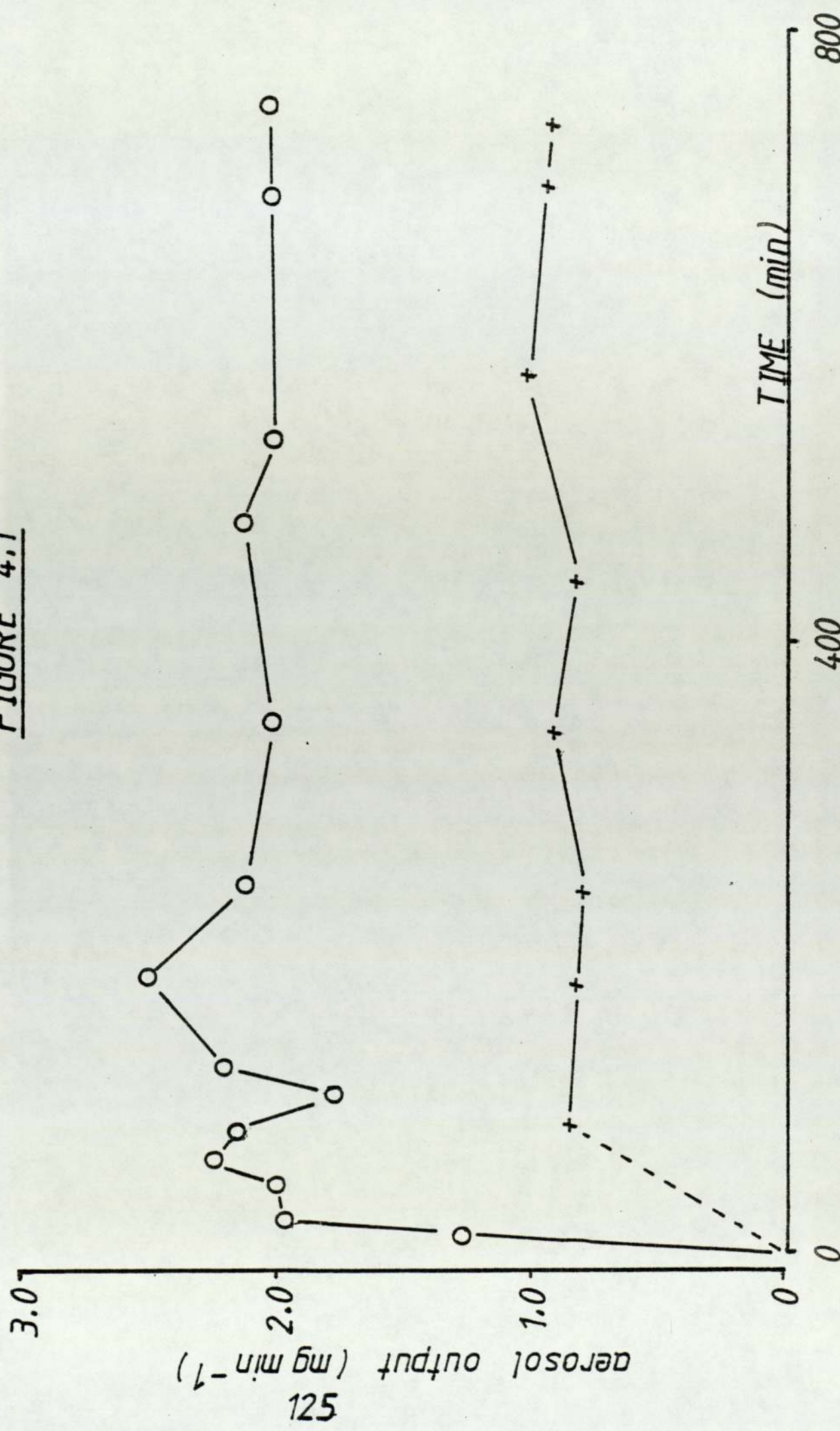


FIGURE 4.2

Schematic diagram of aerosol generation apparatus featuring the constant liquid feed atomiser. Aerosols were characterised at D using identical techniques to those described for the 3400FB (see Figs 4.6 and 4.7).

- i constant liquid feed atomiser
- ii pressure regulator
- iii compressed air supply
- iv flow regulator
- v syringe pump
- vi heated copper piping
- vii dilution air flow
- viii air supply to generator (35 psi)
- ix droplet stream
- B aerosol charge neutralising column
- X silica gel
- C administration tube
- D aerosol sampling connection

FIGURE 4.2

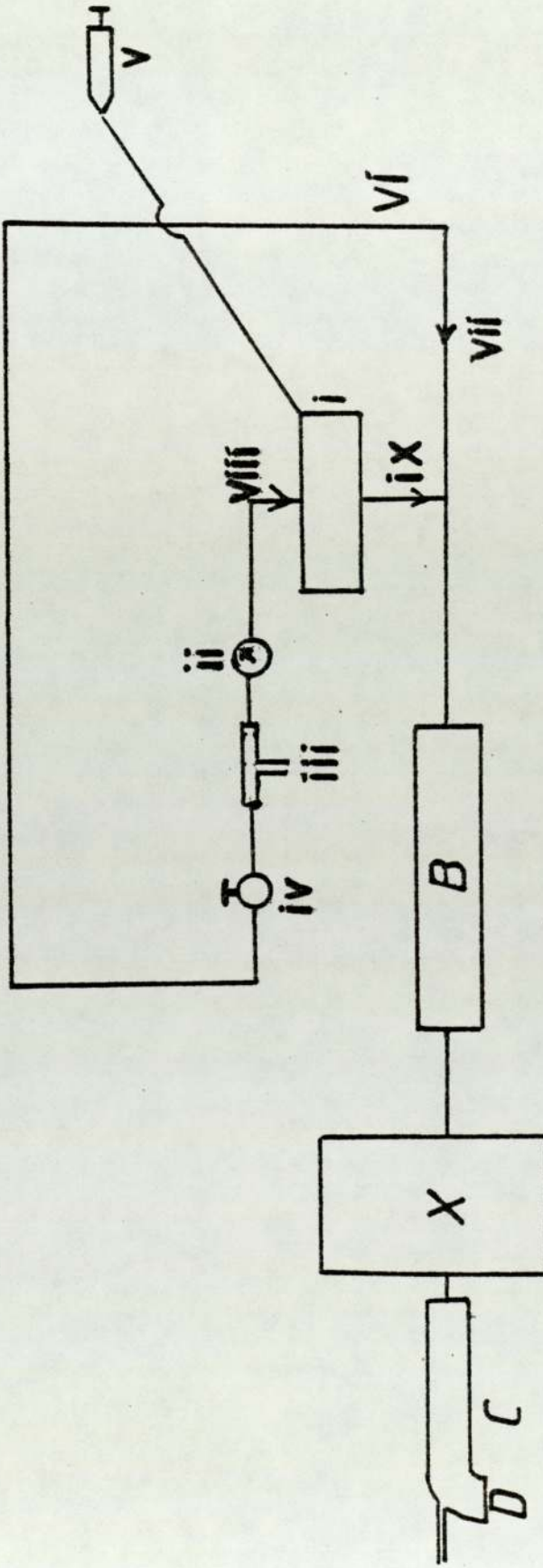


FIGURE 4.3

Schematic diagram (cross sectional view) of 3400FB
(fluidised-bed aerosol generator).

FIGURE 4.3

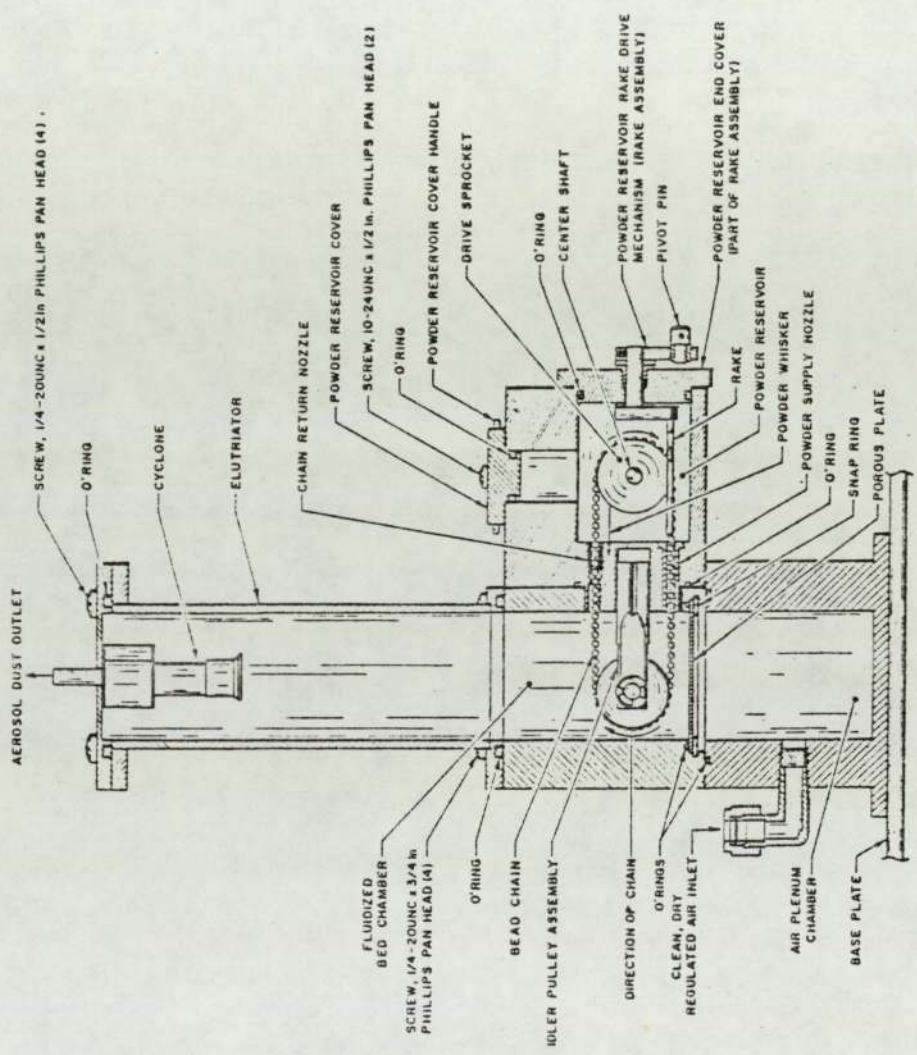


FIGURE 4.4

Design of glass administration tube (C) used in the aerosol administration studies described in Chapter 5.

Length of C	185mm
Length of C to opening of S	170mm
Internal diameter of C	23mm
Internal diameter of C2 and C3	7mm
Length of delivery tube, S	30mm
Internal diameter of S	2mm

x = Ground glass surface

The administration tube bends through 90° as shown, but also through 90° out of the plane of the paper; see Plate 10.

FIGURE 4.4

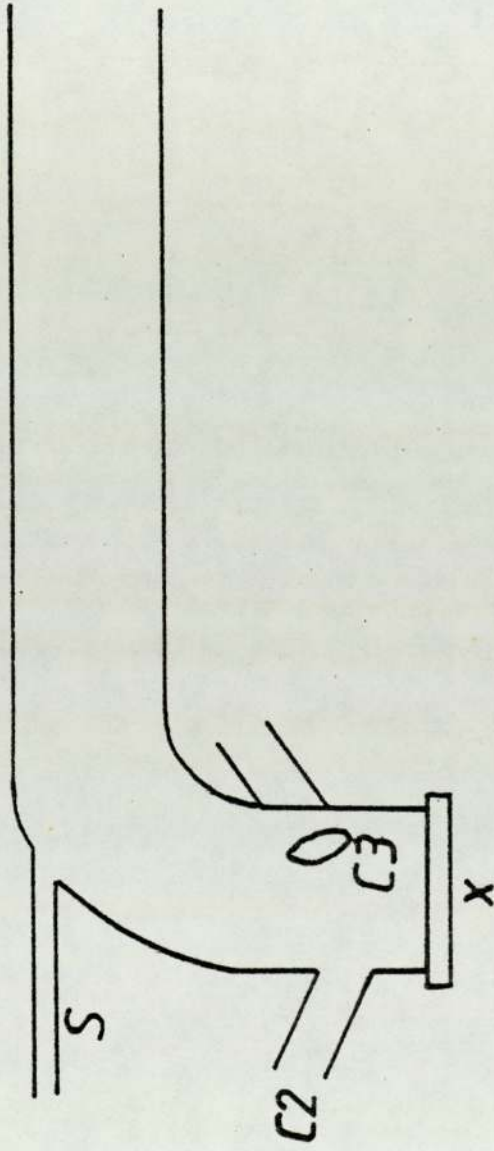


FIGURE 4.5

Air flow rate ($l \text{ min}^{-1}$) from the outlet of the 3400FB aerosol generator versus bed flow rate setting (%) obtained at a variety of bead purge settings.

FIGURE 4.5

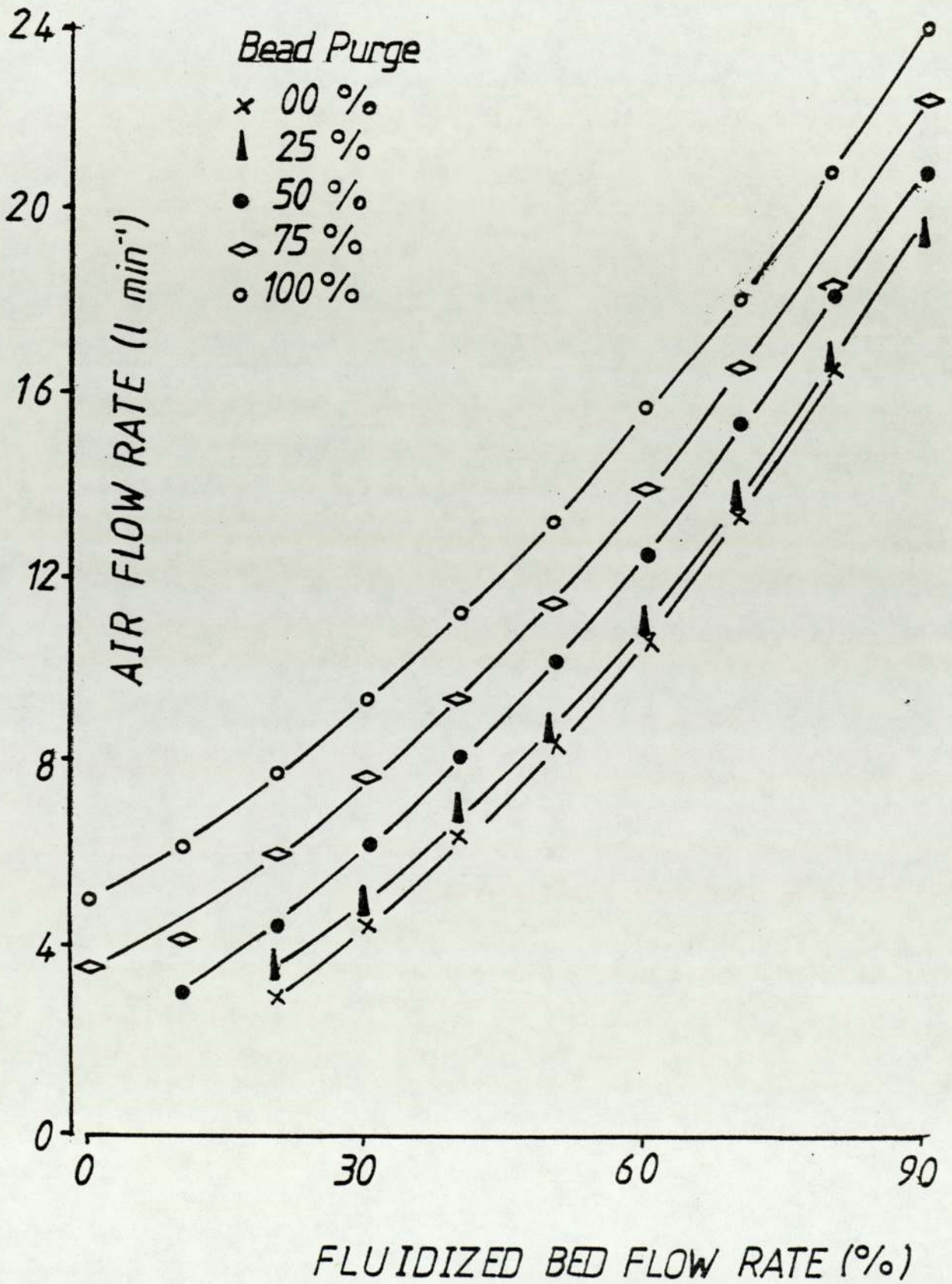


FIGURE 4.6

Schematic diagram of the aerosol generating apparatus featuring the fluidised-bed aerosol generator. The overlay details the apparatus used for determining mass III aerosol output.

A	3400FB
B	aerosol charge neutralising column
C	administration tube
D	removable glass cup (i.d. 23mm, length 40mm)
D'	identical to D, second glass cup
F	filter holder
V1,V2	vacuum pump
S	delivery tube
M1,M2	Water and fibre traps for waste aerosol
S1,C2,C3,D1,R1	Removable tubing clips

FIGURE 4.6

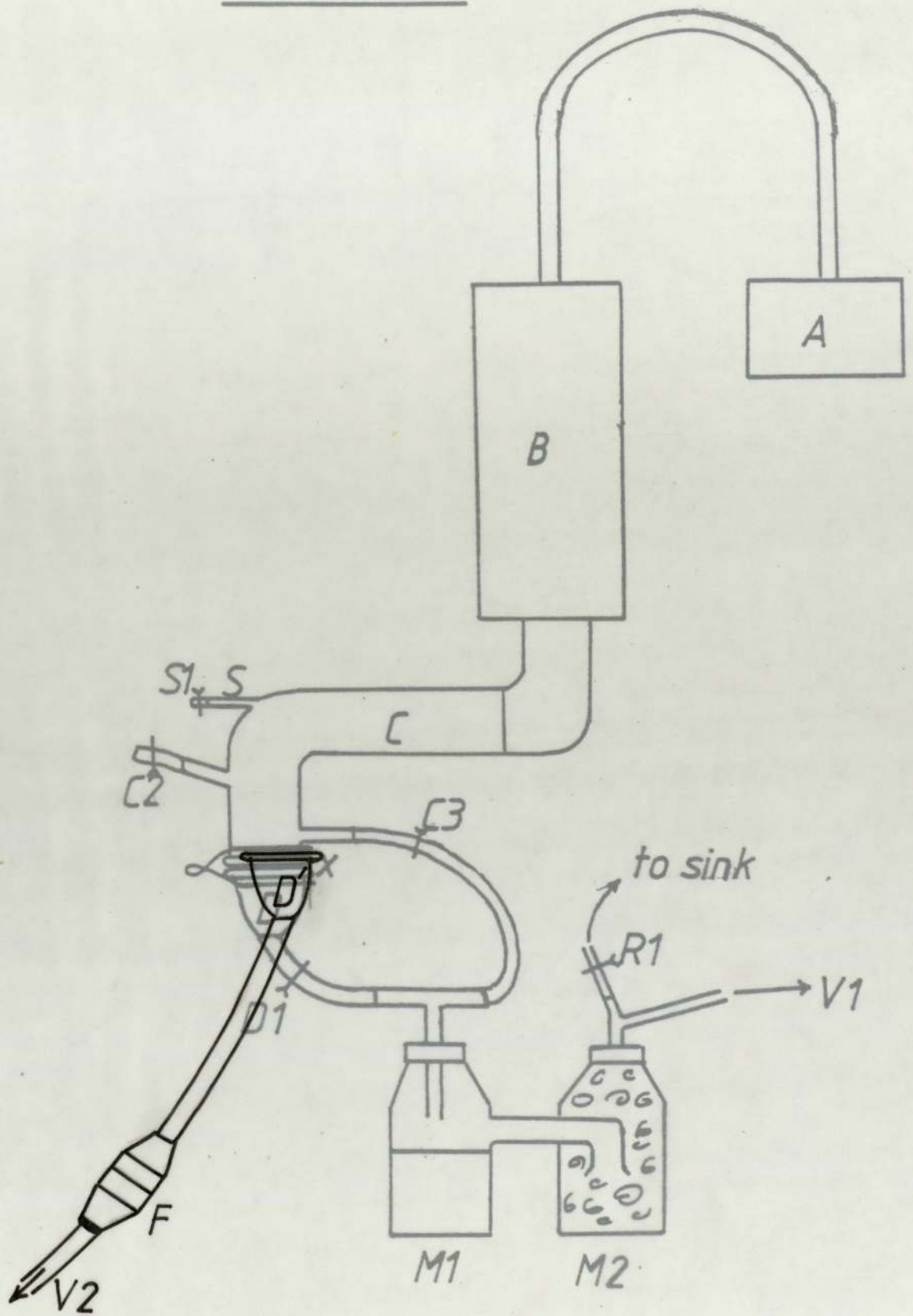


FIGURE 4.6

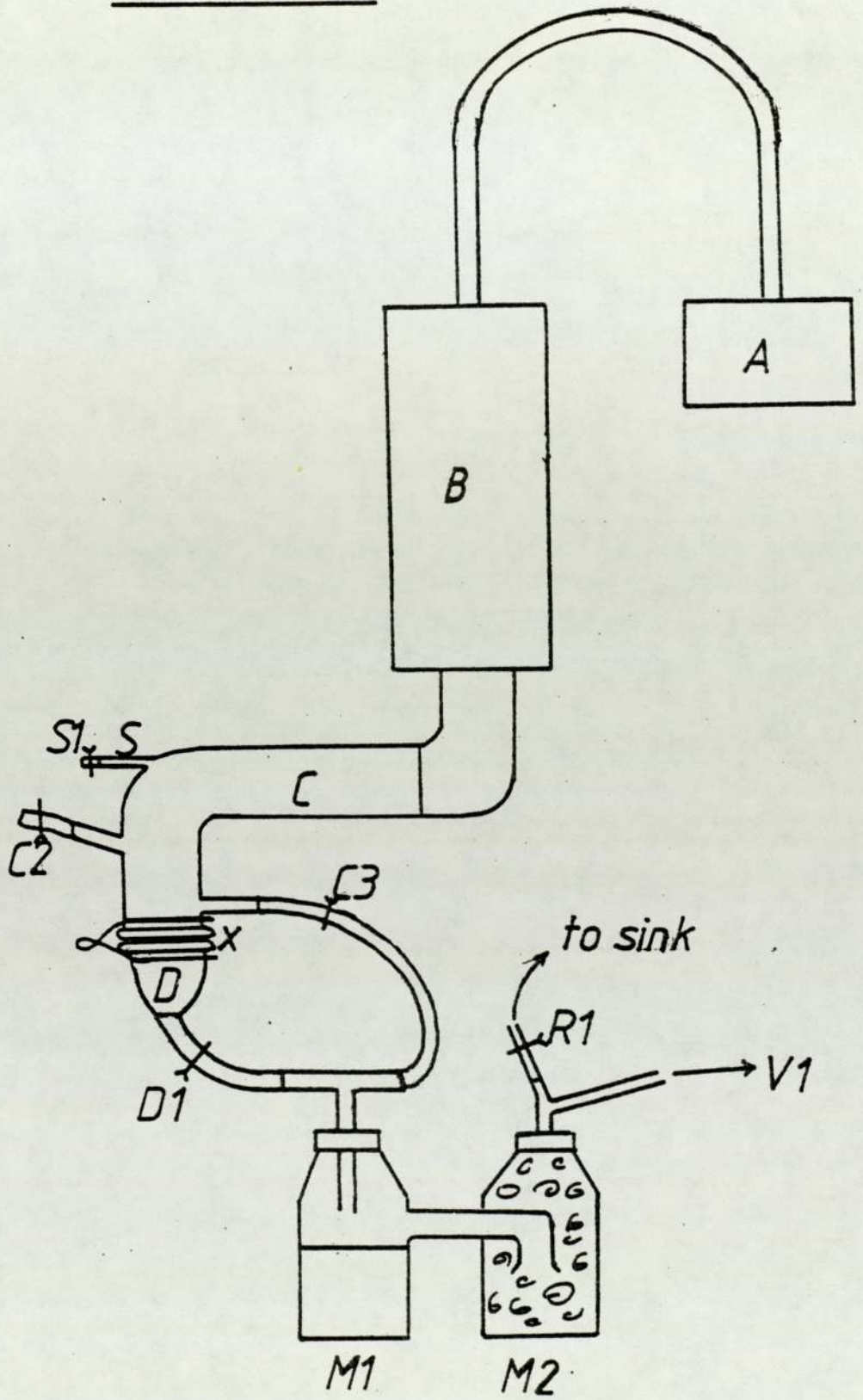


FIGURE 4.7

Schematic diagram of the aerosol generating apparatus featuring the fluidised-bed aerosol generator. The overlay details the apparatus used for determining aerosol particle size distributions utilising a cascade impactor.

A, B, C, D, C2, C3, D1, M1, M2, S, S1, R1 and V1 are as detailed in the legend of Fig 4.6 (page 134).

E Glass tube for conveying aerosol to cascade impactor, I. Ground glass surface at Z for the airtight connection with the administration tube at X (Fig 4.6)

Internal diameter 23mm
length 640mm

G Glass funnel
Internal diameter of neck 23mm
Internal diameter of cone 100mm

I Cascade Impactor

V4 vacuum pump

FIGURE 4.7

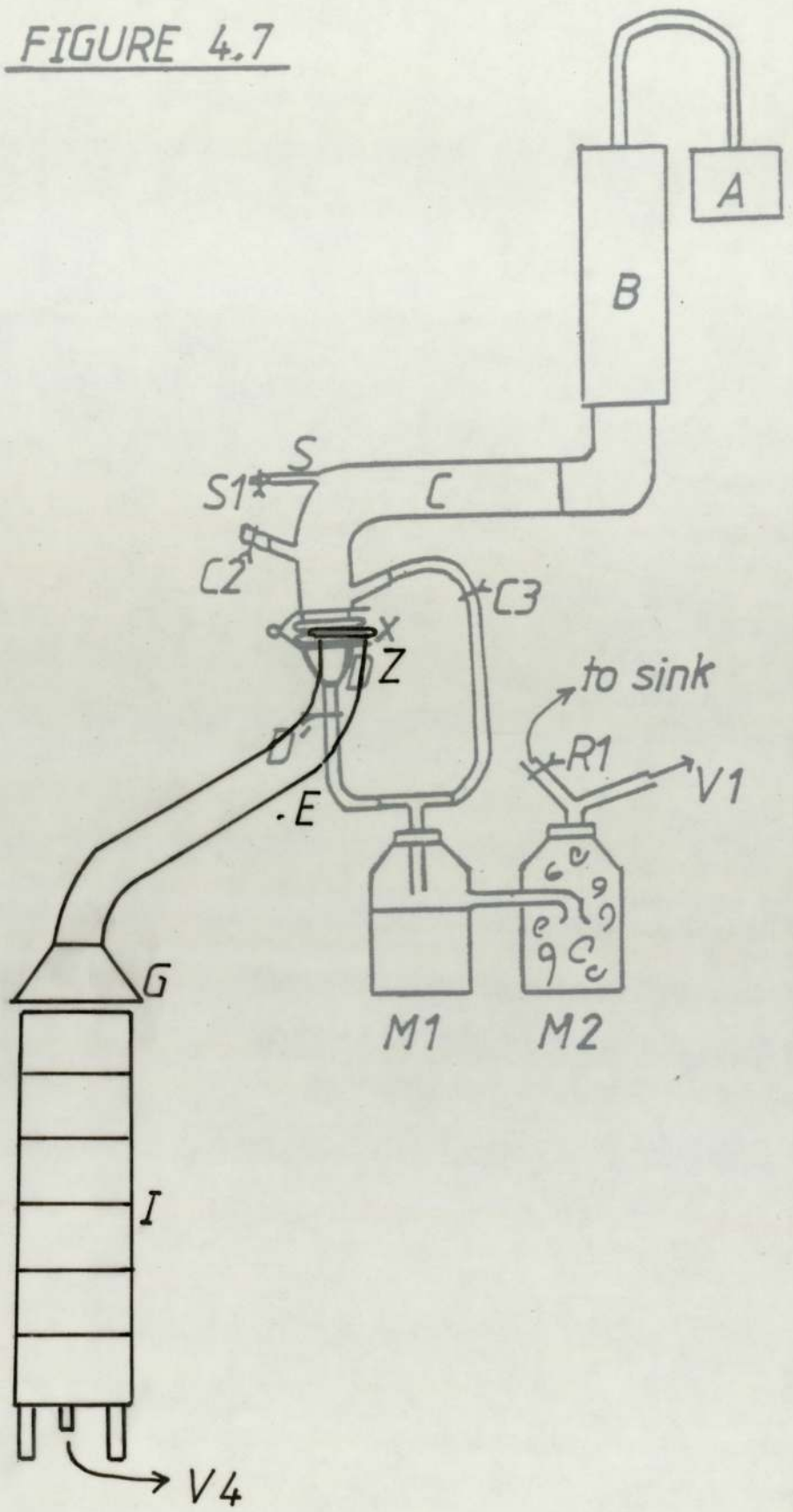
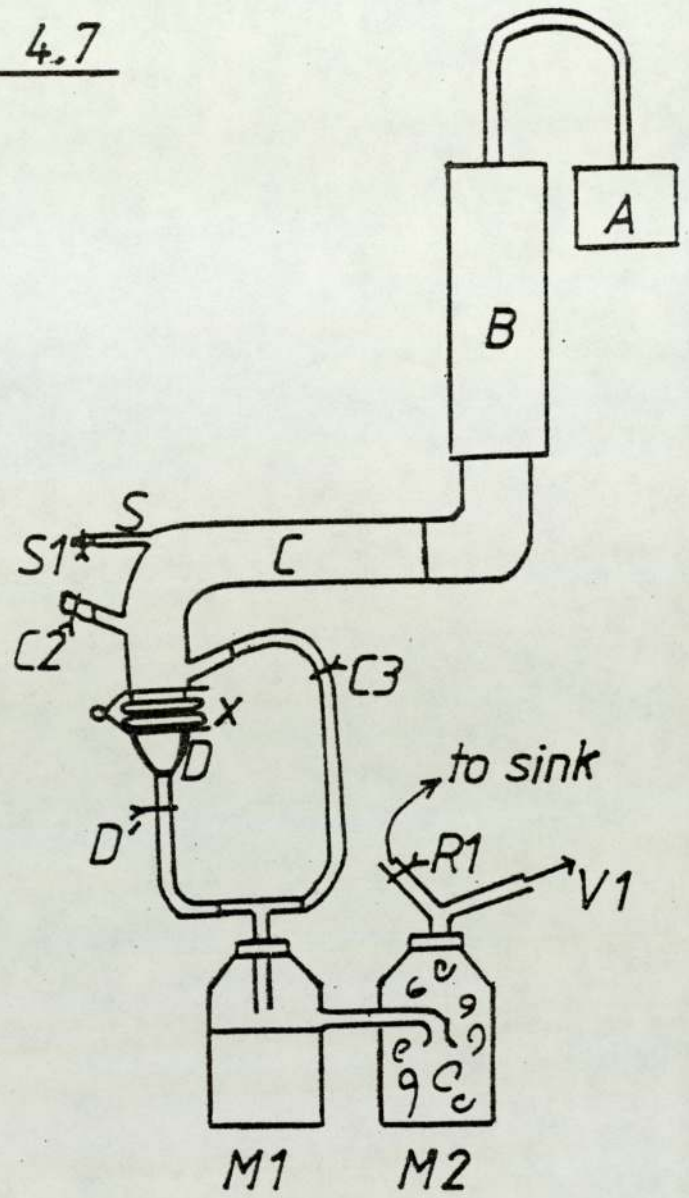


FIGURE 4.7



FIGURES 4.8 to 4.13

Mass III aerosol output versus running time for the 3400 fluidised-bed aerosol generator under the various operating conditions detailed below. Operation commenced at t=0.

Fig II Figure ---Aerosol--- --Operating conditions---

No. batch symbol MMD_{0.5} (um) σ_g a(%) b(%) c(l min⁻¹) d(%)

4.8	A	X	2.62	1.5	50	50	10	25
	A	O	3.05	1.58	50	50	10	100
4.9	D	X	4.31	1.46	50	50	10	50
	D	O	4.00	1.25	65	65	15	50
4.10	C	X	3.88	1.32	50	50	10	50
	B	O	3.9	1.29	50	50	10	50
4.11	D	X	4.31	1.46	50	50	10	50
	B	O	3.9	1.29	50	50	10	50
4.12	B	X	3.38	1.32	50	50	10	50
	B	O	3.9	1.29	50	50	10	50
4.13	A	X	2.62	1.5	50	50	10	25
	A	O	3.59	1.3	50	50	10	25

- a Bead purge setting (%)
- b Bed flow setting (%)
- c Total airflow from 3400FB
- d Chain speed (%)

FIGURE 4.8

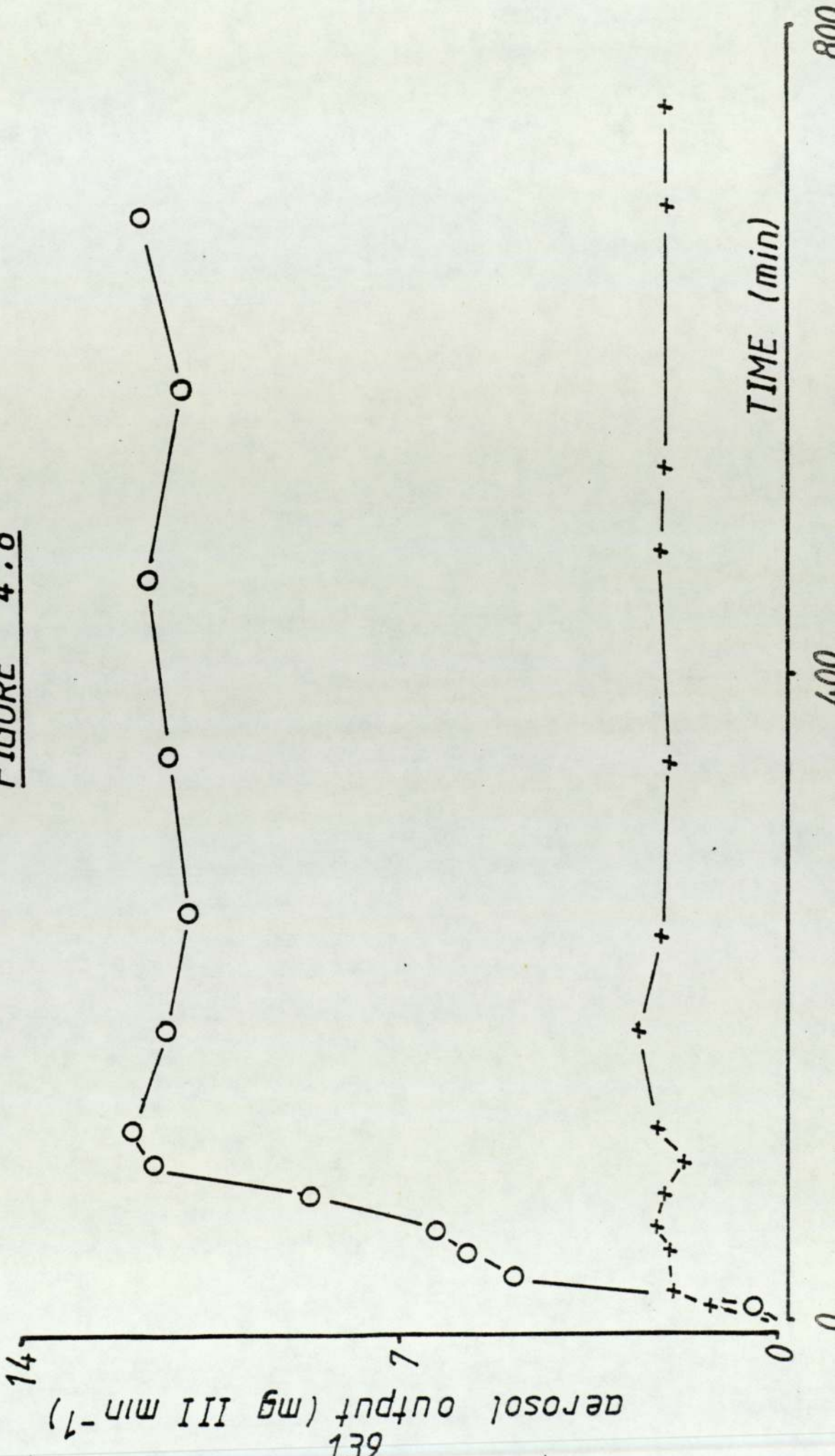


FIGURE 4.9

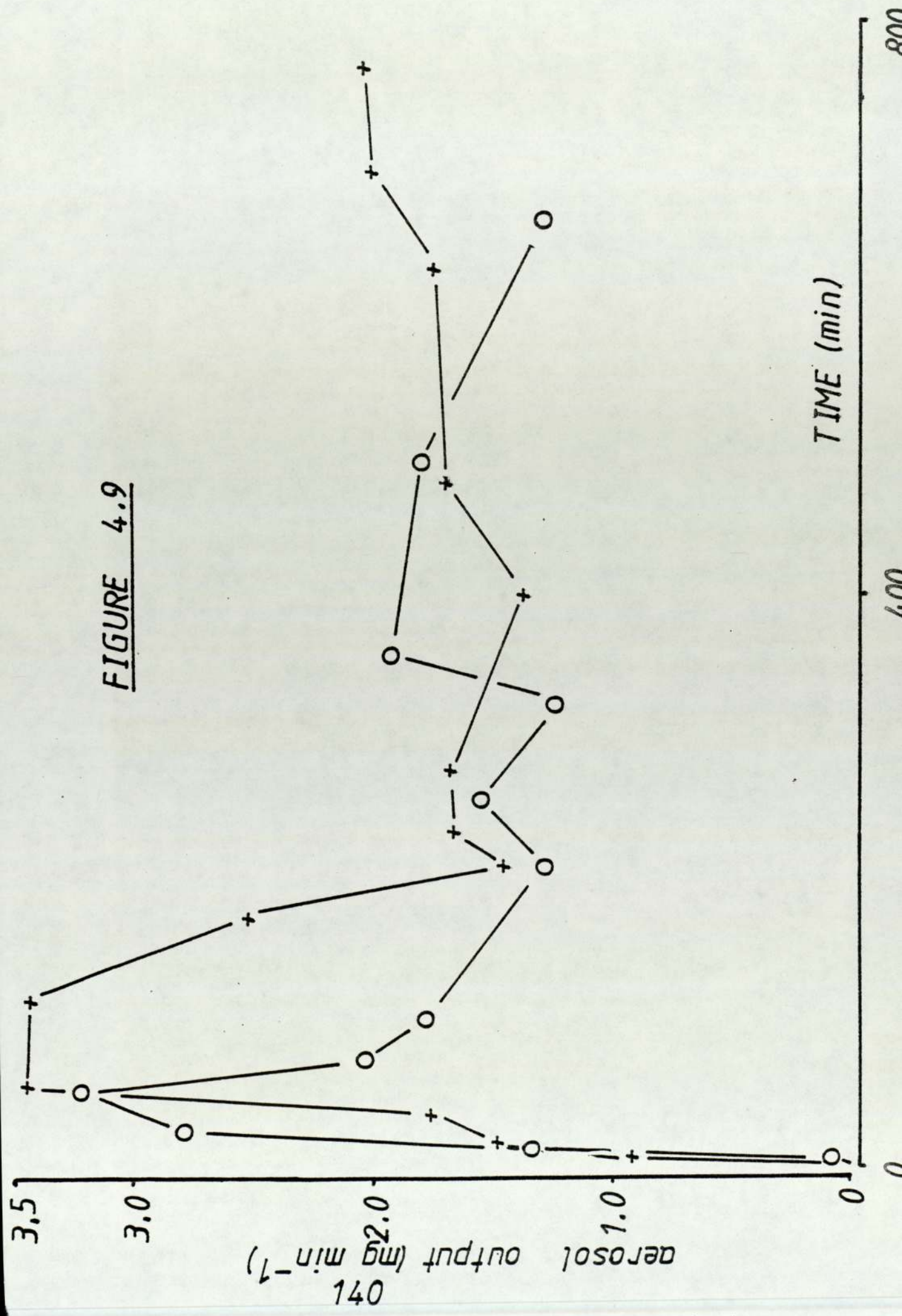


FIGURE 4.10

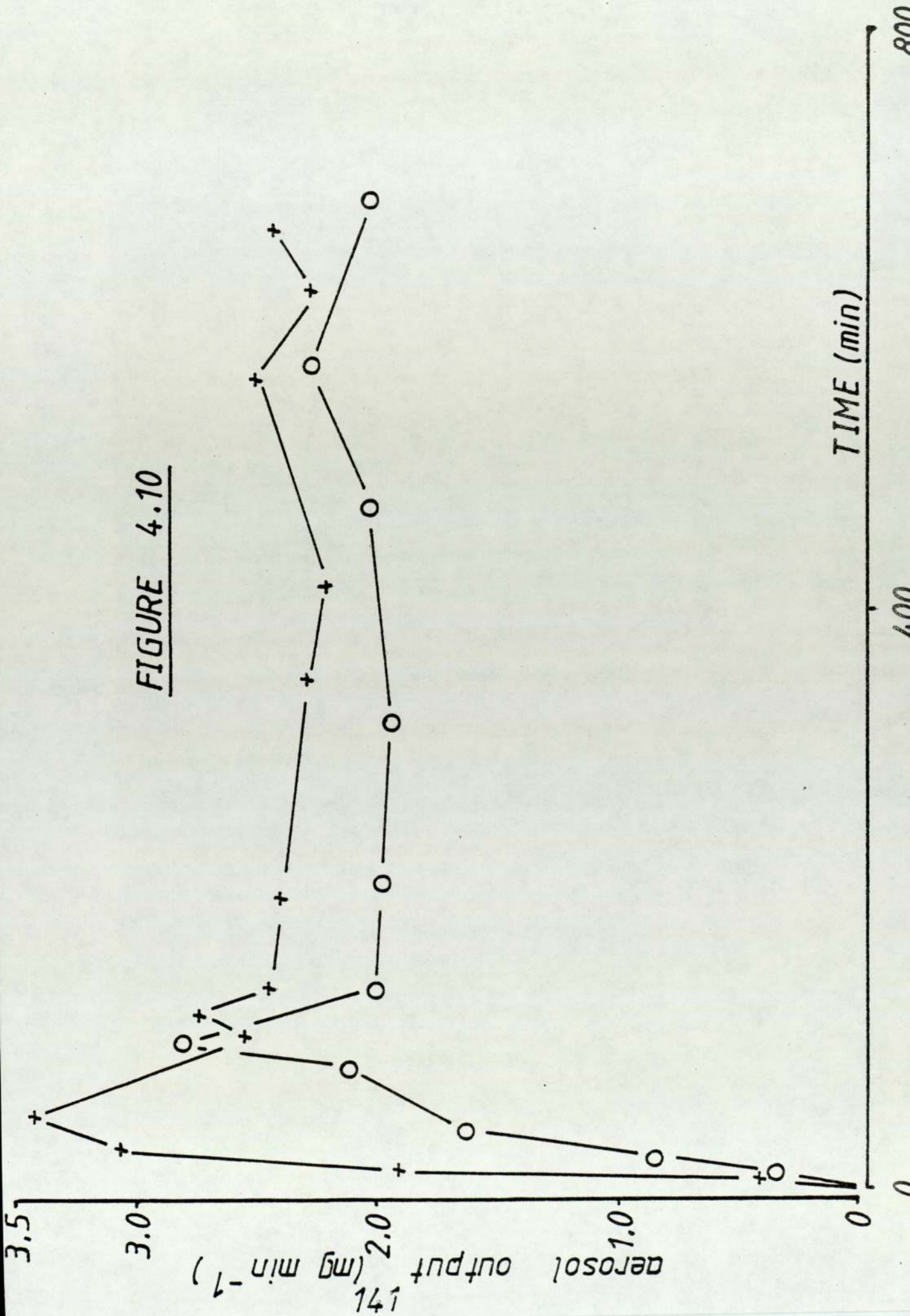


FIGURE 4.11

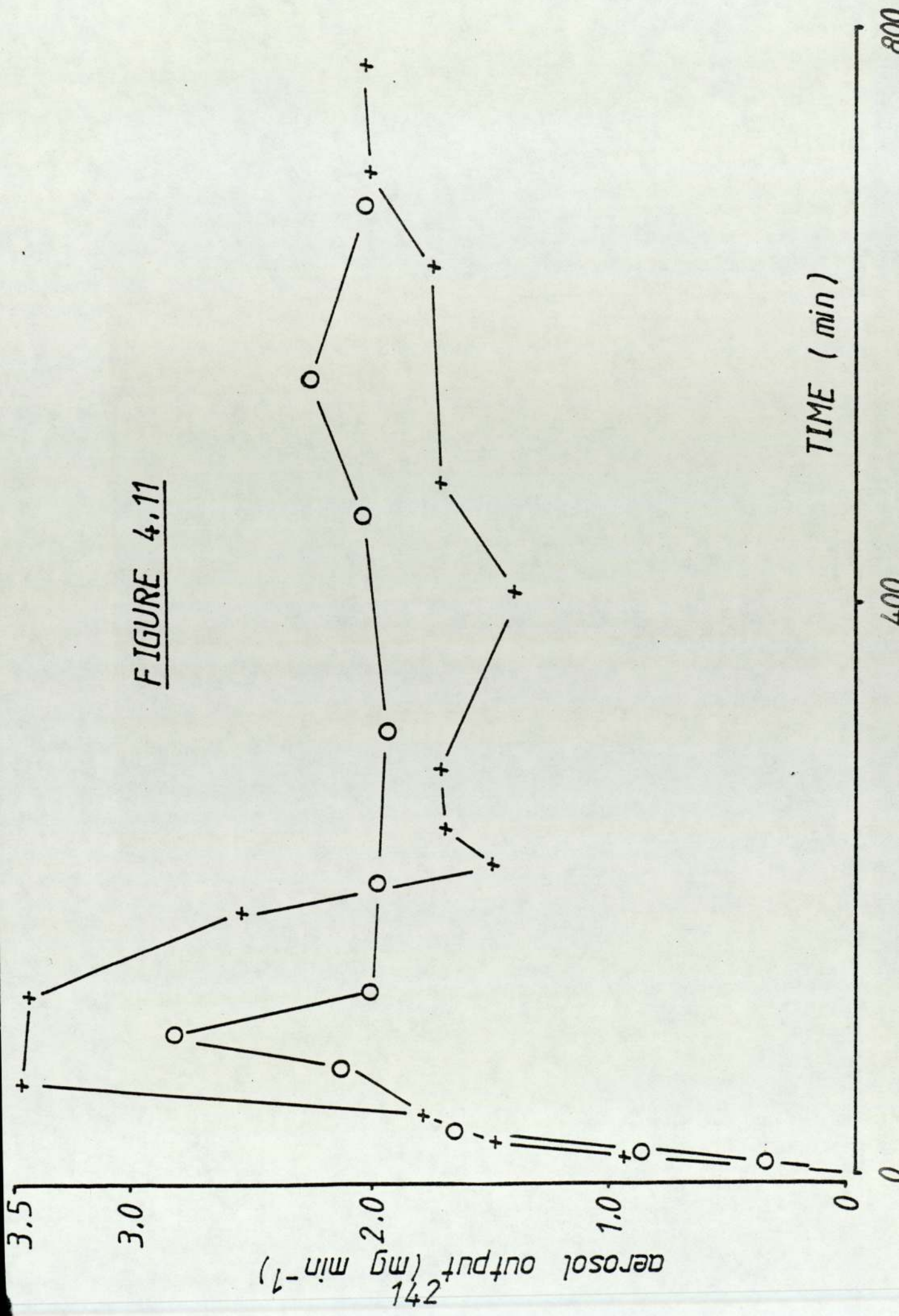


FIGURE 4.12

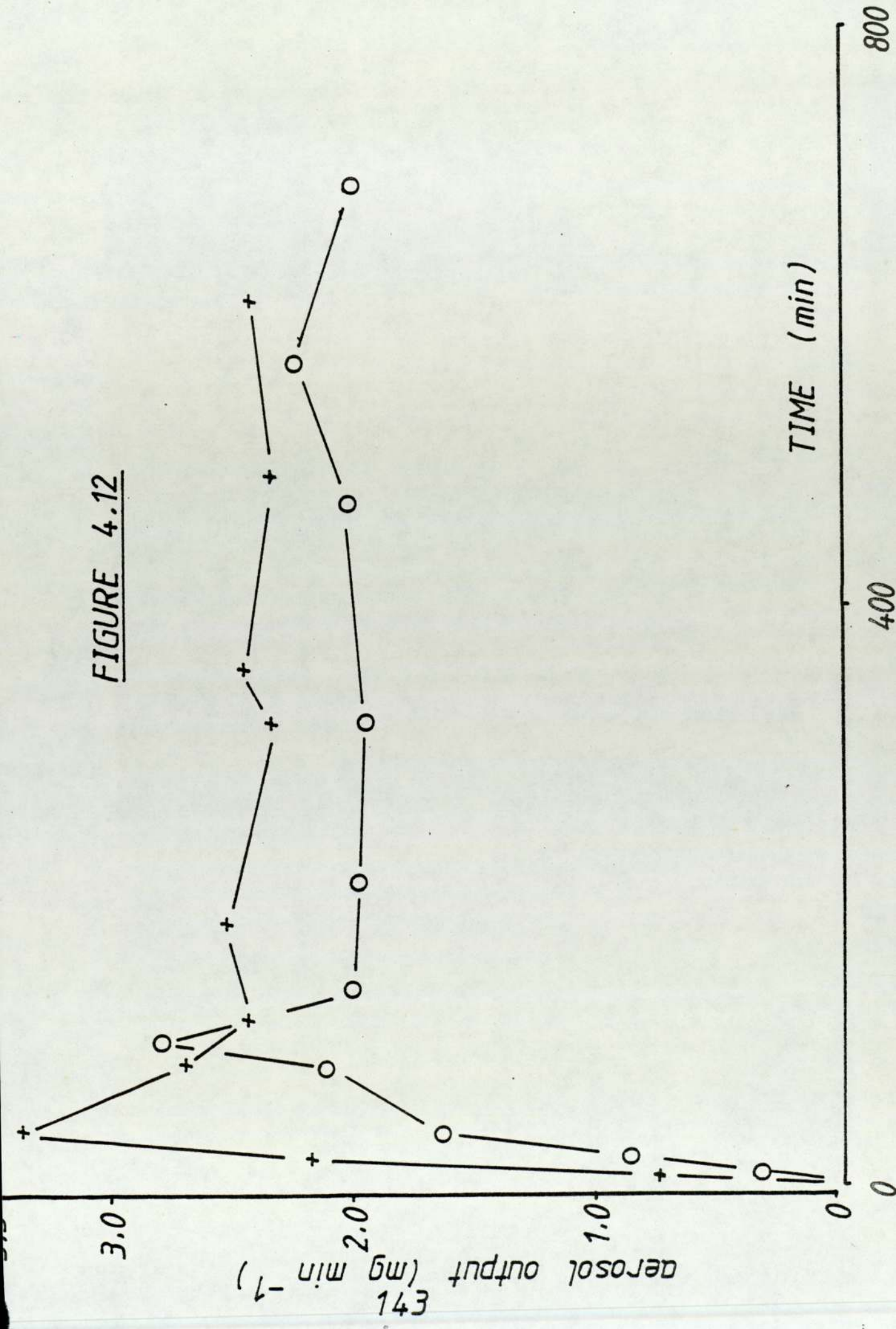


FIGURE 4.13

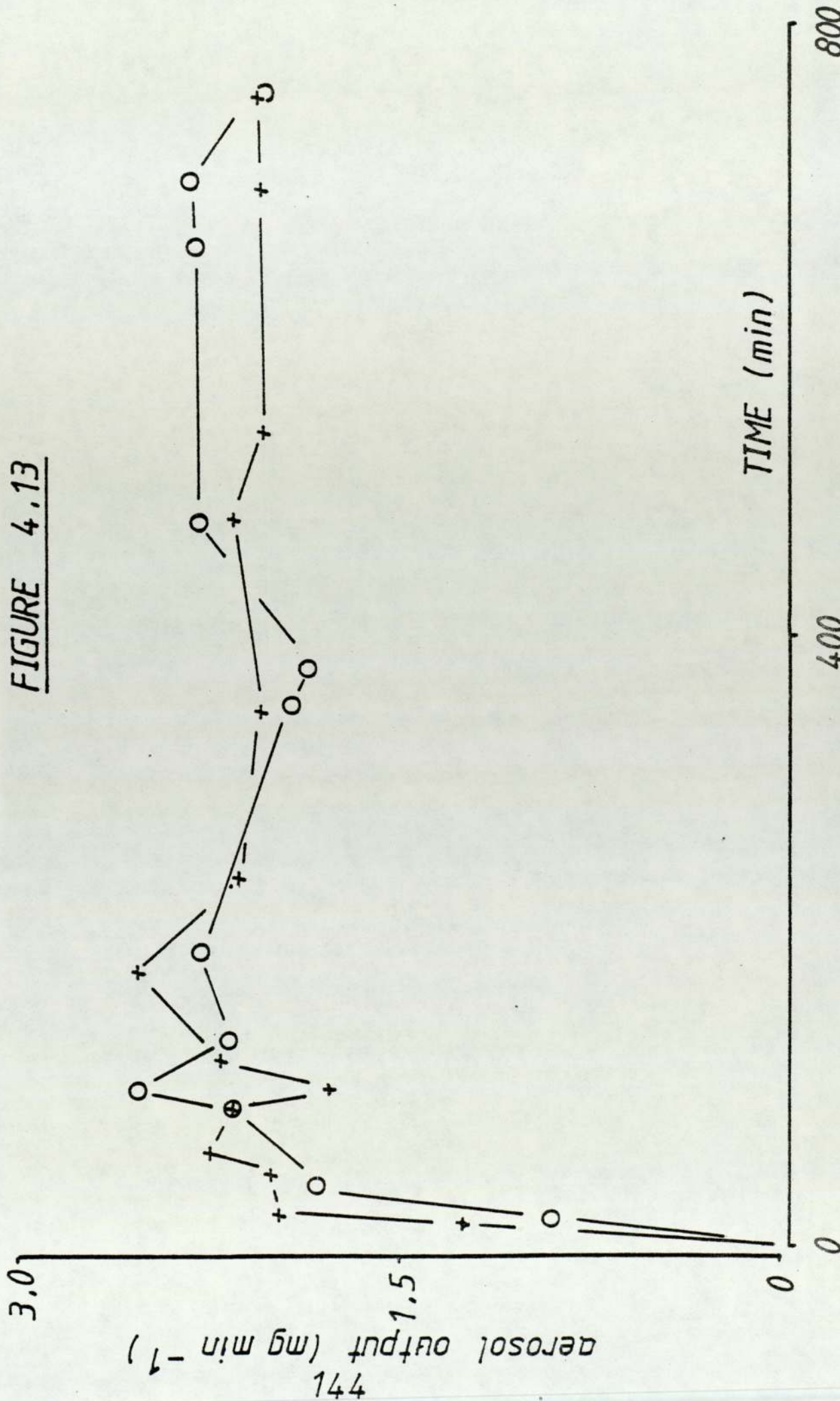


FIGURE 4.14

Concentration (ng ml^{-1}) of III in aerosols generated from powder sub-batch A in (a) main aerosol(☆)stream ($\text{MMD}_{0.5} = 3.6\mu\text{m}$, $\sigma_g = 1.22$) (C, Fig 4.6) and (b) delivery tube (S, Fig 4.6). Aerosols were withdrawn through S at 112 (●), 56 (■) and 28 (▲) ml min^{-1} .

FIGURE 4.14

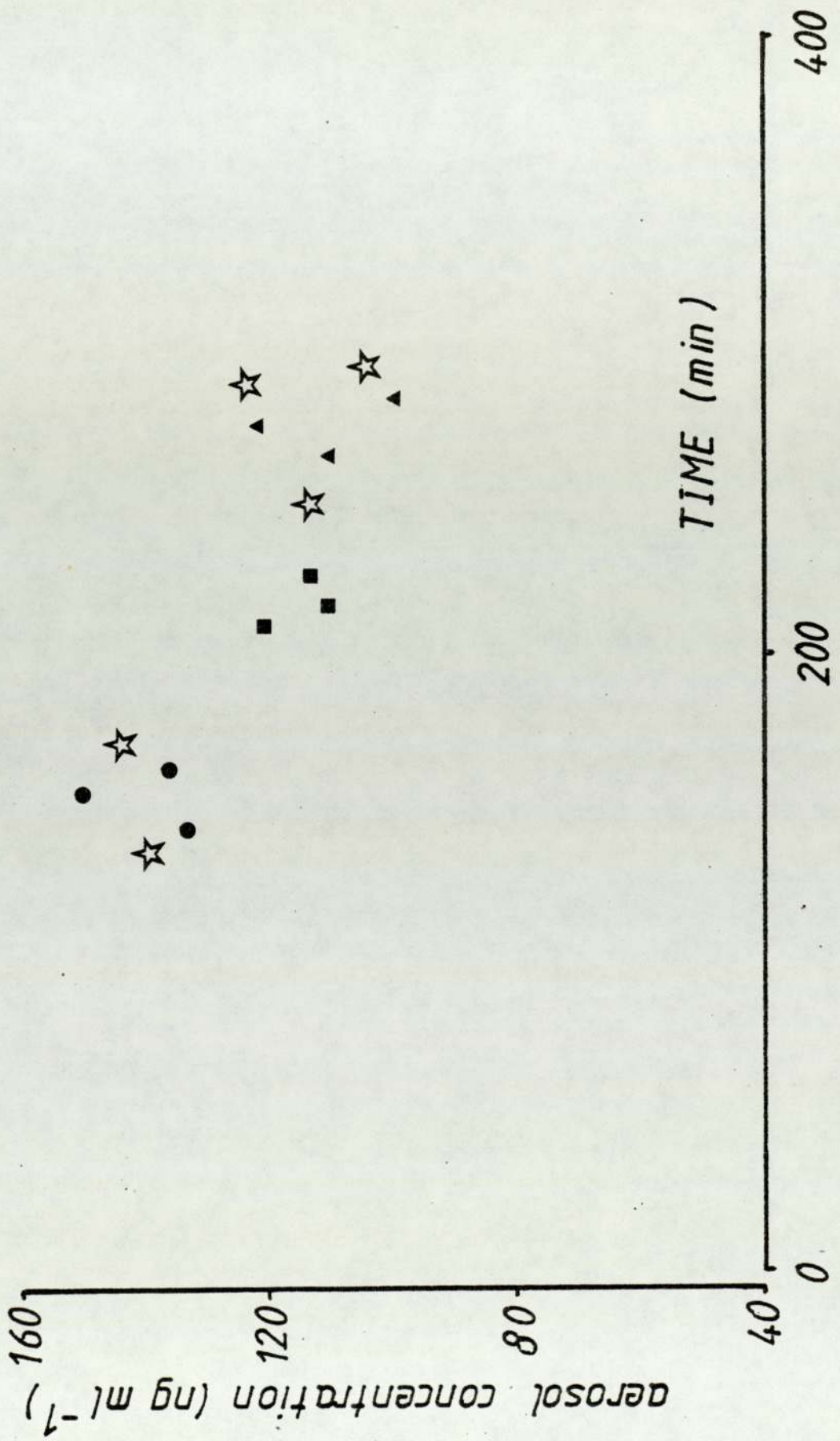


FIGURE 4.15

Concentration (ng ml^{-1}) of III in aerosols generated from powder sub-batch D in (a) main aerosol(★)stream ($\text{MMD}_{\text{aa}} = 4.3\mu\text{m}$, $\sigma_g = 1.35$) (C, Fig 4.6) and (b) delivery tube (S, Fig 4.6). Aerosols were withdrawn through S at 112 (●), 56 (■) and 28 (▲) ml min^{-1} .

FIGURE 4.15

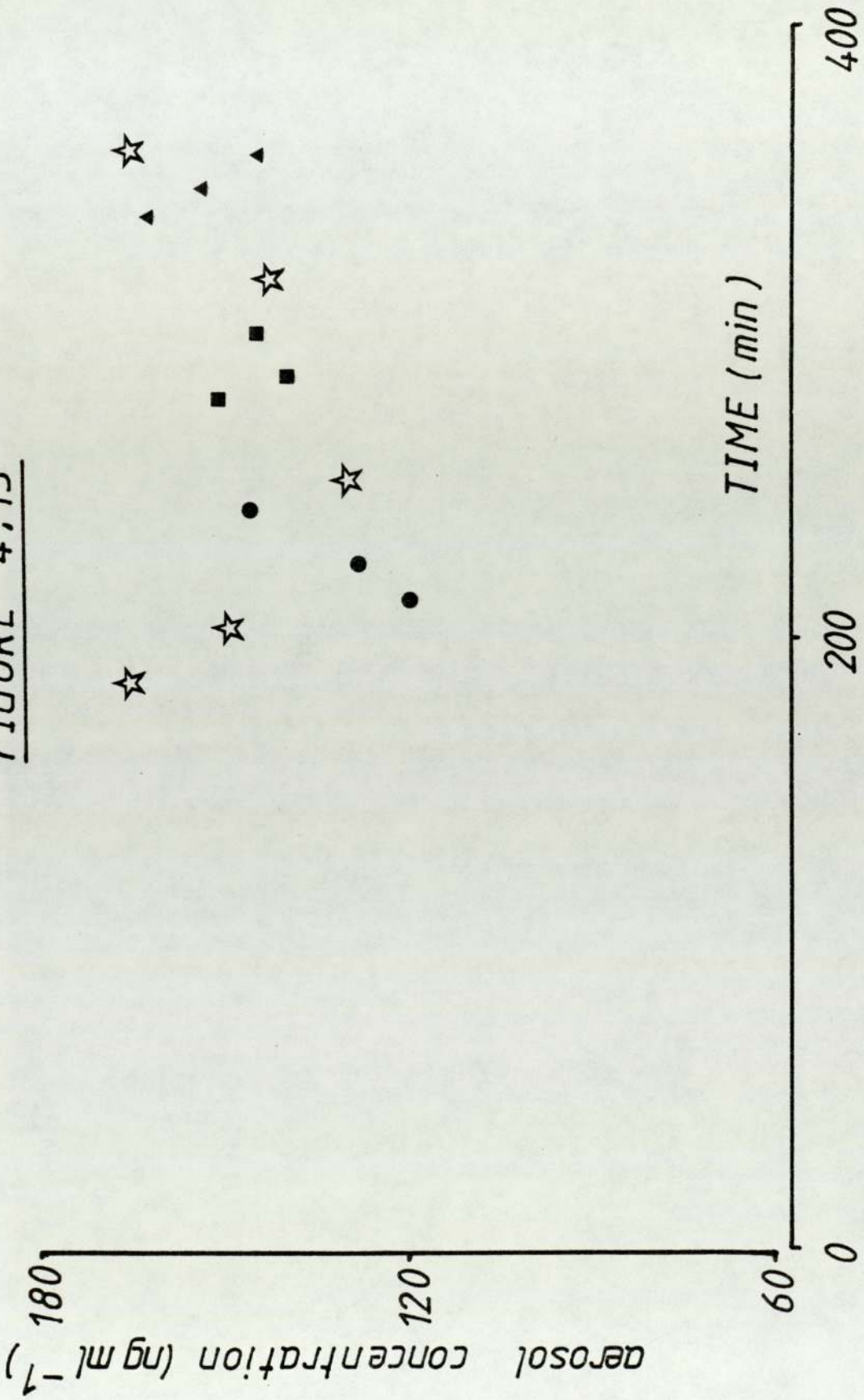


FIGURE 4.16

Aerosol particle size distribution determined using a cascade impactor before aerosol administration to the iprl. Cumulative percent mass less than indicated size (probability scale) is plotted versus aerodynamic diameter (log scale). The hatched line represents the best fit to the experimental data determined by eye.

see text p.118

FIGURE 4.16

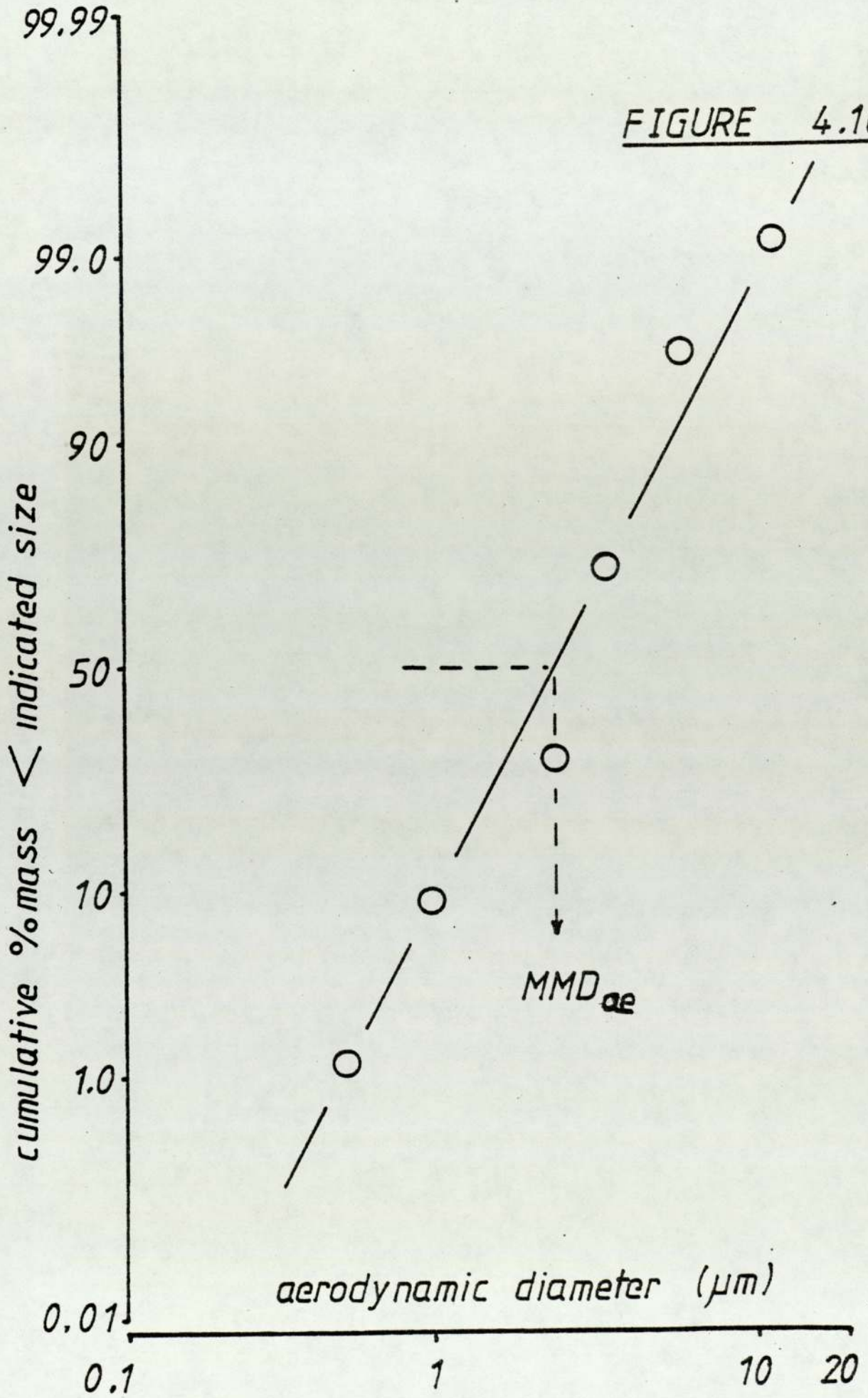
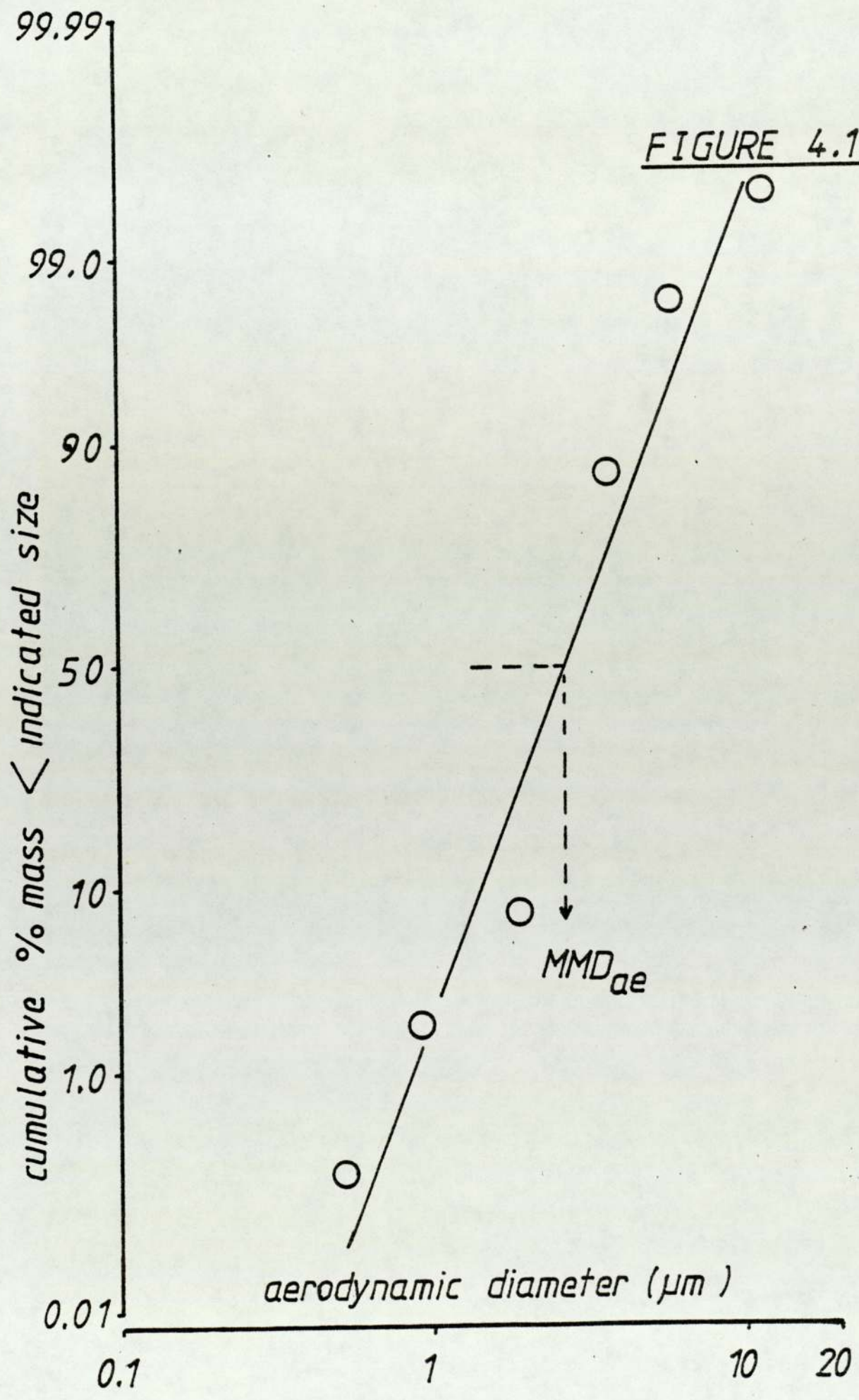


FIGURE 4.17

Aerosol particle size distribution determined using a cascade impactor after aerosol administration to the iprl. Cumulative percent mass less than indicated size (probability scale) is plotted versus aerodynamic diameter (log scale). The hatched line represents the best fit to the experimental data determined by eye.

see text p.118

FIGURE 4.17



CHAPTER FIVE

AEROSOL ADMINISTRATION TO THE ISOLATED, PERFUSED RAT LUNG

5.1 INTRODUCTION

The work described in this chapter concerns the administration of well - characterised aerosols of II to the iprl preparation. The apparatus, surgical and analytical techniques required for this work had been developed and evaluated previously, as described in Chapters 2, 3 and 4.

Experiments designed to assess the reproducibility of II aerosol deposition and subsequent airway-to-perfusate transfer of III in different iprl preparations are described. In these experiments, the aerosol psd, perfusate flow rate, and respiratory regime were held as constant as was practicable for different iprl preparations. The effects of each of these variables upon deposition and transfer, was then made the subject of further investigations. The results were used to assess (a) the likely, primary deposition mechanism for the aerosols studied in this model (b) the probable rate-limiting process for III transfer and (c) the factors affecting aerosol regional deposition and the rates and extent of III transfer to the perfusate. The order of

the kinetic process governing III transfer to the vasculature is deduced and theories advanced concerning the effect of aerosol regional deposition on transfer rate-constants. These theories are used to make deductions concerning the permeability characteristics of the pulmonary epithelium in the perfused regions of the respiratory tract.

5.2 MATERIALS AND METHODS

Aerosols were administered to the iprl preparation using the apparatus shown in Fig 5.1 (Plate 15). This apparatus combined that described in Chapter 2 (Fig 2.5) which housed the isolated lung, with the aerosol generation and administration apparatus described in Chapter 4 (Fig 4.6). The 3400FB reservoir was primed with dried (section 4.3.2.2) powder of II. The generator was switched on and the bead purge and bed flow air supplies adjusted to give a total flow rate of 10 l min^{-1} . The powder feed chain was set in motion at a known rate and the generator allowed to "warm up" for approximately 2.5hr with aerosol going to waste in M1 and M2 (C3 and D1 open, Fig 5.1). Mass III aerosol output samples were taken at various times during the warm up period, using the method described in Chapter 4 (section 4.3.2). At approximately 2.25hr, and following rat anaesthetisation, the rat lungs were isolated using the surgical techniques described in Chapter 2 (section 2.2.6) and suspended horizontally in the AT. The AT was sealed and 4ml air withdrawn from it using a syringe. This manoeuvre drew a small amount of air into the isolated lungs. The iprl preparation was allowed to equilibrate in the AT for 10min. During this period, a 1min aerosol sample was taken to determine aerosol psd, using the cascade impactor, as

described in Chapter 4 (section 4.3.4). The delivery tube, S (Fig 5.1), was connected to the isolated lung by silicone rubber tubing (bore 0.2cm, wall thickness 0.1cm, Esco(rubber) Ltd., Twickenham, U.K.) of minimal length (0.5cm) and therefore, dead space. The tubing clip S1 remained in place. A mass III aerosol output sample was taken. Perfusate in the perfusate reservoir was sampled, and the volume replaced with K4. The clip, S1, was removed and simultaneously, the lungs made to ventilate using negative pressure changes in the AT as described in Chapter 2 (section 2.2.8). The pressure in AT was monitored as a continuous function of time and tidal volume calculated as previously described (Chapter 2, section 2.2.8).

Perfusate samples were taken from the reservoir at specific times after the initiation of ventilation. Each sample was replaced by an equal volume of fresh K4. At precisely 20min after initiation, ventilation was stopped after exhalation and S1 replaced simultaneously. Mass III aerosol output was again sampled. Perfusion and sampling continued for up to 3hr, during which time perfusate pH and volume were maintained as described in Chapter 2 (sections 2.3.5 and 2.2.7).

At the end of an experiment, all electrical apparatus was disconnected, except for the generator, which remained running. The lungs were removed from the AT and homogenised as described in Chapter 3 (section 3.2.2). The tracheal cannula was washed with DDW and the washing made up to known volumes. All samples, perfusate, homogenised lung and cannula washings were stored and assayed as described in

Chapter 3 (section 3.2.2).

A second 200ml aliquot of K4 was then circulated through the iprl apparatus at 37°C, until the pO_2 exceeded 400mm Hg. Another rat was anaesthetised and the procedure described above repeated. Attempts were made to carry out as many administration experiments as possible during each generator run. Mass III aerosol output was determined before and after each ventilation period and aerosol psd samples taken at approximately 2 and 10hr of generator running time. Aerosol samples were treated as described in Chapter 4 (section 4.3.5.1 and 4.3.5.2).

When studying the reproducibility of II aerosol deposition and subsequent airway-to-perfusate transfer of III, following the administration of identical aerosols to consecutive rat lungs, perfusate flow rate (PF), respiratory frequency (RF) and stroke volume of the respirator were held constant. Nevertheless, some variability was present in values for tidal volume (TV) between experiments, due to small differences in lung compliance between rats. Subsequently, the effect of each of aerosol psd, PF, RF and TV were studied by altering each variable in turn, while holding the remainder constant. In order to study the effects of aerosol psd on deposition and transfer, the generator was thoroughly cleaned between experimental runs and different sub-batches of II (section 4.3.2) placed in the reservoir.

The amount of II deposited in the iprl during lung ventilation (expressed in III equivalents throughout) was determined by summing the corrected (section 3.3.5) amounts

found after analysis of the perfusate and lung homogenate. The amount deposited in each experiment was expressed as a fraction of the total amount inhaled (given by the product of III concentration of the aerosol and the total volume inhaled (sum of tidal volumes). Thus the fraction deposited,

$$f_d = (\text{amount III deposited}) / (\text{amount III inhaled}) \quad (\text{Eq 5.1})$$

The amount of III transferred from airway-to-perfusate at any time during an experiment was expressed as a fraction of the total III deposited after the 20min administration period. Thus the fraction transferred was given by

$$f_t = (\text{amount III transferred}) / (\text{amount III deposited}) \quad (\text{Eq 5.2})$$

Fractional deposition (f_d) and the time dependency of fractional transfer (f_t), were studied as functions of aerosol psd, PF, TV and RF, after first examining data variability between iprl preparations.

5.3 RESULTS

A summary of the original data, from which the various figures and tables in this Chapter are constructed, appears in tabulated form in Appendix A.

Figures 5.2 to 5.12 are the fractional transfer versus time profiles resulting from the administration of numerous different aerosols of II (MMD_{50} ranged 2.62 to 4.00 μ m) to a number of iprl preparations under various conditions of PF, RF and TV. All profiles were sigmoidal in shape and reached plateaus approximately 70min after ventilation commenced. Transfer was initially slow, during the 20min ventilation period under all experimental conditions, but increased rapidly once administration of II was complete. The fraction of the asymptote transferred per unit time appeared to be similar in all cases, implying that the half life for transfer of III was also similar. The total fraction transferred as time, $t \rightarrow \infty$ (plateau value, f_{∞}) however, was variable but always less than unity.

5.3.1 Reproducibility

Figure 5.2 shows f_t versus t profiles following administration of the same aerosol ($MMD_{50} = 3.98\mu$ m) to two,

consecutive, isolated lungs. The variables PF, RF and TV were held effectively constant. Rates of transfer and values for f_{∞} (~ 0.4) were extremely reproducible. Similarly, Fig 5.3 shows f_t versus t profiles following administration of a different aerosol ($MMD_{50} = 3.88\mu\text{m}$) to two different iprl preparations. Once more, rates of transfer and f_{∞} were almost identical. The values for fractional deposition, f_d , for each pair of experiments (0.35 and 0.37, Fig 5.2; 0.17 and 0.22, Fig 5.3) were similar; the slight differences may have been due, not only to inter-animal variation, but also to the unavoidable small differences in TV (section 5.3.2.2).

5.3.2 Fractional Deposition

5.3.2.1 Effect of respiratory frequency (RF)

Table 5.1 presents values of f_d resulting from the administration of the same aerosols to different iprl preparations, at three different values for RF while the stroke volume and PF were held constant (TV effectively constant). For one aerosol ($MMD_{50} = 2.62\mu\text{m}$), two-fold decreases in RF, 28 to 14 to 7 cycles min^{-1} , caused approximately two-fold increases in f_d (0.13 to 0.27 to 0.63). A similar effect was observed with the larger ($MMD_{50} = 3.98\mu\text{m}$) aerosol although attempts to study f_d at 7 cycles min^{-1} failed due to onset of pulmonary oedema during administration. It should be noted here, that subsequent aerosol generations, even using the same powder in the

3400FB, were unsuccessful in producing an identical aerosol psd. Because any three experiments took some 15hr to complete, failure at any juncture may result in incomplete data (Table 5.1; ND = no data).

5.3.2.2 Effect of tidal volume

The effect of TV upon fractional deposition in the iprl was dramatic (Table 5.2). When the same aerosol (MMD_{50} 3.96 μ m) was administered to three consecutive preparations, at three different values for TV, increasing TV produced greater values of fd (0.07 to 0.28 when TV ranged 0.92 to 2.25ml, respectively). Similar, but more subtle effects of TV upon fd have probably been observed. Examples are shown in the legends of Figs 5.2 and 5.3 where the much smaller increases in fd correspond to slight increases in TV.

5.3.2.3 Effect of aerosol particle size

Table 5.3 shows that at RFs of 28 and 14 cycles min^{-1} , aerosol psd seemed to have no marked effect upon fd when PF and TV were effectively constant. If anything, a slight increase in fd occurred with increasing MMD_{50} . When RF = 7 cycles min^{-1} however, an increase in MMD_{50} from 2.62 to 3.96 μ m resulted in a decrease in fd from 0.63 to 0.28. An explanation for this phenomenon is advanced in the Discussion section of this chapter.

5.3.3 Fractional Transfer

5.3.3.1 Effect of perfusate flow rate

A three-fold increase in PF, from 5 to 15ml min⁻¹, had no effect upon transfer rate or the value of f_{∞} , when the same aerosol (MMD₅₀ = 3.96 μ m) was administered to two consecutive rat lungs, under similar respiratory regimes (Fig 5.4: RF = 28 cycles min⁻¹, TV \sim 1.5ml). Similarly, Fig 5.5 shows that when two aerosols of approximately the same size (3.59 and 3.88 μ m) were administered (RF = 7 cycles min⁻¹, TV \sim 2ml), the same three-fold difference in PF had little effect on transfer rate or f_{∞} .

5.3.3.2 Effect of respiratory frequency

When the same aerosol (MMD₅₀ = 2.62 μ m) was administered to three iprl preparations at 28, 14 and 7 cycles min⁻¹ (TV \sim 2ml, PF = 15ml min⁻¹) fractional transfer rates and f_{∞} increased with increasing RF (Fig 5.6). The same phenomenon was observed on administration of 3.98 and 3.88 μ m aerosols at 28 and 14 cycles min⁻¹ (Figs 5.7 and 5.8 respectively). For each experiment however, the time taken to reach a particular fraction of the asymptote appeared to be similar and independent of RF or aerosol psd.

5.3.3.3 Effect of tidal volume

When the same aerosol (MMD₅₀ = 3.96 μ m) was

administered to three consecutive iprl preparations, perfused at the same rate and ventilated at the same frequency, an increase in TV from 0.92 to 2.25ml caused a marked increase in transfer rate and f_{∞} . The rates at which the asymptotes were approached, and the half life of transfer however, seemed to be independent of TV (Fig 5.9).

5.3.3.4 Effect of aerosol particle size

Fractional transfer rate and f_{∞} appeared to be dependent upon aerosol psd although, once more, the half lives were similar. At all RFs investigated (28, 14 and 7 cycles min^{-1}), when RF, TV and PF were effectively constant, a decrease in aerosol mass median aerodynamic diameter resulted in increased transfer rates and f_{∞} (Figs 5.10, 5.11, 5.12).

5.3.4 Solution versus aerosol transfer rates

Figure 5.13 compares the f_t versus t profiles following the deposition of II in three iprl preparations, in the form of (a) an aerosol (Experiment A5 (Appendix A), $\text{MMD}_{50} = 2.62\mu\text{m}$; the smallest and most rapidly absorbed aerosol employed in the studies described in this thesis) and (b) an intratracheally instilled solution (Experiments I and II, Chapter 3, Table 3.5). Note however, that f_{∞} was only experimentally determined following aerosol administration. The rates of transfer of III after instillation were faster than for a comparable deposited

amount of aerosol. For instillation however, fluorescein was administered as a bolus (40.57 and 46.87 μ g in experiments I and II respectively) at time, $t = 0$, whereas deposition of 36.6 μ g occurred over a 20min period during the aerosol administration experiment.

If fluorescein transfer to the perfusate after instillation, is assumed to be described by first-order kinetics, as was the case after aerosol administration (section 5.4.4), then log-linear plots of $(f_{\infty} - f_t)$ versus t (first-order plots) may be constructed given estimates for the asymptote f_{∞} . Different values were therefore assigned to f_{∞} using an iterative technique and first-order plots constructed such that correlation coefficients were maximised. These plots are shown in Fig 5.14 (see also Table 5.4) together with a similar plot for the aerosol administration experiment A5 (section 5.4.4). Linear regression analysis of the data also provided estimates of the first-order rate constants for the transfer process as 0.057 and 0.054 min^{-1} for instillation experiments I and II respectively. The average of these two rate constants (0.056 min^{-1}) was similar to the average value (0.054 min^{-1}) for the rate constant, k , calculated from all the aerosol administration experiments performed on the iprl (see Discussion section of this chapter).

5.4 DISCUSSION

All transfer profiles of III from airway-to-perfusate were sigmoidal in shape. Values for the fractional transfer rates and the asymptote, f_{∞} however, varied with TV, RF and aerosol psd. In all cases f_{∞} was less than unity. Its value in a particular experiment was almost certainly due to the relationship between aerosol regional deposition and regional perfusion of the iprl. Figure 5.15 shows the ^{manner in} which the lungs are supplied by the pulmonary circulation. This circulation does not supply the trachea or the upper bronchii. Thus, because other vasculature is removed in the iprl preparation, solid aerosol deposited in unperfused areas was unlikely to be transferable to the perfusate, even given prior dissolution. It follows therefore, that any experimental variable which increases penetration of the lower airways, is likely to increase f_{∞} and the rate of fractional transfer. This argument is based upon that discussed in chapter 3 (section 3.3.6, Scheme 1) and shows how the value of f_{∞} in a given experiment relates to the depth of penetration of the RT.

5.4.1 Reproducibility

When the same aerosol was administered to two

consecutive isolated lungs under similar conditions of PF, TV and RF, both fd and the airway-to-perfusate transfer profiles were almost identical. Due to the length of each administration experiment, and the difficulty of reproducing aerosols on different generator runs however, reproducibility could only be studied in a maximum of two ipr1 preparations. This precluded the application of statistical data analysis for both reproducibility studies and other aerosol administration experiments. The data presented in the f_t versus t profiles (Figs 5.2 to 5.14) was thus derived from one experiment per profile. Nevertheless, Fig 5.2 and 5.3 show the excellent agreement between "duplicate" experiments which involved <7% inter-preparation transfer profile variability.

5.4.2 Effects of respiratory frequency, tidal volume and aerosol particle size upon fractional deposition

The main mechanisms of aerosol particulate deposition within the respiratory tract are considered to be impaction, sedimentation and diffusion (27, 48, 93). The majority of the aerosol particles employed in the investigations described in this thesis were $>1\mu\text{m}$ and therefore, Brownian motion (and thus diffusion) were thought to be unimportant in these investigations (25, 48, 92, 93). Impaction is the dominant mechanism of deposition in many models. Indeed, the mechanism is known to be important during aerosol administration to asthmatic humans using pressure-pack inhalers (93). In such cases, the majority of the metered

dose impacts in the throat, and is subsequently swallowed, never reaching the lungs (93, 95). In the model used in this thesis however, the primary mechanism of aerosol deposition appeared to be sedimentation, rather than impaction (a phenomenon which is known to exist under some conditions in the human RT; 25, 93). This statement is supported by the data presented in Table 5.1. If impaction had predominated then, as RF increased, and the linear velocity with which particles entered the RT increased proportionally, fractional deposition, f_d , should also have increased. Clearly, the opposite was true, f_d decreasing by approximate factors of 2, when RF increased from 7 to 14 to 28 cycles min^{-1} (TV \sim constant 2ml). Because, for these two aerosols (Table 5.1), the slower RF afforded greater particulate residence time in the RT, f_d increased with increasing time available for sedimentation from the aerosol stream.

Fractional deposition increased with increasing TV, at constant PR, RF and aerosol psd (Table 5.2). A larger TV must give rise, at constant RF, to higher linear velocities but, more importantly, greater penetration of the smaller diameter lower airways. Given sedimentation as the major mechanism for deposition, increasing values for f_d should result, due to a decrease in the required sedimentation distance further down the RT in the narrower airways (when the air velocity will be lower, since the total cross-sectional area is greater in the lower, than the upper airways (25)).

Aerosol psd appeared to only slightly affect values for f_d at RFs of 28 and 14 cycles min^{-1} (f_d increased

marginally with increasing particle size, Table 5.3). At 7 cycles min^{-1} however, the opposite occurred and f_d decreased markedly with increased aerosol MMD_{50} . It would be logical to suppose that, if sedimentation was the major deposition mechanism, f_d should increase with increasing aerosol particle size. At first sight, these observations (at 7 cycles min^{-1}) seem difficult to explain. Disodium fluorescein however, is very hygroscopic and its solid particles are likely to hydrate rapidly, not only in the humid environment of the airways, but also in the pipework connecting the iprl to the main aerosol stream. Thus, the smaller the RF (and the larger the residence time), the greater is the opportunity for particles to undergo significant hygroscopic growth and sediment from the airstream. In the cases where f_d apparently decreased with increasing MMD_{50} (7 cycles min^{-1} , Table 5.3), the amount of material washed from the flexible tubing connection and tracheal cannula was double that found in fractional terms at 14 cycles min^{-1} (compare the ratio of amounts in the tracheal cannula to the amount delivered in Tables A6 and A7 of Appendix A). Thus, the reversal in trend (f_d with particle size) shown in Table 5.3 is probably an indication that (a) disodium fluorescein undergoes rapid hygroscopic growth and (b) because of this, the aerosol concentrations actually entering the iprl at low respiratory frequencies, are significantly smaller than those in the main stream (analogous to the term $(1-f_d)AA$ increasing at low RF; Scheme 1, section 3.3.6, Chapter 3). Thus, it appeared as if f_d decreased with increasing MMD_{50} .

When hygroscopic growth occurs during aerosol administration of a highly soluble material to a real lung, the problem of aerosol characteristics changing before particles enter the "lung proper" is inevitable, however the system is designed. It was clear that under the experimental^a conditions described in Chapter 4 (section 4.3.3), when the atmosphere was dry and concentration of aerosol measured in the main stream differed insignificantly from that in the delivery tube (S, Fig 4.6), the sedimentation of particles due to hygroscopic growth, as proposed during administration to the iprl, did not occur.

5.4.3 Effects of perfusate flow, respiratory frequency, tidal volume and aerosol particle size on fractional transfer

Before the airway-to-perfusate transfer of III could occur, deposited disodium fluorescein (II) had first to dissolve within the respiratory tract. Reference has already been made to the hygroscopic nature and extremely high water solubility of II (fluorescein exists largely as the dianion, III, at physiologic pH in aqueous solution). It is likely therefore, that dissolution is rapid, after deposition in the fluid-bathed (24, 40) linings of the RT, and that transfer would be either diffusion or perfusion limited. The iprl would tolerate up to a 3-fold change in perfusate flow, between 5 and 15ml min⁻¹, and still remain viable. Because however, such a change in PF had no effect on either the rate or extent of fluorescein transfer to the perfusate (Fig

5.4 and 5.5), perfusion limitation could be eliminated. Thus, provided transfer was apparent first-order, diffusion could be assumed to be the predominant factor controlling solute transfer in this system. (It has been suggested that only extreme decreases in blood flow, to perhaps 1% of normal, equivalent to $\sim 0.9 \text{ ml min}^{-1}$ in a 400g rat, would slow transfer of lipophobic solutes such as III; 24.)

Effros and Mason (24) presented a collection of literature data on airway-to-vasculature transfer in a variety of different lung models and reviewed evidence to show that fairly high molecular weight, possibly ionised, solutes have absorption rate constants which are independent of blood flow, but appear dependent upon molecular weight, in support of a diffusion-controlled process. Solutes must pass through a number of barriers (pulmonary epithelium, interstitium, capillary endothelium) in order to transfer from the airways to the vasculature. The rate-controlling barrier however, in the case of ionised solutes with molecular weights similar to that of the fluorescein dianion (MW = 330), is believed to be the pulmonary epithelium (24, 96, 97).

The fractional rate of III transfer and f_{∞} were dependent upon lung TV, RF and aerosol psd. It is very probable that each of these three variables affected aerosol regional deposition in the RT (25, 42, 49, 51, 94) and the subsequent transfer of III.

Fractional transfer rates and values for f_{∞} increased with increasing RF, for the three aerosols investigated (Figs 5.6, 5.7, 5.8). This phenomenon was also thought to be

linked to the hygroscopic growth kinetics mentioned earlier. It is well established that droplets or soluble particles grow in environments of high relative humidity (rh) such as the respiratory tract (45, 48, 66, 91). On inhalation, water vapour condenses on the particle, which begins to dissolve and behave like a droplet. Given sufficient time, this droplet should continue to grow until condensation ceases when the vapour pressure of the droplet equals that of the environment. Deposition of II in the iprl was probably a function of the kinetics of this process. Because smaller particles grow faster than larger ones (48) it is possible that, when $RF = 28 \text{ cycles min}^{-1}$, only smaller, low mass particles grew significantly. With the greater residence times associated with $RF = 7 \text{ cycles min}^{-1}$ however, possibly all particles were able to grow. If this were true, then that fraction of the aerosol which was deposited in the lower airways, should be greater with the shorter ($28 \text{ cycles min}^{-1}$), as opposed to the longer ($7 \text{ cycles min}^{-1}$) residence times.

Increasing values for TV, with RF held constant, increased fractional transfer rates and the transferable fraction $F = f_{\infty}$, when the same aerosol was administered to consecutive iprl preparations. This was almost certainly due to an increasing fraction of the inhaled amount, penetrating the lower airways at higher TVs. Studies on the effects of TV in this model were limited to a small range of values. Tidal volumes must be large enough to overcome "dead space" in the pipework connecting the iprl to the aerosol stream ($\sim 0.15\text{cm}^3$ in this system), but not so large as to cause

lung damage (7, 98).

A decrease in aerosol MMD₅₀, at all three RFs investigated, resulted in increased fractional solute transfer rates and f_{∞} . Once again, this was almost certainly due to increased penetration of the lower airways by aerosols consisting of smaller particles, the larger particles sedimenting from the airstream much higher in the RT. Reductions in the value of f_{∞} (= transferable fraction, F; Scheme 1) ^{p. 73} must result from deposition in these upper, unperfused regions of the lung.

In summary to this section therefore, all differences in the fractional transfer versus time profiles, which were observed as functions of aerosol psd, TV or RF, could be explained on the basis of these variables modifying the resultant regional deposition of the aerosolised solute.

5.4.4 Apparent first-order kinetics

Transfer half-lives, which were functions of the rates at which the asymptotes (f_{∞}) were approached (Figs 5.2 to 5.12) following aerosol administration to the iprl preparation, appeared to be similar for each experiment, and independent of f_{∞} , when the value of this transferable fraction of the material deposited, was modified by TV, RF or aerosol psd. The first-order, log-linear plots of ($f_{\infty} - f_t$) versus t were constructed for values of t , after administration was complete ($t = 20\text{min}$) and are shown in Figs 5.16 to 5.25. The use of experimentally observed asymptotes (values for f_{∞} derived from an average value for

f_t when $t > 70$ min) in these plots, produced either positive, negative or negligible deviations from linearity in the final 5% of the transfer profiles. For this reason therefore, values for f_∞ were assigned for each experiment according to the method described previously to linearise solution instillation data (section 5.3.4). These derived values for f_∞ deviated $< 8\%$ from the average values determined experimentally (except in experiments A4 and A10 (see Table 5.5)). Deviation for experiment A4 = 12.1% and was probably due to a falsely low amount of III found in the perfusate at 85min (Table A8, Appendix A). The large deviation of experimental from derived values of f_∞ for experiment A10 was again probably due to inaccuracies, in this instance because of the extremely small amounts of III transferred to the perfusate (Table A10, 0.942ug at $t = 90$ min being equivalent to only 4.6ng ml^{-1} in 200ml perfusate). For this reason, the value for the rate constant, k , for experiment A10 was thought to be unreliable and was not included in the determination of the average rate constant for transfer following aerosol administration. An inspection of the log-linear negative gradients (the apparent first-order rate constants for solute transfer, k) in Figs 5.16 to 5.25 revealed that all transfer rate constants appeared similar. The solid profiles in these Figs (5.16 - 5.25) were drawn after linear regression analysis of the $\ln(f_\infty - f_t)$ vs t data. The transfer rate constants, k , provided by this analysis are shown in Table 5.5. Values for k showed some inter-experiment variation (average $k = 0.054\text{min}^{-1}$, S.D. = 0.009min^{-1}) but certainly, no trends

in any expected direction. Brown and Shanker (40), as was mentioned earlier, implied that transfer rate constants should be faster when solute penetration in the RT is greater. The data in Table 5.5 shows that, for fluorescein, administered as a variety of aerosols, under different respiratory regimes to the iprl, the transfer rate constant, k , was independent of regional deposition of the solute (indicated by a lack of correlation between f_{∞} and k).

Fluorescein, dissolves rapidly at physiologic pH and is transferred by a non-perfusate flow limited process, from the airways to the vasculature in the iprl (section 5.4.3). Thus, transfer is presumably diffusion-limited, in which case, the first-order rate constant for the process should be given by (24)

$$k = (PA)/V \quad (\text{Eq 5.3}),$$

where diffusion occurs through a membrane of permeability, P , of cross sectional area, A , from a donor solution volume, V . If k remains effectively constant throughout the perfused regions of the RT, and the A/V ratio is also fairly constant (24; the progressive increase in area from the upper to the lower airways being accompanied by a proportional increase in fluid volume covering that area), then membrane permeability should also remain constant and regionally independent.

This argument may be extended further by observing that the permeability, P , should be given by

$$P = (DK_D)/h \quad (\text{Eq 5.4}),$$

where K_D is the solute's solution:membrane partition coefficient, D is its diffusion coefficient in the membrane and h is the thickness of the latter. If the rate controlling barrier in the RT is the pulmonary epithelium (24, 96, 97) and P is independent of region, then one possibility is that the barrier is effectively the same, causing all three variables, D , K_D and h to remain constant, throughout the perfused respiratory tract. Enna and Shanker (100) have obtained extremely reproducible solute transfer profiles, following the administration of 0.1ml solutions to the rat RT, despite the non-uniform distribution of the solution throughout the organ. Their data supports the theory advanced here, that pulmonary epithelial permeability remains effectively constant throughout the RT.

These arguments were advanced on the assumption that the transfer process for fluorescein, from the airways to the perfusate in the iprl, was apparent first-order. In order to support this assumption, if transfer was first-order, the rate constant k , should be independent of the amount of fluorescein deposited and transferable in the RT, A ($A = fd.F.AA$; Scheme 1, section 3.3.6). Because $F = f_\infty$, A may be calculated from

$$A = (\text{amount inhaled}).fd.f_\infty \quad (\text{Eq 5.5})$$

Table 5.6 presents values of A , alongside corresponding values of the rate constant, k . When A ranged from 12.28 to

38.05ug, k remained effectively constant and independent of the transferable dose. Additionally, Fig 5.26 shows the airway-to-perfusate transfer profiles for a range of values for A , presented as amount in the perfusate versus time. It is clear from this figure that the rate of transfer was effectively proportional to the transferable amount, a further piece of evidence in support of first-order transfer for the range of A values investigated.

It has been suggested (40), that other anions, the dye phenol red (31) and disodium cromoglycate (35; used in the prophylactic control of allergic asthma) are transferred partly by saturable, carrier-type transport and partly by diffusion, in rat lung. Although there was no substantial evidence for carrier-mediated transport of disodium fluorescein, a limit for diffusion-only transfer may have been approached for $A = 38.05\text{ug}$ (Fig 5.26), although the value of k for this experiment did not reflect this. Further investigations, involving larger transferable amounts are therefore necessary, if such transport processes are to be implicated for fluorescein's passage to the vasculature in the iprl.

5.4.5 Solution versus aerosol transfer rates

The rate of III transfer was faster following solution instillation than that found after aerosol administration. This observation could be explained by the fact that the transferable amounts A , although comparable, were introduced as a bolus during instillation and over a 20min period for

the aerosol. Average values for k after instillation or aerosol however, were very similar (0.056 and 0.054min^{-1} , respectively). Brown and Shanker (40) have previously reported that k from solution was approximately 2-fold less than k following aerosol administration, of the same compound to the rat lung. They suggested that the difference was due to more rapid absorption from the alveolar (aerosol administration) than from the tracheobronchial (instillation) parts of the lung. In the iprl, even though not all of the tracheobronchial regions of the RT are perfused, the findings for fluorescein are clearly different. Brown and Shanker's explanation is initially credible but probably incorrect. Their instillation experiments used the same volume (0.1ml) of donor solution as in these studies with fluorescein. It should be noted that 0.1ml is fairly large relative to the tidal volume of a rat and that Shanker's solutions were isotonic while the instillations in this thesis were performed in simple aqueous (and substantially hypotonic) solutions of II. Because water is known to equilibrate between the airway surfaces and the vasculature of the RT extremely rapidly (24, 40), the hypotonic solutions instilled into the iprl in these investigations was unlikely to disturb the area to volume ratio (A/V ; Eq 5.3) in the airways. Water should have left the donor solution within seconds of its instillation, to bring this solution to effective tonicity. In Brown and Shanker's experiments however, it is likely that A/V fell substantially due to the instilled volume of isotonic solution.

The reduced value for k reported by these authors after solution instillation to the RT therefore, can be explained simply by referring to Eq 5.3. This reveals that a fall in the area to volume ratio, given a constant and regional^l-independent value for the permeability, P , should produce a coincident decrease in the value of the transfer rate-constant, k .

TABLE 5.1

Effect of respiratory frequency (RF) on fractional deposition (fd).

```

*****
RF          -----fd-(*)-----
cycles min-1      Aerosol 1      Aerosol 2
*****

28          0.13 (1.89)          0.15 (1.86)
14          0.27 (2.4)           0.35 (1.92)
7           0.63 (2.2)           ND

*****

ND          no data
*           values in parentheses are tidal
           volumes (ml)

Aerosol 1   MMD50 = 2.62um,   σg = 1.5
Aerosol 2   MMD50 = 3.98um,   σg = 1.19
    
```

TABLE 5.2

Effect of tidal volume (TV) on fractional deposition (fd)
for an aerosol with $MMD_{50} = 3.96\mu m$ and $\sigma_g = 1.29$

TV	fd
----	----

2.25	0.28
------	------

1.35	0.13
------	------

0.92	0.07
------	------

TABLE 5.3

Effect of aerosol particle size distribution
on fractional deposition (fd)

RF = 28cycles min⁻¹

```
*****
MMD50 (um) (*)          fd          TV (ml)
*****
```

2.62 (1.50)	0.13	1.89
3.26 (1.49)	0.15	2.02
3.59 (1.30)	0.13	1.95
3.80 (1.42)	0.20	2.25
3.88 (1.32)	0.15	2.07
3.92 (1.30)	0.15	1.86
3.93 (1.52)	0.23	2.40
4.00 (1.25)	0.22	2.05

```
*****
```

RF = 14cycles min⁻¹

```
*****
MMD50 (um) (*)          fd          TV (ml)
*****
```

2.62 (1.50)	0.27	2.40
3.88 (1.32)	0.17	1.86
3.88 (1.32)	0.22	2.00
3.98 (1.19)	0.35	1.85
3.98 (1.19)	0.37	1.92

```
*****
```

RF = 7cycles min⁻¹

```
*****
MMD50 (um) (*)          fd          TV (ml)
*****
```

2.62 (1.50)	0.63	2.20
3.35 (1.83)	0.37	1.96
3.75 (1.31)	0.27	2.40
3.96 (1.29)	0.28	2.25

```
*****
```

* figures in parentheses are
geometric standard deviations

TABLE 5.4

Amounts of III (ug) and fractions to be transferred, ($f_{\infty} - f_t$), from airway - to - perfusate, with time, for the instillation experiments I and II (Chapter 3).

* Values in parentheses are ($f_{\infty} - f_t$). Estimated values for f_{∞} were 0.615 and 0.79 for experiments I and II, respectively.

```

*****
Time (min)          -----Amount transferred (ug)-(*)-
                    Experiment I           Experiment II
*****
5                   1.7   (0.575)         5.87   (0.670)
10                  6.6   (0.505)         12.77  (0.520)
15                  9.63  (0.375)         19.33  (0.380)
20                  16.37 (0.215)         25.65  (0.250)
30                  18.71 (0.155)         30.09  (0.150)
45                  20.48 (0.115)         32.31  (0.100)
53                  23.88 (0.025)         --     ( -- )
60                  --     ( -- )         35.59  (0.03)

*****
Amount III deposited  40.57ug           46.87ug
*****

```

TABLE 5.5

The lack of correlation between values for f_{∞} (estimated), as an index of depth of RT penetration, and the transfer rate constant, k , for aerosol and instilled solution administration experiments. Results are presented in descending order of f_{∞} .

```

*****
Expt.No.      f∞          % Diff      k(min-1)      r          n
*****
A22(s)        0.790         --          0.054         0.988         7
A18           0.745         0.1         0.051         0.991         7
A3            0.745         5.7         0.049         0.995         7
A19           0.690         4.2         0.059         0.985         6
A16           0.683         3.0         0.046         0.998         7
A20           0.640         0           0.050         0.992         5
A2            0.625         7.5         0.048         0.994         7
A14           0.622         3.1         0.043         0.995         8
A21(s)        0.615         --          0.057         0.954         7
A5            0.595         2.5         0.068         0.989         5
A8            0.592         0.6         0.057         0.986         7
A6            0.582         1.4         0.070         0.995         6
A4            0.555         12.1        0.042         0.964         7
A7            0.522         1.9         0.072         0.965         5
A17           0.520         7.0         0.051         0.886         7
A12           0.470         1.9         0.061         0.898         6
A15           0.420         5.7         0.059         0.988         5
A1            0.413         0.2         0.059         0.998         6
A11           0.410         4.9         0.052         0.980         7
A9            0.380         8.0         0.052         0.993         7
A13           0.358         2.2         0.044         0.997         6
A10           0.273         16.2        0.030         0.994         8
*****

```

```

*****
% Diff        Percentage difference of estimated asymptote
              from the average experimental value
r             correlation coefficient
n            number of co-ordinates
s            solution instillation experiments

```

Average k (aerosol) = 0.054min^{-1} (S.D. = 0.009)
Average k (instillation) = 0.056min^{-1}

TABLE 5.6

Values for the transfer rate constant, k, following the deposition of a range of transferable amounts (A) of III, as aerosol, in the isolated, perfused rat lung preparation.

```

*****
Expt.No.      -----Amount (ug)-----      Rate constant
              deposited      transferable      (min-1)
              a
*****
A3             52.78             38.05             0.049
A16            48.80             34.89             0.046
A5             36.60             26.25             0.068
A2             31.66             20.10             0.048
A12            19.68             12.28             0.061
    
```

```

*****
a             Appendix A
    
```

FIGURE 5.1

Schematic diagram of apparatus used to administer aerosols of II to the isolated, perfused rat lung preparation.

a	heating coil
b	artificial thorax
c	perfusate reservoir
d	pH meter electrode
e	magnetic stirrer
e'	magnetic flea
f	filter
g	oxygen electrode
h	perfusate pump
i	volume-cycle ventilator
j	flow meter
k	flow regulator
l	isolated lungs
m	pressure transducer
n	syringe
o	tracheal cannula
p	narrow-bore side-arm of perfusate reservoir
q	3-way tap
A	aerosol generator
B	neutralising tube
C	administration tube
D	removable glass cup with ground glass upper surface
S	aerosol delivery tube
M1,M2	water and fibre aerosol traps
V1	vacuum source
S1,C2,C3,D1 and R1	removable tubing clips

FIGURE 5.1

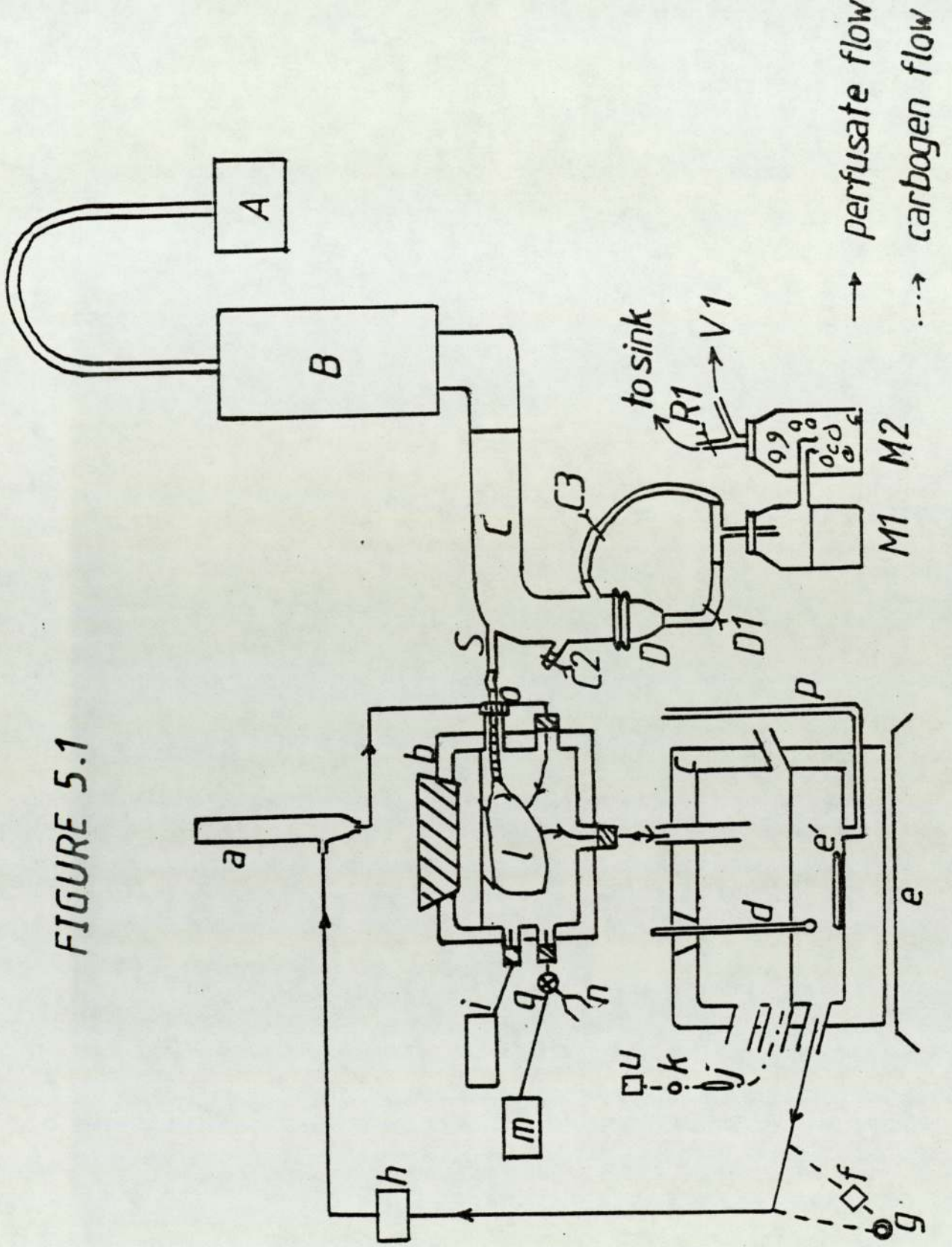


FIGURE 5.2 to 5.12

Fraction transferred versus time profiles resulting from the administration of aerosols of II to a number of isolated, perfused rat lung preparations.

FIGURE 5.2

Test of reproducibility

Symbol	:	O	X
MMD _{0.5} (um)	:	3.98	3.98
σ_g	:	1.19	1.19
TV (ml)	:	1.85	1.92
fd	:	0.35	0.37
PF (ml min ⁻¹)	:	15.0	15.0
RF (cycles min ⁻¹)	:	14.0	14.0
Appendix A		A "	A I

FIGURE 5.2

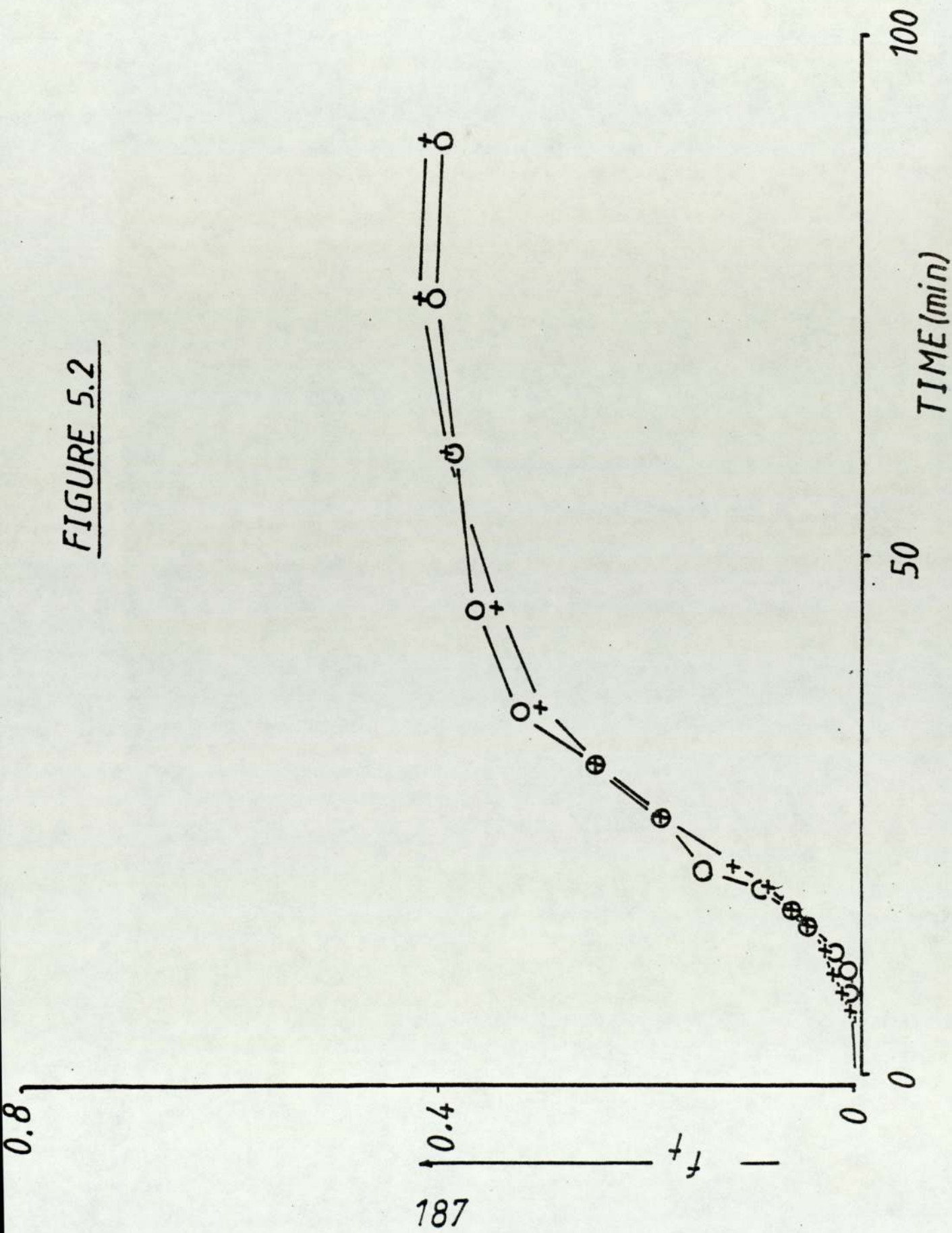


FIGURE 5.2 to 5.12

Fraction transferred versus time profiles resulting from the administration of aerosols of II to a number of isolated, perfused rat lung preparations.

FIGURE 5.3

Test of reproducibility

Symbol	:	O	X
MMD _{0.5} (um)	:	3.88	3.88
σ_g	:	1.32	1.32
TV (ml)	:	2.00	1.86
fd	:	0.22	0.17
PF (ml min ⁻¹)	:	15.0	15.0
RF (cycles min ⁻¹)	:	14.0	14.0
Appendix A		A4	A12

FIGURE 5.3

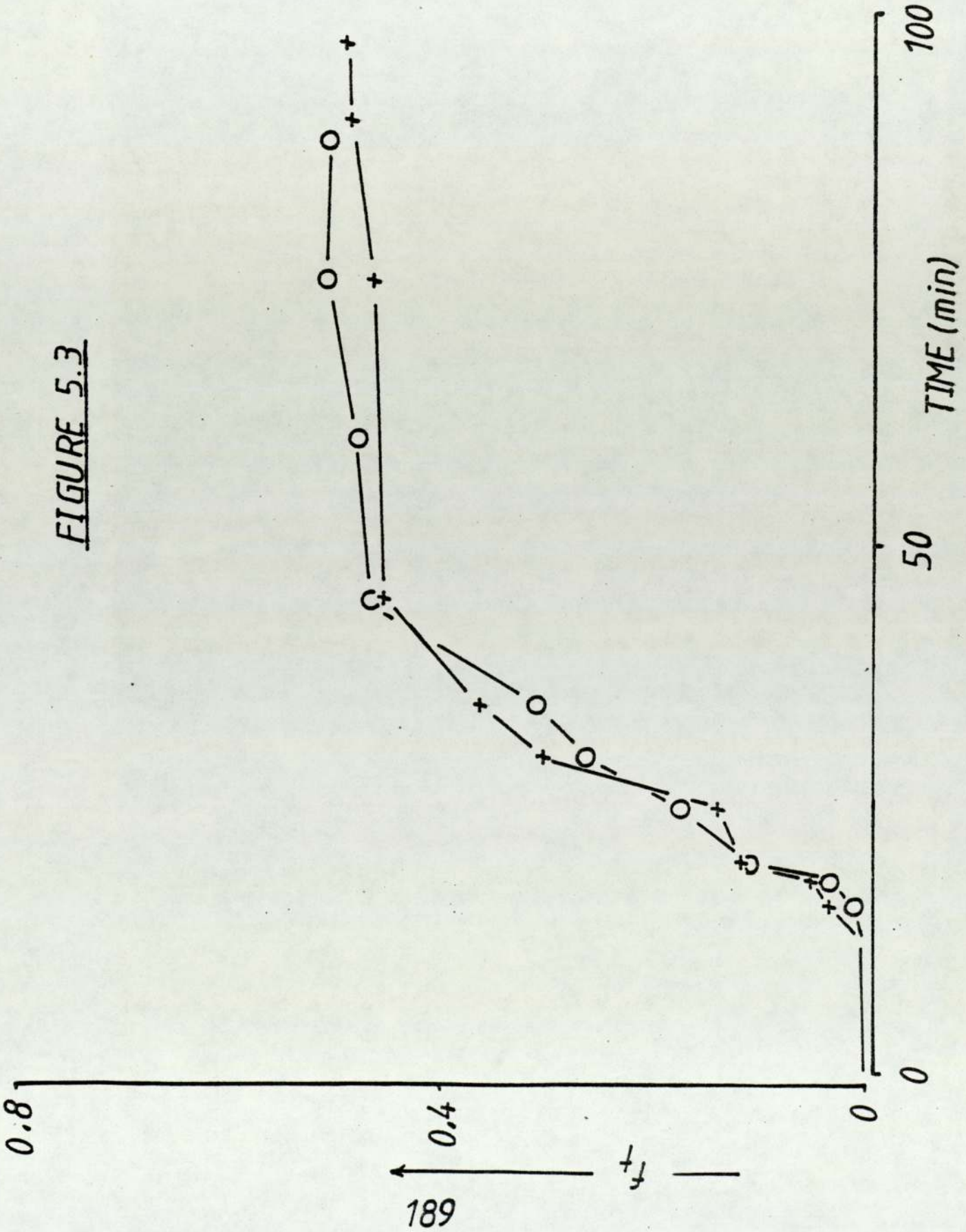


FIGURE 5.2 to 5.12

Fraction transferred versus time profiles resulting from the administration of aerosols of II to a number of isolated, perfused rat lung preparations.

FIGURE 5.4

Effect of perfusate flow rate (PF) on transfer

Symbol	:	O	X
MMD ₅₀ (um)	:	3.96	3.96
σ_g	:	1.29	1.29
TV (ml)	:	1.35	1.64
fd	:	0.10	0.13
PF (ml min ⁻¹)	:	15.0	5.0
RF (cycles min ⁻¹)	:	7.0	7.0
Appendix A.		A9	A13

FIGURE 5.4

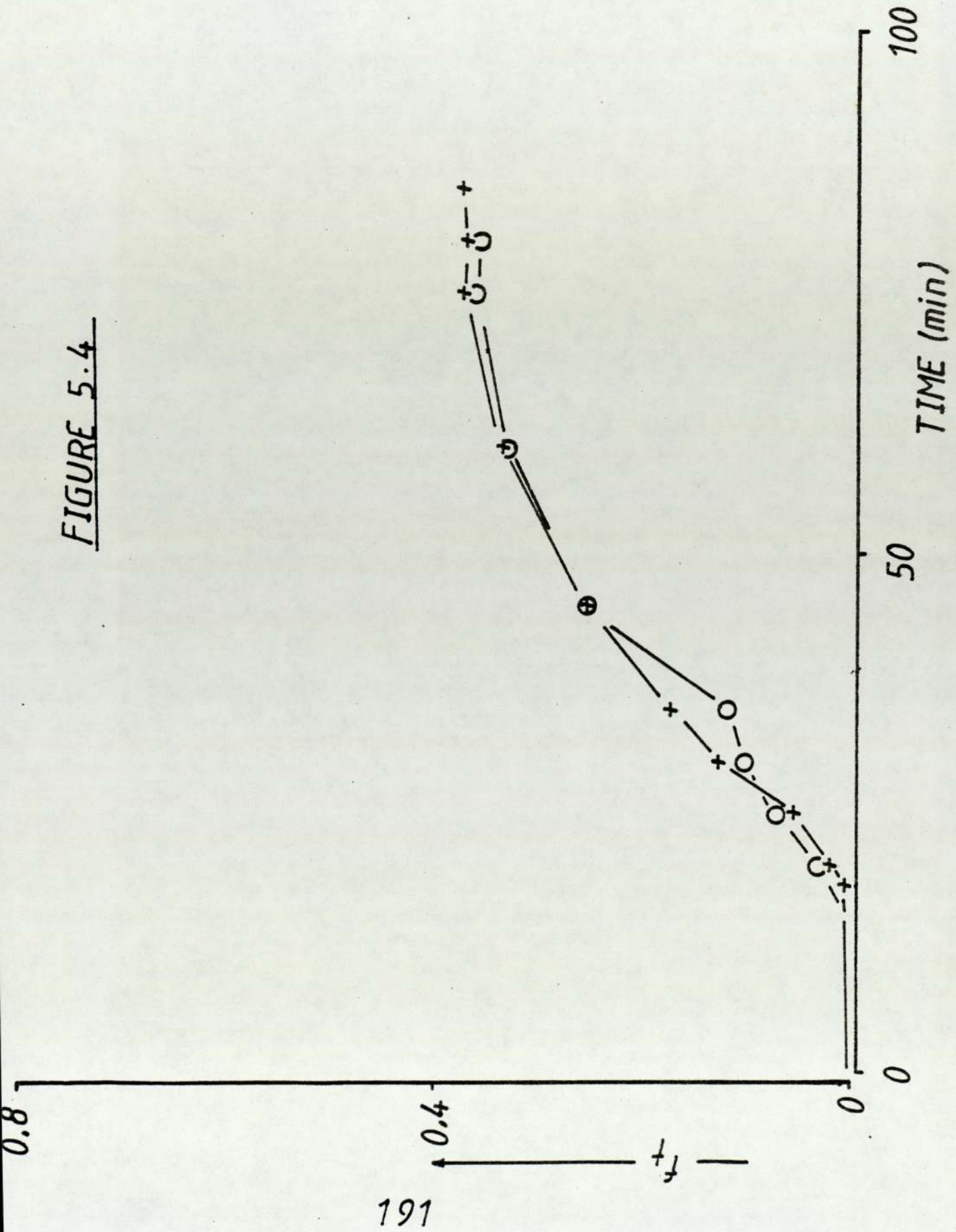


FIGURE 5.2 to 5.12

Fraction transferred versus time profiles resulting from the administration of aerosols of II to a number of isolated, perfused rat lung preparations.

FIGURE 5.5

Effect of perfusate flow rate (PF) on fractional transfer

Symbol	:	O	X
MMD ₅₀ (um)	:	3.88	3.59
σ_g	:	1.32	1.30
TV (ml)	:	2.07	1.95
fd	:	0.37	0.13
PF (ml min ⁻¹)	:	15.0	5.0
RF (cycles min ⁻¹)	:	28.0	28.0
Appendix A		A3	A14

FIGURE 5.5

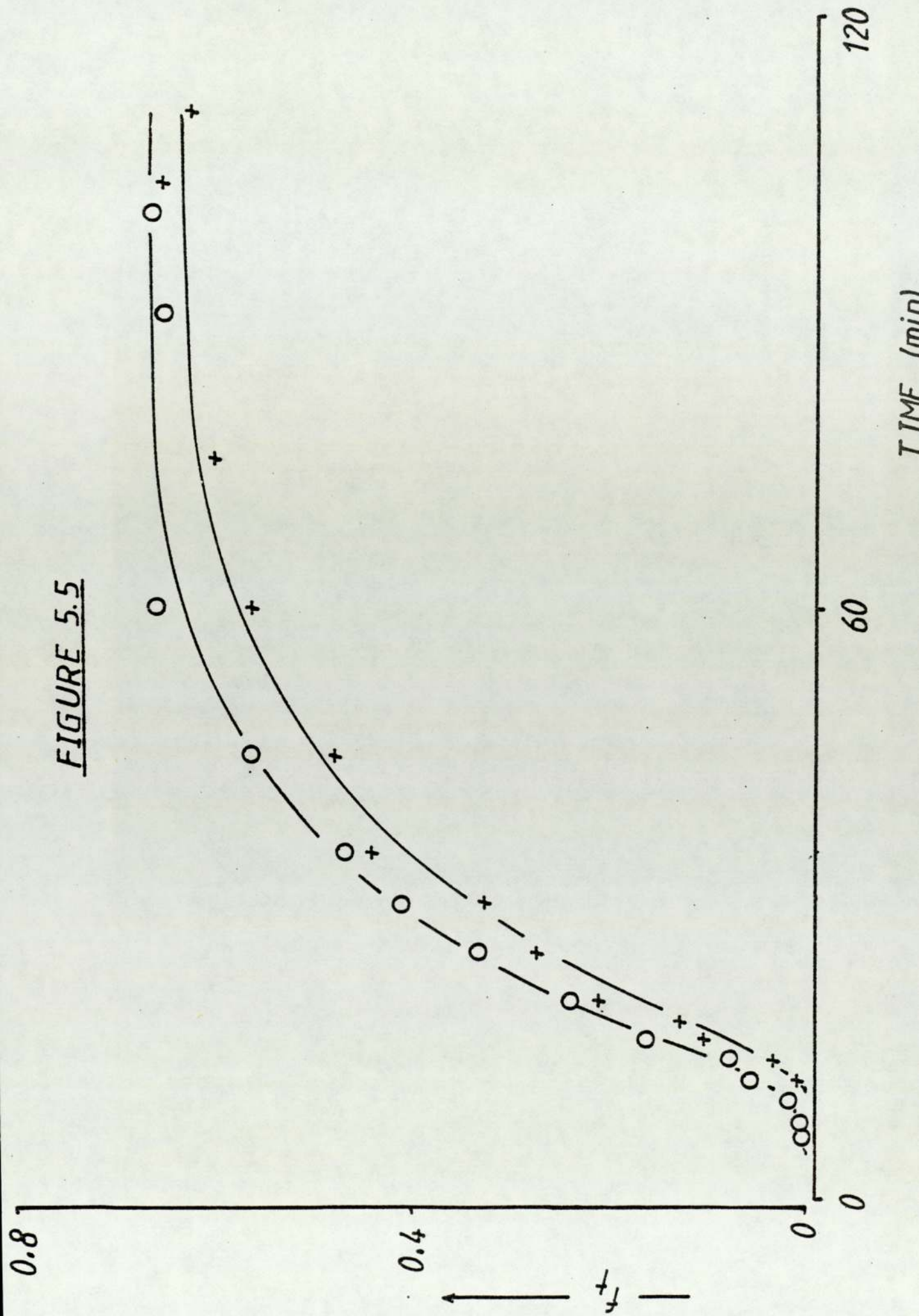


FIGURE 5.2 to 5.12

Fraction transferred versus time profiles resulting from the administration of aerosols of II to a number of isolated, perfused rat lung preparations.

FIGURE 5.6

Effect of respiratory frequency (RF) on fractional transfer

Symbol	:	●	○	■
MMD ₅₀ (um)	:	2.62	2.62	2.62
σ_g	:	1.50	1.50	1.50
TV (ml)	:	2.30	2.40	1.89
fd	:	0.63	0.27	0.13
PF (ml min ⁻¹)	:	15.0	15.0	15.0
RF (cycles min ⁻¹)	:	7.0	14.0	28.0
Appendix A		A7	A6	A5

FIGURE 5.6

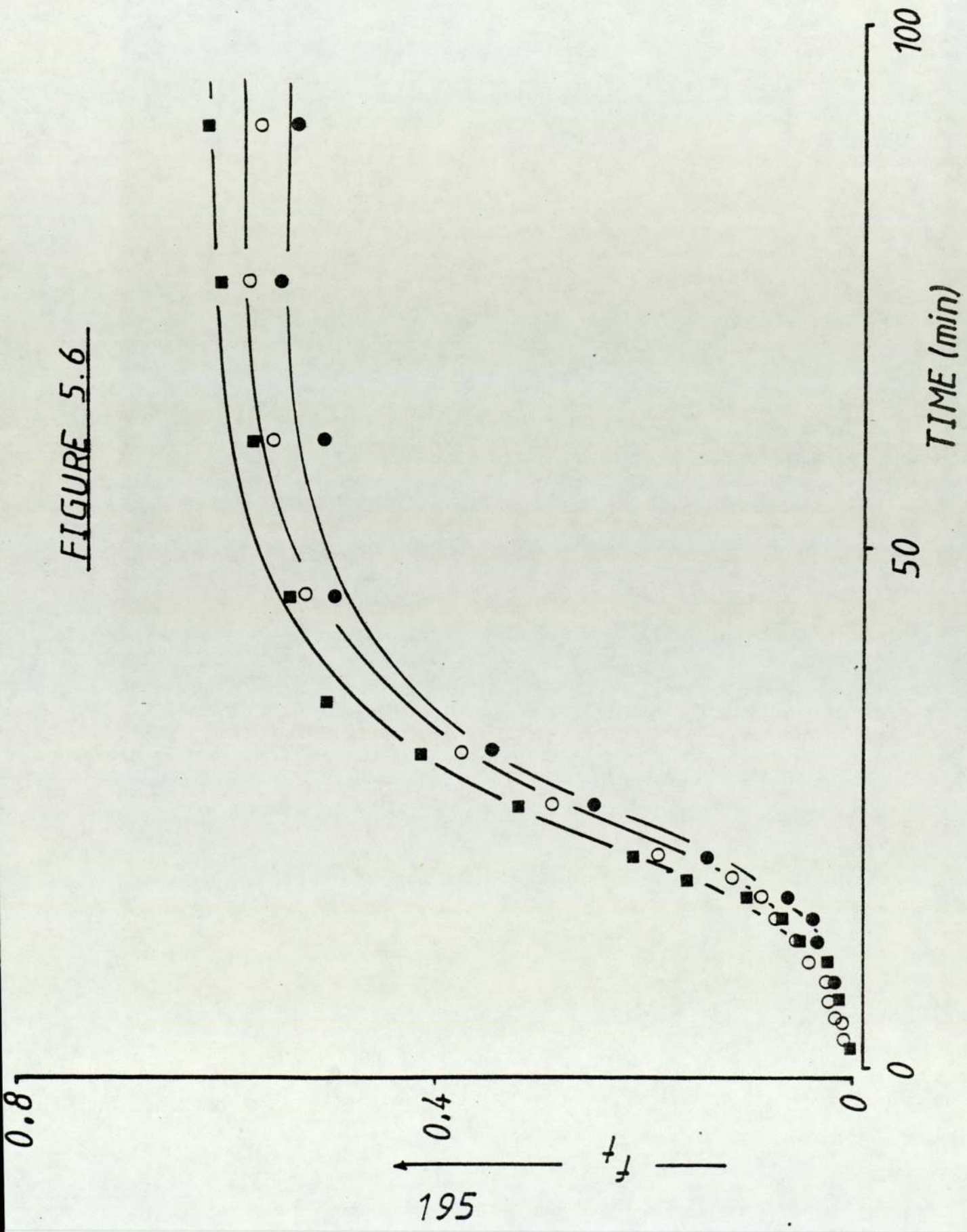


FIGURE 5.2 to 5.12

Fraction transferred versus time profiles resulting from the administration of aerosols of II to a number of isolated, perfused rat lung preparations.

FIGURE 5.7

Effect of respiratory frequency (RF) on fractional transfer

Symbol	:	O	X
MMD ₅₀ (um)	:	3.98	3.98
σ_g	:	1.19	1.19
TV (ml)	:	1.92	1.86
fd	:	0.35	0.15
PF (ml min ⁻¹)	:	15.0	15.0
RF (cycles min ⁻¹)	:	14.0	28.0
Appendix A		A1	A2

FIGURE 5.7

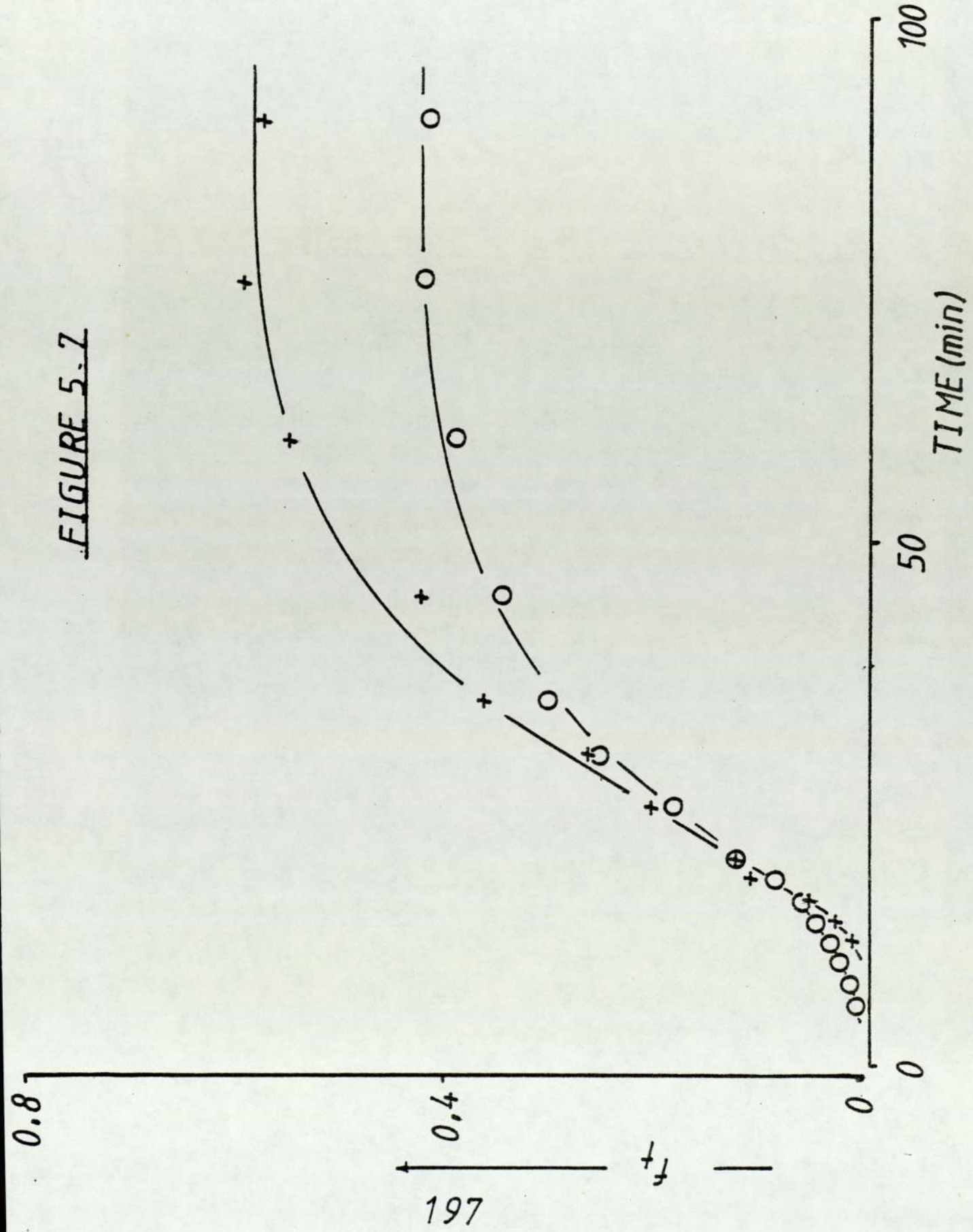


FIGURE 5.2 to 5.12

Fraction transferred versus time profiles resulting from the administration of aerosols of II to a number of isolated, perfused rat lung preparations.

FIGURE 5.8

Effect of respiratory frequency (RF) on fractional transfer

Symbol	:	X	O
MMD ₅₀ (um)	:	3.88	3.88
σ_g	:	1.32	1.32
TV (ml)	:	2.0	2.07
fd	:	0.35	0.15
PF (ml min ⁻¹)	:	15.0	15.0
RF (cycles min ⁻¹)	:	14.0	28.0
Appendix A		A4	A3

FIGURE 5.8

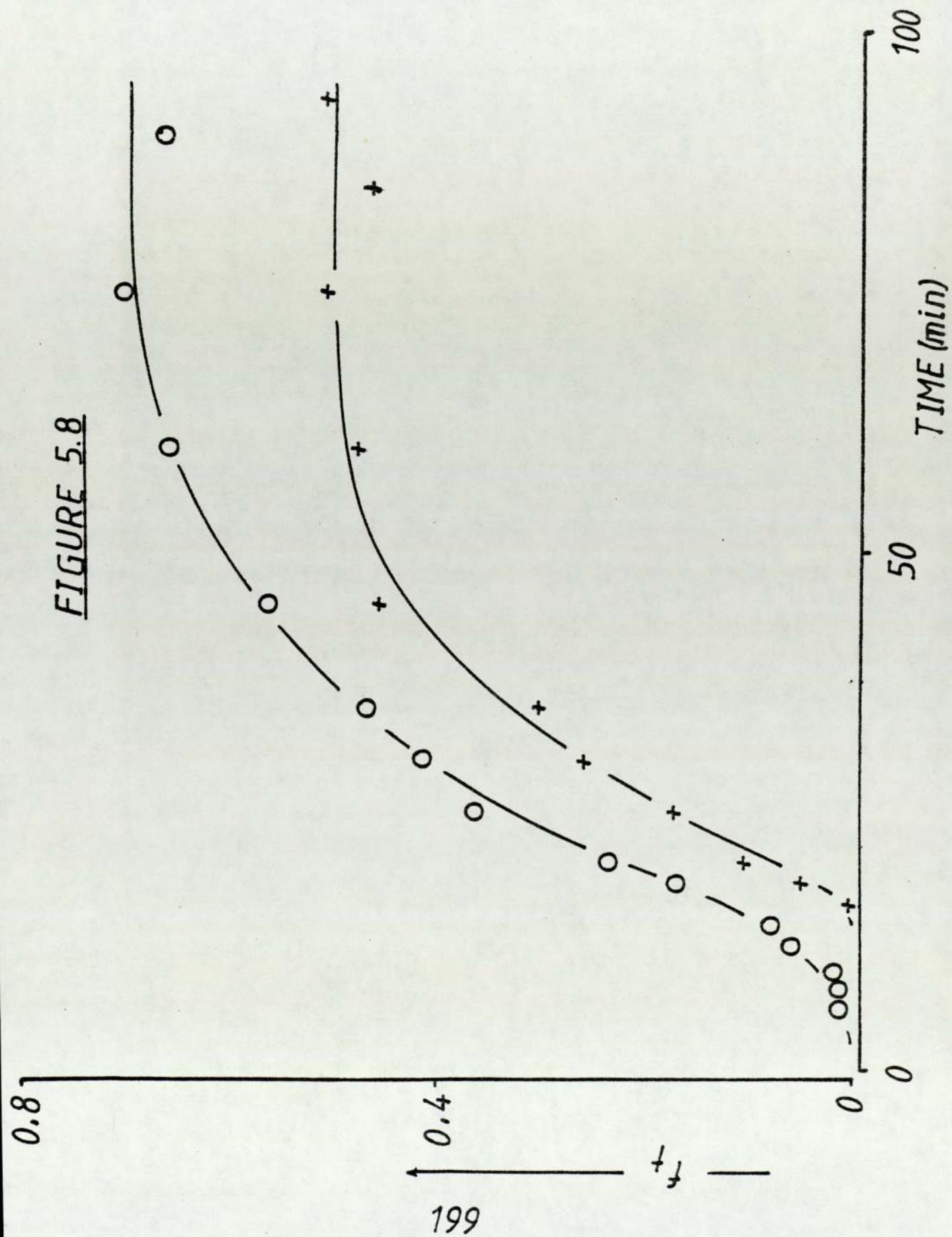


FIGURE 5.2 to 5.12

Fraction transferred versus time profiles resulting from the administration of aerosols of II to a number of isolated, perfused rat lung preparations.

FIGURE 5.9

Effect of tidal volume (TV) on fractional transfer

Symbol	:	●	○	■
MMD ₅₀ (um)	:	3.96	3.96	3.96
σ_g	:	1.29	1.29	1.29
TV (ml)	:	0.92	1.35	2.25
fd	:	0.07	0.13	0.28
PF (ml min ⁻¹)	:	15.0	15.0	15.0
RF (cycles min ⁻¹)	:	7.0	7.0	7.0
Appendix A		A10	A9	A8

FIGURE 5.9

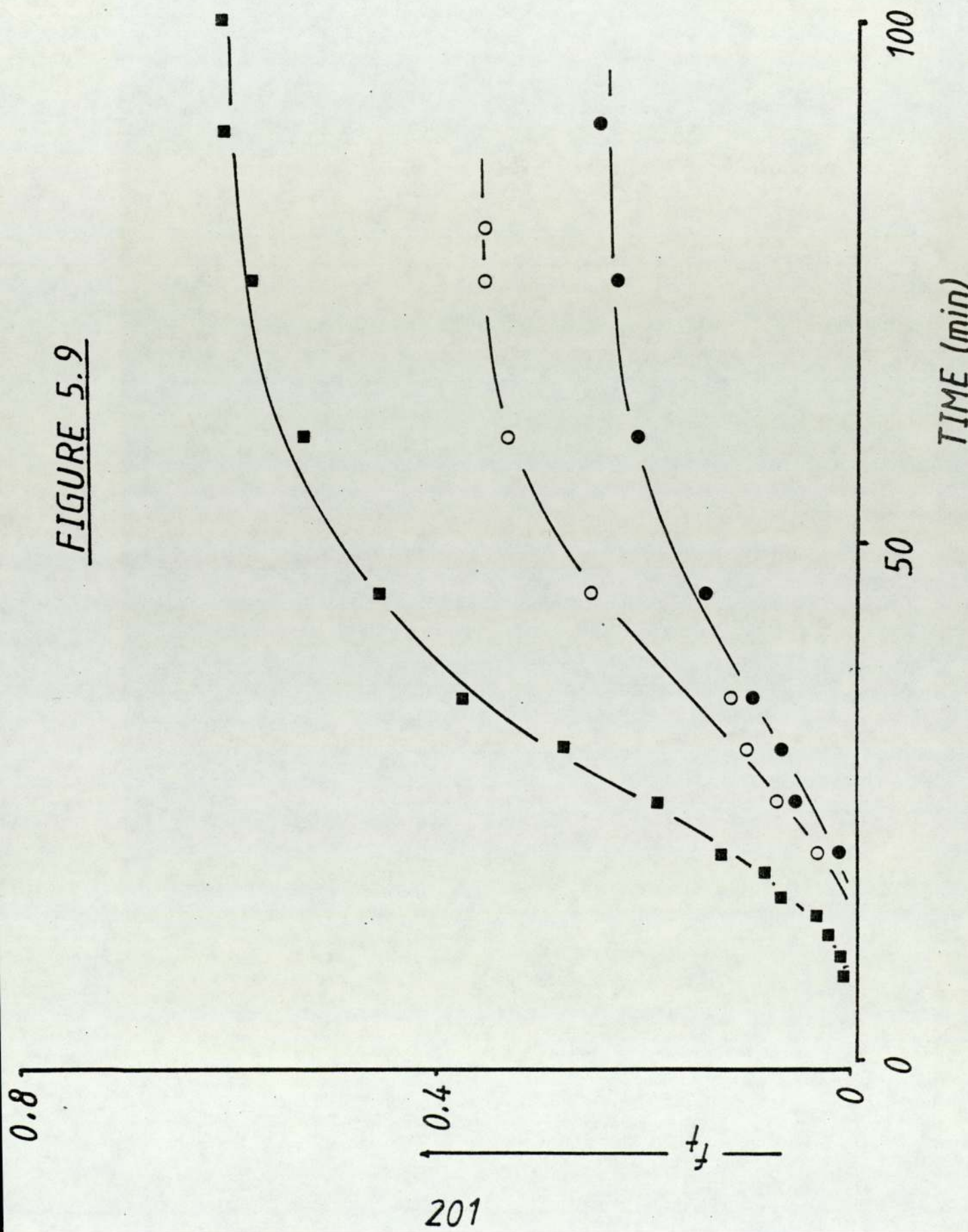


FIGURE 5.2 to 5.12

Fraction transferred versus time profiles resulting from the administration of aerosols of II to a number of isolated, perfused rat lung preparations.

FIGURE 5.10

Effect of aerosol particle size distribution on fractional transfer

Symbol	:	○	×
MMD ₅₀ (um)	:	2.62	3.92
σ_g	:	1.50	1.30
TV (ml)	:	1.89	1.86
fd	:	0.13	0.15
PF (ml min ⁻¹)	:	15.0	15.0
RF (cycles min ⁻¹)	:	28.0	28.0
Appendix A		A5	A2

FIGURE 5.10

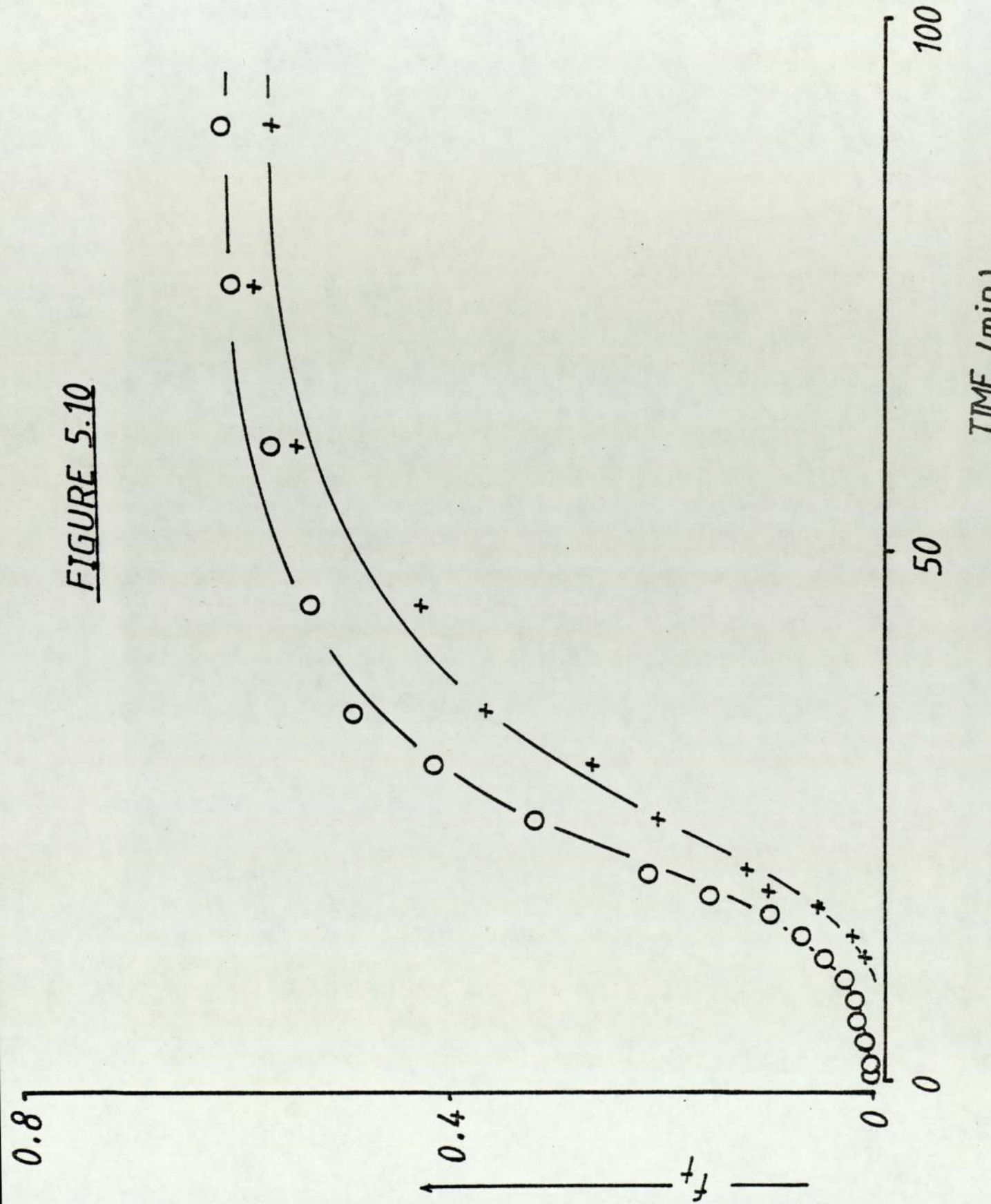


FIGURE 5.2 to 5.12

Fraction transferred versus time profiles resulting from the administration of aerosols of II to a number of isolated, perfused rat lung preparations.

FIGURE 5.11

Effect of aerosol particle size distribution on fractional transfer

Symbol	:	O	X
MMD ₅₀ (um)	:	2.62	3.98
σ_g	:	1.50	1.19
TV (ml)	:	2.4	1.92
fd	:	0.27	0.35
PF (ml min ⁻¹)	:	15.0	15.0
RF (cycles min ⁻¹)	:	14.0	14.0
Appendix A		46	A1

FIGURE 5.11

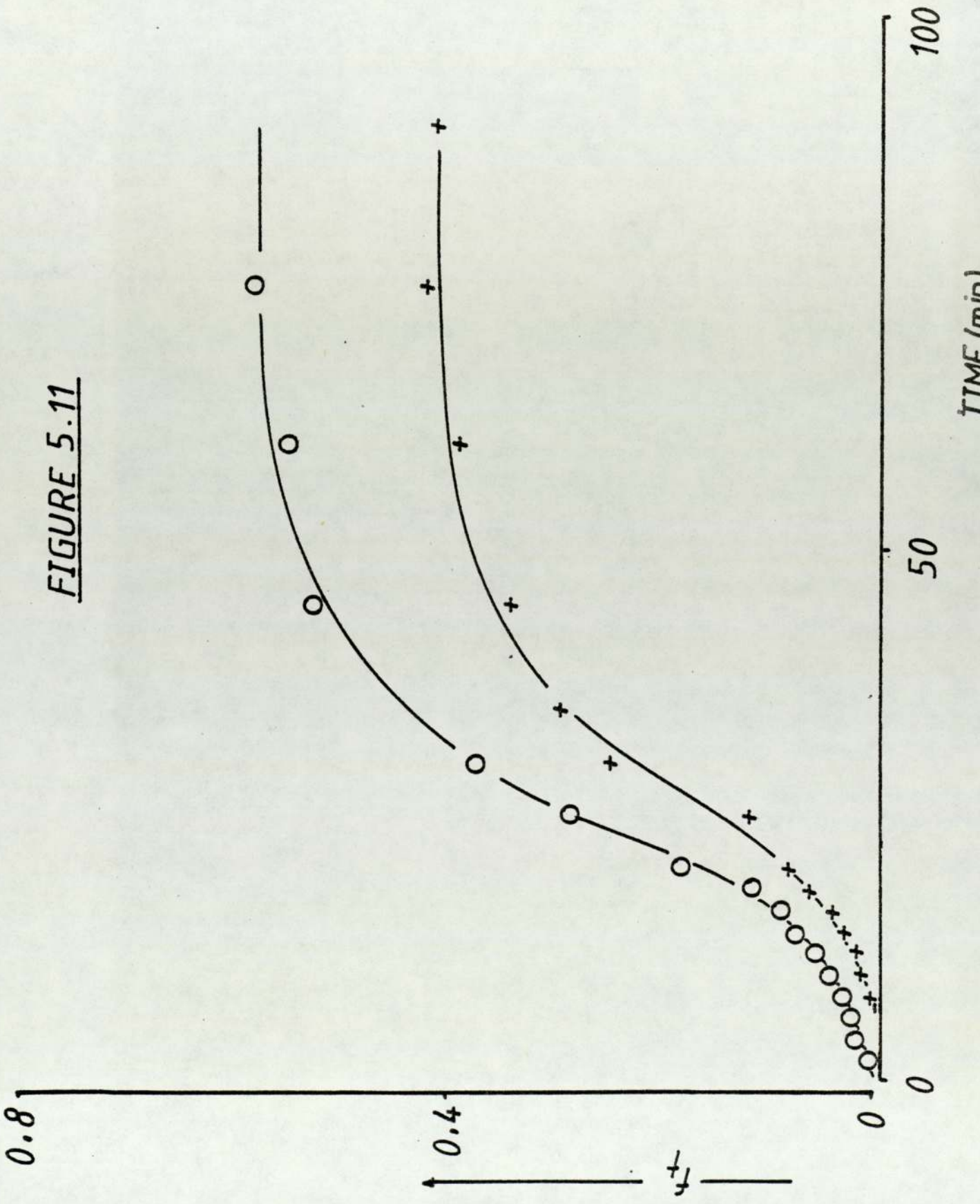


FIGURE 5.2 to 5.12

Fraction transferred versus time profiles resulting from the administration of aerosols of II to a number of isolated, perfused rat lung preparations.

FIGURE 5.12

Effect of aerosol particle size distribution on fractional transfer

Symbol	:	O	X
MMD ₅₀ (um)	:	2.62	3.75
σ_g	:	1.50	1.31
TV (ml)	:	2.20	2.40
fd	:	0.63	0.27
PF (ml min ⁻¹)	:	15.0	15.0
RF (cycles min ⁻¹)	:	7.0	7.0
Appendix A		A7	A15

FIGURE 5.12

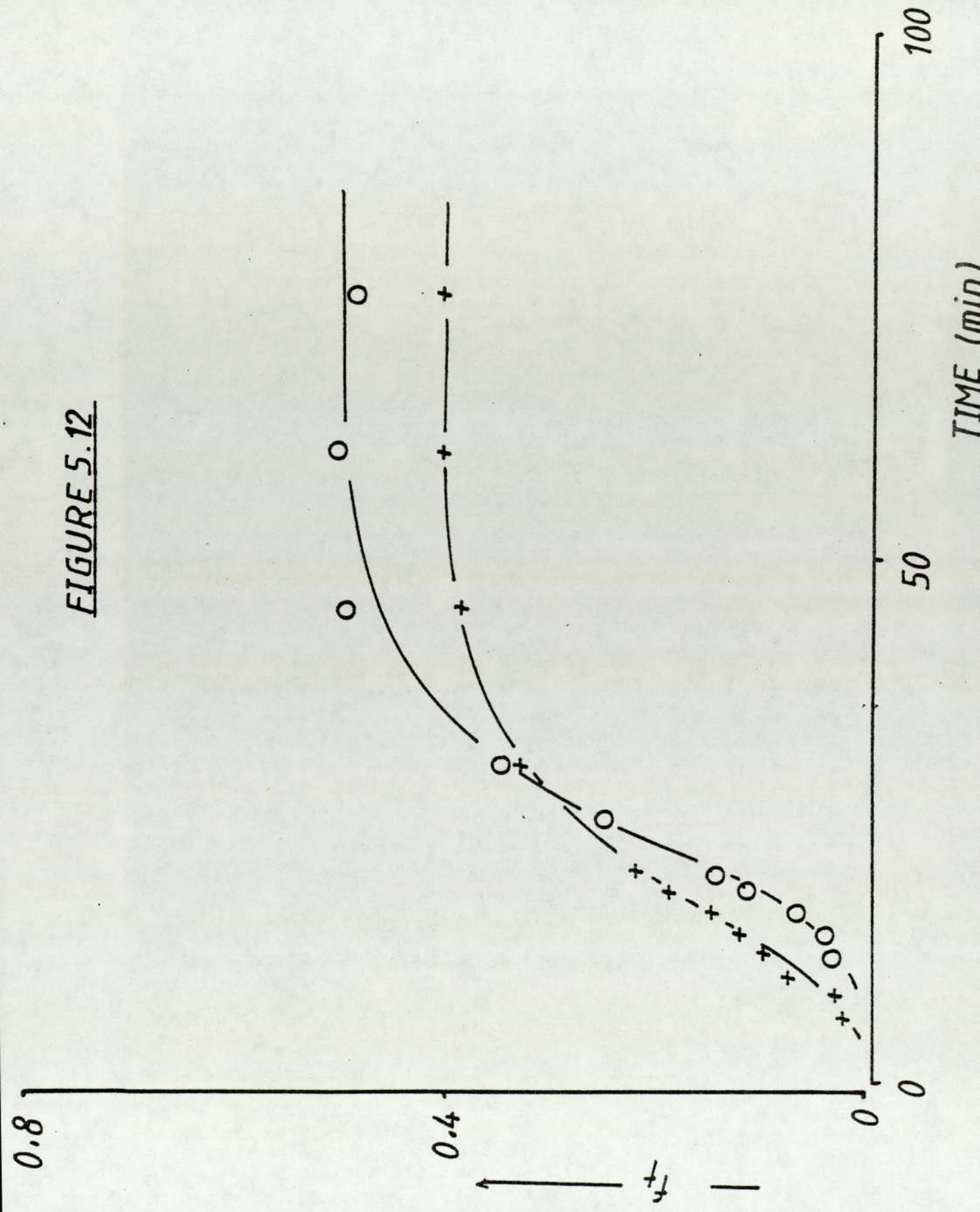


FIGURE 5.13

Fraction transferred versus time profiles resulting from (a) aerosol administration ($MMD_{ae} = 2.62\mu m$; amount deposited = 36.6ug) and (b) solution instillation (deposited amounts = 40.57 and 46.87ug for experiments I and II, respectively (Chapter 3)).

FIGURE 5.13

--- solution Exp. II

— aerosol

--- solution Exp. I

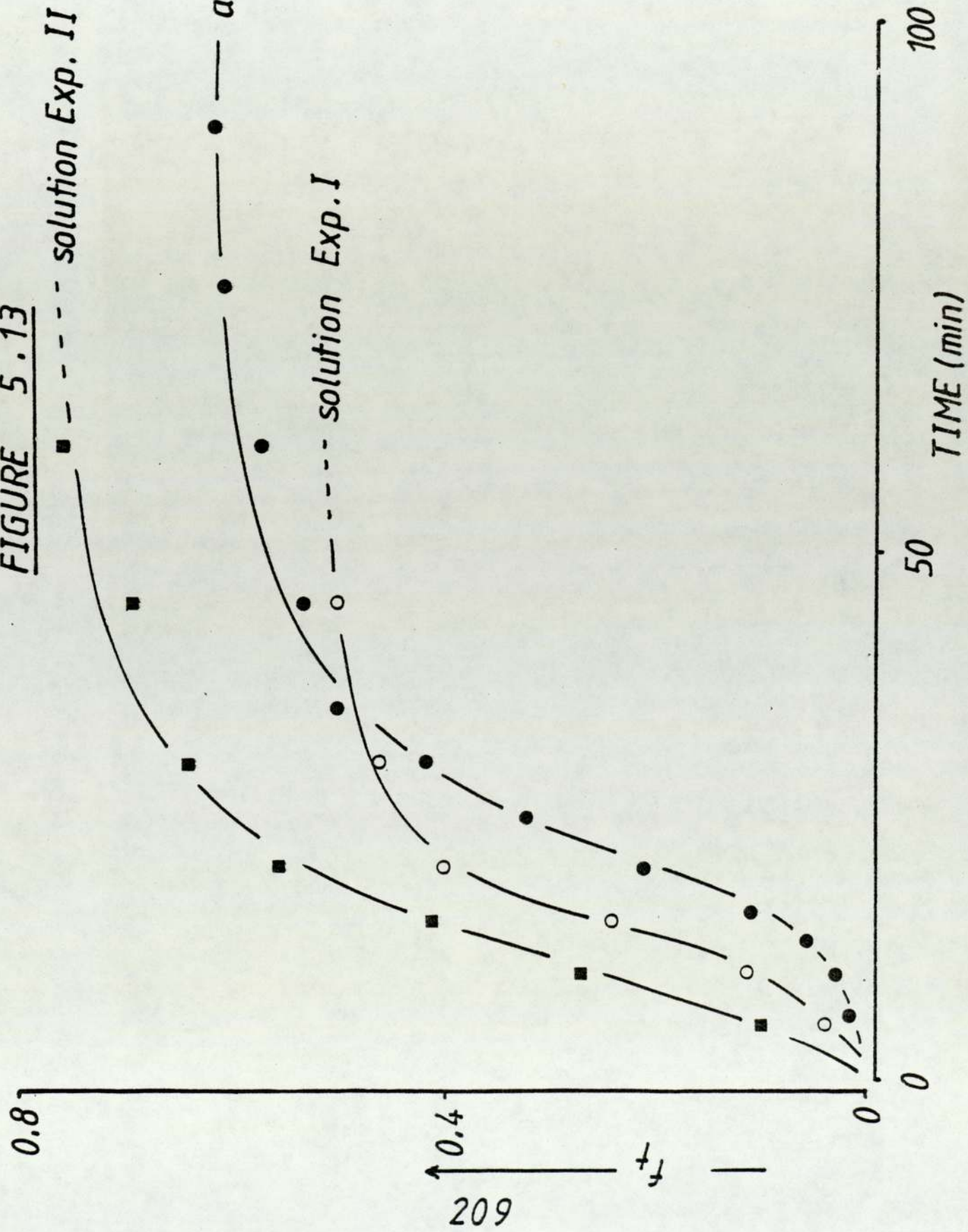


FIGURE 5.14

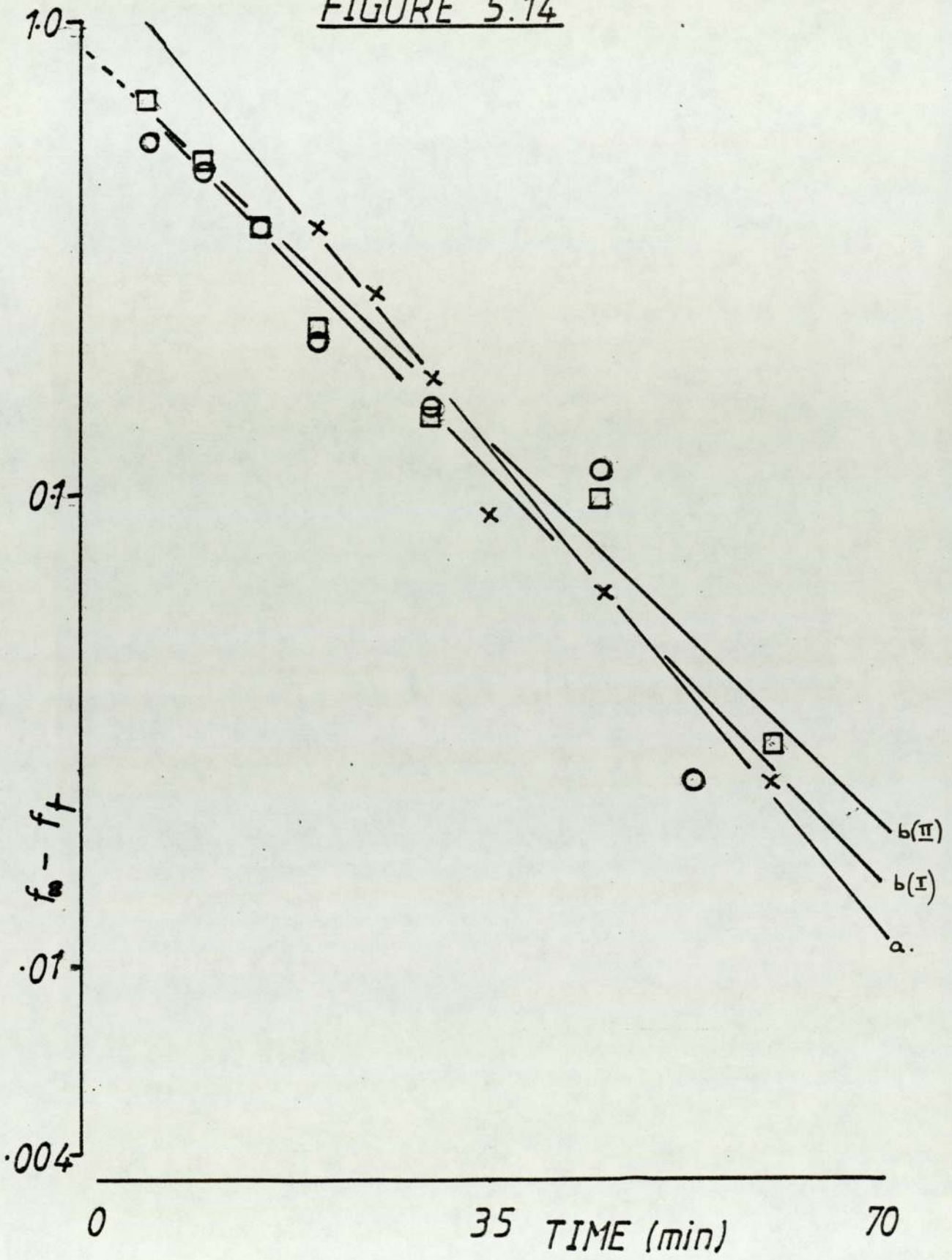


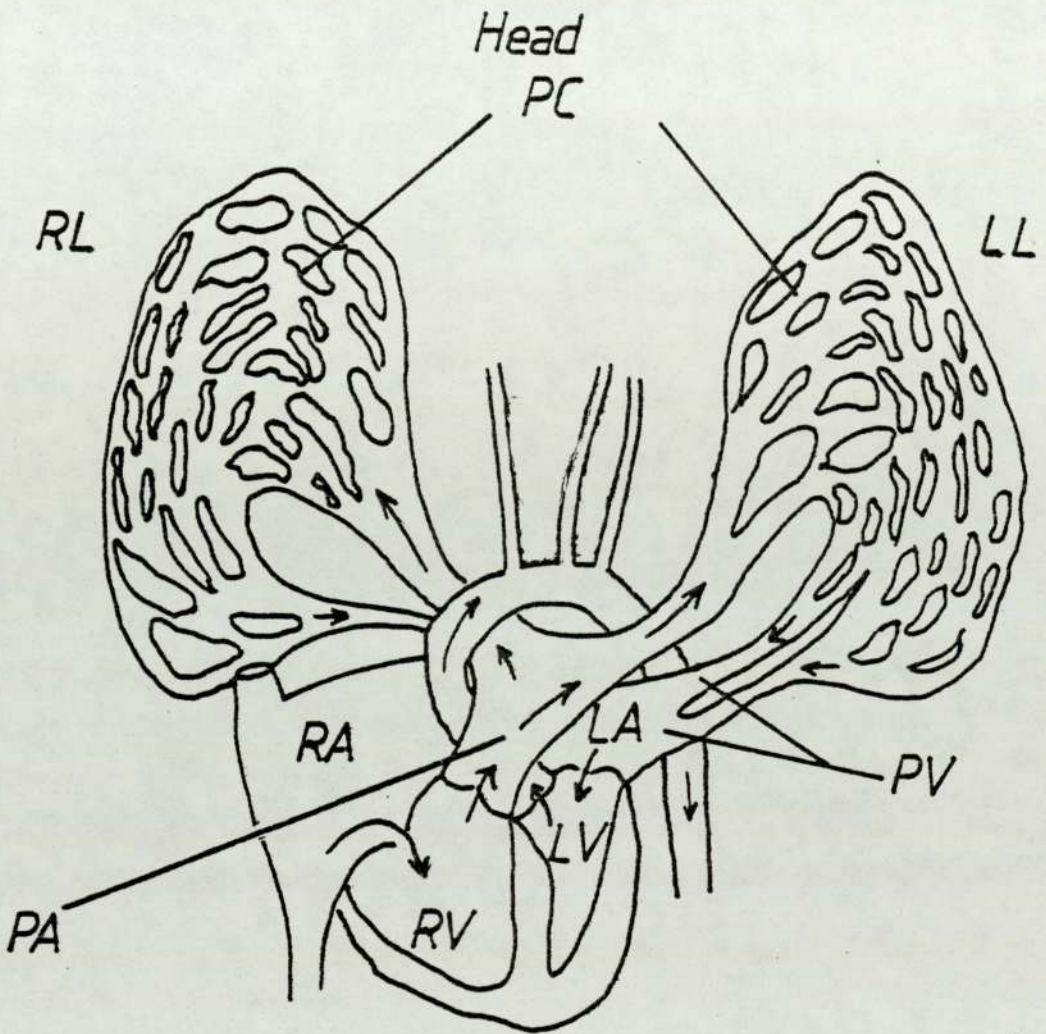
FIGURE 5.15

Schematic representation of the pulmonary circulation.

- RL: right lung
- LL: left lung
- PC: pulmonary capillaries
- RA: right atrium
- LA: left atrium
- PV: pulmonary veins
- PA: pulmonary artery
- LV: left ventricle
- RV: right ventricle

The head of the animal, and the opening of the trachea, is toward the top of the page.

FIGURE 5.15



→ blood flow

FIGURE 5.16 to 5.25

Log-linear plots of fraction to be transferred, $(f_{\infty} - f_t)$, versus time, for values of f_t obtained after aerosol administration was complete ($t > 20\text{min}$).

Fig Experiment number (Appendix A)

5.16	A1 (X) and A2 (O)
5.17	A3 (X) and A4 (O)
5.18	A5 (X) and A6 (O)
5.19	A7 (X) and A8 (O)
5.20	A9 (O) and A10 (X)
5.21	A11 (X) and A12 (O)
5.22	A13 (X) and A14 (O)
5.23	A15 (X) and A16 (O)
5.24	A17 (X) and A18 (O)
5.25	A19 (X) and A20 (O)

FIGURE 5.16

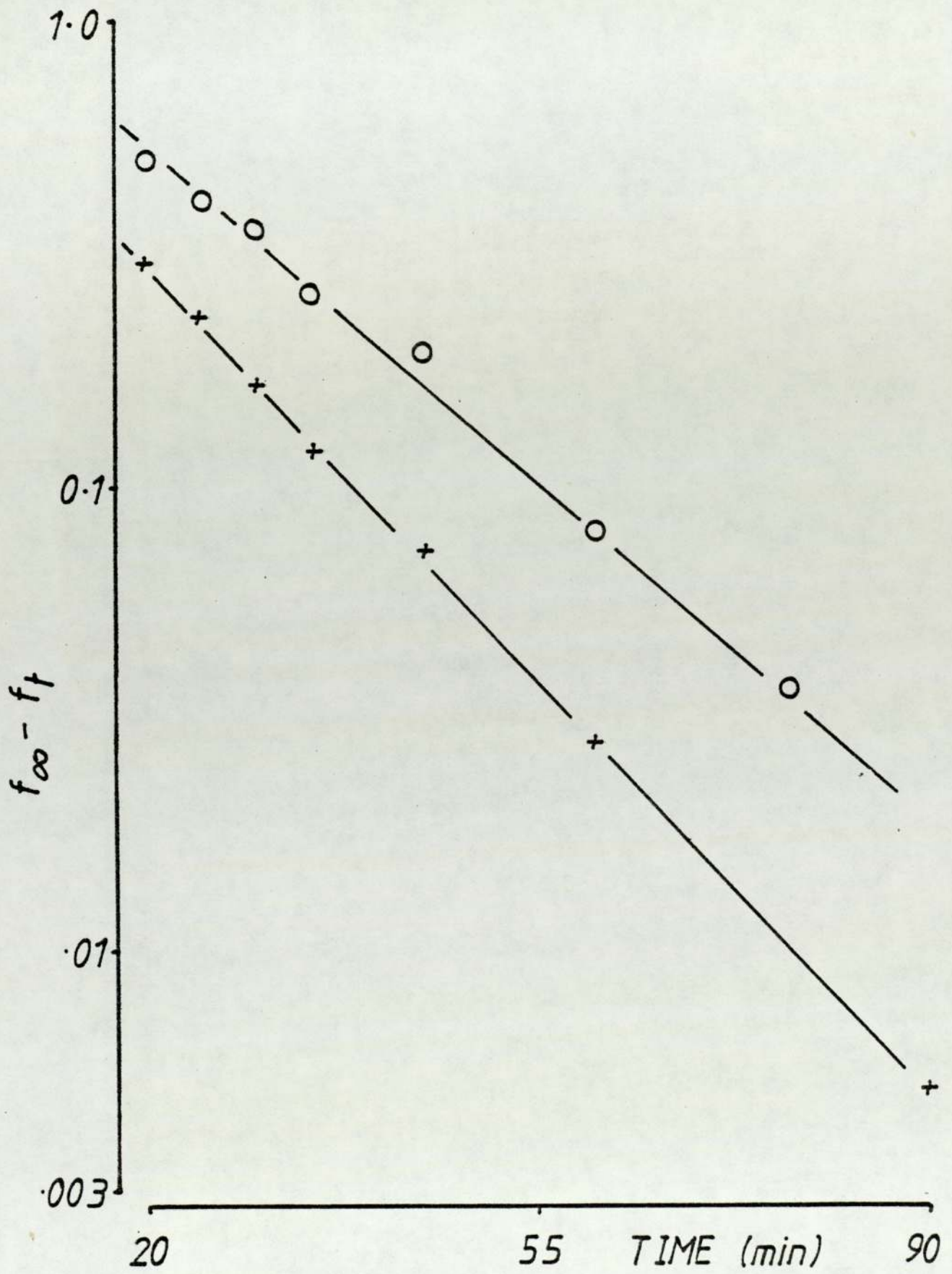


FIGURE 5.17

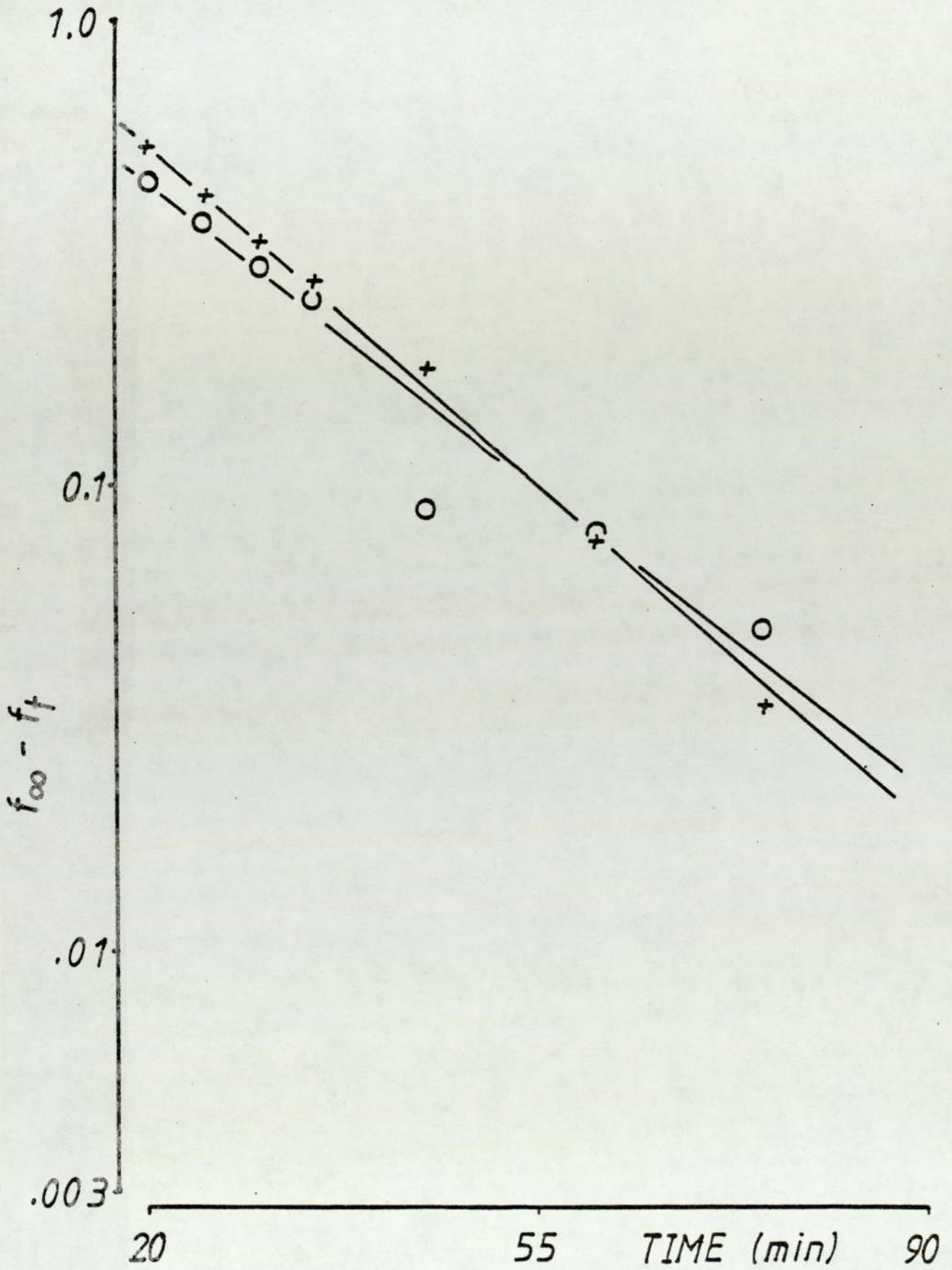


FIGURE 5,18

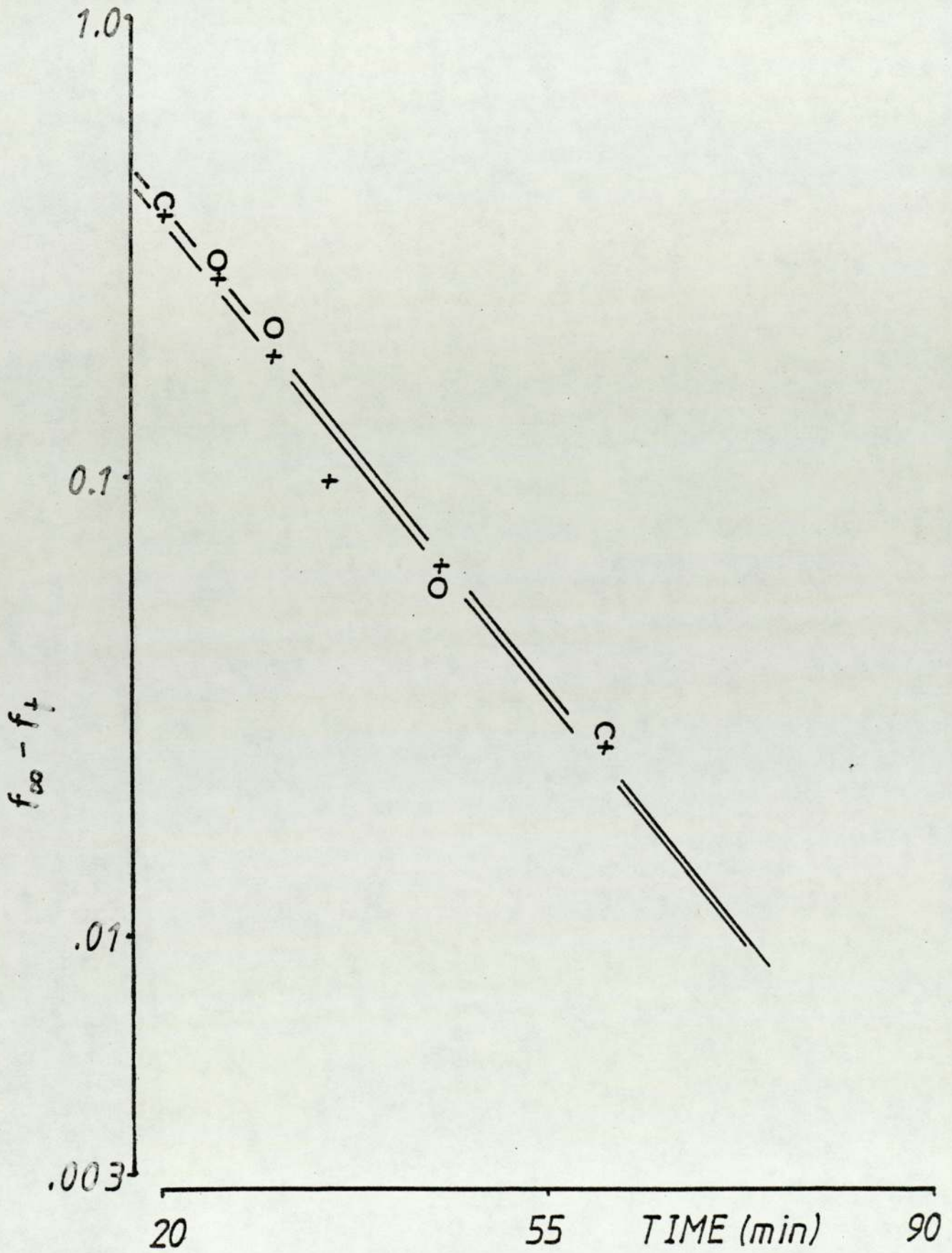


FIGURE 5.19

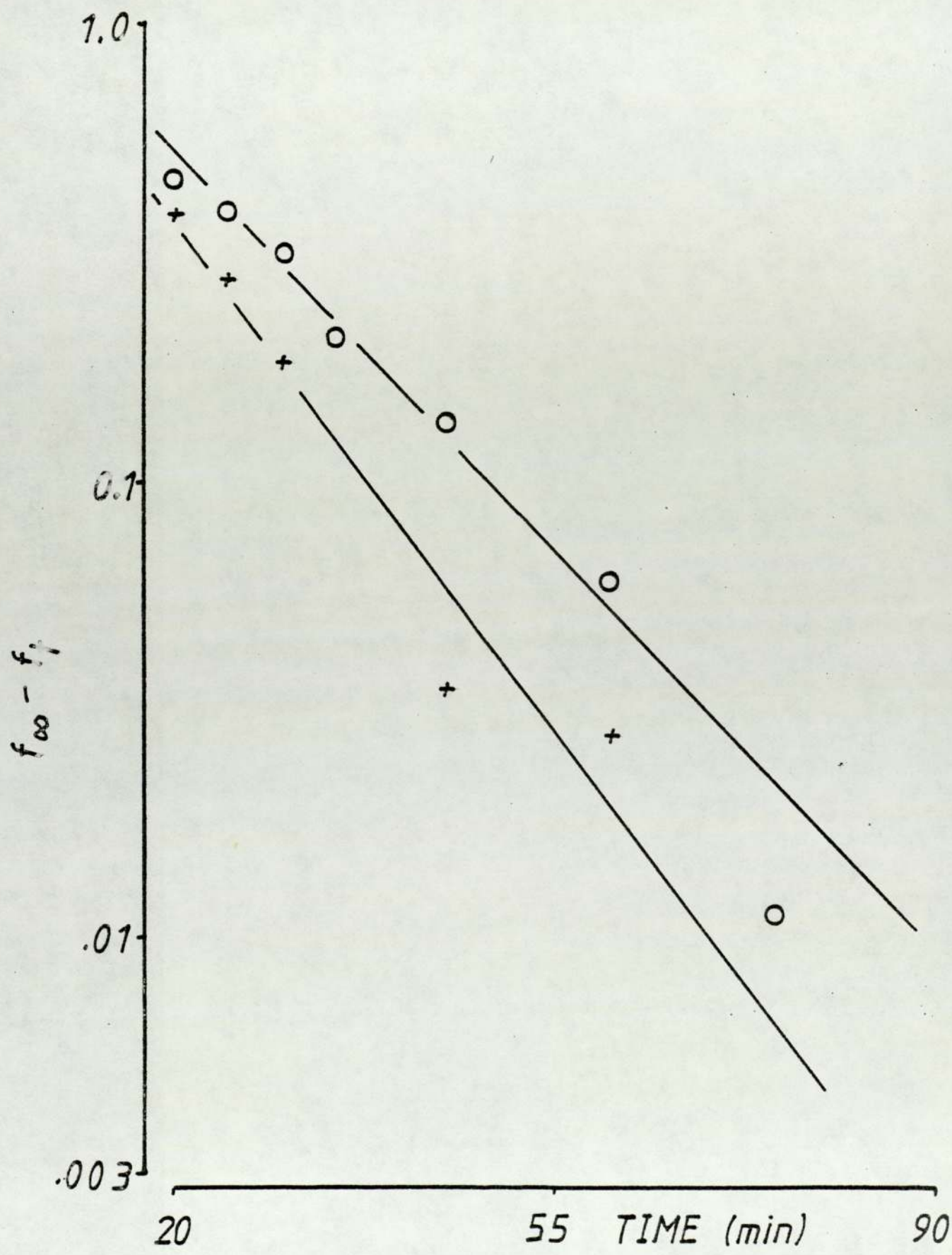


FIGURE 5.20

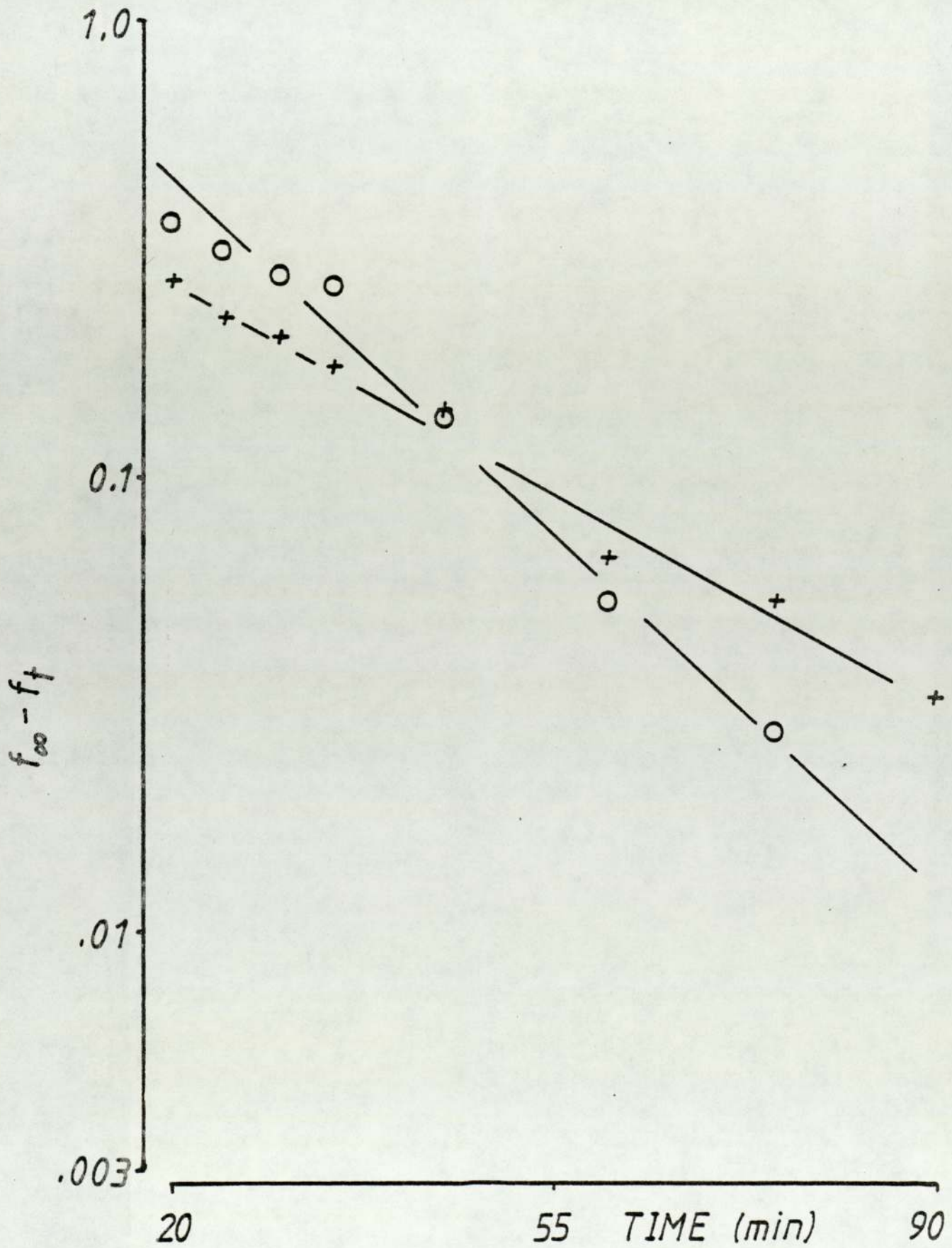


FIGURE 5, 21

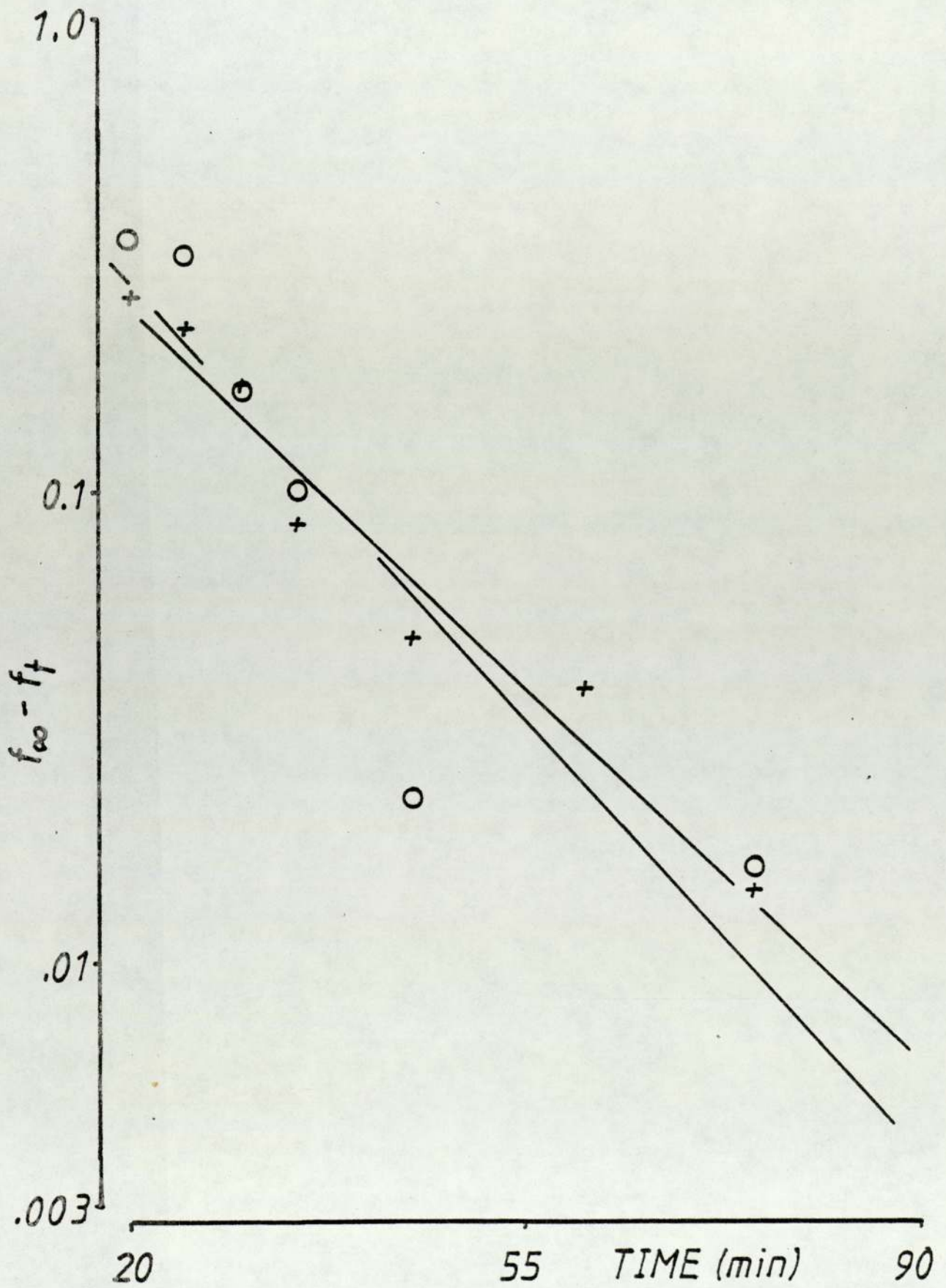


FIGURE 5.22

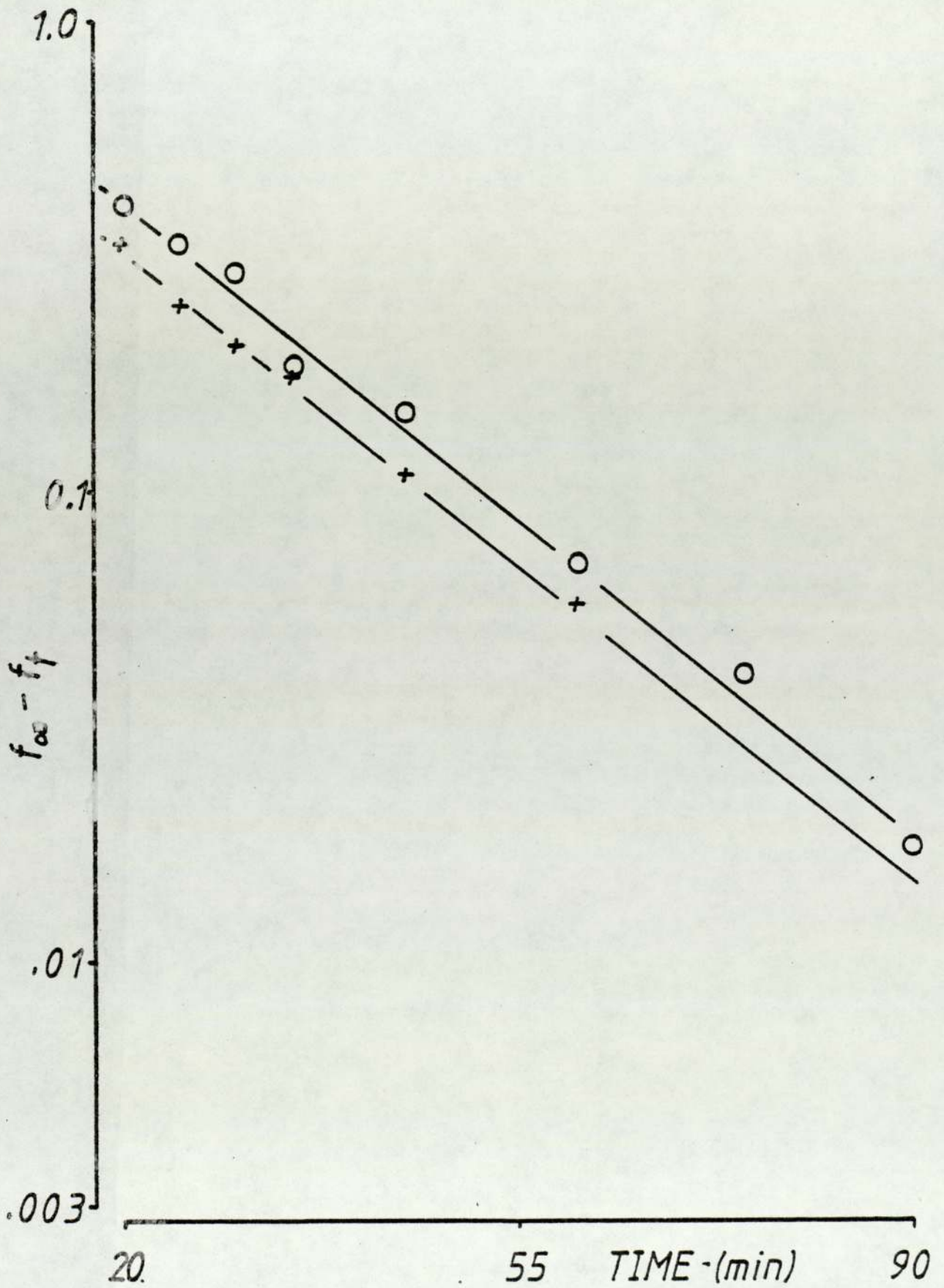


FIGURE 5.23

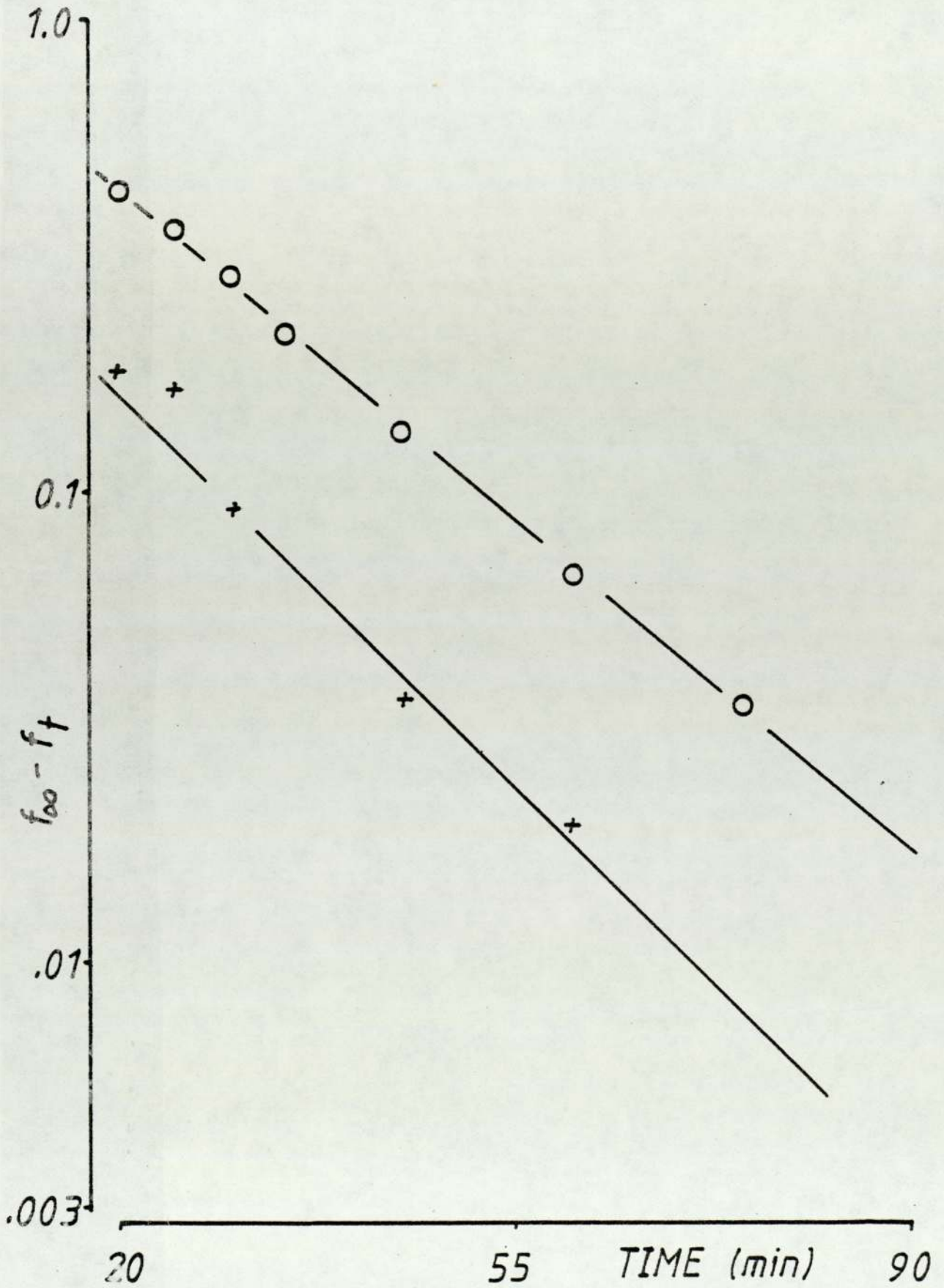


FIGURE 5.24

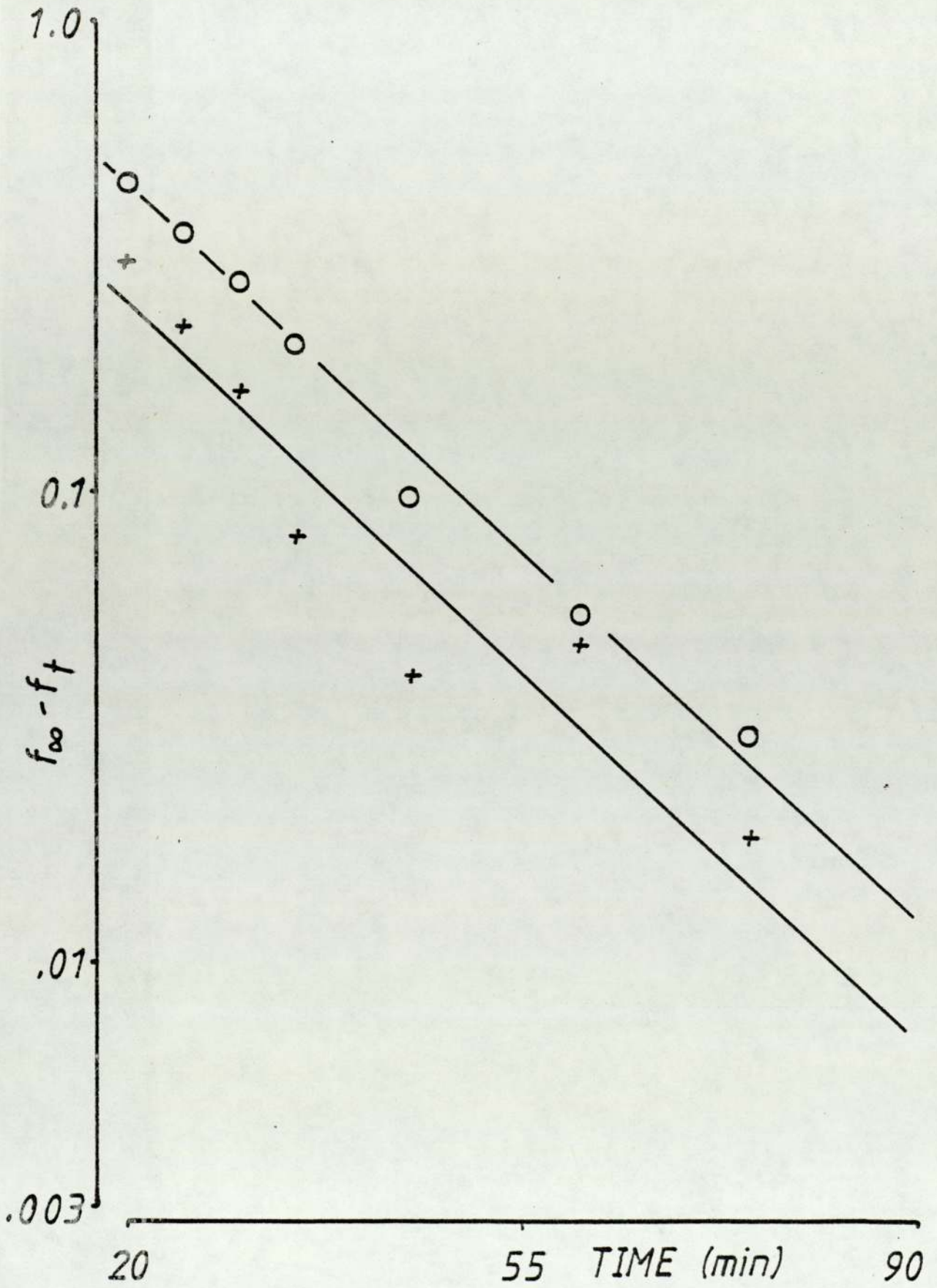


FIGURE 5.25

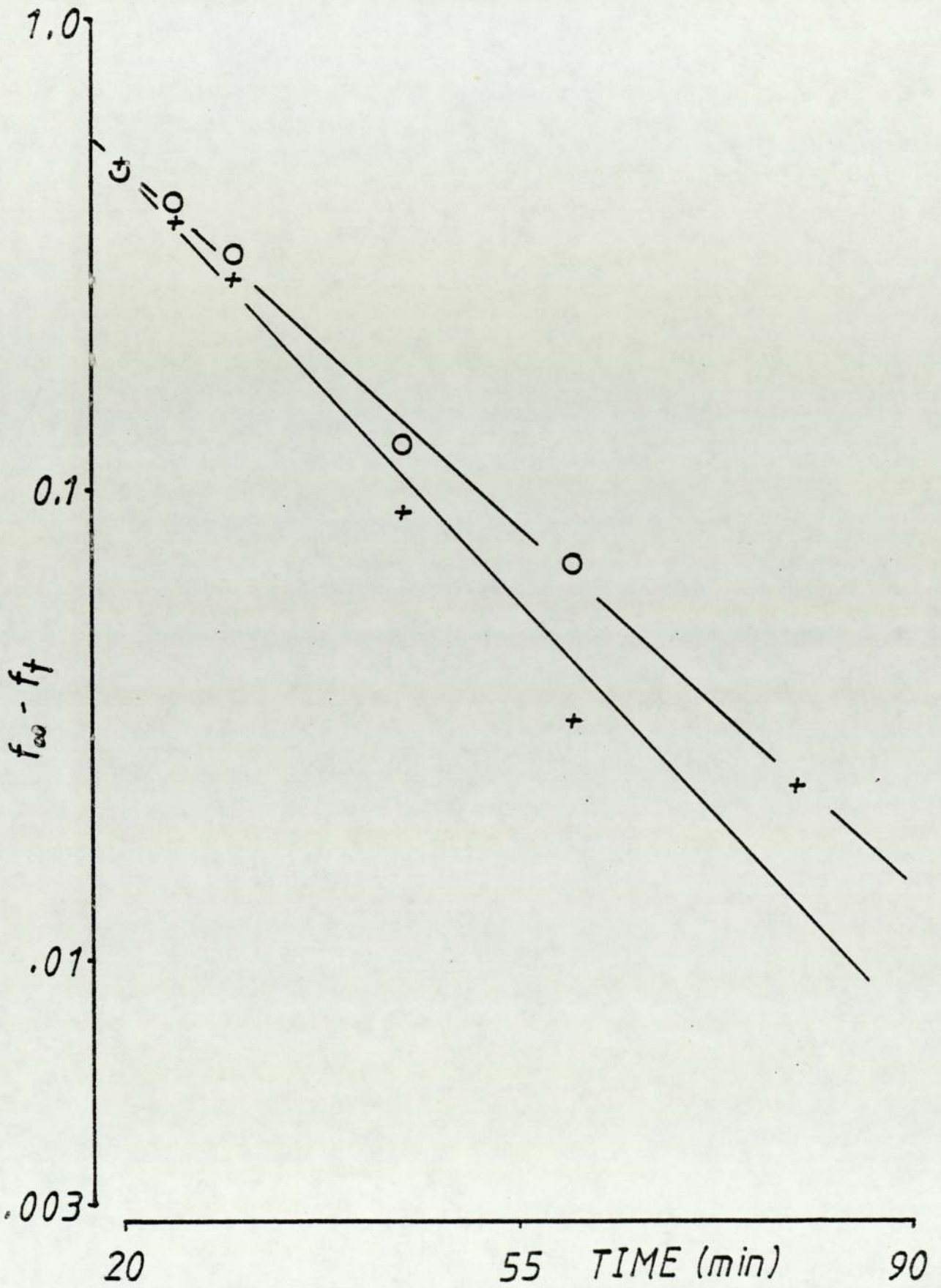
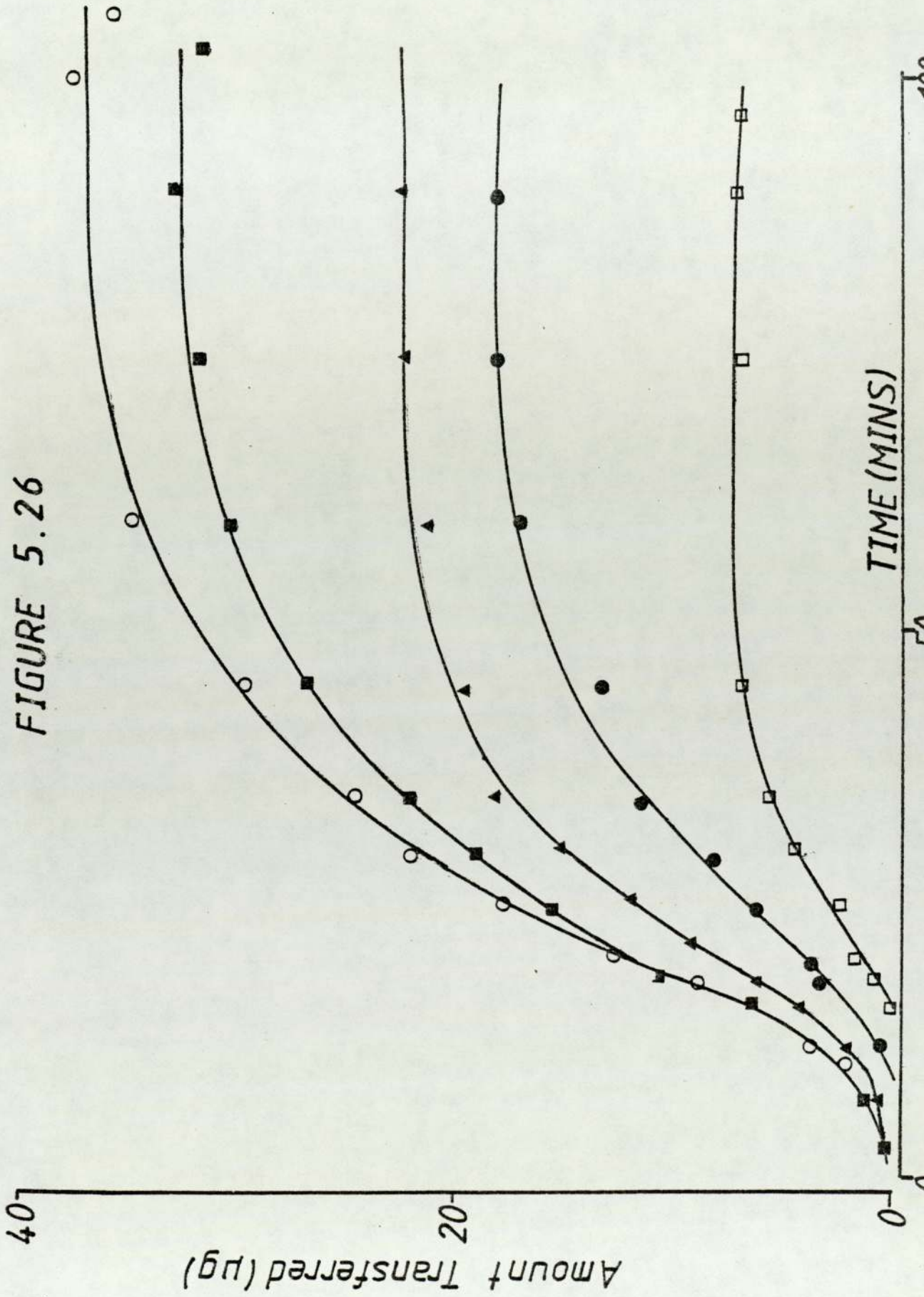


FIGURE 5.26

Amounts of III (ug) transferred versus time (minutes) following deposition, from aerosols, of a range of transferable amounts: (O) 38.05ug, (■) 34.89ug, (▲) 26.25ug, (●) 20.10ug and (□) 12.27ug.

FIGURE 5.26



CHAPTER SIX

GENERAL DISCUSSION

The administration of inhalation aerosols intended for local and systemic activity, such that deposition and solute absorption is reproducible, predictable and within safe therapeutic boundaries, will not be easy to achieve. Exploitation of the respiratory tract as a reliable route for the administration of various solutes depends upon full investigation and comprehension of the many interacting and complicating factors affecting aerosol deposition and solute absorption. A review of the relevant literature indicated the absence of a system in which aerosol deposition and solute transfer across the lung could be quantified and studied as a function of lung respiratory regime and aerosol particle size distribution. The work undertaken in this thesis therefore, described the development of a simple system which consisted of an isolated, perfused rat lung preparation maintained, in a viable condition, in an apparatus designed for ease of aerosol administration to the lungs and subsequent monitoring of airway-to-perfusate solute transfer. Respiratory regimes could be both monitored and varied and perfusate flow rates readily adjusted. Solid

aerosols, of a compound known to be rapidly absorbed via the lungs, were generated in the respirable size range. The aerosols were characterised in terms of concentration and particle size distribution and administered to the isolated lungs in known volumes. Using this system, it was possible to administer known amounts of solute as aerosols of various particle sizes and to quantify deposition and solute transfer as functions of tidal volume, respiratory frequency and perfusate flow rate.

The results of deposition studies presented in this thesis clearly indicated that tidal volume had the most dramatic effect on fractional deposition, f_d . For constant respiratory frequency, a small increase in the tidal volume resulted in a much larger fraction of a given aerosol being deposited in the lungs. Furthermore, f_d appeared to increase at lower respiratory frequencies. Such effects have previously been reported in human models (25, 41, 42, 49, 94) and aerosol deposition is reportedly maximised, for a given respirable particle size distribution, when tidal volume is maximised, inhalation is slow and the breath held for a few seconds (25, 27, 41, 42, 49, 50, 94). Although the effects of breath holding were not investigated in this thesis, the system developed could readily be used for such studies. Aerosol particle size, over the small range investigated, had a less marked effect upon fractional deposition. It seemed probable however, that f_d increased with increasing aerosol mass-median aerodynamic diameter. At the smallest respiratory frequency studied however, the opposite appeared to be true. Here, at 7 breathing cycles

per minute, it was likely that particulate hygroscopic growth was affecting the results, causing greater fractional deposition in the tubing connecting the lungs to the aerosol mainstream. Further studies are necessary to fully determine the effects of aerosol MMD_{50} and σ_g (geometric standard deviation of size distributions) upon deposition in this model. Other workers have established that aerosol deposition efficiencies in the human are largely independent of σ_g and are related primarily to the MMD_{50} of the administered aerosol (42, 47).

The absorption studies described in this thesis indicated that, for the transferable, deposited amounts delivered, airway-to-perfusate transfer of fluorescein anions was an apparent first-order process. The absorption rate constants appeared to be independent of regional deposition, suggesting that pulmonary epithelial permeability was constant throughout the perfused airways of the isolated rat lung. If this statement was also found to be true in vivo then optimising deposition should also optimise systemic transfer rates. Such a phenomenon could be used where rapid absorption is desirable, perhaps in the administration of compounds to neutralise or relieve the effects of ingested, inhaled or even topically absorbed toxic substances. Alternatively, formulation expertise could perhaps be employed to prepare controlled-release therapeutic preparations for inhalation. If these were to contain substances known to exert local pharmacologic activity in the respiratory tract, then provided release from the aerosol formulation was slower than, in this case,

undesirable absorption, some sustained pharmacologic effects may well result. Conversion of prodrugs, to therapeutically active agents within the lungs following inhalation aerosol administration, may be a useful therapeutic tool, employing the drug metabolising spectrum of the organ. Such techniques of "drug engineering" could perhaps reduce the extensive side effects often associated with the use of cytotoxic agents in the treatment of pulmonary carcinoma.

In conclusion, the work described in this thesis presents the development of a system in which deposition and absorption, following administration of a well-characterised aerosol, to the isolated, perfused rat lung, can be quantitatively studied under various experimental conditions. It was envisaged that the detail devoted to the development of the system would enable other workers to easily mimic and utilise a similar experimental arrangement for other aerosol studies. The system is versatile and could be used to investigate deposition and absorption of a wide variety of compounds. These may be intended for local or systemic activity. The effects of broncho-dilating or -constricting agents, on the deposition and absorption of subsequently administered aerosolised solutes could be studied, as could effects of molecular change upon the rates and extent of solute transfer. The model could also perhaps be used for studying the effects of aerosol charge (101, 102) on deposition and transfer.

The potential use of the respiratory tract as an alternative route for either local or systemic drug administration is immense. Successful exploitation of this

delivery pathway however, requires that energy is devoted to careful and stepwise research, in order to establish a data-base for deposition and absorption of a wide variety of compounds, presented in a number of aerosol formulations, according to various respiratory regimes. By such methods, inhalation aerosol science may become predictive and resultant aerosol therapy a lot safer and more reliable than it is at present.

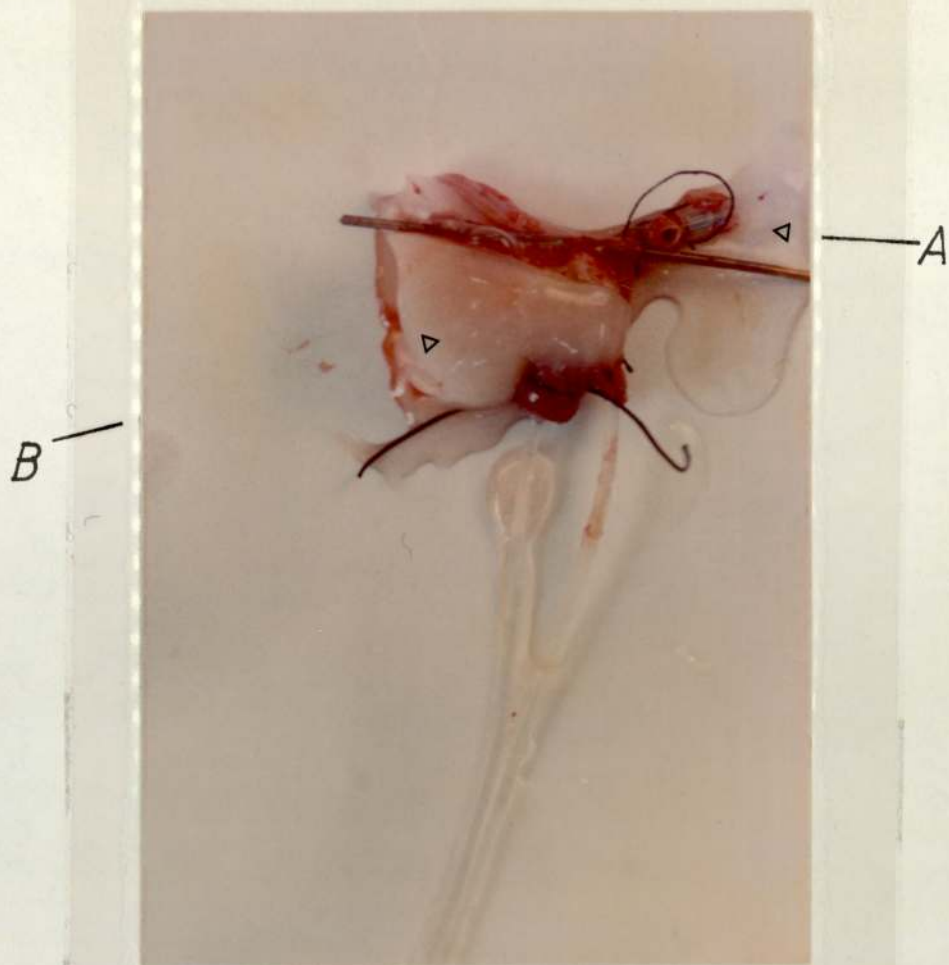


PLATE 1

Dedematous lungs (note glossy appearance and fluid escaping from trachea)

A fluid from trachea
B swollen, glossy lung



PLATE 2

A non-viable lung. Note the mottled right lung (A) becoming oedematous



PLATE 3

A non viable lung after perfusion. Lungs (A) are grey and patchy, indicating loss of viability. Compare with the appearance of the viable lung (Plate 9)



PLATE 4

Tracheotomised rat receiving positive pressure ventilation

A tracheal cannula tied in place

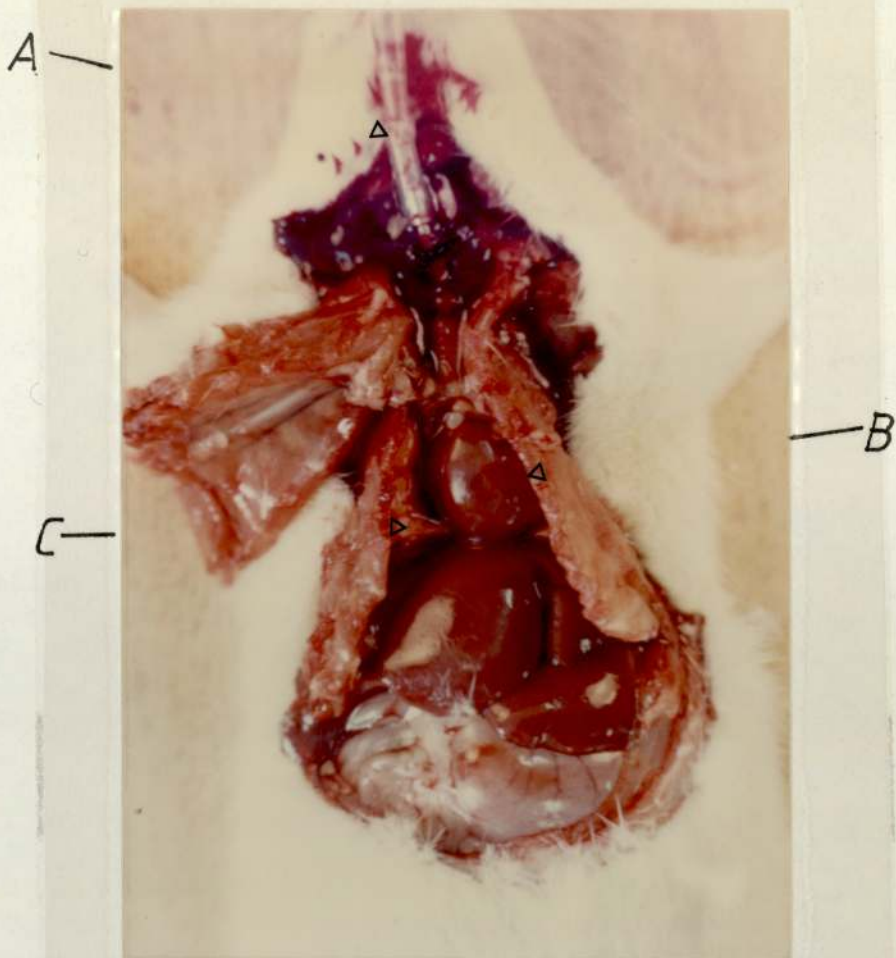


PLATE 5

Tracheotomised rat receiving positive pressure ventilation -
thorax is open, displaying the heart and lungs

A	tracheal cannula
B	heart
C	right lung

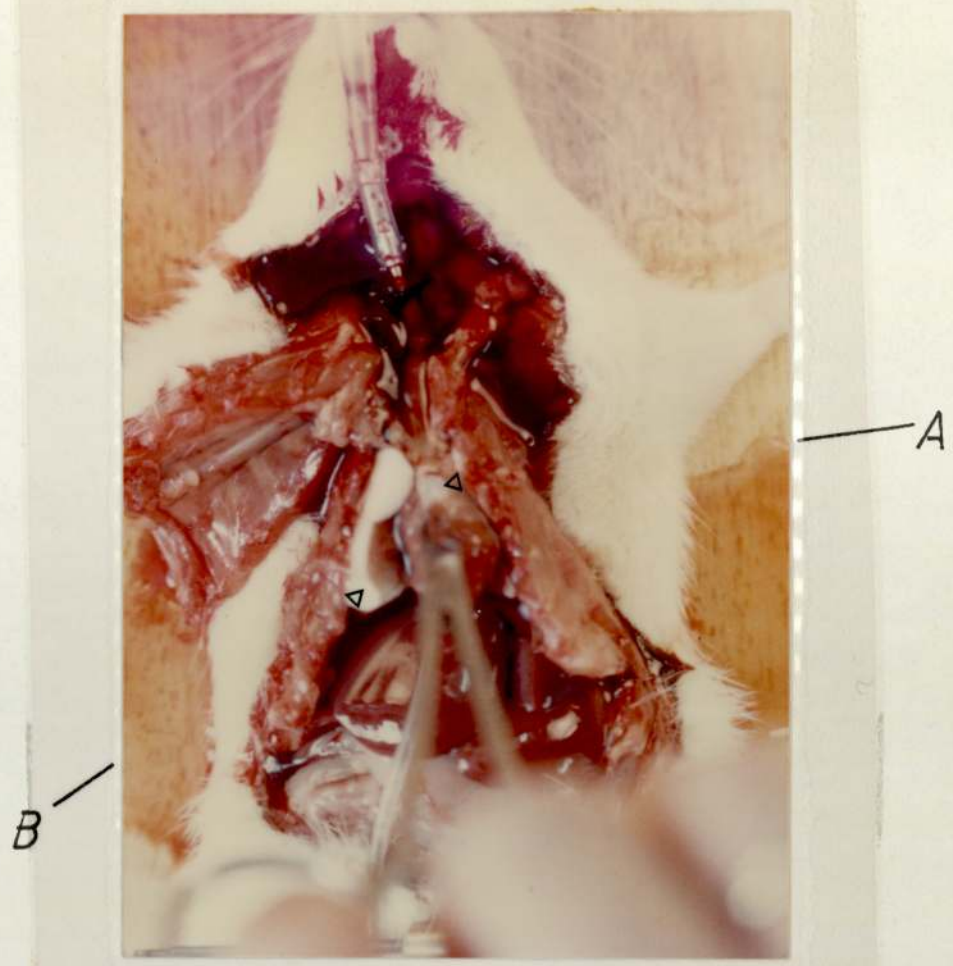


PLATE 6

Cannulation of the pulmonary artery and clearance of blood from the ventilating lungs with K4

- A pulmonary artery cannula
- B right lung cleared of blood

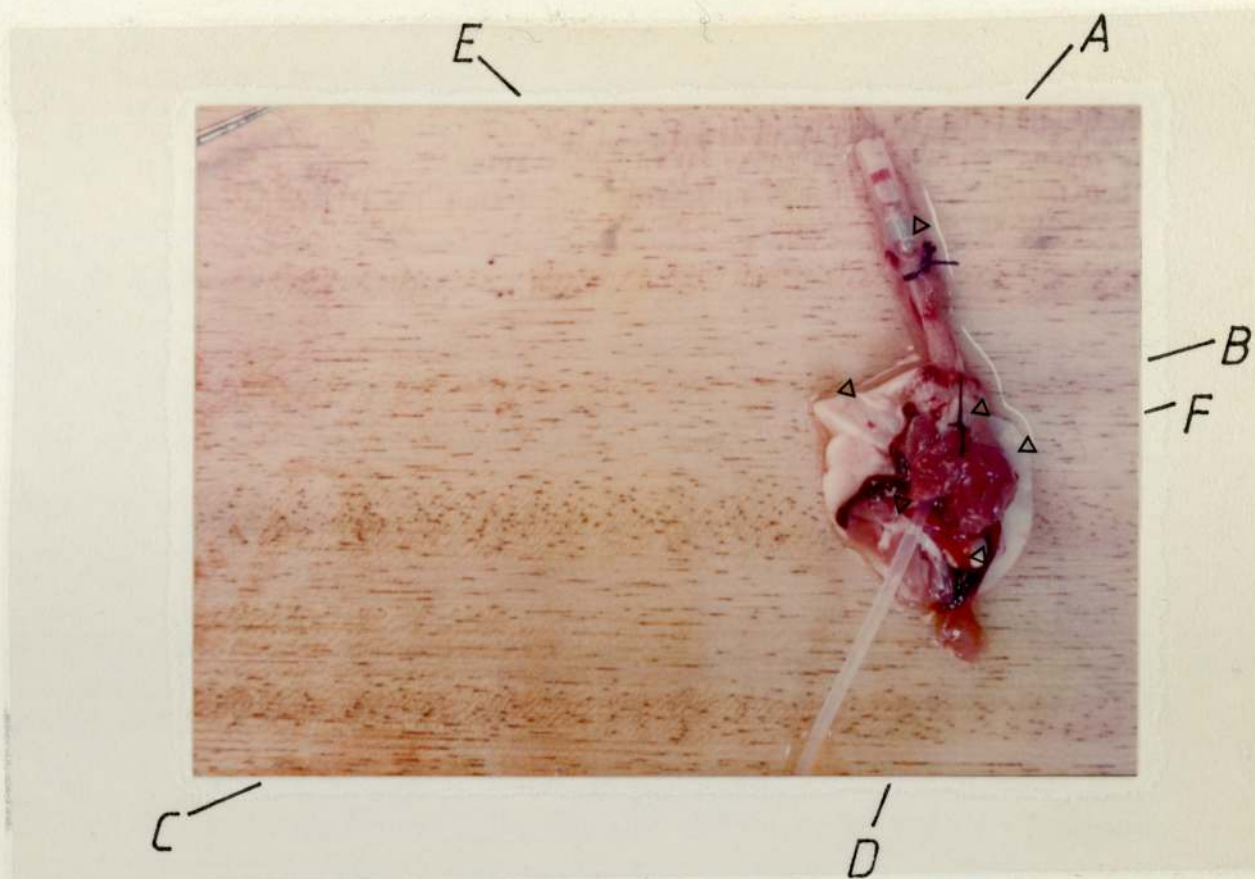


PLATE 7

Isolated, perfused rat lungs, ventral view, with the pulmonary artery cannula tied in place, without ventilation

- | | |
|---|----------------------------------|
| A | cannulated trachea |
| B | secured pulmonary artery cannula |
| C | right ventricle |
| D | tip of heart removed |
| E | right lung |
| F | left lung |

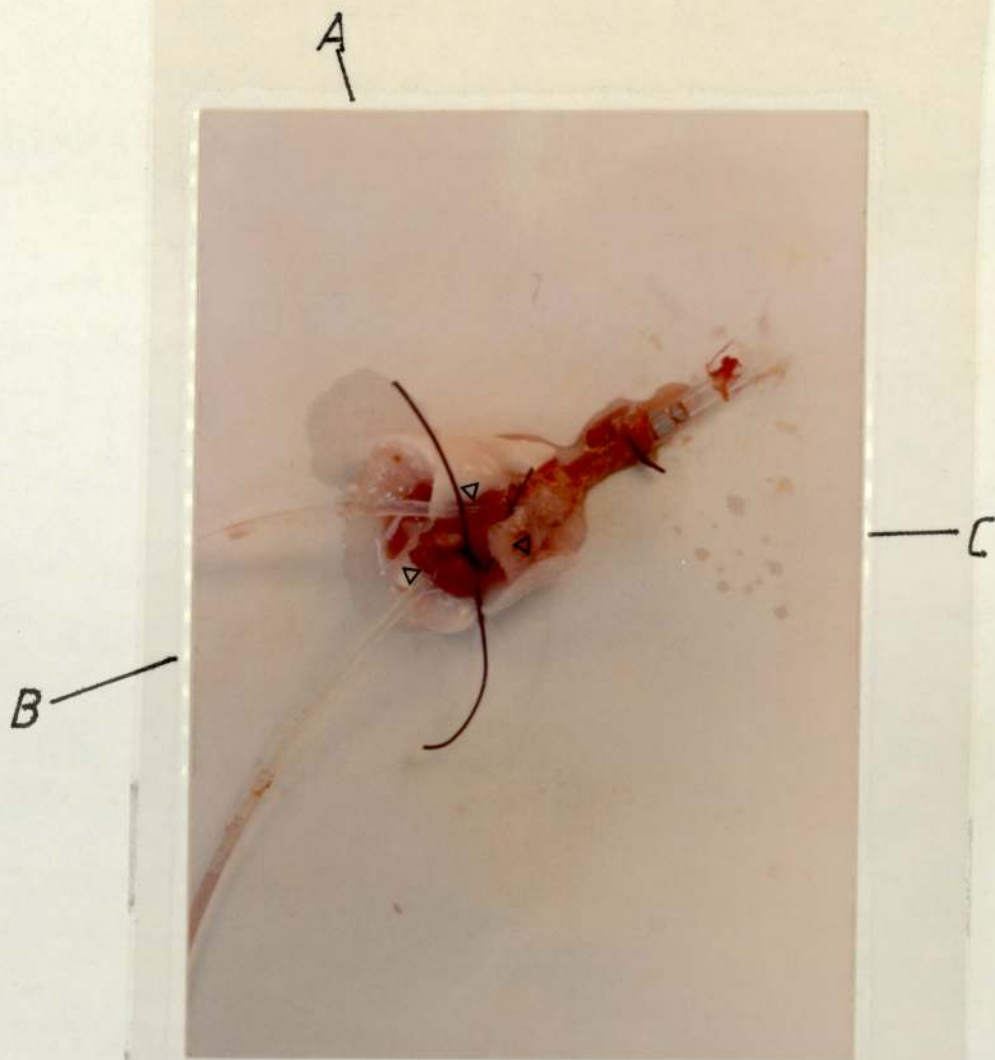


PLATE 8

Isolated, perfused rat lungs, without ventilation. The pulmonary artery and left ventricle are cannulated

- | | |
|---|---------------------------|
| A | pulmonary artery cannula |
| B | cannulated left ventricle |
| C | left atrium |

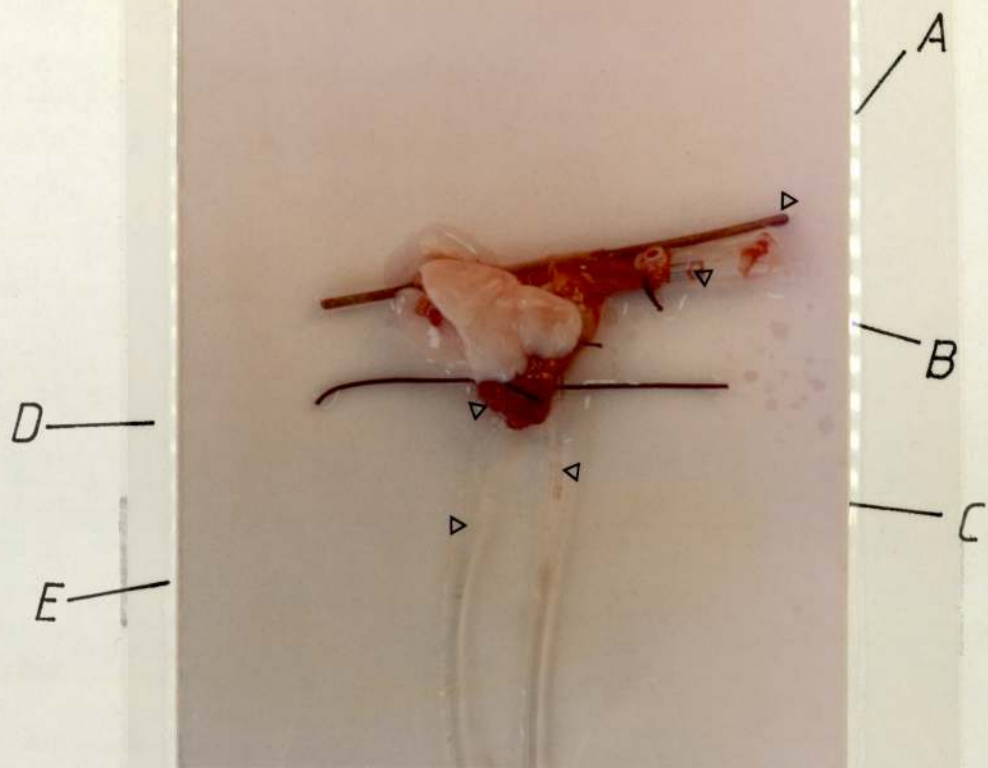


PLATE 9

Viable, unventilated, isolated, perfused rat lung with bar through the oesophagus for horizontal suspension in the artificial thorax

- | | |
|---|--------------------------|
| A | bar through oesophagus |
| B | tracheal cannula |
| C | pulmonary artery cannula |
| D | heart |
| E | left ventricle cannula |

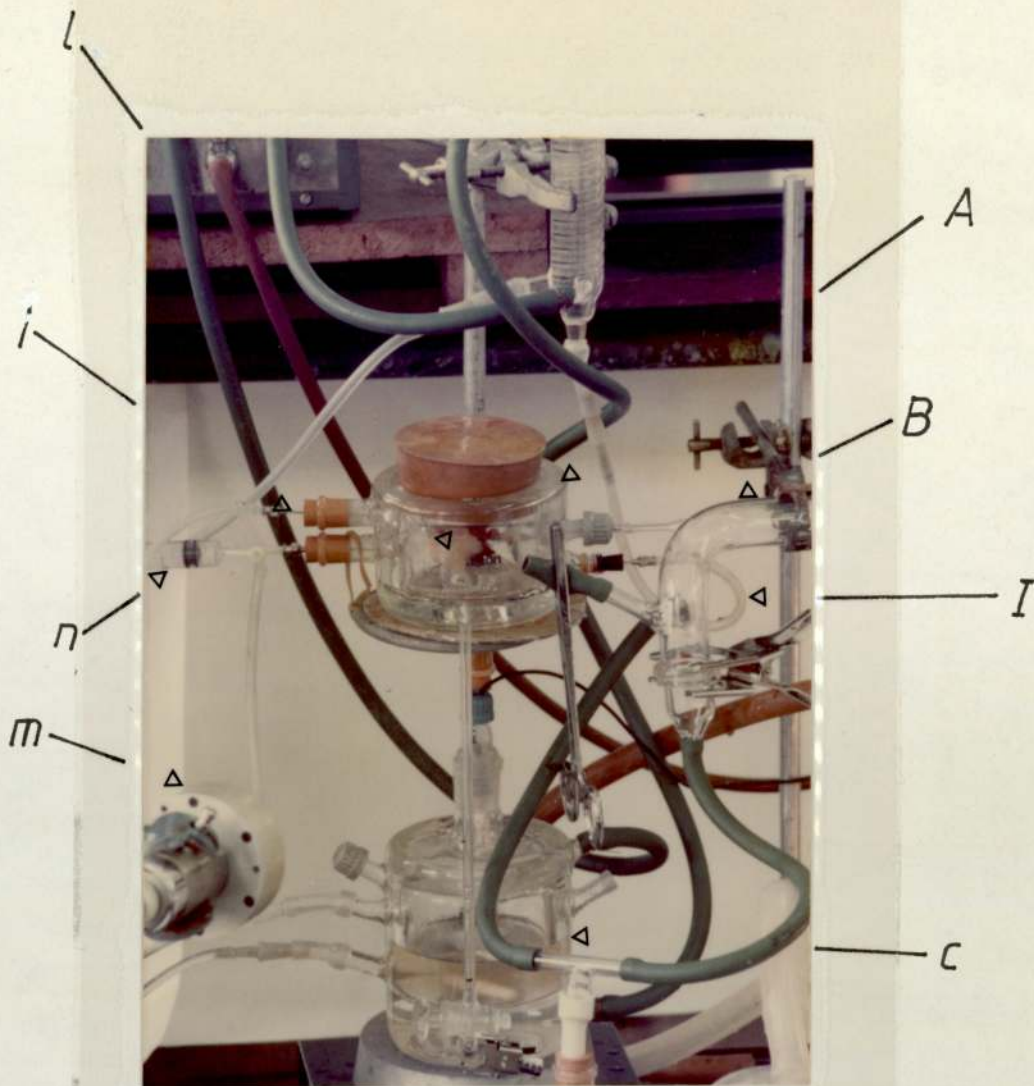


PLATE 10

Isolated, perfused lungs, suspended horizontally in artificial thorax (AT) and maintained under slight negative pressure by withdrawal of air from the AT by syringe

- | | |
|---|---|
| a | artificial thorax |
| C | aerosol administration tube |
| I | perfusate supply to lungs |
| c | perfusate reservoir |
| m | pressure transducer |
| n | syringe |
| i | volume-cycle ventilator connected to AT |
| l | isolated lungs |

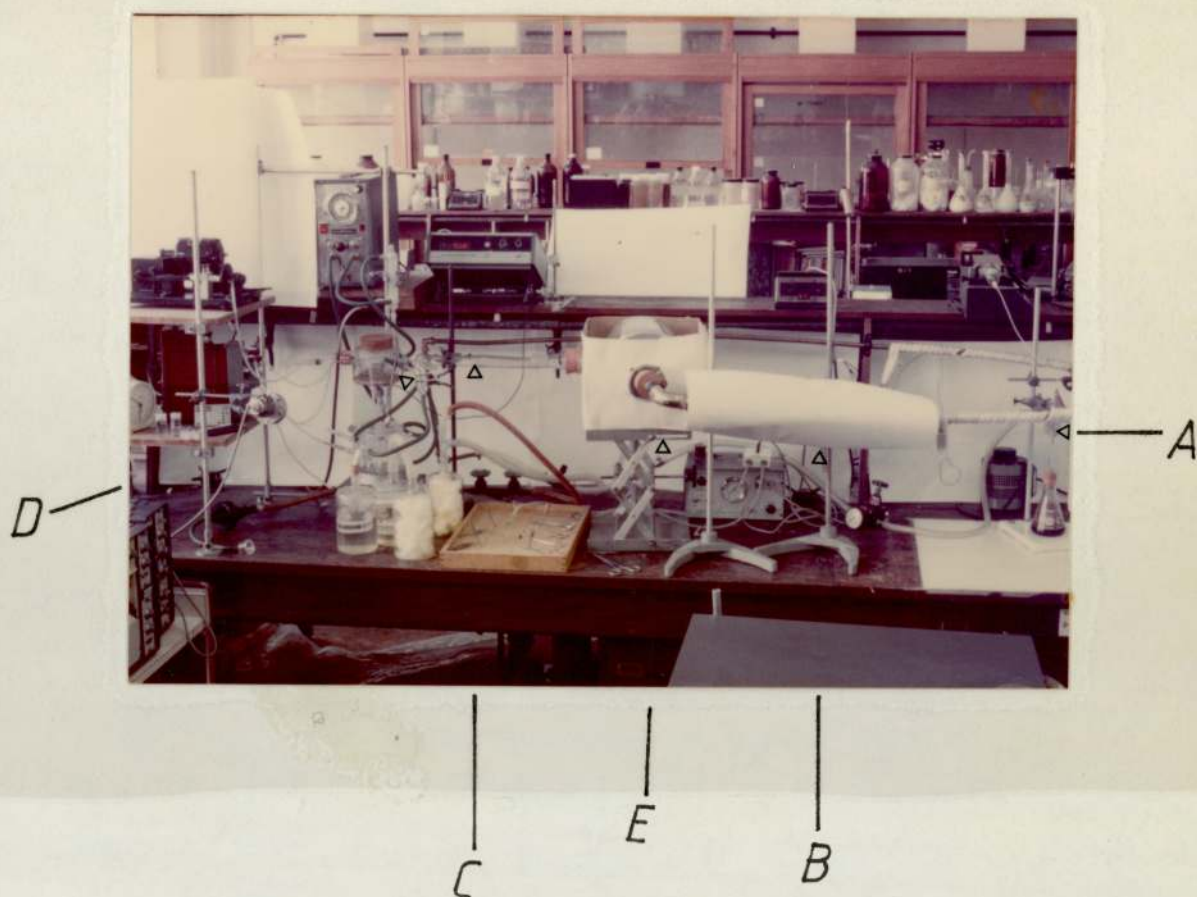
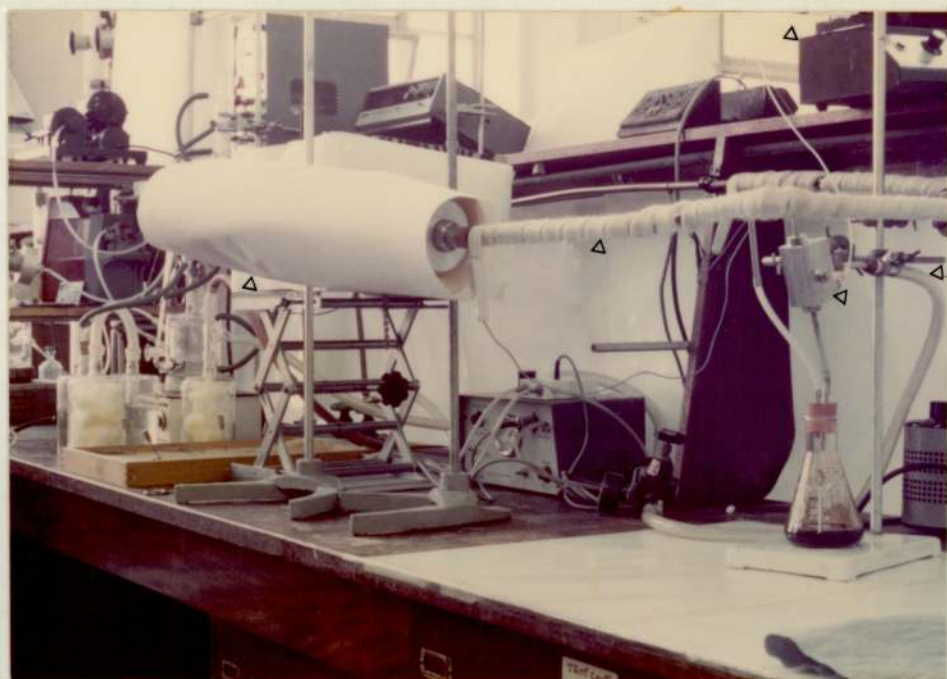


PLATE 11

Aerosol generation apparatus featuring the constant liquid feed atomiser. Aerosols were characterised from D, using the same methods as described for the 3400FB generator (see Fig 4.6)

- | | |
|---|-----------------------------------|
| A | constant liquid feed atomiser |
| B | charge neutralising column |
| C | aerosol administration tube |
| D | aerosol sampling connection point |
| E | silica gel |



B

E

D

A

PLATE 12

Close-up view of constant liquid feed atomiser and associated equipment

- | | |
|---|-------------------------------|
| A | constant liquid feed atomiser |
| B | charge neutralising column |
| C | syringe pump |
| D | compressed air supply |
| E | heated copper tubing |

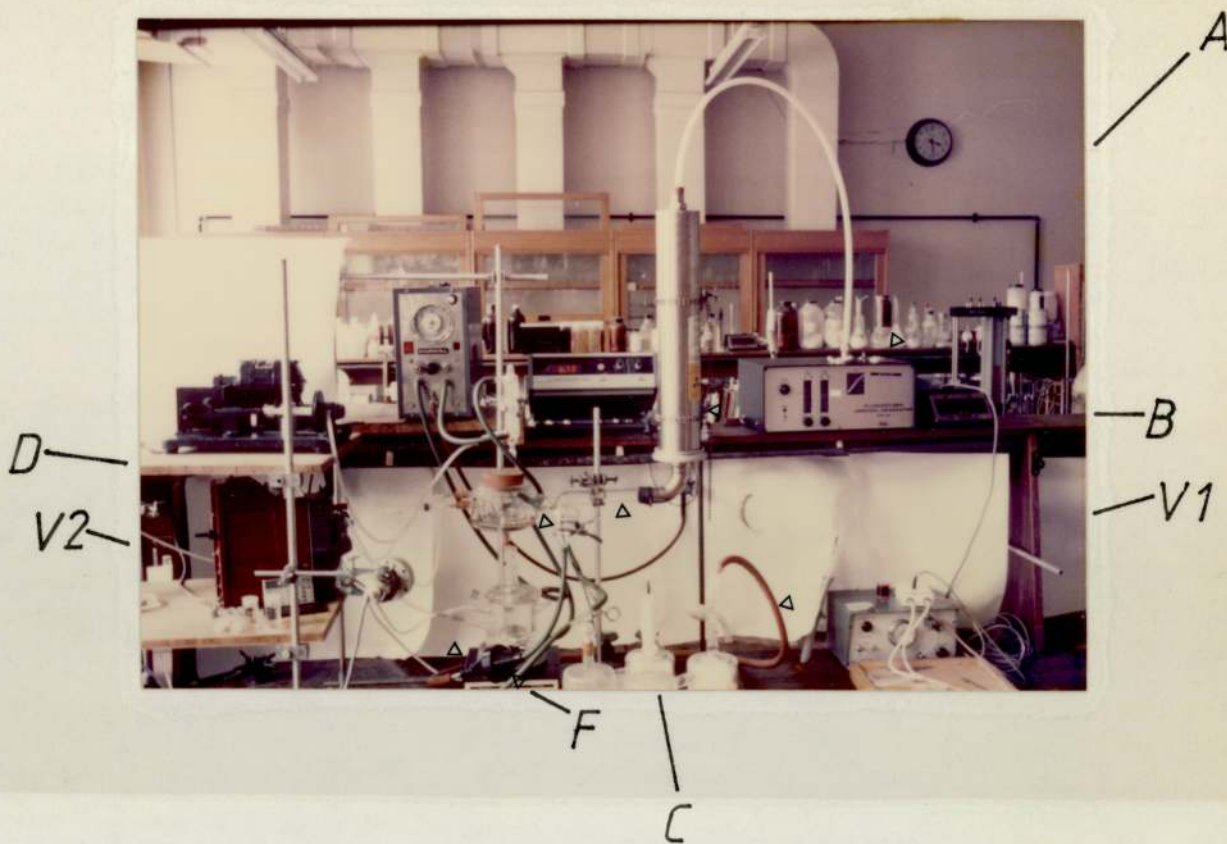


PLATE 13

Aerosol characterisation: determination of aerosol mass output

- | | |
|--------|---|
| A | 3400FB aerosol generator |
| B | charge neutralising column |
| C | aerosol administration tube |
| D | aerosol sampling connection point |
| F | filter in holder, collecting output from 3400FB |
| V1, V2 | connections to vacuum |

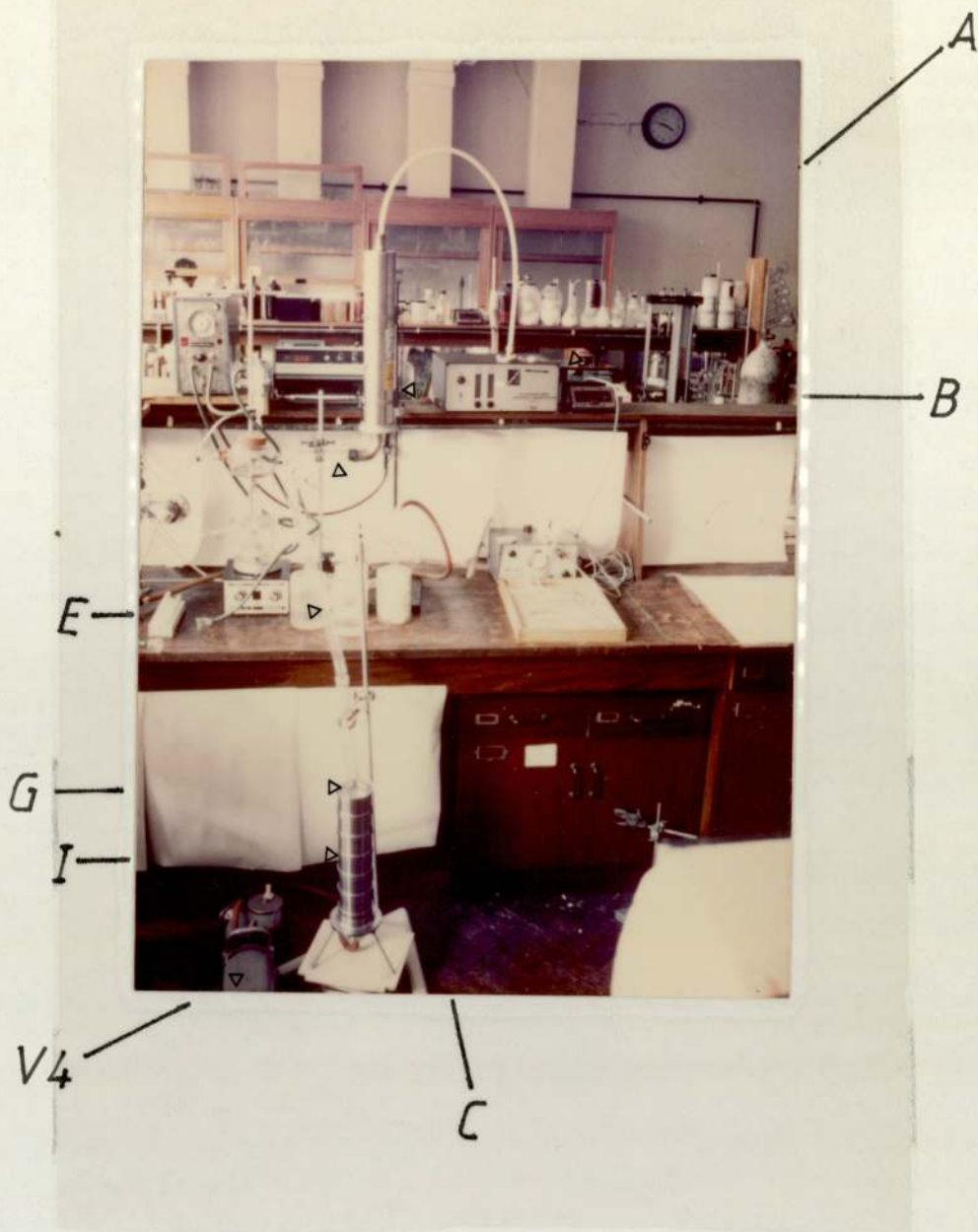


PLATE 14

Aerosol characterisation: determination of particle size distribution using a cascade impactor

- | | |
|--|---|
| <p>A
B
C
E

G
I
V4</p> | <p>3400FB aerosol generator
charge neutralising column
aerosol administration tube
curved tube conveying aerosol to
cascade impactor
inverted funnel
cascade impactor
vacuum pump</p> |
|--|---|

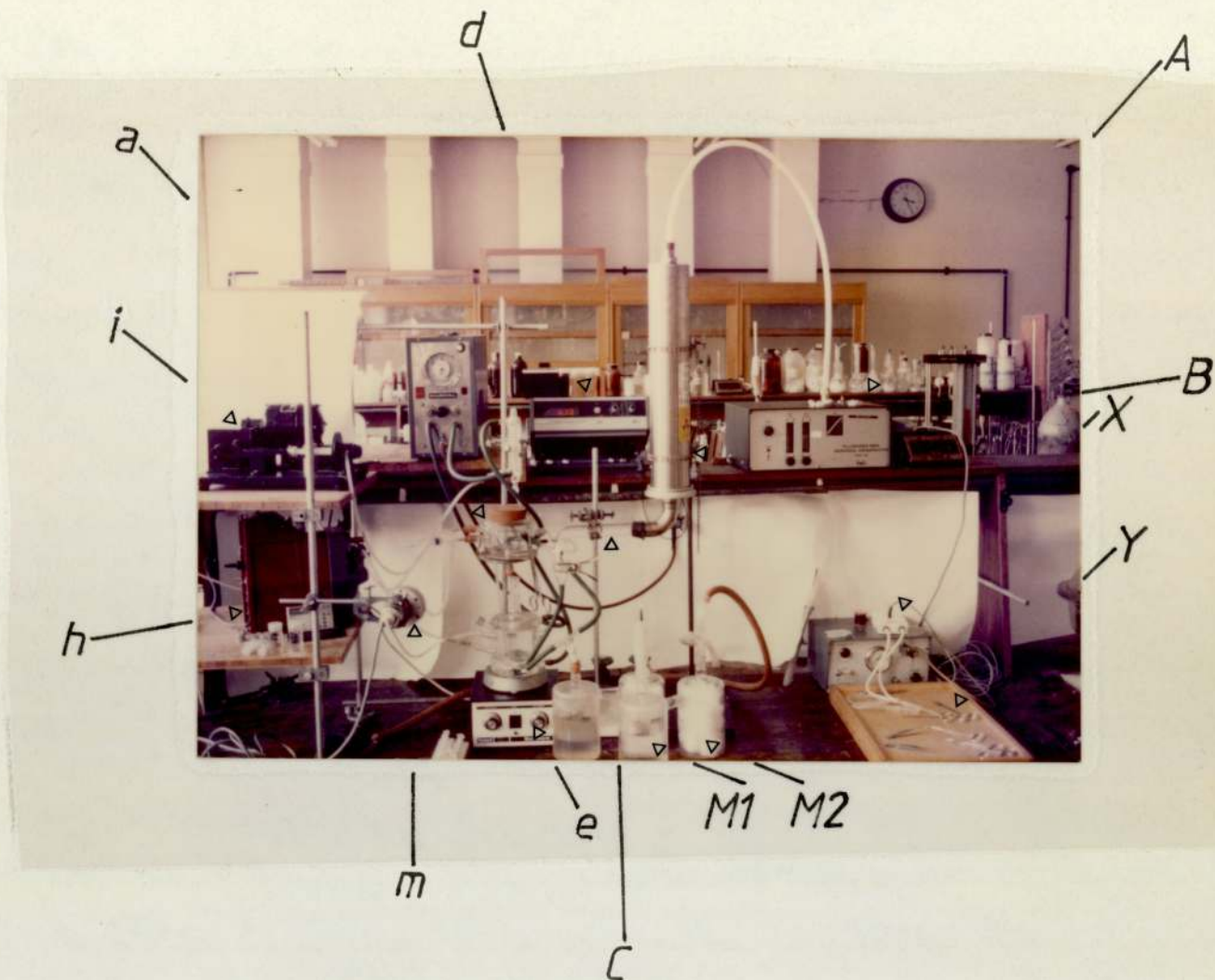


PLATE 15

Apparatus used for aerosol generation and administration to the isolated, perfused rat lung preparation

A	3400FB aerosol generator
B	charge neutralising column
C	aerosol administration tube
M1, M2	aerosol waste traps
i	volume-cycle ventilator
h	perfusate pump
a	artificial thorax
m	pressure transducer
e	magnetic stirrer
d	pH meter
X	pressure-cycle ventilator (for use during surgery only)
Y	operation block

APPENDIX A

TABULATED RESULTS FROM AEROSOL ADMINISTRATION EXPERIMENTS

This appendix lists the results following the III analyses performed after each aerosol administration experiment reported in this thesis. Each Table of results shows data for one experiment. Included, alongside the data for amount in the perfusate versus time, are values for various parameters characterising the aerosol, the respiratory regime, perfusate flow, amount administered or inspired and total deposition.

The amounts of III reported after analysis of the homogenised lungs are corrected for the loss known to occur due to binding to intracellular components. The amounts of III in the perfusate at any given time however, are not corrected for binding losses known to occur within the apparatus. For this reason, and the observation that occasionally, more III was present in the perfusate solution at the true end of an experiment (if viability was lost), the total deposited does not always tally with the sum of the amounts in the perfusate and the homogenised lung.

Values for "theoretical f_{∞} " were calculated according to section 5.4.4 and 5.3.4 and used in constructing the first-order plots shown in Chapter 5.

TABLE A1

Tidal volume	= 1.92ml
Perfusion rate	= 15ml min ⁻¹
Respiratory frequency	= 14 cycles min ⁻¹
MMD ₅₀	= 3.98um
Geometric standard deviation	= 1.19
Aerosol III concentration	= 198ng ml ⁻¹
Amount III in tracheal cannula	= 73.69ug
Amount III in homogenised lung	= 20.7ug
Total deposited	= 39.44ug
Total inspired	= 106.6ug
Theoretical f _∞	= 0.413

Time (min)	Amount III in perfusate (ug)
6.0	0.118
8.0	0.459
10.0	0.802
12.0	1.140
14.0	1.682
16.0	2.303
18.0	3.169
20.0	4.578
25.0	7.058
30.0	9.810
35.0	11.640
45.0	13.740
60.0	15.155
75.0	16.458
90.0	16.082
105.0	16.316

TABLE A2

Tidal volume	= 1.86ml
Perfusion rate	= 15ml min ⁻¹
Respiratory frequency	= 28 cycles min ⁻¹
MMD _{ae}	= 3.92um
Geometric standard deviation	= 1.30
Aerosol III concentration	= 205ng ml ⁻¹
Amount III in tracheal cannula	= 44.715ug
Amount III in homogenised lung	= 11.5ug
Total deposited	= 31.66ug
Total inspired	= 213.53ug
Theoretical f _∞	= 0.625

Time (min)	Amount III in perfusate (ug)
12.0	0.39
14.0	0.617
16.0	1.621
18.0	3.321
20.0	3.761
25.0	6.491
30.0	8.281
35.0	11.518
45.0	13.245
60.0	17.693
75.0	18.574
90.0	17.860

TABLE A3

Tidal volume	= 2.07ml
Perfusion rate	= 15ml min ⁻¹
Respiratory frequency	= 28 cycles min ⁻¹
MMD _{ae}	= 3.88um
Geometric standard deviation	= 1.32
Aerosol III concentration	= 310ng ml ⁻¹
Amount III in tracheal cannula	= 79.0ug
Amount III in homogenised lung	= 14.724ug
Total deposited	= 52.775ug
Total inspired	= 359.35ug
Theoretical f _∞	= 0.745

Time (min)	Amount III in perfusate (ug)
6.0	0.714
8.0	0.730
10.0	0.961
12.0	3.403
14.0	4.178
18.0	9.039
20.0	12.759
25.0	17.727
30.0	21.996
35.0	24.627
45.0	29.677
60.0	34.789
75.0	37.577
90.0	36.397

TABLE A4

Tidal volume	= 2.0ml
Perfusion rate	= 15ml min ⁻¹
Respiratory frequency	= 14 cycles min ⁻¹
MMD ₅₀	= 3.88um
Geometric standard deviation	= 1.32
Aerosol III concentration	= 230ng ml ⁻¹
Amount III in tracheal cannula	= 26.554ug
Amount III in homogenised lung	= 8.751ug
Total deposited	= 28.116ug
Total inspired	= 129.932ug
Theoretical f _∞	= 0.555

Time (min)	Amount III in perfusate (ug)
16.0	0.049
18.0	0.492
20.0	1.937
25.0	3.240
30.0	4.818
35.0	5.551
45.0	8.633
60.0	8.798
75.0	9.371
85.0	8.442
88.0	9.339

TABLE A5

Tidal volume	= 1.89ml
Perfusion rate	= 15ml min ⁻¹
Respiratory frequency	= 28 cycles min ⁻¹
MMD _{ae}	= 2.62um
Geometric standard deviation	= 1.5
Aerosol III concentration	= 260ng ml ⁻¹
Amount III in tracheal cannula	= 38.826ug
Amount III in homogenised lung	= 10.30ug
Total deposited	= 36.60ug
Total inspired	= 275.184ug
Theoretical f _∞	= 0.595

Time (min)	Amount III in perfusate (ug)
1.0	0.154
2.0	0.311
4.0	0.489
6.0	0.637
8.0	0.802
10.0	1.045
12.0	1.923
14.0	2.570
16.0	3.711
18.0	5.747
20.0	7.753
25.0	11.746
30.0	15.168
35.0	18.327
45.0	19.432
60.0	20.867
75.0	22.158
90.0	22.313

TABLE A6

Tidal volume	= 2.4ml
Perfusion rate	= 15ml min ⁻¹
Respiratory frequency	= 14 cycles min ⁻¹
MMD ₅₀	= 2.62um
Geometric standard deviation	= 1.5
Aerosol III concentration	= 203ng ml ⁻¹
Amount III in tracheal cannula	= 19.438ug
Amount III in homogenised lung	= 8.90ug
Total deposited	= 36.70ug
Total inspired	= 136.274ug
Theoretical f _∞	= 0.582

Time (min)	Amount III in perfusate (ug)
2.0	0.277
4.0	0.666
6.0	0.951
8.0	1.109
10.0	1.666
12.0	2.014
14.0	2.796
16.0	3.083
18.0	4.154
20.0	6.781
25.0	10.543
30.0	13.680
45.0	19.260
60.0	20.369
75.0	21.405
90.0	20.685

TABLE A7

Tidal volume	= 2.2ml
Perfusion rate	= 15ml min ⁻¹
Respiratory frequency	= 7 cycles min ⁻¹
MMD ₅₀	= 2.62um
Geometric standard deviation	= 1.5
Aerosol III concentration	= 303.8ng ml ⁻¹
Amount III in tracheal cannula	= 19.047ug
Amount III in homogenised lung	= 13.80ug
Total deposited	= 40.40ug
Total inspired	= 63.80ug
Theoretical f _∞	= 0.522

Time (min)	Amount III in perfusate (ug)
------------	------------------------------

12.0	1.346
14.0	1.539
16.0	2.682
18.0	4.642
20.0	5.616
25.0	9.963
30.0	13.860
45.0	20.011
60.0	20.290
75.0	22.220
90.0	21.412

TABLE A8

Tidal volume	= 2.25ml
Perfusion rate	= 15ml min ⁻¹
Respiratory frequency	= 7 cycles min ⁻¹
MMD ₅₀	= 3.96um
Geometric standard deviation	= 1.29
Aerosol III concentration	= 315ng ml ⁻¹
Amount III in tracheal cannula	= 23.829ug
Amount III in homogenised lung	= 11.62ug
Total deposited	= 36.82ug
Total inspired	= 132.237ug
Theoretical f _∞	= 0.592

Time (min)	Amount III in perfusate (ug)
------------	------------------------------

8.0	0.128
10.0	0.458
12.0	0.663
14.0	1.135
16.0	2.523
18.0	2.969
20.0	4.603
25.0	6.776
30.0	10.089
35.0	13.849
45.0	16.641
60.0	19.241
75.0	21.171
90.0	22.134
110.0	23.458

TABLE A9

Tidal volume	= 1.35ml
Perfusion rate	= 15ml min ⁻¹
Respiratory frequency	= 7 cycles min ⁻¹
MMD ₅₀	= 3.96um
Geometric standard deviation	= 1.29
Aerosol III concentration	= 189ng ml ⁻¹
Amount III in tracheal cannula	= 13.460ug
Amount III in homogenised lung	= 4.994ug
Total deposited	= 8.48ug
Total inspired	= 86.96ug
Theoretical f _∞	= 0.380

Time (min)	Amount III in perfusate (ug)
20.0	0.263
25.0	0.618
30.0	0.824
35.0	0.936
45.0	2.064
60.0	2.736
75.0	2.985
80.0	2.960

TABLE A10

Tidal volume	= 0.92ml
Perfusion rate	= 15ml min ⁻¹
Respiratory frequency	= 7 cycles min ⁻¹
MMD _{ae}	= 3.96um
Geometric standard deviation	= 1.29
Aerosol III concentration	= 409.3ng ml ⁻¹
Amount III in tracheal cannula	= 2.901ug
Amount III in homogenised lung	= 1.865ug
Total deposited	= 3.852ug
Total inspired	= 52.718ug
Theoretical f _∞	= 0.273

Time (min)	Amount III in perfusate (ug)
20.0	0.043
25.0	0.198
30.0	0.251
35.0	0.352
45.0	0.517
60.0	0.794
75.0	0.847
90.0	0.924

TABLE A11

Tidal volume	= 1.85ml
Perfusion rate	= 15ml min ⁻¹
Respiratory frequency	= 14 cycles min ⁻¹
MMD ₅₀	= 3.98um
Geometric standard deviation	= 1.19
Aerosol III concentration	= 207.9ng ml ⁻¹
Amount III in tracheal cannula	= 35.310ug
Amount III in homogenised lung	= 17.822ug
Total deposited	= 37.688ug
Total inspired	= 107.680ug
Theoretical f _∞	= 0.410

Time (min)	Amount III in perfusate (ug)
8.0	0.060
10.0	0.120
12.0	0.514
14.0	1.663
16.0	2.183
18.0	3.329
20.0	5.738
25.0	6.979
30.0	9.227
35.0	12.127
45.0	13.648
60.0	14.033
75.0	14.941
90.0	14.535

TABLE A12

Tidal volume	= 1.86ml
Perfusion rate	= 15ml min ⁻¹
Respiratory frequency	= 14 cycles min ⁻¹
MMD ₅₀	= 3.88um
Geometric standard deviation	= 1.32
Aerosol III concentration	= 224ng ml ⁻¹
Amount III in tracheal cannula	= 8.773ug
Amount III in homogenised lung	= 7.002ug
Total deposited	= 19.680ug
Total inspired	= 116.659ug
Theoretical f _∞	= 0.470

Time (min)	Amount III in perfusate (ug)
16.0	0.583
18.0	0.840
20.0	1.730
25.0	2.072
30.0	4.629
35.0	5.593
45.0	6.796
75.0	6.861
90.0	7.231
97.0	7.229

TABLE A13

Tidal volume	= 1.64ml
Perfusion rate	= 5ml min ⁻¹
Respiratory frequency	= 7 cycles min ⁻¹
MMD ₅₀	= 3.96um
Geometric standard deviation	= 1.29
Aerosol III concentration	= 429.3ng ml ⁻¹
Amount III in tracheal cannula	= 11.85ug
Amount III in homogenised lung	= 7.729ug
Total deposited	= 13.126ug
Total inspired	= 98.567ug
Theoretical f _∞	= 0.358

Time (min)	Amount III in perfusate (ug)
18.0	0.039
20.0	0.270
25.0	1.485
30.0	2.002
35.0	2.340
45.0	3.280
60.0	4.350
75.0	4.884
80.0	4.812
85.0	4.856

TABLE A14

Tidal volume	= 1.95ml
Perfusion rate	= 5ml min ⁻¹
Respiratory frequency	= 28 cycles min ⁻¹
MMD _{aa}	= 3.59um
Geometric standard deviation	= 1.30
Aerosol III concentration	= 114.7ng ml ⁻¹
Amount III in tracheal cannula	= 15.163ug
Amount III in homogenised lung	= 5.134ug
Total deposited	= 16.278ug
Total inspired	= 125.22ug
Theoretical f _∞	= 0.622

Time (min)	Amount III in perfusate (ug)
------------	------------------------------

12.0	0.157
14.0	0.584
16.0	1.787
18.0	2.176
20.0	3.407
25.0	4.527
30.0	5.260
35.0	7.106
45.0	7.707
60.0	9.077
75.0	9.103
90.0	9.831
98.0	10.757
105.0	10.137

TABLE A15

Tidal volume	= 2.4ml
Perfusion rate	= 15ml min ⁻¹
Respiratory frequency	= 7 cycles min ⁻¹
MMD ₅₀	= 3.75um
Geometric standard deviation	= 1.31
Aerosol III concentration	= 277ng ml ⁻¹
Amount III in tracheal cannula	= 18.00ug
Amount III in homogenised lung	= 9.822ug
Total deposited	= 25.137ug
Total inspired	= 93.07ug
Theoretical f _∞	= 0.42

Time (min)	Amount III in perfusate (ug)
------------	------------------------------

6.0	0.459
8.0	0.545
10.0	1.885
12.0	2.523
14.0	3.028
16.0	3.672
18.0	4.691
20.0	5.850
25.0	6.149
30.0	8.798
45.0	9.612
60.0	10.058
75.0	10.031

TABLE A16

Tidal volume	= 2.05ml
Perfusion rate	= 15ml min ⁻¹
Respiratory frequency	= 28 cycles min ⁻¹
MMD ₅₀	= 4.00um
Geometric standard deviation	= 1.25
Aerosol III concentration	= 280ng ml ⁻¹
Amount III in tracheal cannula	= 25.203ug
Amount III in homogenised lung	= 13.919ug
Total deposited	= 48.797ug
Total inspired	= 221.90ug
Theoretical f _∞	= 0.683

Time (min)	Amount III in perfusate (ug)
------------	------------------------------

4.0	0.511
6.0	0.424
8.0	0.824
10.0	2.006
12.0	3.860
14.0	4.818
16.0	7.649
18.0	8.643
20.0	11.819
25.0	15.466
30.0	18.988
35.0	22.122
45.0	26.775
60.0	30.112
75.0	31.561
90.0	32.784
100.0	32.701
105.0	31.629

TABLE A17

Tidal volume	= 1.96ml
Perfusion rate	= 15ml min ⁻¹
Respiratory frequency	= 7 cycles min ⁻¹
MMD ₅₀	= 3.35um
Geometric standard deviation	= 1.83
Aerosol III concentration	= 248ng ml ⁻¹
Amount III in tracheal cannula	= 15.044ug
Amount III in homogenised lung	= 10.718ug
Total deposited	= 25.397ug
Total inspired	= 68.051ug
Theoretical f _∞	= 0.520

Time (min)	Amount III in perfusate (ug)
------------	------------------------------

8.0	0.624
10.0	1.802
12.0	1.814
14.0	2.853
16.0	4.422
18.0	4.822
20.0	5.157
25.0	7.389
30.0	9.078
35.0	11.232
45.0	12.185
60.0	11.899
75.0	12.730

TABLE A18

Tidal volume	= 2.02ml
Perfusion rate	= 5.5ml min ⁻¹
Respiratory frequency	= 28 cycles min ⁻¹
MMD ₅₀	= 3.26um
Geometric standard deviation	= 1.49
Aerosol III concentration	= 213.9ng ml ⁻¹
Amount III in tracheal cannula	= 11.34ug
Amount III in homogenised lung	= 6.676ug
Total deposited	= 36.016ug
Total inspired	= 241.964ug
Theoretical f _∞	= 0.745

Time (min)	Amount III in perfusate (ug)
------------	------------------------------

6.0	0.504
8.0	1.534
10.0	2.247
12.0	3.979
14.0	4.985
16.0	6.732
18.0	7.806
20.0	10.410
25.0	13.840
30.0	16.813
35.0	19.253
45.0	23.434
60.0	24.880
75.0	25.714
90.0	26.420
105.0	27.387
120.0	26.810

TABLE A19

Tidal volume	= 2.40ml
Perfusion rate	= 15ml min ⁻¹
Respiratory frequency	= 28 cycles min ⁻¹
MMD ₅₀	= 3.93um
Geometric standard deviation	= 1.52
Aerosol III concentration	= 200.9ng ml ⁻¹
Amount III in tracheal cannula	= 8.760ug
Amount III in homogenised lung	= 19.14ug
Total deposited	= 61.728ug
Total inspired	= 270.00ug
Theoretical f _∞	= 0.690

Time (min)	Amount III in perfusate (ug)
------------	------------------------------

4.0	0.130
6.0	1.472
8.0	2.128
10.0	3.452
12.0	4.623
14.0	6.255
16.0	7.492
18.0	9.470
20.0	11.826
25.0	19.082
30.0	24.226
45.0	35.830
60.0	39.235
75.0	39.655

TABLE A20

Tidal volume	= 2.25ml
Perfusion rate	= 15ml min ⁻¹
Respiratory frequency	= 28 cycles min ⁻¹
MMD ₅₀	= 3.80um
Geometric standard deviation	= 1.42
Aerosol III concentration	= 192ng ml ⁻¹
Amount III in tracheal cannula	= 41.21ug
Amount III in homogenised lung	= 14.68ug
Total deposited	= 47.51ug
Total inspired	= 242.50ug
Theoretical f _∞	= 0.640

Time (min)	Amount III in perfusate (ug)
------------	------------------------------

1.0	0.353
2.0	0.402
4.0	0.456
6.0	0.978
8.0	1.313
10.0	2.480
12.0	3.059
14.0	4.055
16.0	4.232
18.0	6.499
20.0	8.064
25.0	10.943
30.0	14.811
45.0	24.599
60.0	27.071
75.0	30.363
90.0	30.424
100.0	30.464

TABLE A21

Instillation experiment I

Perfusion rate	= 15ml min ⁻¹
Amount III in tracheal cannula	= 20.70ug
Amount III in homogenised lung	= 15.34ug
Total deposited	= 40.57ug
Total instilled	= 60.97ug
Theoretical f_{∞}	= 0.615

Time (min)	Amount III in perfusate (ug)
5.0	1.70
10.0	6.60
15.0	9.63
20.0	16.37
30.0	18.71
45.0	20.48
53.0	23.88

TABLE A22

Instillation experiment II

Perfusion rate	= 15ml min ⁻¹
Amount III in tracheal cannula	= 12.72ug
Amount III in homogenised lung	= 10.17ug
Total deposited	= 46.872ug
Total instilled	= 61.62ug
Theoretical f _∞	= 0.790

Time (min)	Amount III in perfusate (ug)
------------	------------------------------

5.0	5.872
10.0	12.772
15.0	19.328
20.0	25.647
30.0	30.091
45.0	32.314
60.0	35.586

REFERENCES

1. A. Junod. Uptake, release and metabolism of drugs by the lungs. *Pharmacol. Ther. B.*, 2, 511 - 521 (1976).
2. P. R. Mayer, W. C. Lubawy, P. J. McNamara and H. B. Kostenbauder. Metabolism of isorbide dinitrate in the isolated, perfused rabbit lung. *J. Pharm. Sci.*, 72, 785 - 792 (1983).
3. P. J. Wedlund, S. -L. Chang and R. H. Levy. Steady - state determination of the contribution of lung metabolism to the total body clearance of drugs: application to carbamazepine. *J. Pharm. Sci.*, 72, 860 - 862 (1983).
4. J. M. Collins and R. L. Dedrick. Contribution of lungs to total body clearance: linear and non-linear effects. *J. Pharm. Sci.*, 71, 66 - 70 (1982).
5. T. C. Orton, M. W. Anderson, R. D. Pickett, T. E. Eling and J. R. Fouts. Xenobiotic accumulation and metabolism by isolated, perfused rabbit lungs. *J. Pharmacol. Exp. Therap.*, 186, 482 - 497 (1973).
6. E. Bingham, R. Niemeier and W. Dalbey. Metabolism of environmental pollutants by the isolated, perfused lung. *Federation Proc.*, 35, 81 - 84 (1976).
7. R. Niemeier and E. Bingham. An isolated, perfused lung preparation for metabolic studies. *Life Sci.*, 11, 807 - 820 (1972).
8. M. E. Shaw and R. A. Rhoades. Substrate metabolism in the perfused lung: response to changes in circulating glucose and palmitate levels. *Lipids*, 12, 930 - 935 (1977).
9. E. B. Olson. Jr., M. Ghias-Ud-Din and J. Rankin. Serotonin uptake and metabolism in isolated, perfused fetal, newborn and adult rabbit lungs. *Lung*, 161, 173 - 179 (1983).
10. R. I. Godinez and W. J. Longmore. Use of the isolated perfused rat lung in studies on lung lipid metabolism. *J. Lipid. Res.*, 14, 138 - 143 (1973).
11. R. A. Rhoades. Net uptake of glucose, glycerol and fatty acids by the isolated, perfused rat lung. *Am. J. Physiol.*, 226, 144 - 149 (1974).

12. D. A. Wiersma and R. A. Roth. Clearance of 5 - hydroxytryptamine by rat lung and liver: the importance of relative perfusion and intrinsic clearance. *J. Pharmacol. Exp. Therap.*, 212, 97 - 102 (1980).
13. H. Toivonen, J. Hartiala and Y. S. Bakhle. Effects of high oxygen tension on the metabolism of vasoactive hormones in isolated, perfused rat lungs. *Acta. Physiol. Scand.*, 111, 185 - 192 (1982).
14. D. A. Wiersma, W. E. Braselton and R. A. Roth. The influence of flow on the metabolism of perfused benzo(a)pyrene by isolated rat lung. *Chem. Biol. Interactions.*, 43, 1 - 15 (1982).
15. Y. S. Bakhle, J. Hartiala and P. Uotila. Effects of cigarette smoke on the metabolism of vasoactive hormones in isolated rat lungs. *Brit. J. Pharmacol.*, 65, 495 - 499 (1979).
16. K. M. McCormack, R. A. Roth, K. B. Wallace, L. M. Ross and J. B. Hook. Nonrespiratory metabolic function and morphology of lung following exposure to polybrominated biphenyls in rats. *J. Tox. Envir. Hlth.*, 9, 27 - 39 (1982).
17. K. Okumura, H. Yoshida and R. Hori. Tissue distribution and metabolism of drugs. III. Accumulation of drugs by the isolated, perfused rat lung. *J. Pharm. Dyn.*, 1, 230 - 237 (1978).
18. S. H. Curry. Theoretical changes in drug distribution resulting from changes in binding to plasma proteins and to tissues. *J. Pharm. Pharmacol.*, 22, 753 - 757 (1970).
19. J. A. Burton, T. H. Gardiner and L. S. Schanker. Absorption of herbicides from the rat lung. *Arch. Environ. Hlth.*, 29, 31 - 33 (1974).
20. L. V. Lourenco and E. Cotromanes. Clinical aerosols. II. Therapeutic aerosols. *Arch. Int. Med.*, 142, 2299 - 2308 (1982).
21. A. Ryrfeldt and E. Nilsson. Uptake and biotransformation of ibuprofen and terbutaline in isolated perfused rat and guinea pig lungs. *Biochem. Pharmacol.*, 27, 301 - 305 (1978).
22. A. Ryrfeldt. The physiological deposition of ibuprofen, terbutaline and isoproterenol after endotracheal instillation to rats. *Xenobiotica*, 5, 521 - 529 (1975).
23. L. S. Schanker. Drug absorption from the lung. *Biochem. Pharmacol.*, 27, 381 - 385 (1978).
24. R. Effros and G. R. Mason. Measurements of pulmonary epithelial permeability in vivo. *Am. Rev. Resp. Dis.*, 127, S59 - S61 (1983).
25. R. V. Lourenco and E. Cotromanes. Clinical aerosols. I.

- Characterisation of aerosols and their diagnostic uses. Arch. Int. Med., 142, 2163 - 2172 (1982).
26. G. Oberdorsver, M. J. Utell, D. A. Webb, M. Ivanovich, R. W. Hyde and P. E. Morrow. Reproducibility of lung clearance of ^{99m}Tc - DTPA aerosols for measuring an index of lung permeability. Ann. Occ. Hyg., 26, 205 - 207 (1982).
27. T. F. Hatch and P. Gross. Pulmonary deposition and retention of inhaled aerosols. Academic Press, New York and London, (1964).
28. Z. T. Chowhan and A. A. Amaro. Pulmonary absorption studies utilising in situ rat lung model: designing dosage regimen for bronchial delivery of new drug entities. J. Pharm. Sci., 65, 1669 - 1672 (1976).
29. S. J. Enna and L. S. Schanker. Absorption of drugs from the rat lung. Am. J. Physiol., 223, 1227 - 1231 (1972).
30. R. C. Lanman, R. M. Gillian and L. S. Schanker. Absorption of cardiac glycosides from the rat respiratory tract. J. Pharmacol. Exp. Therap., 187, 105 - 111 (1973).
31. S. J. Enna and L. S. Schanker. Phenol red absorption from the rat lung: evidence of carrier transport. Life Sci., 12, 231 - 239 (1973).
32. J. A. Burton and L. S. Schanker. Absorption of antibiotics from the rat lung. Proc. Soc. Exptl. Biol. Med., 145, 752 - 756 (1974).
33. J. A. Burton and L. S. Schanker. Absorption of corticosteroids from the rat lung. Steroids, 23, 617 - 624 (1974).
34. L. S. Schanker and J. A. Burton. Absorption of heparin and cyanocobalamin from the rat lung. Proc. Soc. Exptl. Biol. Med., 152, 377 - 380 (1976).
35. T. H. Gardiner and L. S. Schanker. Absorption of disodium cromoglycate from the rat lung: evidence of carrier transport. Xenobiotica, 12, 725 - 731 (1974).
36. A. R. Clark and P. R. Byron. Department of Pharmacy, University of Aston, Birmingham U.K., Personal communication of data in press (1983,4).
37. R. K. Brazzell, R. B. Smith and H. B. Kostenbauder. Isolated perfused rabbit lung as a model for intravascular and intrabronchial administration of bronchodilator drugs I: Isoproterenol. J. Pharm. Sci., 71, 1268 - 1274 (1982).
38. R. K. Brazzell and H. B. Kostenbauder. Isolated perfused rabbit lung as a model for intravascular and intrabronchial administration of bronchodilator drugs I: Isoproterenol prodrugs. J. Pharm. Sci., 71, 1274 - 1281 (1982).

39. W. W. Wagner, L. P. Latham, M. N. Gillespie and J. P. Guenther. Direct measurement of pulmonary capillary transit times. *Science*, 218, 379 - 381 (1982).
40. R. A. Brown Jr. and L. S. Schanker. Absorption of aerosolised drugs from the rat lung. *Drug Metabolism and Disposition*, 11, 355 - 360 (1983).
41. J. Heyder, L. Armbruster, J. Gebhart, E. Grein and W. Stahlhofen. Total deposition of aerosol particles in the human respiratory tract for nose and mouth breathing. *J. Aerosol. Sci.*, 6, 311 - 328 (1975).
42. Task Group on Lung Dynamics. Deposition and retention models for internal dosimetry of the human respiratory tract. *Health Phys.*, 12, 173 - 207 (1966).
43. T. B. Martonen. Measurement of particle dose distribution in a model of a human larynx and tracheobronchial tree. *J. Aerosol. Sci.*, 14, 11 - 22 (1983).
44. S. P. Shiah and C. S. Wang. A mathematical model for predicting regional deposition. *J. Aerosol. Sci.*, 12, 212 - 213 (1981).
45. P. E. Morrow. Aerosol factors affecting respiratory deposition. International symposium on deposition and clearance of aerosols in the human respiratory tract. GAF and AeM, Bad Gleichenburg, Austria, 1 - 24, (1981).
46. I. Gonda and P. R. Byron. Perspectives on the biopharmacy of inhalation aerosols. *Drug. Dev. Ind. Pharm.*, 4, 243 - 259 (1978).
47. T. B. Martonen and A. F. Wilson. The influence of hygroscopic growth upon the deposition of bronchodilator aerosols in the upper human airways. *Ann. Occ. Hyg.*, 26, 208 - 211 (1982).
48. A. T. Cocks and R. P. Fernando. The growth of sulphate aerosols in the human airways. *J. Aerosol. Sci.*, 13, 9 - 19 (1982).
49. C. N. Davies. Deposition of particles in the human lungs as a function of particle size and breathing pattern: an empirical model. *Ann. Occ. Hyg.*, 26, 119 - 135 (1982).
50. P. R. Byron, S. S. Davis, M. D. Bubb and P. Cooper. Pharmaceutical implications of particle growth at high relative humidities. *Pest. Sci.*, 8, 521 - 526 (1977).
51. I. Gonda. Study of the effects of polydispersity of aerosols on regional deposition in the respiratory tract. *J. Pharm. Pharmacol.*, 33 (Suppl), 52P (1981).
52. S. Levey and R. Gast. Isolated perfused rat lung preparation. *Brit. J. Pharmacol.*, 40, 468 - 482 (1966).

53. D. J. P. Bassett, A. B. Fisher and J. L. Rabinowitz, Effect of hypoxia on incorporation of glucose carbons into lipids by isolated rat lung. *Am. J. Physiol.*, 227, 1103 - 1107 (1974).
54. D. J. P. Bassett and A. B. Fisher. Metabolic response to carbon monoxide by isolated rat lung. *Am. J. Physiol.*, 230, 658 - 663 (1976).
55. J. D. Brain, D. E. Knudson, S. P. Sorokin and M. A. Davis. Pulmonary distribution of particles given by intratracheal instillation or by aerosol inhalation. *Environmental Res.*, 11, 13 - 33 (1976).
56. H. A. Krebs and K. Henseleit. Untersuchungen über die Harnstoffbildung im Tierkörper. *Hoppe-Seyler's Z. Physiol. Chem.*, 210, 33 - 66 (1932).
57. Y. S. Bakhle, Royal College of Surgeons, London, U.K. Personal communication.
58. H. M. Mehendale, L. S. Angenne and Y. Ohmiya. The isolated, perfused lung - a critical evaluation. *Toxicol.*, 21, 1 - 36 (1981).
59. L. C. Ward and P. J. Buttery. The patho-physiologic basis for tests of viability in isolated perfused organs. *Biomed.*, 30, 181 - 186 (1979).
60. D. A. Wiersma and R. A. Roth. Clearance of benzo(a)pyrene by isolated rat liver and lung: alteration in perfusion and metabolic capacity. *J. Pharmacol. Exp. Therap.*, 225, 121 - 125 (1983).
61. W. A. Colburn. Organ perfusion studies. *J. Pharm. Sci.*, 72, 970 - 971 (1983).
62. E. J. M. McDevitt, W. Wilborn and G. Cassidy. Ultrastructure of the lung after ventilation. *Brit. J. Exp. Path.*, 63, 401 - 407 (1982).
63. G. C. Guilbart. Practical fluorescence, theory, methods and techniques. Marcel Dekker Inc., New York and Basel (1973).
64. S. P. L. Sørensen. Ergänzung zu der abhandlung: Enzymstudien II: Über die messung und die bedeutung der wasserstoffionenkonzentrationen bei enzymatischen prozessen. *Biochem. Z.*, 22, 352 - 356 (1909).

65. A. Aitio. Glucuronide conjugation in the lung. *Agents and Actions*, 6, 531 - 533 (1976).
66. C. V. Groom. Effects of relative humidity on inhalation aerosols. Ph.D. Thesis. University of Aston, Birmingham, U.K. (1981).
67. S. -C. Chen, H. Nakamura and Z. Temura. Determination of fluorescein and fluorescein monoglucuronide excreted in urine. *Chem. Pharm. Bull.*, 28, 2812 - 2816 (1980).
68. Merck Index, 9th Edition, pp. 4043 (1976).
69. T. Wagatsuma and H. Payling-Wright. The estimation of uranin (fluorescein sodium) in blood. *J. Clin. Path.*, 17, 271 - 272 (1964).
70. M. -L. Chen and W. L. Chiou. Adsorption of methotrexate onto glassware and syringes. *J. Pharm. Sci.*, 71, 129 - 131 (1982).
71. N. A. Fuchs and A. G. Sutugin. Generation and use of monodisperse aerosols. in C. N. Davies (ed.): *Aerosol Science*. Academic Press, London, U.K. (1966).
72. K. -W. Tu. A condensation aerosol generator system for monodisperse aerosols of different physicochemical properties. *J. Aerosol. Sci.*, 13, 363 - 371 (1982).
73. T. T. Mercer. Production and characterisation of aerosols. *Arch. Int. Med.*, 131, 39 - 50 (1973).
74. R. N. Berglund and B. Y. H. Liu. Generation of monodisperse aerosol standards. *Environ. Sci. Tech.*, 7, 147 - 153 (1973).
75. Research Engineering Ltd., U.K. (manufacturers of spinning disc generators) Personal communication.
76. W. H. Walton and W. C. Prewitt. The production of sprays and mists of uniform drop size by means of spinning disc type sprayers. *Proc. Phys. Soc.*, 62, 341 - 350 (1949).
77. K. R. May. An improved spinning top homogeneous spray apparatus. *J. Appl. Phys.*, 20, 932 - 938 (1949).
78. K. T. Whitby, D. A. Lundren and C. M. Peterson. Homogeneous aerosol generators. *Int. J. Air. Wat. Poll.*, 9, 263 - 277 (1965).
79. J. P. Mitchell, C. A. Ramsey and N. A. Rowe. The generation of calibration aerosols of known particle number concentrations. *J. Aerosol. Sci.*, 14, 257 - 260 (1983).
80. T. T. Mercer, M. I. Tillery and H. Y. Chew. Operating characteristics of some compressed-air nebulisers. *Am. Ind. Hyg. Assoc. J.*, 29, 66 - 78 (1968).

81. B. Y. H. Liu and K. W. Lee. An aerosol generator of high stability. *Am. Ind. Hyg. Assoc. J.*, 36, 861 - 865 (1975).
82. V. A. Marple, B. Y. H. Liu and K. L. Rubow. A dust generator for laboratory use. *Am. Ind. Hyg. Assoc. J.*, 39, 26 - 32 (1978).
83. R. F. Boucher and A. C. Lua. A stable high-concentration, dry aerosol generator. *J. Aerosol. Sci.*, 13, 499 - 511 (1982).
84. T. T. Mercer. *Aerosol technology in hazard evaluation*. Academic Press. New York and London (1973).
85. B. Y. H. Liu and D. Y. H. Pui. Electrical neutralisation of aerosols. *Aerosol Sci.*, 5, 465 - 472 (1974).
86. A. R. Clark, University of Aston, Birmingham, U.K. Personal communication.
87. C. V. Groom and I. Gonda. Cascade impaction: the performance of different collection surfaces. *J. Pharm. Pharmacol.*, 32 (suppl), 93P (1980).
88. D. G. Raabe. A General method for fitting size distributions to multicompartement aerosol data using weighted least squares. *Environ. Sci. Tech.*, 12, 1162 - 1167 (1978).
89. I. Gonda, J. B. Kayes, C. V. Groom and F. J. T. Fildes. Characterisation of hygroscopic inhalation aerosols. in N. G. Stanleywood and T. Allen. *Particle size analysis*. Wiley Heyden, Chichester, U.K. (1982).
90. M. Post, J. J. Barenburg, E. A. J. M. Schuurmans, V. Oldenburg, A. J. van der Molen and L. M. van Golde. The perfused rat lung as a model for studies on the formation of surfactant and the effect of ambroxol on this process. *Lung*, 161, 349 - 359 (1983).
91. T. B. Martonen, K. A. Bell, R. F. Phalen, A. F. Wilson and A. Ho. Growth rate measurements and deposition modelling of hygroscopic aerosols in human tracheobronchial models. *Proc. 5th Int. Symp. on inhaled particles*, Cardiff, 8-12 Sept. (1980). Pergamon Press, Oxford, U.K.
92. T. B. Martonen and M. L. Clark. The deposition of hygroscopic phosphoric acid aerosols in ciliated airways of man. *Fund. Appl. Tox.*, 3, 10 - 15 (1983).
93. F. Morén. Pressurized aerosols for oral inhalation. *Int. J. Pharm.*, 8, 1 - 10 (1981).
94. D. Pavia, M. L. Thompson, S. W. Clarke and H. S. Shannon. Effect of lung function and mode of inhalation on penetration of aerosol into the human lung. *Thorax*, 32, 194 - 197 (1977).

95. R. V. Lourenco, M. F. Klimek and C. J. Borowski. Deposition and clearance of 2-micron particles in the tracheobronchial tree of normal subjects: smokers and non-smokers. *J. Clin. Invest.*, 50, 1411 - 1420 (1971).
96. A. E. Taylor and K. E. Gaar. Estimation of equivalent pore radii of pulmonary capillary and alveolar membranes. *Am. J. Physiol.*, 218, 1133 - 1140 (1970).
97. J. Theodore, E. D. Robin, R. Gaudio and J. Acevedo. Transalveolar transport of large polar solutes (sucrose, inulin and dextrose). *Am. J. Physiol.*, 229, 989 - 996 (1975).
98. E. A. Egan, R. M. Nelson and R. E. Oliver. Lung inflation and alveolar permeability to non-electrolytes in the adult sheep *in vivo*. *J. Physiol.*, 260, 409 - 424 (1976).
99. J. -J. Kjaergaard, K. Dideriksen and T. Mourits-Andersen. Some aspects of the pharmacokinetics of fluorescein in normal and diabetic subjects. *Int. J. Microcirc. Clin. Exp.*, 2, 191 - 197 (1983).
100. S. J. Enna and L. S. Schanker. Absorption of saccharides and urea from the rat lung. *Am. J. Physiol.*, 222, 409 - 414 (1972).
101. T. L. Chan and C. P. Yu. Charge effects on particle deposition in the human tracheobronchial tree. *Ann. Occ. Hyg.*, 26, 65 - 75 (1982).
102. J. Ferin, T. T. Mercer and L. J. Leach. The effect of aerosol charge on the deposition and clearance of TiO_2 particles in rats. *Environ. Res.*, 31, 148 - 151 (1983).

GLOSSARY OF TERMS

I	Fluorescein (free acid)
II	Disodium fluorescein
III	Fluorescein dianion
	I & II prefixed by "experiment" refer to instillation experiments
K4	Kreb's Ringer bicarbonate solution with 4%w/v bovine serum albumin
KRB	Kreb's Ringer bicarbonate solution
pH12SGB	pH12 Sorensens glycine buffer
pH12K4	Centrifuged supernatant of K4 at pH12
um	micrometers
ug	micrograms
ul	microlitres
RT	respiratory tract
iprl	isolated, perfused rat lung
RI	relative intensity
T_s	fluorescent intensity of sample solution
T_r	fluorescent intensity of reference solution
f_t	fraction transferred
f_d	fraction deposited
F	total transferable fraction
f_∞	fraction transferred at time infinity
3400FB	Model 3400 fluidised bed aerosol generator
MMD_{ae}	mass median aerodynamic diameter
σ_g	geometric standard deviation
TV	Tidal volume
RF	respiratory frequency
PF	perfusate flow rate
psd	particle size distribution
AT	artificial thorax
k	first-order rate constant
P	permeability
P_1 and 2	pressures
A	surface area
K_D	partition coefficient
h	membrane thickness
V	volume